Hydrogen Fuelling Stations

A Thermodynamic Analysis of Fuelling Hydrogen Vehicles for Personal Transportation

Rothuizen, Erasmus Damgaard

Publication date:
2013

Document Version
Publisher's PDF, also known as Version of record

Hydrogen Fuelling Stations

A Thermodynamic Analysis of Fuelling Hydrogen Vehicles for Personal Transportation

PhD Thesis

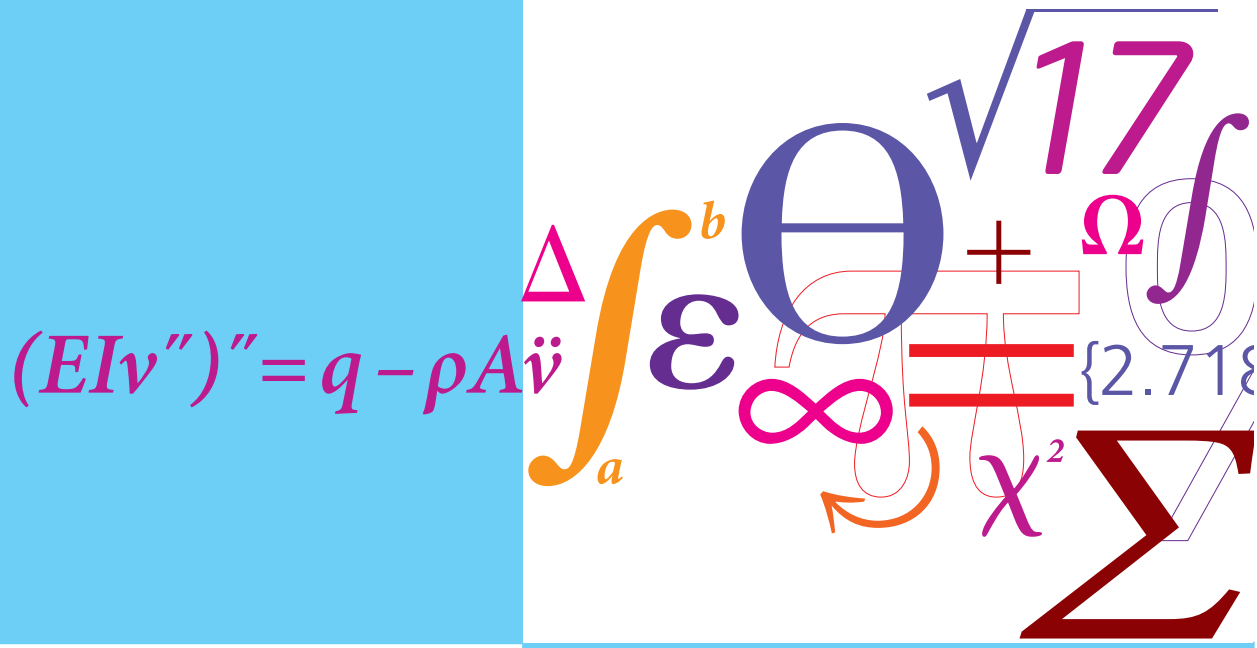

Erasmus Damgaard Rothuizen
DCAMM Special Report No. S161
September 2013

DTU Mekanik
Institut for Mekanisk Teknologi

Hydrogen Fuelling Stations

A Thermodynamic Analysis of Fuelling Hydrogen Vehicles for Personal Transportation

Erasmus Damgaard Rothuizen

Ph.D. Thesis

Kongens Lyngby 2013

Technical University of Denmark

Hydrogen Fuelling Stations
A Thermodynamic Analysis of Fuelling Hydrogen Vehicles for Personal Transportation

Ph.D. Thesis
DCAMM Special Report No. S161
Printed by Rosendahls – Schultz Grafisk A/S
Font: Latin Modern typeset with LaTeX 2_ε

DTU Mechanical Engineering
Section of Thermal Energy
Technical University of Denmark

Nils Koppels Allé, Bldg. 403
DK-2800 Kongens Lyngby
Denmark
Phone (+45) 45 88 41 31
Fax (+45) 45 88 43 25
www.mek.dtu.dk
ISBN: 978-87-7475-371-1

Preface

This thesis is submitted as partial fulfillment of the requirements for the Ph.D. degree at the Technical University of Denmark (DTU).

The thesis was completed at the Section of Thermal Energy, Department of Mechanical Engineering at the Technical University of Denmark. The work was carried out in the three-year period from 1^{st} of October 2010 to 30^{th} of September 2013 under the supervision of Associate Professor Masoud Rokni and the co-supervision of Associate Professor Brian Elmegaard.

An external research stay was undertaken from March 2012 to July 2012 at the Clean Energy Research Center (CERC), Department of Mechanical Engineering, University of British Columbia, Vancouver, Canada. The supervisor was Associate Professor and Head of the Clean Energy Research Center, Walter Mérida.

The Ph.D. study was funded by the Technical University of Denmark and the Danish Energy Agency through the project work group LINK 2009 including H2Logic as an industrial partner.

The thesis is written as a monograph, but a number of papers have been published based on the work in this research study.

Erasmus Damgaard Rothuizen
Kgs. Lyngby, September 2013

Acknowledgements

I would like to express my deepest gratitude to everyone who has assisted and supported me during my Ph.D. project in the last three years.

I would especially like to thank my supervisor Associate Professor Masoud Rokni, who was always available for discussions and good advice when needed. I am also very grateful for the great confidence you showed me. I would also like to thank my co-supervisor Brian Elmegaard for his guidance and discussions.

A special thanks goes to the employees at my industrial partner H2Logic and especially to Morten Wistoft-Ibsen with whom I have had a lot of broad and useful discussions.

I would also like to thank all my colleagues at the section of Thermal Energy, who have contributed to a great working environment and many friendships. I would especially like to thank Torben Ommen for all our lengthy discussions, Martin Kaern for introducing me to Modelica and for the help getting started, Jorrit Wronski for creating the Dymola interface to CoolProp that saved me many hours of simulation time, Wiebke Brix for the broad discussions and Lorenzo Bellemo and Andrea Mazzucco the two Italians, for keeping the spirit high. I would also like to thank Jonas Jensen for taking on my proposed Master project in refrigeration for hydrogen fuelling stations.

My stay at the Clean Energy Research Center at the Department of Mechanical Engineering at the University of British Columbia, Vancouver, Canada, would not have been possible without the kind assistance of Associate Professor Walter Mérida who invited me to his research group. I would like to thank Walter

Mérida for his encouraging guidance and support for my work. I would also like to thank the Otto-Mønsted fund for the economical support making my stay possible.

Last, but not least, I would like to thank my friends and family for all their support and discussions. I am especially grateful to Katrine who has been a solid support at home.

Abstract

This thesis concerns hydrogen fuelling stations from an overall system perspective. The study investigates the thermodynamics and the energy consumption of hydrogen fuelling stations for fuelling vehicles for personal transportation. For this study a numerical library to model the components in a hydrogen fuelling station has been developed in Dymola, which is a commercial software package. The models include the fuelling protocol (J2601) for hydrogen vehicles published by the Society of Automotive Engineers (SAE), and the thermodynamic property library CoolProp is used for retrieving state points.

The components in the hydrogen fuelling library are constructed following the same procedure for each component. This enables components to be connected in any random order when building systems. The systems are made in a graphical interface, where components from the library can be directly added and connected by dragging a line from their input or output port.

A system consisting of one high-pressure storage tank is used to investigate the thermodynamics of fuelling a hydrogen vehicle. The results show that the decisive parameter for how the fuelling proceeds is the pressure loss in the vehicle. The single-tank fuelling system is compared to a cascade fuelling system. This shows that the mass flow and the thermodynamic development in the vehicle are independent of the station design, when the fuelling is according to the protocol published by SAE. Further, the study show that a cascade system is preferable compared to a single-tank system, considering the energy consumption of the fuelling procedure.

Models of cascade systems, consisting of between 1 and 8 tanks, have been used to analyse the effect of the number of tanks at the station with respect to

energy consumption. An optimisation using a parameter variation of the tank volumes and pressures is performed in order to reduce the energy consumption further. The study showed that the energy consumption at the station approaches an exponential function of the number of tanks. The energy saving is highest going from one to two tanks in the cascade system, and the saving levels out when more than four tanks are used. Decreasing the tank volumes to a minimum or decreasing the pressure to a minimum, contributes to the overall savings with approximately 4-5 %.

Two alternative system designs to the cascade fuelling system have been suggested and analysed with respect to thermodynamics, energy consumption and exergy destruction. The first system uses a compressor to fuel the hydrogen vehicle. The second system uses a compressor followed by a small buffer tank. The system fuelling directly from a compressor does not follow the fuelling protocol, though it does not exceed the safety limits. The system using a compressor and a buffer tank does fuelled in accordance with the fuelling protocol. The analysis shows that it is possible to eliminate all the high-pressure storage tanks from the cascade system, using one of the other fuelling systems. The energy consumption of the direct compression system is 18 % lower than for the two other systems. The exergy analysis shows that the largest exergy destruction was in the vehicle tank, due to compression. The compressor and the heat exchanger at the outlet of the compressor also show high exergy destructions in all three systems. The reduction valve, which is eliminated in the direct compression system, has an exergy destruction corresponding to more than 0.75 kWh which is 11-17 % of the total exergy destruction in the two other systems. The direct compression system is the least energy consuming and has the lowest exergy destruction. The cascade system has the highest exergy destruction, while the energy consumption is approximately the same as for the direct compression system with a buffer.

Resumé

Denne afhandling betragter brinttankstationer med fokus på hele systemet. Termodynamikken i en brint tankning og energi forbruget for tankning af en brintbil undersøges og analyseres. Til at lave analyserne er et komponentbibliotek til brinttankning blevet udviklet i den dynamiske software Dymola. Komponentmodellerne inkluderer fyldningsprotokollen (J2601) udviklet af Society of Automotive Engineers (SAE) og de termodynamiske egenskaber findes ved brug a biblioteket CoolProp.

Komponenterne i brint påfyldningsbiblioteket er bygget op efter samme procedure, dette gør det muligt at placere komponenter og sammensætte komponenterne i vilkårlig rækkefølge når et brinttankningssystem skal designes. Systemerne opbygges i en grafisk brugerflade hvor komponenterne kan indføres direkte fra biblioteket. Modellerne forbindes ved at tegne linjer mellem deres porte, der repræsentere strømning ind og ud af modellen.

Et system bestående af en enkelt højtrykstank for brintlagring på tankstationen er brugt til at undersøge termodynamikken af en brintpåfyldning af et køretøj. Resultaterne af undersøgelsen viste at bilens tryktab er den bestemmende parameter for hvordan en brintpåfyldning forløber. Brinttankningssystemet bestående af en højtrykstank er sammenlignet med et kaskadetankningssystem bestående af tre højtrykstanke. Resultaterne viser at massestrømmen og termodynamikken i bil tanken er uafhængig at brinttankstationsdesignet, så længe påfyldningen følger protokollen udgivet af SAE. Endvidere viser sammenligningen af de to systemer at kaskade systemet er at foretrække når energiforbruget af brintpåfyldningen af køretøjet tages i betragtning.

Modeller af kaskadesystemer med mellem 1 og 8 tanke er brugt til at undersøge

hvordan antal tanke i kaskadesystemet påvirker energiforbruget på stationen. En parameter variation hvor tankenes volumen nedsættes til et minimum og en optimering hvor trykkene i tankene reduceres til et minimum er udført for at se effekten på energiforbruget. Analysen viste at energi forbruget på stationen nærmer sig en eksponentiel kurve som funktion af antal tanke i kaskadesystemet. Den største energibesparelse var når man gik fra at have en højtrykstank til to højtrykstanke i kaskadesystemet og energibesparelserne fladede ud når man tilføjede mere end fire tanke i systemet. Minimeringen af volumen of trykket i tankene gav en yderligere energi besparelse på 4 -5 %.

To alternative tanksystemer til kaskadesystemet er blevet foreslået og undersøgt med hensyn på termodynamiske egenskaber, energi forbrug og exergi destruktion. Det første system består af en kompressor der påfylder biltanken direkte. Det andet system består ligeledes af en kompressor, men den er efterfulgt af en lille opsamlingstank. Systemet der fylder direkte fra kompressoren følger ikke brintpåfyldningsprotokollen, men den overtræder heller ikke de fastlagte sikkerhedsgrænser. Systemet der fylder med en kompressor og en lille opsamlingstank følger brintprotokollen for påfyldning. Undersøgelsen viste at det er muligt at eliminere højtrykstankene i kaskadesystemet, ved brug af de to alternative systemer. Energiforbruget ved at fylde direkte med en kompressor var 18 % lavere end for kaskadesystemet og kompressorsystemet med en opsamlingstank. Exergi analysen af de to systemer viste at den største exergi destruktion var i tank, dette skyldes komprimeringen af gassen. Kompressoren og varmeveksleren efter den havde også en høj exergi destruktion for alle tre systemer. Reduktionsventilen som er brugt i kaskadesystemet og systemet med en kompressor og en opsamlingstank havde en exergi destruktion på 0.75 kWh svarende til 11-17 % af den totale exergi destruktion i de to systemer. Dette exergi tab er elimineret for systemet der fylder direkte ved kompression, da kompressoren levere brinten direkte ved det ønskede tryk. Systemet med direkte kompression havde det laveste energi forbrug og exergi destruktion imens kaskadesystemet havde den højeste exergi destruktion. Energiforbruget ved kaskadepåfyldningen og kompressoren med en opsamlingstank var stort set det samme.

List of publications

Journal Papers:

Rothuizen E., Mérida W., Rokni M., Wistoft-Ibsen M., 2013, Optimization of hydrogen vehicle refuelling via dynamic simulation. *International Journal of Hydrogen Energy 38*,4221-4231.

Rothuizen E., Rokni M., 2013, Optimization of the overall energy consumption in cascade fueling stations for hydrogen vehicles. *International Journal of Hydrogen Energy 39*. 582-592.

Jensen J., Rothuizen E., Brix W., 2013, Entropy generation minimization of one and two stage tube in tube evaporators cooling high pressure gaseous hydrogen for vehicle refueling. Special issue of *Energy Conversion and Management* dedicated to ECOS 2013. The 26th International Conference on Efficiency, Costs, Optimization, Simulation and Environmental Impact of Energy Systems. Submitted.

Peer-reviewed conference papers

Rothuizen E., Abel M., Rokni M., Elmegaard B., 2011, Using a potassium acetate solution for cooling high pressure hydrogen in a prototype heat exchanger. In 23rd International Congress of Refrigeration. IIR/IFF. Prague, Czech Republic.

Rothuizen E., Rokni M., 2013, The effect on overall energy consumption at a hydrogen refueling station by cascade fueling a hydrogen vehicle. In: 6th In-

ternational Conference of Sustainable Energy and Environmental Protection. SEEP. Maribor, Slovenia.

Contents

Nomenclature

Roman

A	Area of tank, m^2
a	Thermal diffusivity, m^2/s
c	Specific heat capacity, $J/(kgK)$
d	Diameter, m
e	Specific exergy, J/kg
E	Exergy, J
f	Friction factor, -
g	Gravity, m/s^2
h	Enthalpy, J/kg
k	Conductivity, $W/(mK)$
k_v	Pressure loss constant, m^3/h
k_p	Pressure loss constant,-
L	Length, m
$\dot{m}$	Mass flow rate, kg/s
M	Mass, kg
n	Number of strokes, $strokes/s$
Nu	Nusselt number, -
p	Pressure, Pa
Q	Heat loss, J/s
R	Resistance, (J/K)
r	Roughness, mm
Ra	Rayleigh number, -

Roman continued	
$\dot{s}$	Surface energy conversion, J
s	Entropy, J/kg
T	Temperature, K or $°C$
t	Time, s
U	Internal energy, J
V	Volume, m^3
$\dot{V}$	Volume flow, m^3/s
v	Velocity, m/s
W	Work, J/s
x	Thickness, m

Greek	
α	Heat transfer coefficient, $W/(m^2K)$
β	Thermal expansion coefficient, T^{-1}
η	Efficiency, $-$
γ	Heat capacity ratio, -
μ	Dynamic viscosity, $kg/(sm)$
ρ	Density, kg/m^3

Subscript	
0	Reference properties
1	Entrance number
2	Entrance number
3	Entrance number
a	Ambient
cv	Control volume
cyl	Cylinder
D	Destruction
E	Exergy
g	Gas
i	Node number

Subscript continued	
in	Into component
is	Isentropic
k	Conductivity
L	Total thickness
out	Out of component
P	Pressure
poly	Polytropic
s	Solid
T	Temperature
v	Volumetric
w	Wall
water	Water properties at $15°C$

Abbreviations	
APRR	Average pressure ramp rate
COP	Coefficient of performance
Comp	Compressor
HPL	High pressure loss
HRS	hydrogen refuelling station
HSS	hydrogen storage system
LPL	Low pressure loss
PL	Pressure loss
RV	Reduction valve
SAE	Society of Automotive Engineers
SOC	state of charge
TIR	Technical information report

Chapter 1

Introduction

1.1 Motivation

The history of fuel cell powered vehicles is relatively short as the first commercial hydrogen vehicle was introduced in 1992. The technology gained more attention as climate change, security of supply and fossil fuel depletion became well-known issues at the end of the 20th century. At that time the fuel cell powered vehicles did not have the attention of the public and the research committed within the field was limited, although the development of the proton exchange membrane fuel cell accelerated during the 1990s. At the same time as the vehicle manufacturers started gaining interest in hydrogen vehicles the Society of Automotive Engineers (SAE) started developing protocols to assure the safety of hydrogen fuelling and to provide guidelines for specific components and system designs. This was done in close cooperation with several of the larger vehicle manufacturers in the world. In 2008 some of the major car manufacturers released the early stages of a fuelling protocol in a paper [24] and the SAE released a protocol on how to connect a hydrogen vehicle to a fuelling station [35]. In 2010 a protocol describing a fuelling procedure was released [34]. A result of the close cooperation between manufacturers and the SAE is that nearly all vehicle manufacturers produce their vehicles according to the SAE guidelines, and almost all new hydrogen fuelling stations are built according to the fuelling protocol. The early protocols have given fuel cell vehicles and hydrogen fuelling stations a good basis for further integration, assuring that hydrogen fuelling stations and vehicles can be produced independently and still function together worldwide. These standards serve to promote

the technology for funding, as there are no competing hydrogen fuelling technologies. Another large cooperation among those promoting hydrogen vehicles was formed in 2009 when Toyota, Daimler, GM and four other car companies signed a statement of intent to produce 100000 hydrogen vehicles by 2015.

The protocol for hydrogen fuelling is called "Fueling protocols for light duty gaseous hydrogen surface vehicles" and it is a technical information report [34]. The goal of the report is to achieve a safe, costumer-acceptable fuelling, meaning a fast fuelling without exceeding the limitations of pressure, temperature and density. The protocol is still under development, and a new improved protocol is expected to be released by the end of 2013. The protocol is based on tests conducted by Power Tech and simulations done by Wenger Engineering. The safety and fuelling requirements for the fuelling stations are high, and the fuelling station manufacturers have been struggling to fulfil the requirements satisfactorily. Though some of the newly introduced stations have shown satisfying results.

The research conducted within the field of high-pressure hydrogen fuelling is primarily done within industry, and it is therefore not accessible to the public. The speed of development within hydrogen fuelling stations is fast, and at the moment different companies are at the moment competing to get the early market shares. The information available from the manufacturers is limited as they keep their research internal so their rival companies cannot use it. The work in this project has been carried out in collaboration with H2Logic who builds hydrogen fuelling stations, but in order to keep their technology secret, the study does not include specific technology from their stations.

The basic understanding of the thermodynamic development of hydrogen during a fuelling process and which components influence the process of the fuelling are still unexplored in the literature even though this information is commercially known. Without the basic understanding of hydrogen fuelling, it is impossible to address problems within the system. Further, the understanding of how the fuelling protocol affects the fuelling is needed in order to improve station designs and fuelling methods.

The hydrogen fuelling stations today all use a cascade system to fuel the vehicles. The process of getting the system to perform satisfactorily has been the main priority until now, and little concern has been given to the energy consumption of the station. The number of tanks in the cascade system and the effect of volumes and pressures in the tanks have not yet been investigated with respect to the energy consumption of the station. Potentially there could be a large energy savings by optimizing the cascade systems.

Other system designs for fuelling hydrogen vehicles have been discussed, in-

cluding fuelling directly from a compressor. While cascade systems are widely used, the advantages and disadvantages compared to other systems have not been investigated. More efficient fuelling technologies could potentially still be revealed.

1.2 Literature review

Even though the procedure for hydrogen fuelling is on the way to being standardized, the subject of hydrogen fuelling is relatively new from a scientific point of view. Literature within the field of hydrogen fuelling is limited to the specific analysis of the behaviour of the compressed hydrogen on-board and the heat transfer through both Type III and Type IV tanks. In addition, a few analyses have been conducted from a broader system perspective, though only Maus et al. are using the fuelling protocol [24]. The paper by Maus et al. is the first paper describing the fuelling protocol released in 2010.

Some of the first comprehensive studies on compressed hydrogen fuelling were carried out by Dicken and Mérida, [7]. They placed 63 thermocouples in a Type III tank while fuelling to 350 bar. The study showed a non-uniform temperature distribution with up to a $6°C$ temperature difference. Further, the study showed that the main contributor to the heat development in the tank was the compression rather than the Joule-Thomson effect.

Although the study of Dicken and Mérida showed a non-uniform temperature distribution during the fuelling, it is generally accepted that in mathematical models the temperature can be assumed uniform, according to the research conducted by Monde and Woodfield. Further they showed that new tanks have a distributor at the inlet to ensure a more uniform temperature distribution [27] [26] [37].

Work similar to that of Dicken and Mérida has been carried out by Kim, who found that the temperature at the upper part of the cylinder was higher than in the lower part due to the buoyancy effect, and for their experiment the maximum allowed temperature of 85 $°C$ was exceeded [19].

Monde and Woodfield have made different models of both analytical and numerical transient heat transfer from the hydrogen through the tank wall, and to the ambient. Depending on the nozzle design in the tank (e.g., advanced or straight nozzles) the average local hydrogen heat transfer coefficient inside the tank during a fuelling can vary between 150 and 500 $W/(m^2K)$ [27] [38]. For discharging vessels, Daney's relation has been shown valid for a large range of Rayleigh numbers [38].

The thermodynamics of filling a hydrogen tank has been investigated through exergy analysis, and it has been shown that increasing the initial pressure increases the exergy efficiency and the final temperature in the hydrogen tank was lower [14]. Similar work has been conducted by Ozsaban [29].

Galassi has conducted experiments on the life-time of the tanks, and the local temperature inside the tank has been measured and compared to the outside temperature. The results were used to validate a CFD model of the tank during fast filling [12]. Similar work has been carried out by Heitsch [13] and Abhilash [1].

Li has done investigations on the temperature rise inside the hydrogen tank. Fuellings using a constantly decreasing mass flow rate were compared with fuellings using a constantly increasing mass flow rate. It was found that the lowest temperature increase was obtained when filling with constantly decreasing mass flow rate[23].

Farzaneh-Gordi has done a comparison between cascade fuelling and fuelling from a single tank. The results revealed that the filling time of the single tank was faster than for the cascade system but, it was also accompanied with a much higher entropy generation. The study also revealed that filling the single tank and the cascade system tanks again after a vehicle fuelling, required less work for the compressor for the cascade system [10].

Zhao has conducted research using numerical simulations to predict the temperature rise in the hydrogen tank during filling. The results showed that with increased mass flow rates, the temperature would increase and with an increasing initial pressure, the temperature decreases [40]. Further he has developed a CFD model with an analysis of the thermodynamic response to different pressure rise patterns and filling times within a Type III cylinder [41].

The fuelling time due to the thermodynamics in the tank has been investigated by Yang. The fuelling time is compared to the upper and the lower limit of the tank properties for both adiabatic and isothermal conditions. The fuelling time was shortest under adiabatic conditions [39].

1.3 Thesis statement

The overall aim of this research is to contribute to the understanding of hydrogen fuelling from an overall system perspective. This includes thermodynamic understanding of the whole system, energy consumption in the system and optimisation of the overall energy performance of fuelling systems. As mentioned

in the motivation, most research is done in industry and not published. In order to developed better fuelling systems, the basic understanding of fuelling systems and the different parameters that influence the fuelling process need to be determined.

More specifically, the research aims to:

- Develop a component library for thermodynamic modelling of whole hydrogen fuelling systems including; tanks with heat transfer, different pressure losses, heat exchangers, compressors and other needed components. Further, the model should enable simulations using the fuelling protocol developed by the Society of Automotive Engineers.
- Investigate the thermodynamics of hydrogen fuelling and how the different components influence the fuelling process.
- Optimise the fuelling process of a cascade system with respect to the number of tanks, volumes and pressure of the tanks.
- Compare the cascade system to other alternative fuelling systems, with respect to thermodynamics, complexity and energy consumption.
- Point out the components in the fuelling systems which have the largest influence on the energy consumption and provide suggestions for improvement.

1.3.1 Methodology

The applied methodology for the present research study above can be divided into six steps.

- Develop of a thermodynamic component library for hydrogen fuelling. The model should be able to simulate different hydrogen fuelling systems and show the thermodynamics in each component and for the overall system.
- Perform a thermodynamic analysis of a simple hydrogen fuelling process from one high-pressure tank to the vehicle tank following the fuelling protocol, and show the effect of using a cascade system instead.
- Conduct a parametric study of the energy consumption in a cascade system with variation in the number of tanks, the pressure in the tanks and the volumes of the tanks.
- Compare different fuelling systems and analyse the thermodynamics of each system. Analyse the energy consumption of each system with respect to the main energy-consuming components.

- Implement equations for exergy analysis in the components in the library.
- Perform an exergy analysis on the different fuelling systems, point out the components with the highest exergy destruction and discuss how these can be reduced.

As mentioned, the aim is to improve the thermodynamic understanding of a complete hydrogen fuelling system and to optimize the system with respect to different parameters, but the scale of the component library could be more extensive for future use in other projects or by industry.

1.4 Thesis outline

The thesis contains 8 chapters and 2 appendices besides the published papers.

Chapter 1 is the introduction containing the motivation for the study, the literature review, the thesis statement, the methodology and the thesis outline.

Chapter 2 contains the basic principles of the hydrogen fuelling method, station designs and a description of the fuelling protocol developed by the Society of Automotive Engineers.

Chapter 3 contains a description of the numerical model formulations used in all the models for simulation of hydrogen fuelling systems. For critical components like the tank and the compressor, the different technologies are discussed.

Chapter 4 presents the component library made in Dymola, the methode used and a verification and validation. It explains some of the principles behind the modelling of flows and enthalpies. The verification and validation are comparisons between the Dymola model and a MatLab model developed by industry and test data from a fuelling station.

Chapter 5 summarises the important and general assumptions for the analysis. First the thermodynamic assumptions, second assumptions regarding to the fuelling protocol and third assumptions regarding the flow where Turbulent flow and tube dimensions are discussed.

Chapter 6 analyses hydrogen fuelling from one tank to the vehicle and from three tanks to the vehicle. The two systems are analysed thermodynamically, and correlations between components and the procedure for the fuelling are discussed. At the end the two systems are compared with respect to energy usage.

Chapter 7 is a parameter variation study of the tanks in a cascade system with respect to energy usage of fuelling a vehicle and afterwards recovering the

cascade system. The energy usage for compression and cooling are shown in detail. The different parameters are the number of tanks in the cascade system, the volume of the tanks and the pressure in the tanks.

Chapter 8 analyses and compares a cascade fuelling system, a direct compression system and a direct compression system with a buffer. The analysis is done with the cascade system as the reference. First, a thermodynamic analysis of the system is done, analysing and explaining the principles and differences of the fuelling systems. Afterwards an energy analysis is carried out to see which system uses the least energy. Then there is an exergy analysis of each system, pointing out the largest exergy-destructive components.

Chapter 9 summarises the most important findings in the thesis and gives suggestions for further work within the field.

Chapter 2

Introduction to hydrogen fuelling

This chapter describes the basic principles of a hydrogen fuelling station and how it functions, including the basics of hydrogen fuelling using the pressure difference in a cascade system and the storage of hydrogen at the station. Then there is an explanation of the fuelling protocol used for hydrogen fuelling to obtain a costumer acceptable, secure and fast fuelling of a vehicle.

2.1 Introduction

The objective of this chapter is to provide an understanding of hydrogen fuelling. First, the simplest way to fill a tank is introduced, followed by the complications that are associated with the fuelling of hydrogen tanks. This sets in perspective why a standardised fuelling protocol is needed. The parts of the fuelling protocol that are of interest for this project are explained. The fuelling protocol is very important for the dynamic simulations done later in the thesis, as they all apply to the protocol. Further, the fuelling protocol is integrated in the library for hydrogen fuelling introduced in chapter 4. The last part of the chapter contains general information about today's fuelling station design and operation strategy.

2.2 The basics of hydrogen fuelling

This section describes the simplest systems for fuelling a hydrogen tank and the complications of hydrogen fuelling, when done within a reasonable time.

2.2.1 Procedure of a simple fuelling

Fuelling into a tank can in principle be done in two different ways, either by compressing directly into the tank or by having a tank at higher pressure. Considering a tank at higher pressure, the pressure difference is used to force hydrogen from the higher pressure to the lower pressure tank. The most common way to fuel hydrogen vehicles is by using tanks at higher pressure. The two different systems are shown in Figure 2.1 When fuelling from a high-pressure

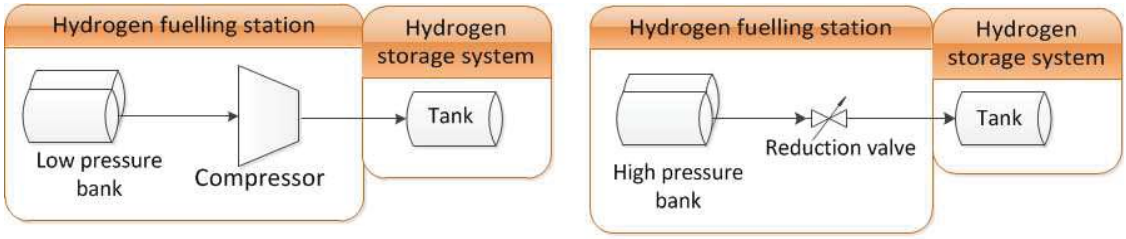

Figure 2.1: Sketch of the simplest way to fill a vehicle hydrogen tank. Left: Compressor fuelling from a low-pressure tank to high pressure. Right: pressure forced fuelling between a high pressure and low-pressure tank
.

tank to a low-pressure tank, the hydrogen needs to be pressurised in the high-pressure tank using a compressor. The advantage of the pressure levelling fuelling is that it can fuel at high mass flow rates. For the compressor system the mass flow is limited by the capacity of the compressor. The two systems shown would be able to fuel a hydrogen vehicle, but due to the properties of hydrogen and compression, the fuelling would take a long time in order to be done safely.

2.2.2 Complications of hydrogen fuelling

Hydrogen fuelling is not as simple as shown in Figure 2.1. First, hydrogen is explosive and needs to be handled with care. Second, the properties of hydrogen and the high working pressures of hydrogen, complicate a safe fuelling process. The pressure for storing hydrogen needs to be high. If a decent driving range is to be obtained, the hydrogen should be stored in the vehicle at 350-700 bar. The primary reason for the high-pressure storage is that hydrogen is stored as a gas and not as liquid. Storing it as liquid would require it to be

cooled down to beneath -253°C. Further more, hydrogen has the lowest density of all elements, 0.089 kg/m^3, at atmospheric pressure and 0°C. Therefore it requires either a large volume or high pressure to store between 3 and 7 kg of hydrogen in the vehicle. The large volume is not an option in a vehicle for personal transportation. The hydrogen is therefore stored at 350 or 700 bar in cylinders of up to 0.172 m^3, corresponding to 7 kg at 700 bar. When hydrogen is fuelled into a vehicle there are several factors to account for during the fuelling. The temperature of the hydrogen is, for safety reasons, not allowed to exceed 85°C. When hydrogen is compressed into a cylinder, the temperature of the hydrogen increases due to the heat of compression and if filled fast, the temperature exceeds the limit. Fuelling a hydrogen vehicle just using a high-pressure tank with a valve reducing the pressure into the vehicle, would take hours if a sufficient amount of hydrogen is to be transferred between the tanks, without exceeding the temperature safety limit. Therefore the hydrogen needs cooling before entering the vehicle. The size of the vehicle tank varies depending on the vehicle type and manufacture. It is therefore necessary to be able to do a safe fuelling independent of the volume of the vehicle tank. This is done using an average pressure ramp rate that fuels with a constant pressure rise at the station's exit. In this way all tanks can be fuelled safely because the pressure rise in the tank is controlled; hence, the mass flow is automatic adjusted for the volume of the tank. If the volume of the tank is known the mass flow rate could also be set according to it, and the average pressure ramp rate would not be necessary. The most critical part when fuelling a tank with hydrogen is to assure that the pressure and the temperature do not exceed the safety limits. Following the fuelling protocol published by the Society of Automotive Engineers, the safety of the fuelling is met and all vehicles can be safely fuelled when knowing the type of tank, the ambient temperature and the initial pressure in the tank. The following sections explain the important part of the protocol with respect to the work in this thesis.

2.3 Hydrogen fuelling protocol

The hydrogen fuelling protocol is an industrial technical information report describing how to fuel different vehicle tanks with regards to volume and maximum allowed pressure. The protocol is called "Fueling of light duty gaseous hydrogen vehicles" and has the journal number J2601 [34]. The protocol is often referred to as "SAE TIR J2601" or just "SAE J2601". This section outlines the most important guidelines regarding safety and measurements of the mass fuelled compared to the reference state.

2.3.1 SAE TIR J2601

The purpose of SAE J2601 is to achieve a consumer-acceptable fuelling which does not compromise safety. The "consumer-acceptable" fuelling refers to the time it takes to fuel the hydrogen vehicle. In order to convince people to use new technologies like hydrogen vehicles, the technology needs to be equally or more convenient to use than the existing technology. The hydrogen fuelling should therefore happen within a reasonable amount of time; hence, the time equal to fuel a petrol vehicle. The fuelling should not exceed the safety limits of temperature, pressure and density during or after the fuelling period. The SAE J2601 for industrial implementation contains guidelines for hydrogen fuelling at two net working pressures (NWP) 35 MPa and 70 MPa and for four different pre-cooling temperatures of the station dispenser; A, B, C and D. The NWP of a station is limited by the pre-cooling in the station dispenser. The fuelling stations are categorised depending on their net working pressure and dispenser cooling capacity. Table 2.1 shows the different maximum allowed NWP depending on the pre-cooling temperature of the hydrogen in the dispenser. The

Table 2.1: Hydrogen fuelling station categories

Type	NWP [bar]	Dispenser pre/cool temperature [C]
A70	700	-33 to -40
A35	350	
B70	700	-17.5 to -22.5
B35	350	
C35	350	-2.5 to 2.5
D35	350	Ambient ± 5

two protocols with dispenser pre-cooling to 0 $^{\circ}C$ and ambient temperature are not recommended to use, though they are useful in the case of a breakdown of a cooling facility, as backup protocols. The maximum storage capacity of the vehicle for the two target pressures is 10 kg for stations categorised "70" and 7.5 kg for stations with a "35". For a "70" the common target is 7 kg as 10 kg requires the vehicle to have multiple storage tanks. The maximum mass flow allowed during a fuelling is 0.06 kg/s. The protocols for fuelling at the different categorised stations contain lookup tables for an average pressure ramp rate which depends on the ambient temperature and the initial pressure in the vehicle tank, the target pressure in the tank and the target state of charge of the tank. The average pressure ramp rate assures that the fuelling proceeds safely within a given time. The target pressure is the pressure the tank should have at the end of the fuelling in order to be filled to the maximum capacity. The state of charge is a measurement of the actual final density in the tank compared to the target density. The target density is the density of the net

working pressure at 15 $°C$. State of charge is calculated by eq. 2.1.

$$SOC = \frac{\rho(T,p)}{\rho(15°C, NWP)}100\% \tag{2.1}$$

For an "A70" fuelling (-40$°C$ and 700 bar) the target density is 40.2 kg/m^3. If the fuelled tank by the end of the fuelling has a lower density than the reference density it is under-filled, and if the density is higher it is over-filled. Figure 2.2 shows the target density for an "A70" fuelling as a function of the final pressure and temperature in the vehicle tank with the boundary conditions of the maximum allowed pressure and temperature. Considering Figure 2.2, if the vehicle

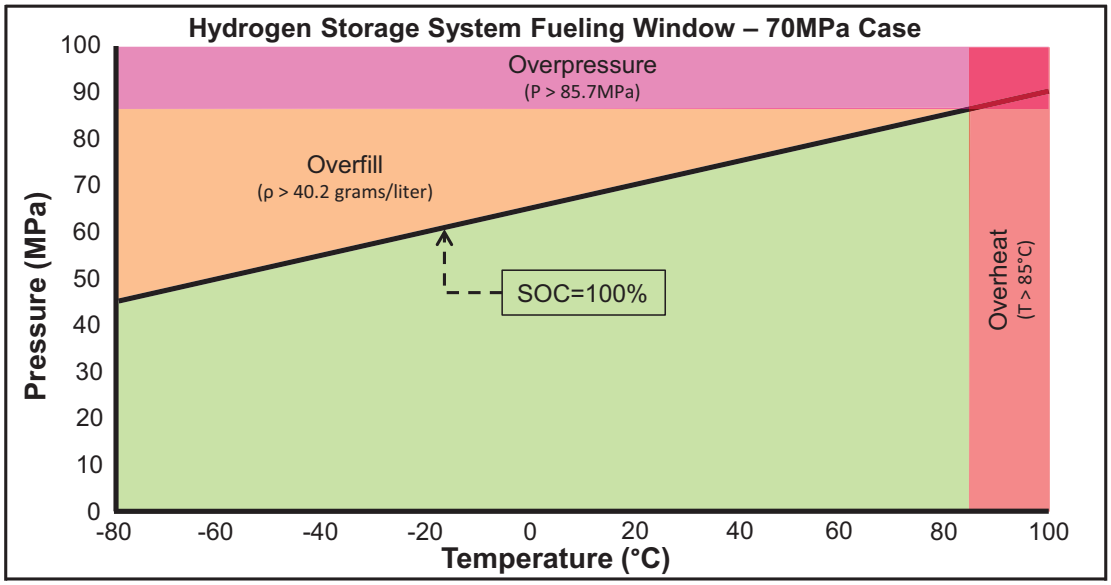

Figure 2.2: Fuelling window from 80$°C$ to 100$°C$ though according to the SAE J2601, fuelling is not allowed at temperatures lower than 40$°C$ [34] [16].

has a final pressure and temperature resulting in the density being below the reference density, the tank is under-filled; if the properties result in a higher density it is over-filled. The target is therefore to get as close to the target density without exceeding into the overpressure or overheat area. Typically the hydrogen in the tank is between 50 and 80$°C$ when the fuelling finishes, and the pressure is lower than needed for a 100% state of charge; thus the vehicle is under-filled. The different fuelling protocols take into account the heat up of the hydrogen during fuelling, and thus the target final pressure in the tank is higher than the net working pressure, to compensate for the heat up. Figure 2.3 shows an example of a lookup table for fuelling at an "A70" station; the values have been modified in order not to break copyrights, although the trends in the table are valid. As the lookup table in Figure 2.3 shows, the average pressure ramp rate depends on the ambient temperature. This is because

A-70 1-7kg		Average Pressure Ramp Rate [MPa/min]	Fuelling Target Pressure [MPa]										
			Initial tank Pressure [MPa]										
			2	5	10	15	20	30	40	50	60	70	>70
Ambient Temperature [C]	>50	no fuelling	no fuelling	no fuelling	no fuelling	no fuelling	no fuelling	no fuelling	no fuelling	no fuelling	no fuelling	no fuelling	no fuelling
	50	16	75	75	75	75	75	70	70	70	70	70	no fuelling
	45	20	75	75	75	75	75	75	70	70	70	70	no fuelling
	40	24	75	75	75	75	75	75	70	70	70	70	no fuelling
	35	27	75	75	75	75	75	70	70	70	70	70	no fuelling
	30	28	75	75	70	70	70	70	70	70	70	70	no fuelling
	25	28	75	75	70	70	70	70	70	70	70	no fuelling	no fuelling
	20	28	75	75	70	70	70	70	70	70	70	no fuelling	no fuelling
	10	28	70	70	70	70	70	70	65	65	65	no fuelling	no fuelling
	0	28	70	70	70	70	65	65	65	60	65	no fuelling	no fuelling
	-10	28	70	70	70	65	65	65	65	60	no fuelling	no fuelling	no fuelling
	-20	28	70	70	65	65	65	60	60	60	no fuelling	no fuelling	no fuelling
	-30	28	70	65	65	65	65	60	60	55	no fuelling	no fuelling	no fuelling
	-40	28	65	65	65	65	65	60	60	55	no fuelling	no fuelling	no fuelling
	<-40	no fuelling	no fuelling	no fuelling	no fuelling	no fuelling	no fuelling	no fuelling	no fuelling	no fuelling	no fuelling	no fuelling	no fuelling

Figure 2.3: Lookup table for the average pressure ramp rate for a 1-7 kg A70 fuelling. The values in the table have been modified and are thus not the same values as in the SAE J2601.

the protocol assumes that the temperature inside the tank is the same as the ambient temperature. Further more, as the ambient temperature decreases, the final pressure decreases as the final temperature in the tank is going to be lower; hence, see Figure 2.2. With an increasing initial pressure, the final pressure decreases, and at temperatures below $-40°C$ or above $50°C$ and for some pressure/temperature combinations above 50 MPa, the vehicle can not be fuelled.

Depending on the vehicle and the station, the fuelling can proceed either with or without communication between the station and the vehicle. The fuelling without communication measures the pressure and the volume of the tank by sending an impulse of a known mass into the tank to measure the pressure increase. The fuelling is done following the tables from the protocol, and the fuelling finishes as the pressure at the exit of the station reaches the target pressure. This often results in under-filling of the tank, as the pressure in the vehicle tank is lower than at the exit due to pressure losses in the vehicle. Another contribution to under-filling is the gas temperature inside the tank that is higher than expected resulting in a lower density for the final pressure. If communication is present between the vehicle and the station, the vehicle can be fuelled to the reference density as the pressure and temperature of the vehicle are transmitted to the station. If either the pressure or the temperature reaches the maximum allowed limit, the fuelling can abort, before reaching a state of charge of 100%.

This thesis considers hydrogen fuelling of type "A70" as it is the most demanding fuelling protocol to meet, and if an "A70" fuelling can be done successfully,

the other protocols can also be met. Further more, the stations constructed today all aim to comply with an "A70" fuelling as it enables fuelling of all hydrogen vehicles. In Chapters 6 and 7 there is analysis for fuelling systems without communication and in Chapter 8 for fuelling systems with communication.

2.4 Hydrogen fuelling systems

This section explains how hydrogen fuelling systems are designed and operated. The first part contains information on how fuelling stations are made today with respect to the SAE J2601. The second part explains how hydrogen is stored at the station and gives an example on how it can be operated utilizing a large amount of hydrogen.

2.4.1 Hydrogen fuelling stations complying with the SAE J2601

Hydrogen fuelling stations complying with the SAE J2601 are in principal designed as the system shown in Figure 2.4. The hydrogen is stored in the cascade

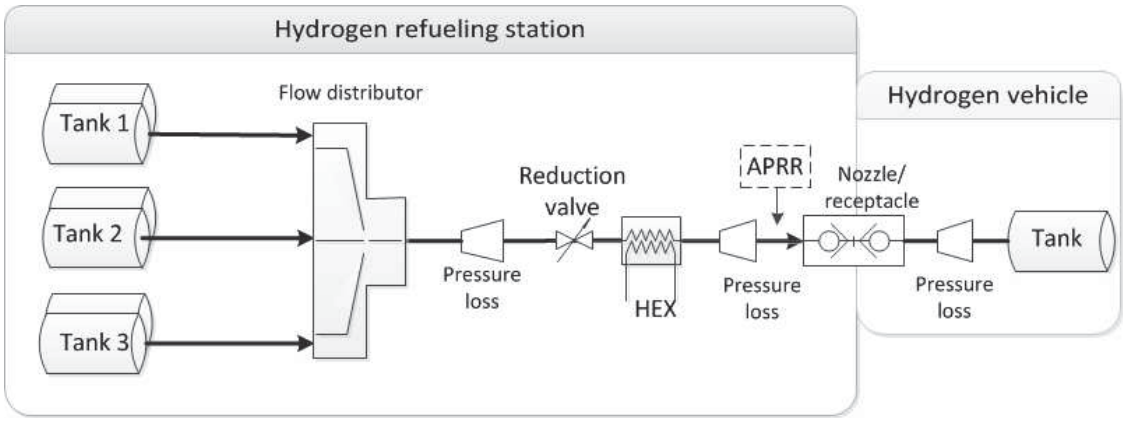

Figure 2.4: Sketch of the principles of a real hydrogen fuelling station complying with the SAE J2601.

system consisting of "tank 1", "tank 2" and "tank 3". The pressure of the tanks is typically between 400-600 bar for "tank 1", between 600-800 bar for "tank 2" and 900-1000 bar for "tank 3". The fuelling proceeds by levelling the pressure between the tank in the vehicle with tanks at the station, starting with the tank with the lowest pressure, and when the pressure across the reduction gets too low to keep the average pressure ramp rate, the station switches to the next tank in the cascade system. The average pressure ramp rate is maintained at the outlet of the station; this has the effect that the reduction valve needs to compensate for pressure losses between it and the outlet. The reduction valve

is controlled by measuring the pressure at the outlet of the station. Before the hydrogen leaves the station it needs to be cooled down. This is done in a heat exchanger placed after the reduction valve. The reason it should be placed after the reduction valve is that hydrogen heats up when throttled, and the protocol requires the hydrogen out of the station to have a precooled temperature at the exit of the station. Typically the hydrogen fuelling station is split up into two parts, a storage part and a dispenser part. The storage part consists of the cascade system and the related components, such as the compressor and bank as shown in Figure 2.1. The dispenser module typically consists of the heat exchanger, the pressure gauge for controlling the reduction valve and the nozzle for connecting to the vehicle. The reduction valve can be placed in either part of the system. It should be noted that this is a design question. Some fuelling stations have a separate dispenser module placed away from the rest of the station while others have everything in the same unit, and the different systems can not be distinguished by sight from the outside.

2.4.2 Hydrogen supply and storage

Storing hydrogen at a fuelling station is done at low pressures compared to the target pressure in a vehicle fuelling. The hydrogen is typically stored at 200 to 300 bar in steel cylinders that are either filled externally and then trucked to the facility or an on-site electrolysis facility delivers hydrogen at 10 to 20 bar which is compressed to 200 to 300 bar. The storage for a station with hydrogen trucked in has to be larger than for a station with continuous on-site production, as the continuous on-site production can cover the demand partly or fully. Today's hydrogen fuelling stations usually have hydrogen trucked to the station at high pressure from time to time, although some of the facilities have on-site electrolysis for hydrogen production but the production is typically lower than the demand for fuelling vehicles. An example of hydrogen storage at a fuelling station could be as follows. A bundle of tanks are delivered at 300 bar. The fuelling station empties the tanks to a pressure of 200 bar. From a compression point of view, it would then be energy-wise to split up the bundle into two: one used for recovering the fuelling station cascade system and one used to maintain the pressure in the storage; see Figure 2.5. In this way the hydrogen utilization for the storage is enhanced. The following example explains the principle in more detail. A $100m^3$ storage at 300 bar is delivered to a fuelling station. The storage contains approximately 360 kg of hydrogen stored between 200 and 300 bar; this corresponds to more than 60 vehicle fuellings. When the storage reaches 200 bar $90m^3$ is dismantled and used as supply for the other 10 m^3. The 10 m^3 is then kept at a pressure of 200-300 bar while the 90 m^3 decreases in pressure as it fills up the 10 m^3. If the minimum pressure allowed in the 90 m^3 to supply the 10 m^3 is 40 bar, there is another 632 kg of hydrogen available corresponding to more than 100 fuellings. In total the 100 m^3 of delivered hydrogen can fuel more than 160 vehicles. The volume

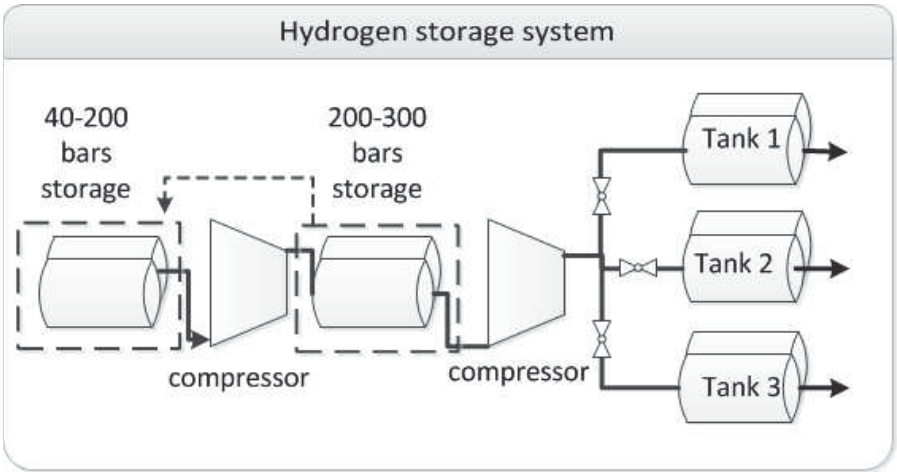

Figure 2.5: The storage system of a hydrogen fuelling station.

of the storage and the total mass are proportional, so if the volume decreases with 50 % the total mass decreases accordingly. For 25 m^3 of delivered storage, approximately 40 vehicles can be fuelled. This is only valid for stations without on-site production, as the on-site production increases the capacity and if the capacity is large enough, trucked in hydrogen is eliminated.

In this study the hydrogen supply is not considered, and the analysis in the later chapters assumes that hydrogen stored at between 200-300 bar is available at the station.

Chapter 3

Component model formulation

This chapter explains the fundamental mathematical equations used for the main component models that are implemented in Dymola, which is an software built with the Modelica language. The chapter provides a background to the model formulation and theory, necessary for the further investigations of hydrogen fuelling stations. The chapter works as documentation of the modelling formulation.

3.1 Introduction

The object of the modelling is to predict the behaviour of hydrogen during a fuelling process to a tank storing high-pressure gaseous hydrogen at temperatures between $-40°C$ to $85°C$. The model can handle pure fluids. The model is capable of handling mass flows, pressure drops and energy changes. The equations chosen are based on real gas equations. The approach for pressure drop models has been chosen on the basis of equations used by industrial partners and component manufacturers. Pressure drops cover tubing, mass flow meters, filters and valves, including the control valves of the system. The models for energy balances are based on the first law of thermodynamics. Mass conservation is applied to all models, assuring mass balance throughout the calculations of a hydrogen fuelling. The tank in the vehicle and the tanks at the stations are dynamic so that they model the hydrogen migration between them. The

heat transfer is also modelled dynamically, taking into account the change of hydrogen properties as heat dissipates through the walls. Quasi-static model formulations are used for the pressure losses and the compressor.

The chapter describes all the mathematical models. For each model there is a short introduction followed by general information and properties of the component and then the model description. Focus is on the tank models with 1-dimensional transient heat transfer. The chapter provides a basic understanding of the pressure losses, the compressor and heat exchanger.

3.2 First principles

The component models used for the simulation of hydrogen fuelling systems are based on the first law of thermodynamics, Newton's second law for force and the mass-conservation statement. The three laws are used for energy balance, momentum balance and mass balance, respectively. The first law of thermodynamics is stated in eq. 3.1.

$$\begin{aligned}\frac{dE}{dt} = Q - W + \frac{d}{dt}(m(u + \frac{V^2}{2} + gz)) \\ + \sum(\dot{m}(h + \frac{V^2}{2} + gz))_{in} \\ - \sum(\dot{m}(h + \frac{V^2}{2} + gz))_{out}\end{aligned} \tag{3.1}$$

For all the components it has been assumed that the gravitational potential energy is neglected, and the kinetic energy is simplified through compressible gas flow relations. The gravitational potential energy has been neglected as there is no significant difference in height. The kinetic energy is included in the enthalpy as the specific stagnation enthalpy has been used throughout the system; see Section 3.3 for further explanation. This leaves us with the energy balance for an open system, where the specific enthalpy is the stagnation enthalpy.

$$\frac{dE}{dt} = Q - W + \frac{d(m \cdot u)}{dt} + \sum(\dot{m}h)_{in} - \sum(\dot{m}h)_{out} \tag{3.2}$$

For steady state which is used in the quasi static models, the change of energy is zero, hence $dE/dt = 0$. Newton's second law states that the change of momentum can be expressed through change in pressure as shown in eq. 3.3.

$$\sum F = A_1 \frac{p_1}{dt} - A_2 \frac{p_2}{dt} \tag{3.3}$$

Where $A_1 = A_2$ and knowing that $p = F/A$, the momentum balance yields a pressure difference.

$$dp = p_1 - p_2 \tag{3.4}$$

The mass balance which originates from the first law of thermodynamics states that the change in mass for an open system is

$$\frac{dm}{dt} = \sum \dot{m}_{in} - \sum \dot{m}_{out} \tag{3.5}$$

In general eqs. 3.2, 3.4 and 3.5 are present for all the models. The guideline for drawing the control volumes of the components is that only the energy contributions from eq. 3.2 which are possible are included. If there is no volume, the internal energy is not included, while heat and work contributions are included, but not necessarily present for the component.

3.3 Compressible gas flow relations

The compressible gas flow relation considers two kinds of enthalpy and kinetic energy. The two kinds of enthalpies are stagnation or total enthalpy and static enthalpy. The stagnation enthalpy (h) is the static enthalpy of the stream (h_s) added with the kinetic energy of the stream [8] .

$$h = h_s + \frac{1}{2}v^2 \tag{3.6}$$

The kinetic energy is included in the stagnation enthalpy. Figure 3.1 shows a very simple hydrogen system with the respective enthalpies and velocities. The

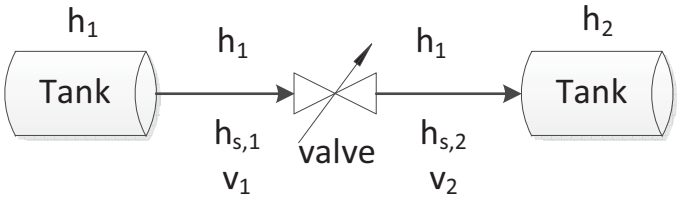

Figure 3.1: A simple system with mass flow from left to right. Both the stagnation enthalpy and the static enthalpy are shown.

specific stagnation enthalpy in the high-pressure tank is $h = h_s + 0.5v^2$ but as the velocity is negligible $h = h_s$. The specific enthalpy flow out of the tank is assumed to be the stagnation enthalpy. The valve uses the stagnation enthalpy at the inlet and outlet, and thereby includes the kinetic energy. In the receiving low-pressure tank the stagnation enthalpy is entering and used for the energy balance; hence, it is assumed that all kinetic energy is transformed to enthalpy

once inside the tank as the velocity is assumed to be zero. The set of energy balance equations for the figure is thus in the tank $h = h_s$ out of the tank $h_1 = h_{s,1} + 0.5v_1$ and after the valve $h_1 = h_{s,2} + 0.5v_2$. In the receiving tank the change in specific enthalpy is $dh_2/dt = 1/M(\dot{m}h_1)$. Thus the real specific enthalpies and velocity change across the valve, but the stagnation enthalpy is the same.
Using the stagnation enthalpy instead of the static enthalpy can cause a difference in the thermodynamic properties of the hydrogen if the kinetic energy composes a significant part of the stagnation enthalpy, though in this thesis it never composes more than 2% during a hydrogen fuelling. Thus, the difference between using static or stagnation enthalpy is negligibly small.

3.4 Tank

This section covers the modelling of the tanks with first an introduction with some general information about hydrogen tanks and then an explanation the modelling theory.

3.4.1 Tank types for storing hydrogen

There are four different types of tanks for storing hydrogen; they are categorized as Type I, Type II, Type III and Type IV. As a general rule of thumb, the higher the type number, the higher pressure it is capable of storing and the more expensive the tank. Type I is made of stainless steel and can typically handle 200-350 bar pressure, but it has been made for pressures up to 500 bar. Type II is made from aluminium, it is lighter than Type I and can handle the same pressures. Type III is a composite tank, made with a thin aluminium liner wrapped in carbon fibre. It is lighter than Type I and Type II and can store hydrogen at pressures up to 1000 bar. Type IV is a composite tank with a plastic liner wrapped in carbon fibre, it is lighter than the other three types and can withstand pressures up to 1000 bar. Type I and II tanks are typically applied for hydrogen storage when pressures are below 350 bar and weight is not an issue, e.g., as buffer tanks at the hydrogen fuelling station or as lower pressure tanks in a cascade fuelling system. Type III and IV are used when the pressures exceed the limitations of Type I and II and when weight is an important parameter, e.g., high-pressure tanks in a cascade fuelling system and tanks used in the vehicle's storage system.

3.4.2 Tank model

Figure 3.2 shows the control volume around a tank. The walls are in-compressible and no work is done to the tank, therefore $W = 0$. The momentum balance is $p = p_1 = p_2$ so that the pressure into the tank is the same as in the tank; hence,

there is no pressure loss at the entrance. The thermal boundary condition for

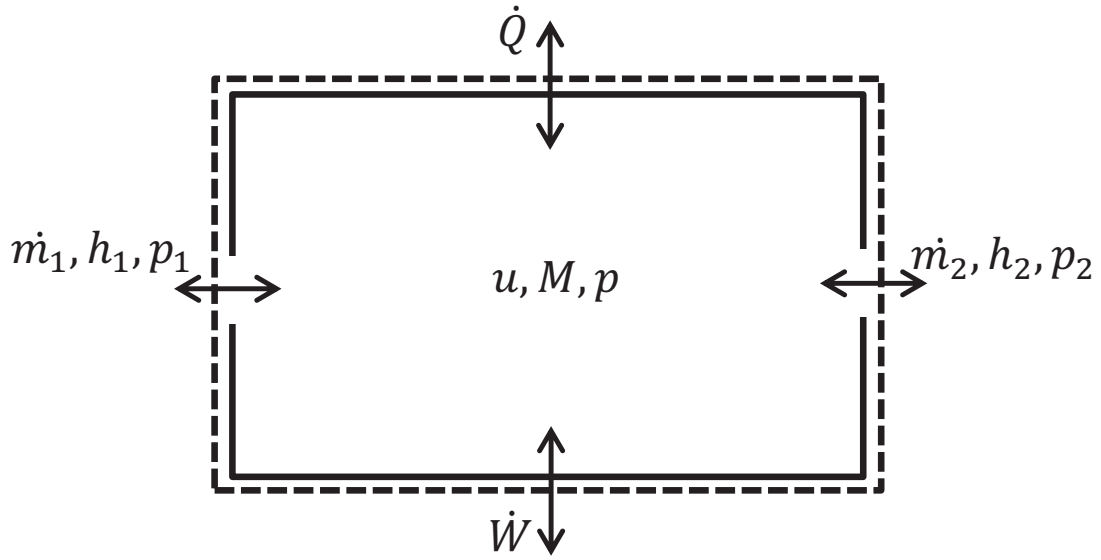

Figure 3.2: A tank with the defined control volume, there are two entrances into the tank where mass can enter or exit.

the actual tank is defined by the heat exchange with the surroundings, but the general tank model is adiabatic with the possibility of adding heat transfer. The mass balance for the control volume is

$$\frac{dM}{dt} = \dot{m}_1 + \dot{m}_2 \tag{3.7}$$

Introducing $M = V * \rho$ and assuming a constant volume of the tank, eq. 3.7 can be expressed as

$$V\frac{d\rho}{dt} = \dot{m}_1 - \dot{m}_2 \tag{3.8}$$

The thermodynamics of the tanks can be stated from the first law of thermodynamics for an open system without any work added. The energy balance for one tank is the change in internal energy as mass leaves or enters the tank and the heat dissipation through the tank wall. The change in internal energy can be found from eq. 3.9.

$$\frac{dU}{dt} = h_1\frac{dm_1}{dt} + h_2\frac{dm_2}{dt} + \frac{dQ}{dt} \tag{3.9}$$

where dU/dt is the change in internal energy of the system h_1 and h_2 is the enthalpy leaving or entering the tank at each opening, dm/dt is the mass flow rate and dQ/dt is the heat rate entering or leaving the system, where entering

is considered positive. Using the rewriting from the mass balance to eq. 3.9, $U = Mu = V\rho u$ gives

$$V\frac{d\rho u}{dt} = h_1\frac{dm_1}{dt} + h_2\frac{dm_2}{dt} + \frac{dQ}{dt} \tag{3.10}$$

Two different rewritings of eq. 3.10 have been used in the simulations. The first expresses the energy balance through internal energy with time derivatives of pressure and enthalpy and partial derivatives of density. The second rewriting is into enthalpy change in the tank, but also with time derivatives of pressure and enthalpy.

Internal energy

Introducing $u = h - pv$, the internal energy inside the tank where $v = \rho^{-1}$ can be described through derivatives of enthalpy and pressure [17].

$$\frac{dU}{dt} = V(\rho\frac{dh}{dt} + h\frac{d\rho}{dt} - \frac{dp}{dt}) \tag{3.11}$$

where h and P are the enthalpy and the pressure in the tank, and ρ is the density. V is the volume of the tank. The time derivative of ρ can be expressed through the derivative of enthalpy and pressure

$$\frac{d\rho}{dt} = \frac{\partial\rho}{dp}|_h \cdot \frac{dp}{dt} + \frac{\partial\rho}{dh}|_p \cdot \frac{dh}{dt} \tag{3.12}$$

Enthalpy

Rewriting and substituting internal energy with enthalpy $u = h - pV$ into eq. 3.13 gives

$$\frac{dh}{dt} = \frac{1}{M} \cdot (h_1\frac{dm_1}{dt} + h_2\frac{dm_2}{dt} + V\frac{dp}{dt} + \frac{dQ}{dt}) \tag{3.13}$$

The two different expressions of the conservation of energy give the same results, but rewriting the equation in terms of enthalpy instead of internal energy enables the possibility of flow in both directions using the same model of a tank. Using internal energy, the flow of the hydrogen is defined by the model formulation which uses either the enthalpy of the tank (mass flow from the tank) or the mass flowing into the tank; hence, the tank can only operate with flow in one direction during a simulation. The formulation using enthalpy enables the possibility of changing the flow during a simulation, and only one tank model is needed as it can both receive and release hydrogen.

3.5 Heat transfer model

The main heat transfer formulation used in the thesis is conduction through a wall. This formulation is valid for both the tanks which store the hydrogen

and for the tubes in which the hydrogen flows. For both the tanks and the tubes the heat transfer is unsteady. In the tanks the temperature changes due to the heat of compression or expansion as the hydrogen flows to or from the tanks. For the tubes the hydrogen changes temperature as it flows through the tube. The second observation concerns whether or not a lumped model or a 1-dimensional model of the heat conduction should be used. Studying the tanks used for high-pressure hydrogen storage, one sees they are made of composite material with low heat conduction properties and that the walls are thick. From experiments at Saga University, the thermal conductivity of the liner and carbon fibre wrapping of the tanks have been measured and the properties are shown in Table A.1 in Chapter 4. For the tube the Biot number was calculated, and it showed that a lumped model is insufficient. Therefore a 1-dimensional model is necessary for both the tank and the tube model.

3.5.1 1-dimensional unsteady heat transfer

The heat transfer through the tank is assumed to be 1-dimensional unsteady heat conduction (the temperature of the gas changes when gas is leaving or entering the tank). Figure 3.3 shows the control volume around the walls setting the heat exchange with the surroundings on each side as the boundary conditions. The general heat equation and the boundary conditions of heat

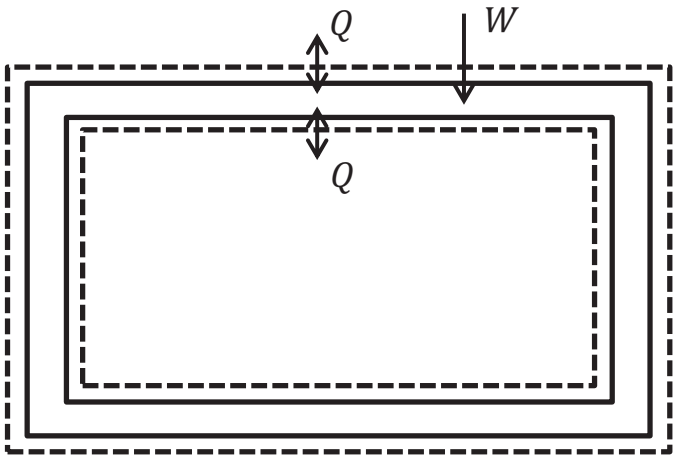

Figure 3.3: A control volume around the wall of a tank, the only exchange of energy to the wall from the surroundings is heat.

exchange through the wall are given in eqs. 3.14, 3.15 and 3.16.

$$\frac{d^2T_s}{\partial x^2} = \frac{1}{\alpha}\frac{\partial T_s}{dt} \tag{3.14}$$

$$k\frac{dT_w}{dx}|_{x=0} = \alpha_g(T_g - T_w|_{x=0}) \tag{3.15}$$

$$k\frac{dT_w}{dx}|_{x=L} = \alpha_a(T_w|_{x=L} - T_a) \tag{3.16}$$

where T_w is the wall temperature, T_g the gas temperature in the tank and T_a the air temperature outside the tank. k is the thermal conductivity, and α_g and α_a are the heat transfer coefficients of the gas in the tank and the air outside the tank, respectively. A numerical solution to eq. 3.14 can be obtained with a capacitance resistance method which corresponds to a finite small-volume analysis [18]. A node system can be defined with i as the subscript identifying a node where the heat transfer occurs, Figure 3.4. Assuming a uniform tempera-

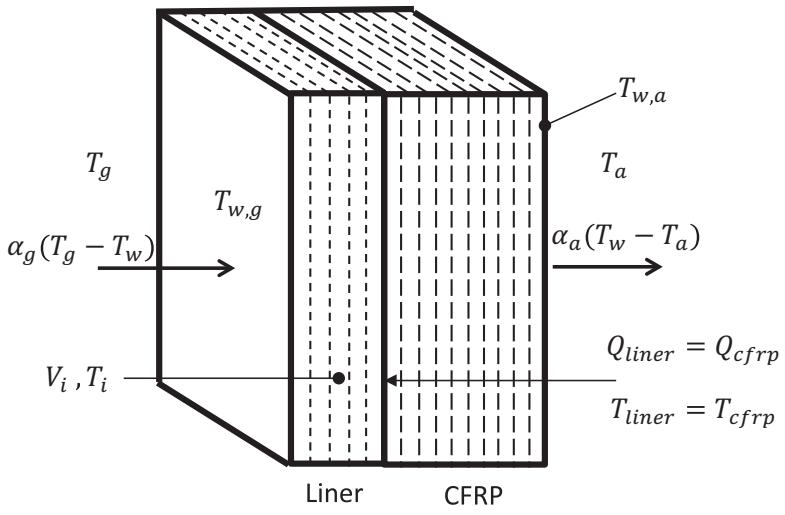

Figure 3.4: Diagram of heat transfer through a wall section

ture distribution, and a wall acting like a plain wall, the resistance capacitance method can be applied to the hydrogen tank using eqs. 3.17 and 3.18.

$$Q_{A,i} = \sum_j Q_{k,i-j} = (Q_k)_{i,\ i-1} + (Q_k)_{i,\ i+1} \tag{3.17}$$

and

$$Q_{A,i} = (\rho c \Delta V)_i \frac{dT_i}{dt} + \dot{s}_i \Delta V_i \tag{3.18}$$

where the subscript i is the node where the temperature is calculated, and $\dot{s}_i$ is the rate of surface energy conversion. The resistance capacitance method simplifies the partial differential eq. 3.14 into an ordinary differential equation,

eq. 3.18. The heat transfer $(Q_k)_{i\ to\ i-1}$ and $(Q_k)_{i\ to\ i+1}$ can be found from eqs. 3.19 and 3.20.

$$Q_{k,i-j} = \frac{T_i - T_{i-1}}{R_{i,\ i-1}} \tag{3.19}$$

$$Q_{k,i+j} = \frac{T_i - T_{i+1}}{R_{i,\ i+1}} \tag{3.20}$$

where R is the thermal resistance of the volume, $R = dx/(Ak)$. The boundary conditions for eqs. 3.17 and 3.18 are given by eqs. 3.21 and 3.22.

$$\frac{dT_i}{dx}|_{x=0} = \frac{\alpha_g}{k}(T_g - T_i|_{x=0}) \tag{3.21}$$

$$\frac{dT_i}{dx}|_{x=L} = \frac{\alpha_a}{k}(T_i|_{x=L} - T_a) \tag{3.22}$$

Equations 3.19 and 3.20 are linked to the temperature change in time through eq. 3.23.

$$Adx\rho * \frac{dT_i}{dt} = Q_{k,i-j} + Q_{k,i+j} \tag{3.23}$$

where A is the area of the tank, dx the thickness of the tank layer considered, ρ the density of the material and dT_i/dt the change of temperature over time at the point.

Tank

For filling a hydrogen tank there is no known mathematical correlation between the tank design and the heat transfer coefficient. The heat transfer coefficient depends on the tank design, the mass flow rate into the tank and the nozzle at the inlet. The heat transfer coefficient for a specific tank design can be estimated using CFD software. For deciding the heat transfer coefficient in the tank, several experiments have been carried out and they show that the heat transfer coefficient α_g varies between $150W/(m^2K)$ and $500W/(m^2K)$ [27] [38]. For emptying a tank, experiments have shown that Daney's correlation gives an acceptable approximate value [38]. Nusselt's number for Daney's correlation is given by eq. 3.24 [6].

$$Nu = 0.104Ra^{0.352} \tag{3.24}$$

where the Rayleigh number (Ra) is given by eq. 3.25.

$$Ra = \frac{g\beta(T_w - T_g)d^3}{va} \tag{3.25}$$

where g is gravity, β is the thermal expansion coefficient, d is the inside diameter of the tank, v is the dynamic viscosity of the gas and a the thermal diffusivity which is $a = k/(\rho c_p)$, the thermal conductivity (k) divided by the density (ρ)

and the specific heat capacity c_p. The outer tank wall is in contact with the ambient environment, and the heat transfer coefficient for the outside surface of the tank depends on different parameters, such as air flow, direction of the cylinder and if it is free or forced convection. The tanks are typically stored inside or on top of the station, where natural convection is common. The heat transfer coefficient is thus typically between $5W/(m^2K)$ and $30W/(m^2K)$ depending on the conditions.

Tubes

Hydrogen flowing through the tubing conducts heat through the tube wall. The heat transfer between the hydrogen and the wall is forced convection as the flow is turbulent. The heat transfer number is found from the following set of equations [15].

$$\alpha = \frac{Nu \cdot k}{d_h} \tag{3.26}$$

$$Nu = 0.023 Re^{4/5} * Pr^{0.3} \tag{3.27}$$

$$Pr = \frac{c_p \mu}{k} \tag{3.28}$$

$$Re = \rho \frac{\dot{V}}{A_{cross}} \frac{d_h}{\mu} \tag{3.29}$$

where α is the local heat transfer coefficient, Nu is Nusselt's number, Pr is Prandtl's number which is a property parameter and Re is Reynolds number. d_h is the hydraulic diameter, k is the thermal conductivity coefficient, c_p the specific heat, μ the viscosity, $\dot{V}$ the volume flow, ρ the density and A_{cross} the cross-sectional area of the tube. The heat transfer coefficient for the outside of the tube may be approximated using the same value as for the outside of the tank.

3.6 Pressure losses

This section covers the different components which cause pressure losses when hydrogen flows through. The pressure losses considered are either general pressure loss equations or equations given by manufacturers. Pressure losses in hydrogen fuelling stations are not different from pressure losses of any other gas flow system. The components used are the same as for other high-pressure systems.

3.6.1 General pressure loss model

There are three different pressure loss components which have the same energy and mass and momentum balance, but the final equation for calculating the pressure loss is different. Figure 3.5 shows a pressure loss with a control volume drawn around it. In the pressure loss components, there is no work

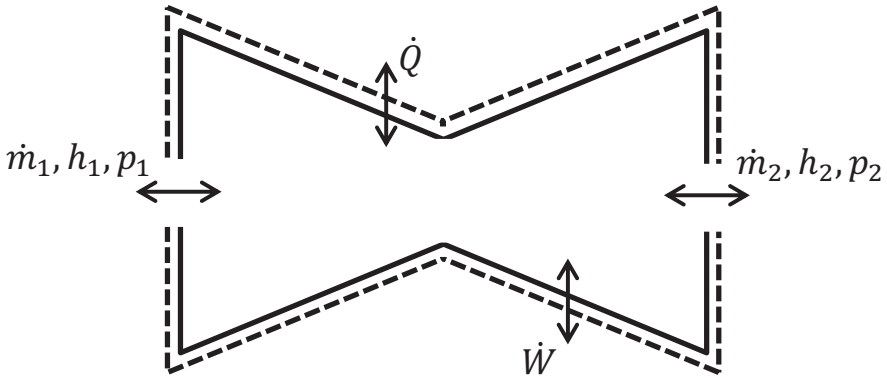

Figure 3.5: Control volume around a pressure loss

added ($W = 0$) and the process is adiabatic ($Q = 0$). The mass entering the component must be the same as the mass leaving ($\dot{m}_1 + \dot{m}_2 = 0$) and the enthalpy is constant ($h_1 = h_2$). The momentum balance yields a pressure difference $dp = p_1 - p_2$, where dp is the pressure loss for each component. The changes when hydrogen undergoes a negative change in pressure are the pressure and the properties of the hydrogen. As the enthalpy is constant across the components and the pressure changes, the hydrogen changes temperature, density, etc. When hydrogen is throttled, the temperature increases due to the Joule-Thomson effect, which has a negative coefficient for hydrogen. Unlike most gases, hydrogen heats up when throttled at temperatures higher than 200 K. The difference in temperature is approximately $0.04°C$ per 1 bar pressure drop. Figure 3.6 shows the Joule-Thomson coefficient for hydrogen. During hydrogen fuelling the Joule-Thomson coefficient is within the window called the HRS range.

3.6.2 Valves

The pressure loss through a valve is calculated in different ways depending on the type of valve and the information which can be obtained from the manufacturer. Valves without information on their pressure loss constant can typically be calculated as a length equivalent pressure loss using the formulation for pressure loss through a tube. If the pressure loss constant (k_v) of a valve is known, a more precise pressure loss calculation can be obtained using the

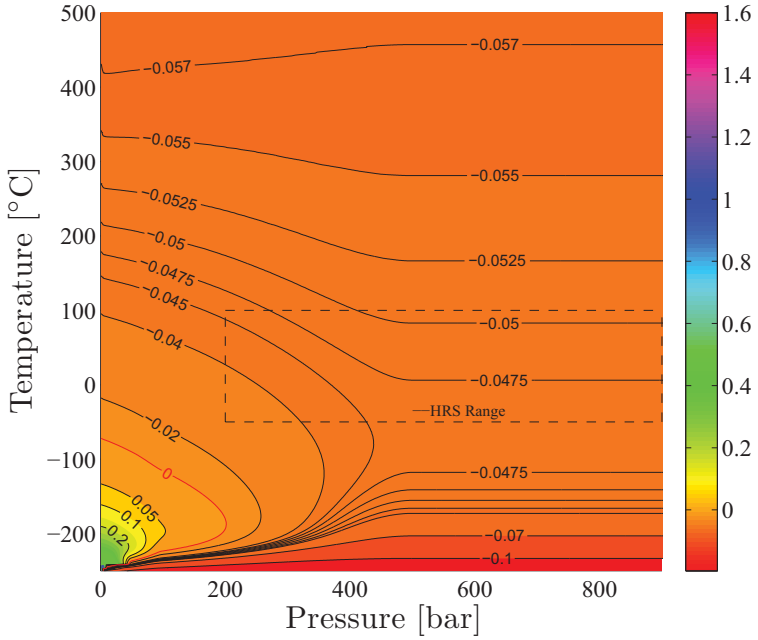

Figure 3.6: The Joule-Thomson coefficient for hydrogen as a function of pressure and temperature [16].

following equation [4].

$$\Delta p = \frac{\rho}{\rho_w (\frac{k_v}{\dot{V}})^2} \tag{3.30}$$

where k_v is the pressure loss constant, and the lower the pressure loss constant is, the higher the pressure loss. The density of water ρ_{water} is found for water at $15°C$. k_v is given for water and therefore the ratio between the hydrogen density and the water density is present. In eq. 3.30 $\dot{V}$ is in m^3/h and the pressure loss is in bars.

3.6.3 Filter and mass flow meter

Pressure losses in mass flow meters and filters in the system are calculated differently from pressure drops for valves. The pressure drop depends on a pressure loss constant k_p and the cross-sectional area in the mass flow meter or filter; as the cross-sectional area is constant the pressure loss constant can be obtained from the manufacturer. Equation 3.31 gives the pressure loss through a component with a constant cross-sectional area and a given pressure loss constant [20].

$$\Delta p = 0.5 k_p \rho \dot{V}^2 \tag{3.31}$$

The volume flow rate ($\dot{V}$) is in m^3/h and the pressure loss in bars. The higher the pressure loss constant in eq. 3.31 the higher the pressure loss, and if the

mass flow is increased by a factor of two, the pressure loss increases by a factor of four.

3.6.4 Tube and length equivalent pressure losses

Pressure losses in the tubing and in components that are not covered by eqs. 3.30 and 3.31 can be found using the general pressure loss equation. The pressure loss depends on the friction factor and the length to diameter ratio. Pressure losses such as bends or ball valves are given in length equivalent. The pressure loss for tubes is given by eq. 3.32.

$$\Delta p = (f\frac{L}{d} + k)\frac{\rho v^2}{2} \tag{3.32}$$

where k is the length equivalent of a component; for a straight tube $k = 0$, but if there is a bend or a valve, the approximate length equivalent value can be added. The length equivalent factor also enables the possibility to add many pressure losses together by just adding another pressure loss equivalent to eq. 3.32. Length equivalent values for different pressure losses can be found in textbooks. The friction factor f is given by eq. 3.33.

$$f = (-1.8log((\frac{6.9}{Re}) + (\frac{3.7r}{d})^{1.11}))^{-2} \tag{3.33}$$

The friction factor is a function of Reynolds number (eq. 3.29), the roughness of the tube and the diameter. The roughness r depends on the material of the tube and should be given by the manufacturer, or approximate values can be found in textbooks.

3.7 Compression of hydrogen

This section covers the compression of hydrogen. The equations used are real gas equations, and the efficiencies are found by general first estimate equations as efficiency curves for compressors are dependent on the type of compressor, the design of the compressor and the manufacturer. General first estimate equations have therefore been chosen in order to make general considerations.

3.7.1 Compressors used for hydrogen

How to compress hydrogen is an on-going discussion and several traditional compressor types are on the market while new compression technologies are undergoing extensive research. The main concerns for hydrogen compression are the explosion danger and the leakage of hydrogen through gaskets. Therefore hydrogen compressors have to be explosion-secure and the gaskets need

to be specifically tested with hydrogen in order to make sure there is no leakage. The range of compressor types that is used for hydrogen compression is extensive. There are three overall categories of hydrogen compressors, each of which contains several different compressor types. The list below shows the subdivision of the compressors in the three main categories.

- Positive displacement compression
  - Reciprocating compressors
  - Membrane/diaphragm compressor
  - Ionic liquid compressor
  - Cryo pump
- Dynamic compression
  - Centrifugal compressor
- Thermal and electrochemical methods
  - High-pressure electrolysis
  - Electrochemical compressor
  - Metal hydride compressor

The above list does not cover all the compressors that are used in hydrogen fuelling stations. The most common compressor type is the positive displacement compressor, which works by decreasing a closed volume with hydrogen in order to compress it. The main differences between them are that a reciprocating compressor uses a moving piston in a cylinder, the membrane uses a fixed membrane with hydrogen on one side and an incompressible liquid on the other side, and the pressure on the membrane is pushing the membrane towards the hydrogen decreasing the area of the hydrogen volume. An ionic liquid compressor is in-between the reciprocating and the membrane compressor. It pumps an incompressible ionic liquid into a cylinder which contains hydrogen, hence like the membrane compressor without the membrane. The volume of the hydrogen in the cylinder is decreased by the liquid, hence a fluid piston. The hydrogen cannot dissolve into the liquid. The positive displacement compressors can be used for pressures of more than 1000 bar. The cryo-pump uses liquid hydrogen which it turns into high-pressure hydrogen using a pump with liquid at the suction side and gas at the discharge side; the gas is then heated to the desired temperature and pressure. The centrifugal compressors are typically used for compressing to medium pressure, 500 bar. The thermal and electrochemical compression methods are still under on-going research and have not yet been seen in hydrogen fuelling stations. The high-pressure electrolysis compression produces high-pressurized hydrogen by electrolysing water at high pressures. An electrochemical compressor uses a membrane to split the hydrogen using

electricity to transport the proton through the membrane before merging with the negative loaded hydrogen atom at high pressure. A metal hydride compressor absorbs hydrogen at low pressure and temperature, and then afterwards it is thermally heated releasing the hydrogen at a higher pressure. It is beyond the scope of this thesis to discuss the compression methods thoroughly and do comparisons; therefore a more general approach has been made. The two compression methods included are reciprocating compression and centrifugal compression. The equation used might also be valid for other types of compressors but this is not verified.

3.7.2 Compressor model

The compressors considered are either reciprocating or centrifugal; for the reciprocating compressors the heat loss is dependent on the type and manufacture, but it is typically 5% or less; the compression has therefore been assumed adiabatic. Figure 3.7 shows the control volume around a compressor. There

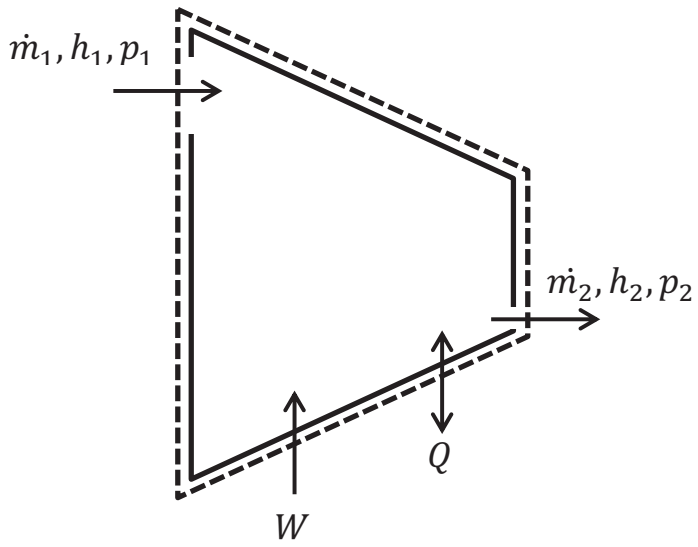

Figure 3.7: Control volume around a compressor.

is a mass balance through the compressor ($m_1 + m_2$=0), the compression is adiabatic ($Q = 0$), and there is work done on the hydrogen in the compressor corresponding to

$$W = \dot{m}(h_{out} - h_{in}) \tag{3.34}$$

The pressure at the discharge side of the compressor is naturally higher than at the inlet so the momentum balance yields the pressure difference $dp = p_1 - p_2$, where dp is the pressure increase from the compression. In order to find the enthalpy out of the compressor, the mass flow and the discharge pressure need

to be known. The mass flow of the compressor is calculated defining the volume of the cylinders (V_{cyl}), piston strokes per second (n) and a defined function for the volumetric efficiency η_v.

$$\dot{m} = V_{cyl} \cdot \rho_{in} \cdot \eta_v \cdot n \tag{3.35}$$

The volumetric efficiency is highest at a low-pressure ratio across the compressor and decreases close to proportional as the pressure ratio increases. For this model the volumetric efficiency has the highest efficiency of 90% at a pressure ratio of one, and it is decreasing with 5% per increased pressure ratio across the compressor. The energy balance of the compressor is the energy flow into the compressor, the energy flow out of the compressor and the work added in the compressors shown in eq. 3.34. Depending on the type of compressor, the enthalpy out can be found from either an isentropic efficiency or a polytropic efficiency estimate. The enthalpy of the discharge of the compressor is found from eq. 3.36.

$$h_{out} = \frac{h_{out,\eta} - h_{in}}{\eta} - h_{in} \tag{3.36}$$

where η is the isentropic or polytrophic efficiency and $h_{out,\eta}$ is the enthalpy for an isentropic or polytrophic compression.

Isentropic compression

The isentropic efficiency is used when considering reciprocating compressors. A first general estimate of the isentropic efficiency is given by eq. 3.37 [36].

$$\eta_{is} = 0.1091 \cdot log(\frac{p_{out}}{p_{in}})^3 - 0.5247 \cdot log(\frac{p_{out}}{p_{in}})^2 + 0.8577 \cdot log(\frac{p_{out}}{p_{in}}) + 0.3727 \tag{3.37}$$

where p_{in} is the suction pressure and P_{out} is the discharge pressure. Equation 3.37 is valid in the range $1.1 < \frac{P_{out}}{p_{in}} < 5$. The pressure ratio never exceeds 5 in the calculations.

Polytropic compression

The polytropic efficiency is used when considering centrifugal compressors. The polytropic efficiency is different from the isentropic efficiency as it is a function of the volume flow rate. Typically the polytropic efficiency has very little variation for a compressor. An estimate of the polytropic efficiency can be found from eq. 3.38[36].

$$\eta_{poly} = 0.017 * log(\dot{V}) + 0.7 \tag{3.38}$$

where $\dot{V}$ is the volume flow of hydrogen.

3.8 Energy balance models

The following section considers different types of components that have not yet been described. The components include heat exchangers, flow mixers and the exergy equations.

3.8.1 Heat balance model

The model of the heat exchanger is done as a heat balance equation transferring all the heat from one side to another. The only thing that is calculated is the cooling capacity needed for the hydrogen to reach the desired temperature. This simple approach has been chosen although other projects at DTU have worked with the refrigeration of high-pressure hydrogen; however they are confidential and thus cannot be included in the thesis. Further more, the inclusion of a total refrigeration facility would be extensive and beyond the scope of this thesis. The cooling capacity is calculated by eq. 3.39.

$$Q = \dot{m}(h_{in} - h_{out}) \tag{3.39}$$

where Q is the cooling demand.

3.8.2 Mixer models

The mixers are components with three connections allowing two streams to meet into one or splitting one stream into two. Figure 3.8 shows the control volume around a mixer. There are two different kinds of mixers: ideal mixing in a point and ideal mixing in a volume. Ideal mixing in a point mixes the streams in a black box, only considering the mass flow in and out, the enthalpy in and out and the pressure. The ideal mixing in a volume considers the mixing inside a small volume which corresponds to a tank with three entrances or exits.

Ideal mixing without a volume

The mass balance of the streams entering the mixer is $m_1 + m_2 + m_3 = 0$. The pressure of the streams must be the same $p_1 = p_2 = p_3$. The energy balance for the mixer is as from eq. 3.40.

$$dE/dt = \dot{m}_1 h_1 + \dot{m}_2 h_2 + \dot{m}_3 h_3 \tag{3.40}$$

The mixer is described by the mass, energy and momentum balances for the three flows.

Ideal mixing with a volume

The mixer with a volume corresponds to a tank with three entrances. The difference between the described tank model and the mixer with a volume is

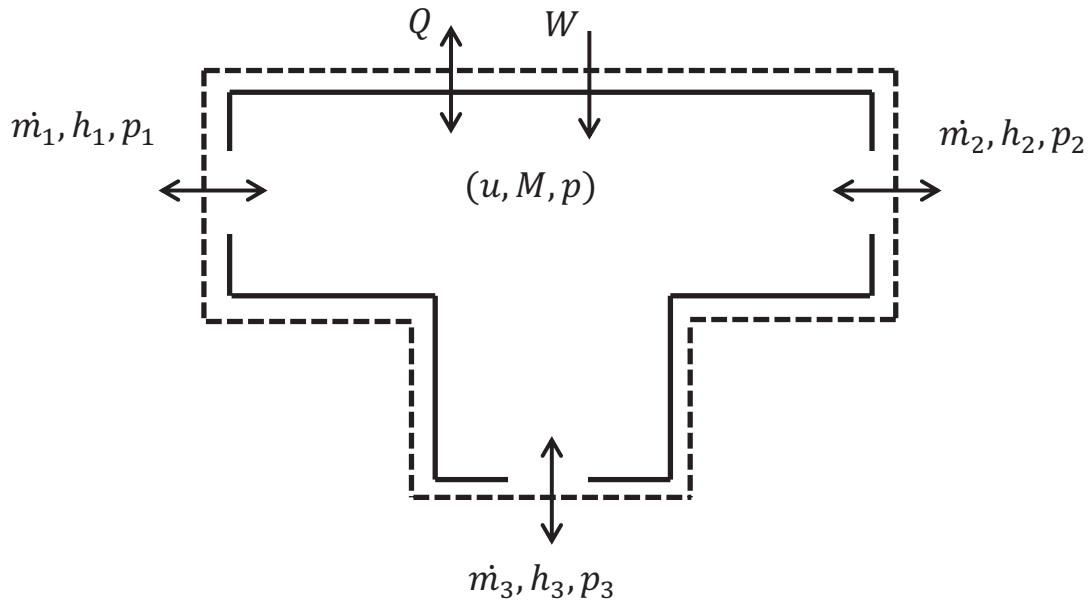

Figure 3.8: Control volume around a mixer.

found in the mass balance eq. 3.8 and the energy balance eq. 3.13. The mass and the energy balance equation for three entrances is given by eq. 3.41 and eq. 3.42, respectively.

$$V\frac{d\rho}{dt} = \dot{m}_1 + \dot{m}_2 + \dot{m}_3 \tag{3.41}$$

$$\frac{dh}{dt} = \frac{1}{M} \cdot (h_1\frac{dm_1}{dt} + h_2\frac{dm_2}{dt} + h_3\frac{dm_3}{dt} + V\frac{dp}{dt}) \tag{3.42}$$

The equation for the derivative of density is the same as eq. 3.12. The volume of the mixer is considered very smal;l thus heat transfer has been neglected. The pressures at the port and in the mixer are all the same, $p = p_1 = p_2 = p_3$.

3.9 Energy optimization

The optimization of hydrogen fuelling stations with respect to energy usage can be done in different ways. Studies of different parameters, such as the number of tanks in the fuelling stations cascade system, the pressure in the tanks and the volume of the tanks, can outline the best setup of the station. The energy savings obtained in the compressor and heat exchangers by adding another tank or changing the pressure or volume can be directly found, and the trade-off between investment cost and running costs can be used to find the best setup for the manufacturer of the station. Another way to optimize

a system is to perform an exergy analysis on the fuelling system. The exergy analysis reveals the components with the largest destruction of energy.

3.9.1 Exergy

Exergy is a way to express the quality of the energy in a system with respect to a reference state. It can be used to point out degradation of useful energy in components in a system and thereby identify which components are the most critical in the system. There are four different kinds of exergy: physical, kinetic, potential and chemical exergy. Physical exergy is the change in thermodynamic properties such as temperature and pressure. Kinetic exergy is bound to the velocity of the fluid. Potential exergy is usable energy due to the height difference and chemical exergy is the energy due to chemical reactions. This section only considers the physical and the kinetic exergy as there is no chemical exergy destruction in a hydrogen fuelling system, and the potential exergy has been neglected as there is no significant height differences in the system.

Considering physical exergy, there are different methods to apply depending on if the component contains a volume or only has a flow passing through. For a volume the general exergy equation is shown in eq. 3.43 [2].

$$\begin{aligned}\frac{dE_{cv}}{dt} = &\sum(1 - T_0/T)\dot{Q} - (\dot{W}_{cv} - p_0\frac{dV_{cv}}{dt}) \\ &+ \sum \dot{m}_{in} * e_{in} - \dot{m}_{out} * e_{out} - \dot{E}_D\end{aligned} \tag{3.43}$$

where dE_{cv}/dt is the change of exergy in the volume, $(1 - T_0/T)\dot{Q}$ is the contribution from the heat transfer using the Carnot efficiency to express the quality of the energy and $(\dot{W}_{cv} - p_0 dV_{cv}/dt)$ is the contribution from the work done by the volume. The specific exergy entering or leaving the volume is expressed with e_{in} and e_{out}, respectively. Multiplying the specific exergy with the mass flow gives the exergy entering or leaving the volume. The exergy destruction, which is the lost exergy or energy, is $\dot{E}_D$.
The exergy of a control volume can be found by eq. 3.44.

$$E = (U - U_0) - p_0(V - V_0) - T_0(S - S_0) \tag{3.44}$$

where U is the internal energy, V the volume, S the entropy, p the pressure and T temperature. The subscript 0 is the reference state to which the exergy is measured. Typically it is the ambient properties around the system. The specific exergy of a stream of matter is shown in eq. 3.45.

$$e = (h - h_0) - T_0(s - s_0) + \frac{1}{2}v^2 + gz + e^{ch} \tag{3.45}$$

where $(h-h_0)-T_0(s-s_0)$ is the physical exergy, h is the specific enthalpy and s the specific entropy. $0.5v^2$ is the kinetic exergy, gz the potential exergy and e^{ch} the chemical exergy. The potential and the chemical exergy are disregarded as there are no height differences and no chemical reactions taking place. The kinetic exergy is assumed to be a part of the energy balance for the specific stagnation enthalpy as the h is the specific stagnation enthalpy of the stream, which corresponds to the specific enthalpy at a point in the stream added with the kinetic energy $h = h_s + 0.5v^2$, as explained in Section 3.3. When considering eq. 3.45 it can be seen that this is an assumption, as the kinetic energy in a system can be directly converted into exergy without any losses, while the physical exergy consists of losses due to entropy generation. The assumption results in a slightly lower exergy, as there is a loss connected to kinetic exergy when including it in the physical exergy.

The exergy destruction across a component is expressed as in eq. 3.45, while the exergy destruction is expressed in eq. 3.46.

$$E_D = m_{flow,in} * e_{in} - m_{flow,out} * e_{out} + W + Q(1 - T_0/T) \tag{3.46}$$

The exergy destruction is a measurement of the useful energy which is lost in the system through the specific component. Another way to express the energy destruction in a component is through its exergy efficiency as shown in eq. 3.47.

$$\eta_E = E_{out}/(E_{in} + W + Q(1 - T_0/T)) \tag{3.47}$$

In general exergy is a useful tool to analyse systems for optimization as it takes enthalpy and entropy generation into account, giving an energy expression that includes the quality of the energy. Exergy can be considered as comparable to electricity as electrical energy can be directly converted to exergy without loss.

3.9.2 Exergy in hydrogen fuelling stations

Using exergy analysis on a hydrogen fuelling system can reveal where the significant exergy losses are. However, considering a fuelling system, some exergy losses are easier to optimize than others. The pressure losses throughout the system result in increased temperature of the hydrogen due to the Joule-Thomsen effect, increasing the thermal exergy when decreasing the mechanical exergy. In hydrogen fuelling systems the mechanical exergy is worth more than the thermal; therefore lower pressure losses result in lower exergy destructions. Further, if there were less or lower pressure losses in the system, the cascade system could operate at lower pressures. This would decrease the exergy destruction in the compressor due to a lower pressure ratio which also results in less heat up of the hydrogen; this is again directly related to eq. 3.45 as the enthalpy of the hydrogen would be lower, eq. 3.36. The pressure losses that

can be hard to improve from an exergy destruction point of view are the reduction valve and the pressure loss in the vehicle. The reduction valve reduces the pressure according to the average pressure ramp rate and the pressure out is therefore specified. The exergy destruction is specified by the pressure reduction across the valve; so in order to reduce the exergy destruction, the pressure reduction should be smaller or work should be produced during the expansion. The hydrogen being compressed or expanded inside the tanks changes temperature due to the heat of compression/expanding. These are exergy losses which can not be avoided. Lower temperature changes inside the tanks would decrease the exergy destruction. Longer fuelling times would allow a higher heat dissipation through the tank wall resulting in a lower heat up. A lower temperature results in a higher density at the same pressure, decreasing the exergy destruction in the tank during fuelling due to a higher mechanical exergy which is worth more than the thermal exergy. After the fuelling the heat dissipation through the tank wall results in an exergy loss, as the pressure decreases, though longer fuelling time violates the average pressure ramp rate given by the fuelling protocol.

In order to asses different hydrogen fuelling systems, an exergy analysis can be used to compare the system performance from an energy point of view. In this case the individual exergy destruction is of less interest because it is the systems which are being compared. When comparing systems it is important that the boundary conditions are the same and the fuellings proceed as similarly as possible. This includes the same total mass filled in approximately the same time interval, the same pressure loss constants and the same properties of the tanks in each system. The comparison between the systems reveals which system has a better energy usage, and in general, the lower the exergy destruction of a system, the better the performance and the less energy is required.

Chapter 4

Hydrogen fuelling library

This chapter provides the rationale behind of the choices made with respect to the Dymola programming, namely, the stream concept, the choice of thermodynamic package and a short introduction to the hydrogen fuelling library. A model of a fuelling station is compared to another model of the same fuelling station developed in MatLab by H2Logic to verify the model. Then test data from a real fuelling is compared to a model made in Dymola of the same system.

4.1 Introduction

The object of the model for hydrogen fuelling is to have a tool that can be used when designing and dimensioning hydrogen fuelling stations. The model is designed with four main criteria in mind. The model must be dynamic, flexible, user-friendly and open to further third party development. The hydrogen fuelling library can be found at: GitHub in the group "DTU_TES". The direct link to the library is:
`https://github.com/DTU-TES/Hydrogen-Fuelling-Station`.

The two most important features regarding the results of this thesis are the dynamic modelling and the flexibility of the model. Hydrogen fuelling is complex with constantly changing mass flows, pressures and temperatures, and therefore it is vital for the model to be able to predict these developments in order to design and optimize fuelling stations. The possibility of easily varying parameters

in the components, changing the layout of the hydrogen fuelling station and adding or removing components enables the possibility to explore endless designs and gain understanding of the influence of each component on the system.

Though the other two criteria regarding easy layout and availability for use by people other than the developer, are not the priority of this thesis as are dynamic and flexible modelling, the vision is that the library should be the first dedicated library for hydrogen which can be used for research at universities and by industry when designing and optimizing fuelling stations. Therefore a lot of effort has been put into streamlining the component and model design. Further more, the interactions between the components have been kept simple. Even though in this study particular attention has been given to compressed gaseous hydrogen storage systems, the developed fuelling station model is valid (and can be simulated) for all storage systems which require high-pressure fuelling in the gas phase, with no interest in the phenomena occurring inside the on-board tank [30] [28] [21]. Only the tank model must be changed accordingly and the same input and output be used.

The first part of this chapter gives a short introduction to Dymola, the flow and stream concept, and discusses external libraries used in the hydrogen fuelling library. The user is assumed to have prior knowledge of Modelica or Dymola and to have a basic understanding of hydrogen fuelling in order to be able to use the hydrogen fuelling library. The second part of this chapter considers a verification of the Dymola model by comparing it to another model developed in MatLab by H2Logic. Then the dymola model is compared to data obtained from a real hydrogen fuelling of a vehicle, in order to demonstrate the the close similarity between a real fuelling and the model developed.

In addition to this chapter, Appendix A is a manual for the library containing detailed description of the components modelled in Dymola. Appendix B contains a validation of each component based on parametric studies and is complementary material to the verification in this chapter.
For further information on the Modelica language and modelling concept, literature such as Modelica's own "The Modelica Language Specification" [25] or Fritzon's textbook "Principles of object oriented Modelling and simulation" [11] are available.

4.2 Introduction to Dymola and Modelica

4.2.1 History

Modelica and Dymola are dynamic modelling software. They originate from the same programmer, Hilding Elmqvist from Sweden. Dymola was first re-

leased in 1978, but has since undergone several extensive changes. In 1992 it was transformed into C++ programming language in a similar form as known today. Modelica was first released in 1997; the goal was to develop an object-oriented language for modelling dynamic systems where the dynamic models could be exchanged and reused in a standardized format. Modelica is developed with the Dymola software, but other modelling languages have been used to improve the Modelica language. The first edition of Modelica was for implementation in Dymola, and for some years Dymola could run both the Dymola and the Modelica language before it fully transitioned to Modelica in 2002. Now Dymola is a front-end user-interface to Modelica with more options in addition to the Modelica standard library.

4.2.2 Building models in the Modelica language

The language of Modelica is a unified object-oriented language for physical system modelling; the approach is non-casual and uses true ordinary differential equations. The language enables graphical editing so that component models may be used graphically to create systems, similar to the interface of Simulink. Building a model in Modelica requires decision-making in different stages. First the type of model has to be decided, then the data types which should be in the model and at last the kind of equations that should be used. When designing a component model, the model classes are either *Model*, *Function*, *Connector*, *Block*, *Record* or *Package*. In the models the data types can be defined as *Real*, *Integer*, *Boolean* and *String* with additional specifying keywords, such as *Parameter*, *Constant*, *Input*, *Output*, *Inner* and *Outer*. All data types used in a class are to be declared. The declaration of the data types is done at the top of the class. Other important declarations of data types which are of dedicated usage to the connectors are the concepts of *Flow* and *Stream*. With the data types declared, the equations describing the class can be declared. The equations can be declared as *Equations* or *Algorithms*.

Equations

Using *equations* the equation written does not describe assignment, but equality of the variables written on both sides of the equal sign, eq. 4.1. Using *algorithms* assigns a value to the left-hand side, eq. 4.2.

$$a + x = b * c \tag{4.1}$$

$$y := ax + b \tag{4.2}$$

The options of using if-expressions, if-clauses, when-clauses and for-loops are also supported in Modelica. The if- and when-clauses are used only in *algorithms*, while the if-expressions and for-loops are used in *equations*.

Flow and stream

Two concepts which have been used throughout the modelling are the assignation of *flow* and of *stream* to a data type. The two assignations are used in connectors but influence the model concept of all models. The *flow* specifies the material flow between models, through the flow connectors. If the mass balance is written correctly, it assures that the flows are assigned the right direction in and out of the component. The programmer does therefore not have to assign negative or positive mass flow to the ports, as the flow command assures this. *Stream* can be assigned to a variable which is carried by the flow, such as chemical composition or enthalpy of a flow. The stream concept makes it possible to have zero mass flow in components without having trouble solving the energy balance. Without the *stream* assignation to the enthalpy, the energy equation for a valve $\dot{m}_1 h_1 + \dot{m}_2 h_2 = 0$ would create singularity with a mass flow of zero, as the enthalpy out of the component cannot be determined. The enthalpy is given by the previous component which would have the same problem. Assigning *stream* to the enthalpy in the port, the enthalpy in a component is assigned the value the enthalpy would have if the mass was flowing out of the component, regardless of the real flow direction. This is convenient as it is possible to have zero mass flow, but inconvenient as the programmer has to handle enthalpy from both directions, even though there is only one flow direction. Figure 4.1 shows an example of a simple system with the enthalpies at the different entrances and exits. h_1 exists inside the tank to the left and at

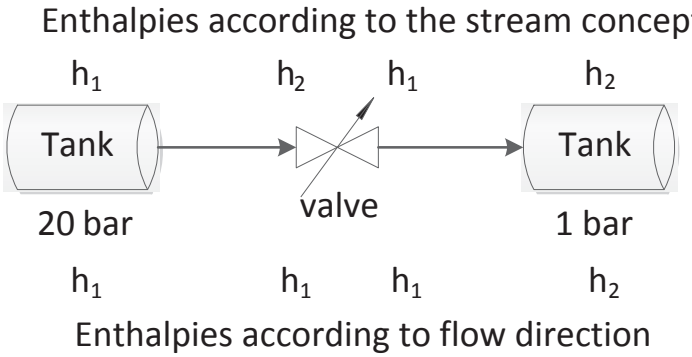

Figure 4.1: Simple system showing the enthalpies in the flow direction and the enthalpies which are present in the point due to the stream concept.

the exit of the valve; this is the actual enthalpy of the mass flow, h_2 is present in the receiving tank, which is correct but it is also the enthalpy in the connector at the entrance of the valve, which is incorrect according to the flow direction. This has to be taken into account not only when formulating the mathematical equations in the components, but also when analysing the results. When modelling it is possible to retrieve the correct enthalpy at the entrance of the valve by calling the enthalpy using the command *instream*. *instream* uses the

entering enthalpy, so it is the opposite of the enthalpy which is carried into the component by the flow connector as it assumes the flow is leaving.

It should be noted that the flow and stream concept has been used in all the models. Therefore all component models naturally work with flow entering from either port.

4.2.3 Thermodynamic properties

Modelling and simulation of thermodynamic systems, such as hydrogen fuelling stations, requires access to thermodynamic properties. There are several different thermodynamic property libraries available for Modelica/Dymola. The most common is available through the licensed TIL package [31] the models have to use components from the TIL library. An alternative is to use *RefProp* [22] which requires a license as well, though it can be used with multiple software as it is a standard .ddl library file which then needs a wrapper for integration into the platform used. For Modelica there is a wrapper called *RefProp2Modelica* which is free to download and use. The *Refprop2Modelica* wrapper uses the Modelica standard library. One alternative to avoid using a third party licensed library for Dymola is to use *CoolProp*. *CoolProp* is open-source and 100% free to use. Free wrappers for different software packages are available; for Modelica it is called *CoolProp2Modelica*. *Coolprop* is like the *Refprop* library which can be used with multiple software packages, and it is a cross-platform software for Microsoft Windows, Linux/Unix and Mac OSX. The results of *CoolProp* have been successfully validated by comparison to both *TIL media* and *Refprop*. The calls for the thermodynamic states can be very time-consuming; especially in larger systems the simulation time depends on the speed of the thermodynamic calls. *Coolprop* has shown itself to be faster than the *Refprop* solution and comparable to *TIL Media* in calculation speed [3]. The purpose of *HydrogenFueling* library is to be a stand-alone library for Dymola; therefore *CoolProp* has been chosen for the thermodynamic calculations. Furthermore, *CoolProp* has the potential to become much faster than *TILMedia*, but as it is still under development it has not been implemented in the wrapper for Modelica yet.

4.2.4 Modelica standard library

The Modelica standard library has many of the predefined components within the field of engineering, built-in units for most properties and many predefined constants. The predefined models have not been used in the library for hydrogen fuelling, as the components needed for the hydrogen fuelling station are specific. The Modelica models were too general and complicated. However, it is worth noting that the predefined units are useful when designing a component, as Modelica does unit checks on all equations before simulation. If some

equations do not match in units a warning is given, and thus this helps securing that the equations add up.

4.2.5 Library descriptions

The library for hydrogen fuelling has a simple structure compared to the Modelica standard library and the TIL library. The specific definition of the library purpose enables the possibility of an easier component structure. Multiple layers and hierarchical composition of components have been avoided for a clearer library structure. Each model is complete in itself and avoids several small partial models. Exceptions are the connectors and the thermodynamic properties that are used in every model; they are retrieved from their original placement in the library for each model. The heat transfer model is built up in three layers reusing models from lower layers. Though the lower layer models could be used instead directly in the systems, the heat transfer models have been made to simplify and ease the implementation of heat transfer in the systems. The library consists of folders or packages where each folder represents a specific kind of component. The different categories are as follows:

- Ports
- Tanks
- PressureLosses
- Compressors
- Mixers
- Switches
- HeatExchangers
- HeatTransfer
- Controls
- Functions
- Templates
- Models

All the models have been made from scratch, and the standard Modelica library has only been used to retrieve units for the data types and to retrieve constant values, such as π and gas constants.

The models in the library are explained in detail in Appendix A. Here more

general information about the models is given with respect to the implementation in Dymola. All the different packages which can be found in the hydrogen fuelling library can be found in Appendix A, and the code from Dymola is shown for each component in Appendix C.

4.3 Verification and validation of the model

This section compares the Dymola model to a Matlab model made by H2Logic, and it also compares the trends of a model with experimental data from a 700 bar hydrogen fuelling. The results are compared with respect to temperatures, pressures and mass flow rates at different places in a fuelling station. In Appendix B a validation of each model is made on the basis of a parametric study.

4.3.1 Comparison of models

The two models compared are the Dymola model developed during this Ph.D. and a MatLab model developed by the company H2Logic. Both models fuel vehicles according to the fuelling protocol, the SAE J2601. The results shown here are for an A70 fuelling of a 0.161 m^3 tank with an initial pressure of 20 bar. The three tanks in the cascade system at the station are all pressurised to 950 bar. The pressure losses are calculated with the same equations in the two models, and the same pressure loss coefficients have been used. The tanks are dynamic in both models, and the same materials and dimensions were used in both models, though the heat transfer model in the Dymola model is more advanced. The average pressure ramp rate for both systems was set at the exit of the station. Figure 4.2 shows a very simplified sketch of a fuelling

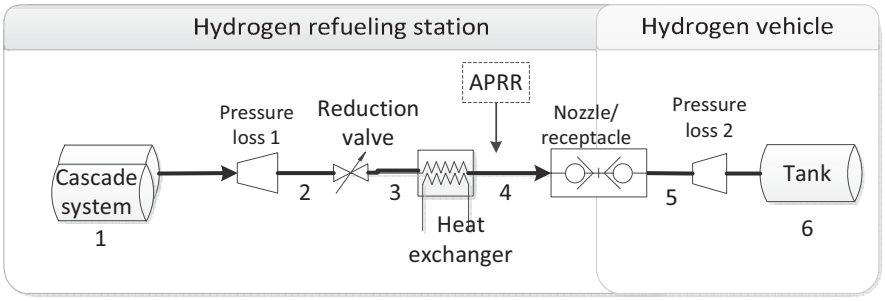

Figure 4.2: Sketch of a fuelling station pointing out where the pressures and temperatures shown in Figure 4.3 and Figure 4.4 are taken from the calculation.

system in order not to show any confidential information. Pressure losses have been collected in two places. The real station modelled had more pressure losses and a lot more parameters, which will not be mentioned as they are confidential. The numbers on the sketch correspond to the temperatures and

pressures shown in Figure 4.3 and Figure 4.4. Point (1) in Figure 4.2 is in the tanks in the cascade system, point (2) is before the reduction valve, point (3) is after the reduction valve, point (4) is after the heat exchanger and just before the outlet of the station, point (5) is after the receptacle in the vehicle and point (6) is inside the vehicle tank. In the following figures the data from the MatLab model is noted with a (M) and the data from the Dymola model is labelled (D).

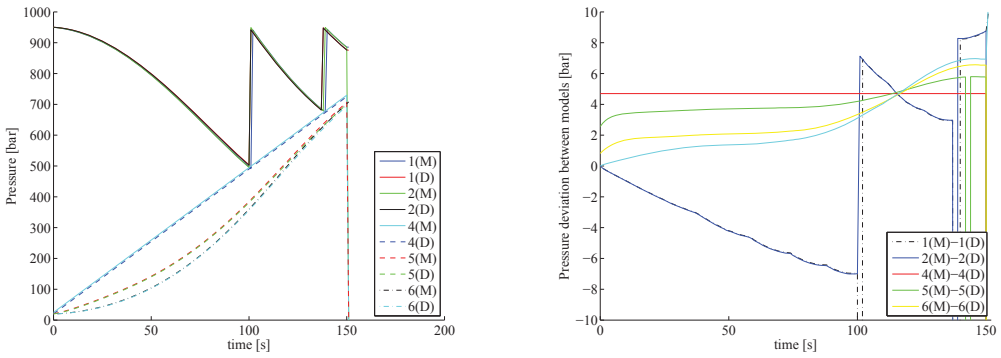

(a) Pressures in the system during a fuelling. (M) Matlab, (D) Dymola

(b) Deviation in pressure between the two models. (M) Matlab, (D) Dymola

Figure 4.3: The pressure throughout the fuelling station during a fuelling. The pressure is shown for both the MatLab and the Dymola model together with the deviation between the two models.

Figure 4.3 shows that the pressure development during a fuelling is almost identical for the two models. The largest pressure difference between the two models is 7 bar, which is acceptable when considering the large pressure losses that are present in the system. The vertical lines going down for the MatLab simulation is a result of changing the tank in the cascade system at the station; the value of the pressure drops to zero bar at this point. The vertical lines should therefore be disregarded. The temperature calculated for the fuelling from both models can be seen in Figure 4.4. They are very similar for both models, and the largest difference is in the vehicle tank with approximately 3 C° difference at its peak. This was expected as the heat transfer in the two models is calculated differently. Comparing Figure 4.3(a) of the pressure and Figure 4.4(a) of the temperature, it can be seen that when there is a pressure drop the temperature of the hydrogen rises, due to the Joule-Thomson effect. The mass flow of the two simulations is shown in Figure 4.6(a). The matlab model has a slightly higher mass flow rate for the first 120 seconds before the two curves cross and the Dymola model has a little higher mass flow rate. Considering the deviation it is approximately 1 g/s, which is less than 2 % of the peak mass flow rate at just over 50 g/s.

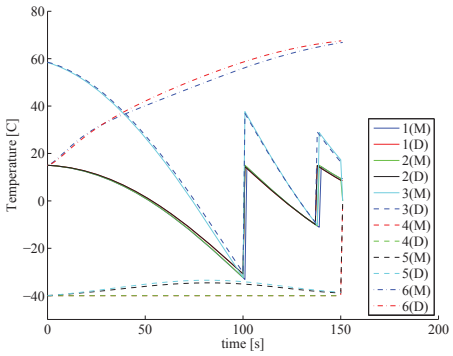

(a) Temperatures in the system during a fuelling. (M) Matlab, (D) Dymola

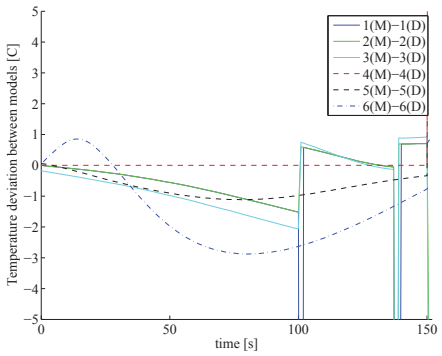

(b) Deviation in temperature between the two models. (M) Matlab, (D) Dymola

Figure 4.4: The temperatures throughout the fuelling station during a fuelling. The temperatures are shown for both the MatLab and the Dymola model together with the deviation between the two models.

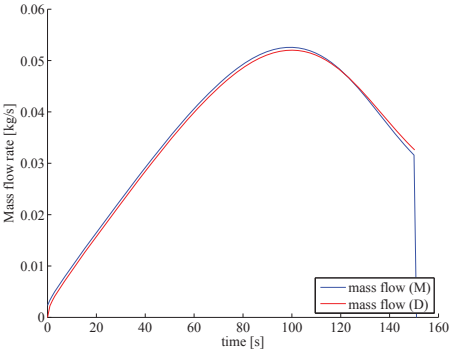

(a) The mass flow rate during a fuelling. (M) Matlab, (D) Dymola

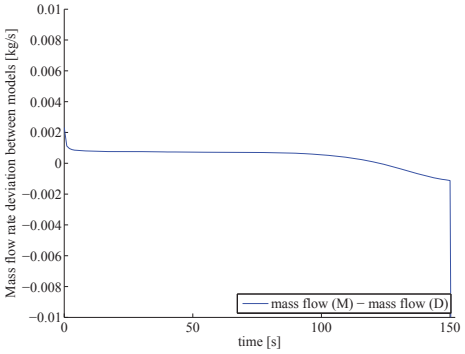

(b) Deviation in mass flow rate between the two models. (M) Matlab, (D) Dymola

Figure 4.5: The mass flow rate of the fuelling simulated. The mass flow rate is shown for both the MatLab and the Dymola model together with the deviation between the two models.

The two models, which are mainly developed independent of each other, give very similar results. The deviations between them are small, and both models perform as expected. The two models have been used to verify one another. Furthermore, the model from H2Logic has been successfully verified to other models developed by Wenger Engineering, who does calculations for the development of the fuelling protocol SAE J2601, and H2Logic has performed a number of tests which have been compared to their model with success.

4.3.2 Comparing to test data

The following section considers data from a real hydrogen fuelling of a 350 bar tank. The data was extracted in 2011 from a H2Logic fuelling station; since the design of the fuelling station is confidential, the design will not be further discussed. Pressures and temperatures were measured at different places in the system. Unfortunately the thermocouples at the exit of the tanks at the station were broken; therefore, the temperature obtained is limited to before and after a heat exchanger placed after the reduction valve in the system. The pressure was measured at the outlet of each tank and before and after the reduction valve. In addition, a mass flow meter measured the mass flow rate in the system. The data from the test is compared to a simulation which follows the fuelling protocol, hence constant average pressure ramp rate and -40 C° out of the heat exchangers. The model used for the simulations is a copy of the real station, where pressure losses are collected were appropriate. The purpose of comparing test data with a simulation is not to get the exact same values, but to see if the trends are the same, as there are too many unknown parameters at the real station not taken into account in the simulation. One important parameter is the control of the real fuelling station which does not function ideally as does the simulation. Furthermore, not all data was given for the tested fuelling station so assumptions about pressure losses had to be made for the simulation. The simulation has been fitted as close to the measured data as possible, while completing an A70 fuelling according to the protocol. The tanks at the station are the same size as is the tank in the vehicle. The pressure losses in the simulation have been fitted to the data from the test. The tested fuelling station had two heat exchangers, whereas only information on the second placed after the reduction valve was available. The model also had two heat exchangers which both were working ideally, hence cooled the hydrogen to -40 C°. The average pressure ramp rate used in the model was changed, so the average ramp rate for both the model and the test were the same, when a complete fuelling is considered. Figure 4.6(a) shows the measured pressure out of the tanks at the fuelling station compared to a simulated pressure of an ideal fuelling. The tanks have the same initial pressure for both the test and the model. The final pressure in each tank is also approximately the same. The change between tanks at the hydrogen fuelling station is different, since the test data's average pressure ramp is not constant as it is for the simulation; however, the final pressure in each tank is the same, and hence, the same amount of mass is removed from the tanks for both the test and the simulation. Considering Figure 4.6(b) which is the pressure on both sides of the reduction valve, it can be seen that the average pressure ramp rate is the same for both the test and the simulation for a complete fuelling. The fuelling stops during the test at each tank shift, which results in a break and some waiting time which is not present in the simulation. The shift between the tanks at the station happens at approximately the same pressure in the test and in the simulation. The tem-

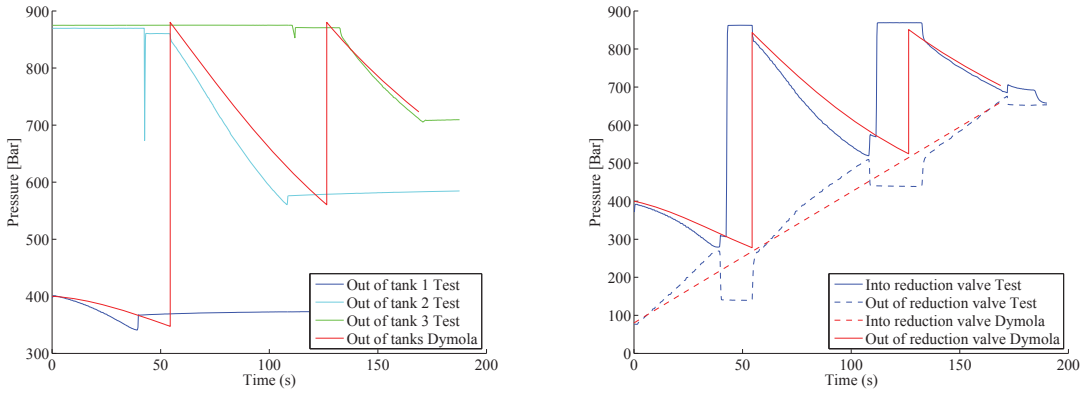

(a) Pressure out of the tanks (b) Pressure on each side of the reduction valve

Figure 4.6: Pressure across the reduction valve.

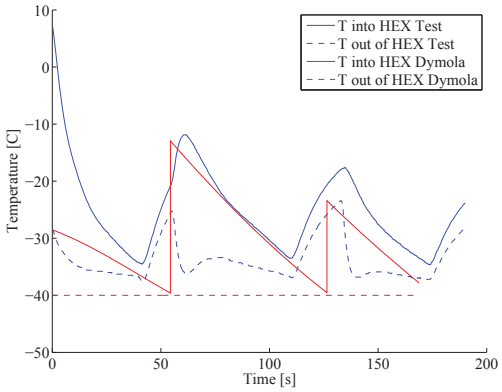

Figure 4.7: The temperature into and out of the heat exchanger for both the test data and a simulation of an ideal fuelling.

perature, shown in Figure 4.7, into and out of the heat exchanger follows the same pattern. As the hydrogen is cooled down before the reduction valve, the temperature of the hydrogen is a result of the Joule-Thomson effect across the valve, hence the pressure difference. In the simulation the hydrogen is cooled down to -40 $C°$ before the valve, and for the test the inlet temperature to the reduction valve is unknown. The comparison shows that the pattern of the temperature before and after the heat exchanger is similar for the test and the model. The differences should be found in the cooling capacity of the hydrogen in the test, which is lower than needed by the demand for cooling to -40 $C°$. The mass flow of the test and the simulation can be seen in Figure 4.8. The mass flow rate seems a little higher for the simulated fuelling; this could be

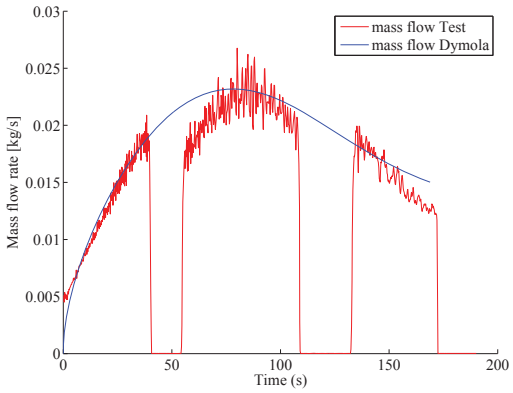

Figure 4.8: The mass flow rate for both the test data and a simulation of an ideal fuelling.

due to an inaccuracy in a tank dimension or the pressure loss in the vehicle is set too low. The two mass flow rates are similar in curve shape, despite the test results have the fuelling break when switching tanks in the cascade system.

The comparison between the test data and the simulation shows that the trends of the simulation are similar to a real hydrogen fuelling. The pressure drops, the Joule-Thomson effect and the temperatures seem to behave similarly in the simulation and in the test. Furthermore, the pressure in the tanks at the station end at the same pressure as for the test data as does the outlet of the reduction valve. The comparison shows that the model for hydrogen fuelling can simulate hydrogen fuelling close to real-life hydrogen fuellings.

4.3.3 Remarks about verification and validation

The comparison of the MatLab model with the Dymola model showed almost identical results. The differences were negligibly small taking into account that the models use different equations and different solvers. The comparison between the data of a real hydrogen fuelling and the model showed that the model's ideal fuelling is quite close to how a real fuelling station operates. The largest difference between the data and the model, was that during a real fuelling there is a break when changing the tank at the station. The temperature into the heat exchanger followed the same pattern for the model as for the data, though the temperature out was different as the station did not cool down to -40 $C°$. The mass flow rates were similar too, for the model and the data. The comparison between the MatLab and the Dymola model, the Dymola model and the data from a real fuelling and the validation based

on a parametric study in Appendix B, shows that the Dymola model works as expected. It can therefore be used for dynamic simulations of hydrogen fuelling stations.

Chapter 5

Assumptions

This chapter summarises and collects the important assumptions used in the analysis of hydrogen fuelling stations. Most of the assumptions have been mentioned in the previous chapters. The chapter also has some general explanation of the flow of hydrogen through the three different pressure loss models described in Chapter 3.

5.1 Introduction

This section has been divided into three parts: thermodynamic assumptions, assumptions regarding the fuelling protocol and assumptions regarding flow characteristics. The three different sections summarises assumptions which are made throughout the thesis and for the flow characteristics considerations that are relevant for the analysis in Chapters 6, 7 and 8 are discussed.

5.2 Thermodynamic assumptions

The assumptions made in the component model formulation are for the first principles equations, that potential energy is neglected and the kinetic energy is partly taken into account through the stagnation enthalpy. There is no noticeable height difference between the fuelling station storage and the vehicle; therefore, the potential energy has been neglected. The kinetic energy is partly included in the stagnation enthalpy used throughout the calculations. The dif-

ference from using the real enthalpy and the kinetic energy compared to the stagnation enthalpy is that the thermodynamic properties would be a little different as the properties should be found using the real enthalpy. Using kinetic energy and the real enthalpy results in an iteration, since the kinetic energy depends on the thermodynamic properties and the enthalpy would depend on the kinetic energy. The stagnation enthalpy has been used to avoid the iteration process between finding the real enthalpy and the kinetic energy, as the kinetic energy accounts for a maximum of 2 % of the total energy in a hydrogen stream. The assumption is also based on that all kinetic energy is transformed to enthalpy when the hydrogen enters the tank in the vehicle. See Chapter 3 for further explanation.

Considering the exergy, the same assumption about the kinetic energy and the stagnation enthalpy has been made. The kinetic exergy is therefore partly included in the physical exergy, though the kinetic exergy is considered as pure exergy, while the physical exergy has entropy generation, and therefore an exergy loss when undergoing a change in pressure and temperature. This assumption has been made on the same basis as for using the stagnation enthalpy for thermodynamic properties, as the kinetic energy accounts for a maximum of 2 % of the total energy in the stream. See Chapter 3 for further explanation.

The ambient temperature is assumed to be 20 C° if nothing else is given. The ambient temperature is also the initial temperature of the hydrogen in the tanks and the tank walls. The heat exchangers are assumed to have the capacity to cool down to the given temperature during the whole simulation, hence constant temperature out of the heat exchanger which is independent of the mass flow rate. The volume of the vehicle tank is assumed to be 0.172 m^3 corresponding to a total mass of 7 kg. The tanks at the station are typically 1 m^3 or less.

5.3 Assumptions from the fuelling protocol, SAE J2601

The assumptions which have been made on the basis of the fuelling protocol [34] are primarily the boundary conditions for the simulations, securing that the fuelling proceeds according to the protocol. The boundary conditions for the pressure losses during a fuelling are that the maximum pressure loss in the vehicle can not exceed 200 bar. Another boundary condition is that the flow can not exceed a mass flow rate higher than 0.06 kg/s, which is obtained if the pressure drop in the vehicle is low. These two boundary conditions have been used when deciding the pressure loss coefficients used in the vehicle. Section 5.4 has further explanation of the hydrogen flow in the system.

The hydrogen fuelling stations which have been simulated, all have hydrogen available in their banks at pressures between 200-300 bar. The hydrogen is assumed to be trucked in, and the work done to pressurise the hydrogen in the banks has not been considered. Only the work done at the station is taken into account. This does not influence comparisons between different fuelling station designs as they all have premises for the hydrogen storage bank.

Hydrogen fuelling of a vehicle can be done with and without communication. For Chapters 6 and 7 the fuellings are simulated without communication. The fuelling does therefore end when the pressure out of the fuelling station reaches the final pressure given in the protocol. The final pressure is for the tank in the vehicle, but when a fuelling proceeds without communication, it is not possible to know the pressure inside the tank or the pressure drop in the vehicle. Therefore, the vehicle tank is assumed to have the same pressure as at the exit of the station, in order not to compromise safety. In Chapter 8 the fuellings are assumed to be with communication, and the fuelling proceeds until the target density of 0.0402 kg/m^3 is reached. This could be either below or above the final pressure depending on the temperature of the hydrogen. With communication the safety limits of both the temperature and the pressure are taken into account, and therefore it is possible to deliberately exceed the final pressure given, as long as the tank is not overheated or over-pressured according to Figure 2.2.

For the simulations the average pressure ramp rate is assumed to be followed strictly, though the protocol allows more flexibility during fuelling so it is possible to stop the fuelling while changing the tank in the cascade system at the station. In the simulations the tank shift is assumed to happen immediately without any interruption of the fuelling.

5.4 Flow assumptions

The assumptions made about the flow of hydrogen are related to the assumptions made on the basis on the fuelling protocol, SAE J2601. Though when considering the flow through a component, the assumptions are more specific than considering the fuelling protocol.

The three pressure losses given in eq. 3.30, 3.31 and 3.32 are for valves, mass flow meter/filter and tubes, respectively. The three equations are very similar as they can be rewritten into eq. 5.1.

$$\Delta p = K \rho \dot{V}^2 \tag{5.1}$$

where K is a constant which for eqs. 3.31 is $K = k_p/2$ and for eq. 3.30 is $K = 1/(k_v^2 \rho_w)$. For eq. 3.32 $K = (fL/d + k)/(2A^2)$, this is not a constant as f is a function of the Reynolds number; but when turbulent flow is present, the value can be assumed to be constant. The diameter, the length and the area are all constants during a simulation. The three different equations used can therefore be fitted to give the same results by altering the constant value K; hence, the three equations are the same but due to the different constant parameters, they can be used for different applications. In Chapters 7 and 8 the pressure losses for each part of the system have been added together to one pressure loss expressing the total pressure loss. This assumption is valid as the pressure loss equations only differ by the constant values used; hence, they all have the same shape and peak at the same time. Considering an example, where first the pressure loss constant k_v, k_p and the length L are for a volume flow of $\dot{V} = 0.001$ and a pressure loss of 100 bar found to be $k_v = 0.07721$, $k_p = 0.33548$ and $L = 30.21299$ m. The obtained pressure losses values are inserted into the equations, and the pressure loss for the three equations are found for volume flows between 0.0001 and 0.002, which have been chosen as hydrogen fuellings typically have volume flows in this range. Figure 5.1(a) shows the three equations compared to each other. The differences between the equations are shown in Figure 5.1(b). The deviation between the pressure

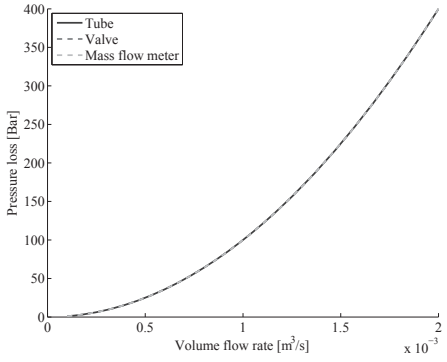

(a) Comparison between pressure loss equations. All three equations use the corresponding pressure loss coefficient to a pressure loss of 100 bar at a volume flow of 0.001 m^3/s.

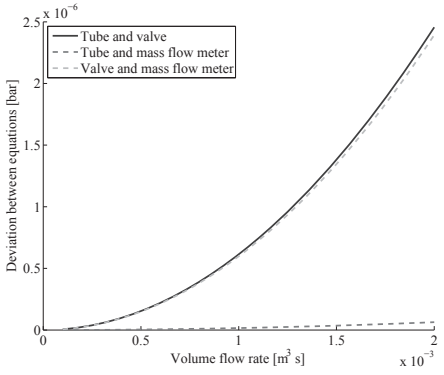

(b) The deviation between the pressure loss calculated from the three different equations.

Figure 5.1: Comparison between the three pressure loss equations.

losses as a function of the volume flow shows that there are almost no differences in the equations as the differences are less than 10^{-5} bar.

All the flows are assumed to be turbulent; for hydrogen there are four different sizes of tubes which currently are used by the fuelling station manufacturers. They range by inside diameter of; $d1 = 0.00517$ m, $d2 = 0.00793$ m, $d3 =$

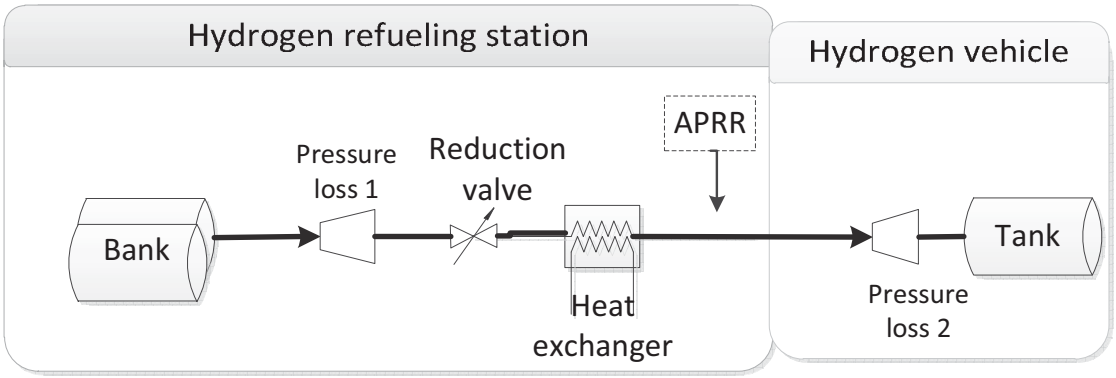

Figure 5.2: A simple fuelling system, the Reynolds numbers are calculated at the highest and lowest pressures of the flow, namely, before pressure loss 1 and at pressure loss 2.

0.01193 m and $d4 = 0.01427$ m. These are from Maximator's catalogue for medium-pressure applications, up to 1500 bar, but the sizes can deviate a little between different manufacturers. Figure 5.2 shows a simple system for the simulation of hydrogen fuelling. The Reynolds numbers have been found during a fuelling where the pressure is highest in the system and where it is lowest, pressure loss 1 and pressure loss 2, respectively. The Reynolds number of the flow at the two different places in the system and for all four diameters are shown in Figures 5.3(a) and 5.3(b) for a vehicle with a high pressure loss, as the Reynolds number increases as the pressure loss in the vehicle decreases. The mass flow rate of the fuelling is shown in Figure 5.4. The Reynold numbers are only laminar when the fuelling begins, but in less than 0.2 seconds the flow is turbulent at both places in the system and for all tube sizes. The tubing at the hydrogen fuelling station has not been taken into account in Chapter 6, but in Chapters 7 and 8 the pressure losses have been collected into one loss for each part of the system, where the tubing is assumed included in these losses. For the vehicle it does not matter if the pressure losses are due to valves, filter, fittings or tubing as the maximum allowed pressure loss does not specify components. It is the manufacturers of the vehicles who are to make sure that the system does not have a higher pressure loss than 200 bar when fuelling according to the protocol. At the fuelling station pressure losses are critical as higher pressure losses result in a higher storage pressure of the hydrogen. During all the simulations, the tubes have been assumed to be 0.00519 m in inside diameter, thus the smallest tube with the highest pressure loss. The pressure loss is a function of the volume flow or velocity squared, thus increasing the cross-sectional area by a factor of two would decrease the pressure loss by a factor of four. Figure 5.5(a) shows the pressure loss during fuelling for the four different diameters; it is obvious that increasing the diameter decreases the

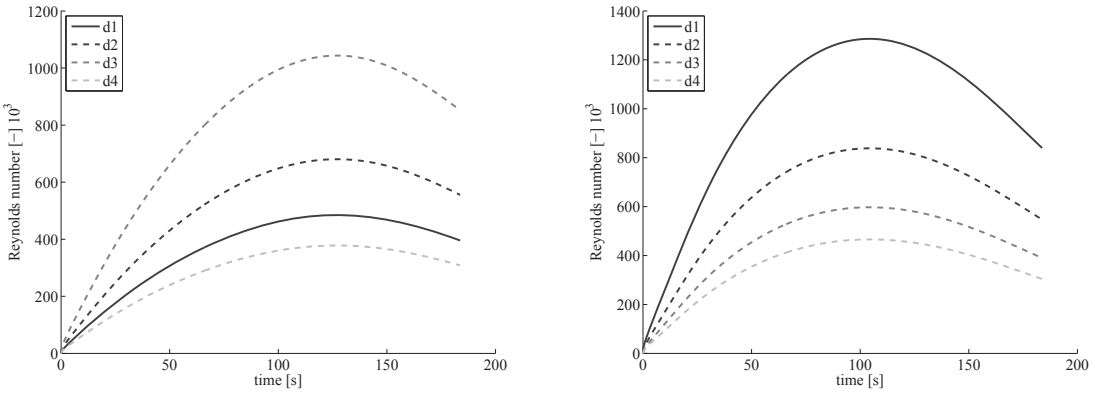

(a) At pressure loss 1

(b) At pressure loss 2

Figure 5.3: The Reynolds numbers obtained during a simulation of a hydrogen fuelling for four different inside tube diameters. These are the lowest Reynolds numbers which can be achieved for a fuelling of a vehicle with a high pressure loss (200 bar).

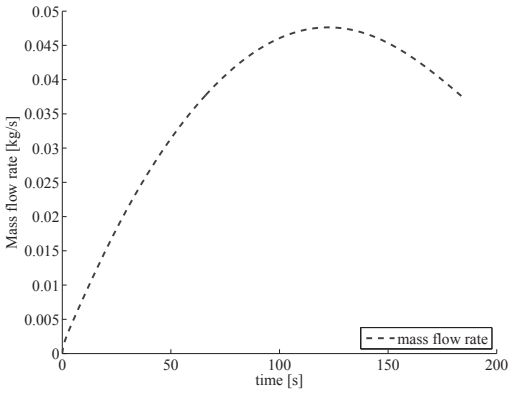

Figure 5.4: Mass flow rate for fuelling of a vehicle with a high pressure loss (200 bar).

pressure loss. Figure 5.5(b) shows the ratio between the pressure losses for the different diameters. It shows that going from the smallest to the largest tube diameter can reduce the pressure loss with a factor of 200, though it should be noted that the largest tube has a pressure limit of 1050 bar, while the other three tubes have a maximum pressure limit of 1500 bar. The pressure losses related to the tubes vary a lot depending on the diameter, and choosing a large tube dimension will result in a small pressure loss through the tubes, thereby improving the system as the stored hydrogen at the station can be at a lower

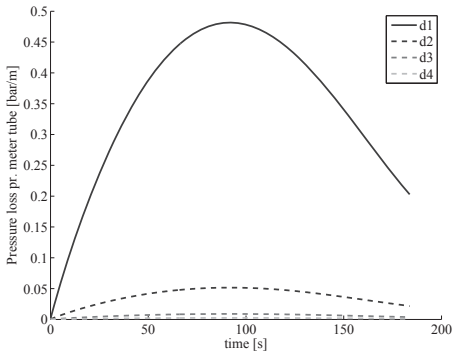

(a) Pressure loss in 1 meter tube during a fuelling of a high pressure loss vehicle

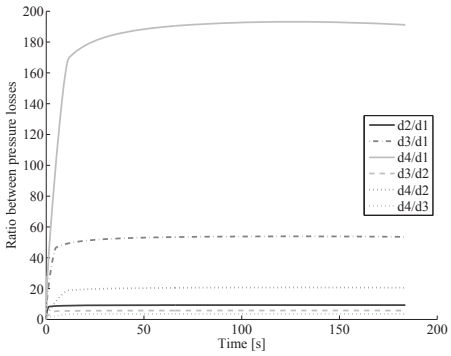

(b) The ratio between the pressure losses as a function of the tube diameter during a fuelling

Figure 5.5: The pressure loss in one meter of tube as a function of the diameter and the ratio of pressure loss between the four different tube diameters. The mass flow rate corresponds to Figure 5.4.

pressure.

Chapter 6

Thermodynamics of hydrogen fuelling

This chapter contains a thermodynamic analysis of a hydrogen fuelling using one high-pressure tank to fuel the vehicle. The fuelling is done in accordance with the fuelling protocol, SAE J2601. The effect of using cascade fuelling is analysed and discussed with respect to the system only having one tank at the station. The chapter provides an basic understanding of the thermodynamics of hydrogen fuelling and which components influence the fuelling process.

The presented results are also discussed in Rothuizen et al. [32].

6.1 Introduction

The documentation on hydrogen fuelling is limited and no full thermodynamic analysis of hydrogen fuelling applying the SAE J2601 has yet been published. Understanding the thermodynamics of the fuelling process and the influence of the fuelling protocol is the first step toward designing and optimising hydrogen fuelling systems.

The first analysis considers an A70 fuelling station with one high-pressure tank fuelling a 7 kg vehicle tank with an initial pressure of 20 bar. The ambient temperature is 25 $^{\circ}C$, and the fuelling is done without communication; see

Chapter 2 for further explanation. The pressure loss in the vehicle peaks at 200 bar, which is the highest allowed. The analysis shows the pressure and temperature development in the system, together with the mass flow and the cooling demand. This provides a thermodynamic understanding of hydrogen fuelling.

The second part contains a parameter variation of the pressure loss in the vehicle. This is relevant as different vehicles have different pressure losses. The influence of the vehicless pressure loss on the fuelling process is shown on the final temperature in the vehicle tank, the final pressure in the vehicle tank, the mass flow of the fuelling process and the cooling demand during the fuelling. The purpose of this part is to clarify the influence of the vehicle on the fuelling process.

The third part contains a thermodynamic analysis of using multiple tanks at the station instead of one tank. The system is analysed with respect to pressure and temperature development in the system during the fuelling. The energy consumption of the system with multiple tanks is compared to the implementation with a single tank. The thermodynamic analysis shows the differences between fuelling from a single tank and multiple tanks.

6.2 Thermodynamics of hydrogen fuelling

A hydrogen refueling station is a high-pressure system in which the pressure and the temperature of the hydrogen change over time within the different components. A diagram for a conceptual hydrogen fuelling station is shown in Figure 6.1. It is a simplified model made to show the thermodynamic evolution over time.

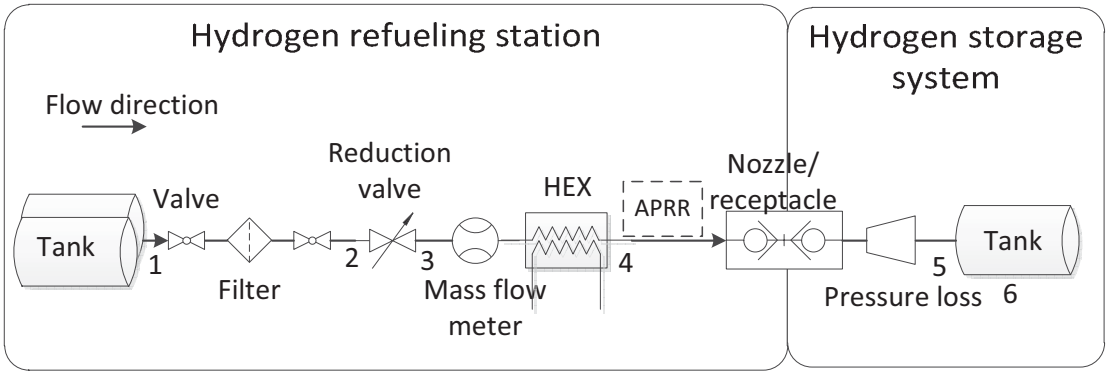

Figure 6.1: Simple hydrogen fuelling station, reference model.

The model has one hydrogen tank with a pressure of 90 MPa at the hydrogen

fuelling station. The APRR is controlled at the station's outlet. However, the pressure reduction valve is placed before the heat exchanger; hence, the reduction valve compensates for the pressure losses across the components between itself and the nozzle. The pressure loss in the hydrogen storage system is given by the same equation as the pressure loss in the mass flow meter, eq. 3.30. As the pressure loss in the hydrogen storage system is different for different vehicle models, it is impossible to predict it in general, though it is not allowed to exceed 20 MPa at any time [34]. The thermodynamics of a full fuelling event according to J2601 are shown in Figure 6.2. The temperature and the pressure at different locations are plotted and they correspond to the numbers in Figure 6.1; the tank outlet of the hydrogen fuelling station (1), before and after the reduction valve (2 and 3), after the heat exchanger (4), at the inlet to the tank in the hydrogen storage system (5) and in the tank in the hydrogen storage system (6). These points were identified as critical locations in the overall system. Figure 6.2(a) shows the temperatures throughout the system. The temperature out of the tank (T1) at the hydrogen fuelling station is decreasing as mass is removed. The temperature increases across components where there are pressure losses present. This is due to the negative Joule-Thomson coefficient of hydrogen; it is especially significant across the reduction valve (points 2-3). The temperature rise (poinst 4-5) is parabolic as the pressure drop is a function of the mass flow; the temperature rise is therefore due to the Joule-Thomson coefficient. The hydrogen gas temperature into the tank at the hydrogen storage system is much lower than the hydrogen gas temperature inside the tank; this is due to the heat of compression inside the tank. Figure 6.2(b) shows the pressures through the system; the pressure out of the tank at the hydrogen fuelling station decreases as mass leaves the tank. Conversely, the pressure increases in the hydrogen storage system tank due to mass being transferred to it. Figure 6.2(c) shows the mass flow of the hydrogen and the cooling demand to cool the hydrogen to $-40°C$. As the system is fuelling with an APRR, the mass flow varies depending on the back pressure in the hydrogen storage system; this will be explained in more detail in Section 6.3. The cooling demand is a function of the mass flow and enthalpy. It is very similar to the mass flow curve, though it peaks earlier due to a higher enthalpy. The enthalpy is highest at the start and decreases during the fuelling as mass is leaving the tank at the hydrogen fuelling station, reducing the pressure and decreasing the temperature. Figure 6.2(d) shows the gas temperature development in both the tank at the hydrogen fuelling station and the tank in the hydrogen storage system during a period of an hour starting with a fuelling. The temperature either increases or decreases rapidly during the fuelling. The thermal conductivity of the carbon fibre wrapping is low [27], and therefore it takes a long time before the tanks are back at ambient conditions after the fuelling (with no mass leaving or entering). Steel tanks would have a higher heat conduction and therefore faster return to ambient, but due to the high pressures of > 500 bar, it is not possible to use steel tanks.

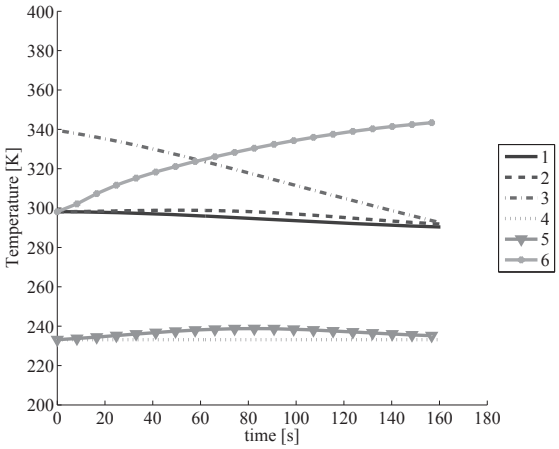

(a) Temperatures in the system

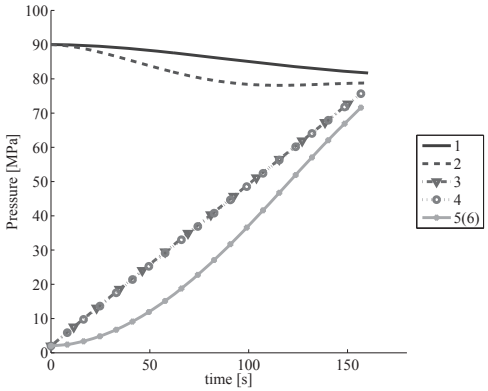

(b) Pressures in the system

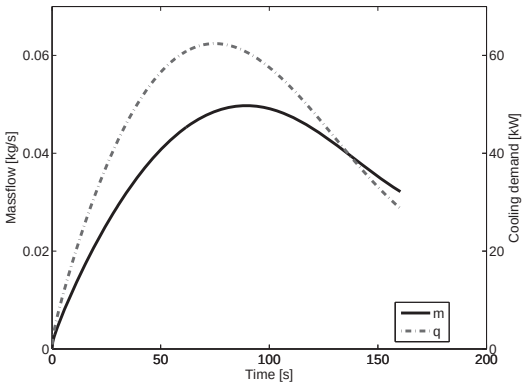

(c) Mass flow and cooling demand

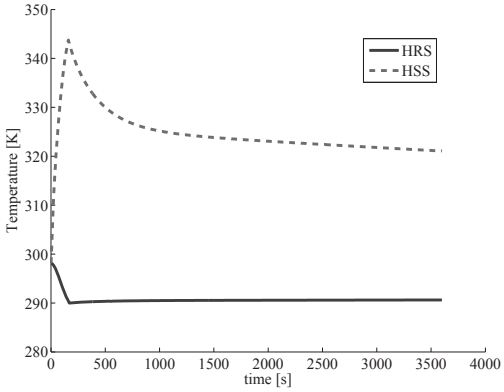

(d) Temperature development in tank at the hydrogen fuelling station (HRS) and the temperature in the tank in the hydrogen storage system (HSS) for a fuelling and 1 hour afterwards

Figure 6.2: The thermodynamics of hydrogen fuelling.

6.3 Effect of pressure loss in a hydrogen storage system on the hydrogen fuelling station

As shown in Figure 6.1 the system consists of the hydrogen fuelling station and the hydrogen storage system. J2601 prescribes the outlet conditions of the hydrogen at the hydrogen fuelling station: the pressure increase should be the APRR, 28.2 MPa/min and the temperature $-40°C$ for an A70 station at an ambient temperature of 25°C filling from 2 MPa to 70 MPa. This means that the pressure losses in the hydrogen fuelling station do not influence the fuelling

of the hydrogen storage system. The pressure losses of the hydrogen storage system, however, have an influence on the hydrogen fuelling station.

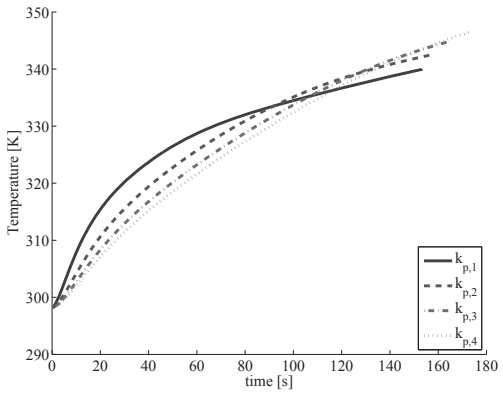

(a) Higher pressure loss in the vehicle results in a larger temperature rise in the hydrogen storage system tank.

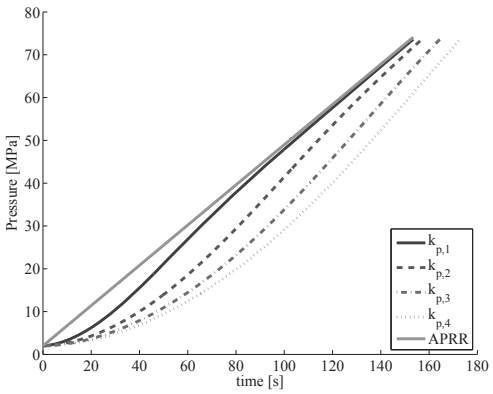

(b) Higher pressure loss in the vehicle results in longer filling times before the pressure has reached the target pressure in the tank.

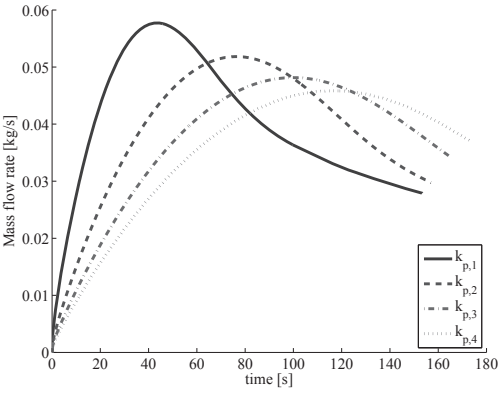

(c) Higher pressure loss in the vehicle results in lower peak mass flow and the mass flow peaks later during the filling.

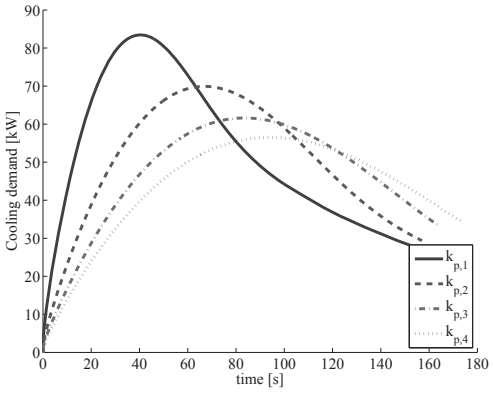

(d) Higher pressure loss in the vehicle results in lower peak cooling demand.

Figure 6.3: The effect of the pressure loss in the hydrogen storage system (vehicle) on the hydrogen fuelling.

The tank in the vehicle and the pressure losses between the hydrogen fuelling station and the tank in the hydrogen storage system determine the mass flow rate and the fuelling time. Figure 6.3 shows the pressure, temperature, mass flow and cooling demand for four different pressure losses in the hydrogen storage system. The pressure loss is calculated from eq. 3.31, where k_p values have been chosen to show almost no pressure loss across in the vehicle resulting in the highest allowed mass flow rate of 60 g/s and to illustrate the highest allowed pressure loss of 20MPa in the hydrogen storage system. Both limits are ac-

cording to J2601 [34]. The dimensionless pressure loss values are $k_{p,1} = 0.035$, $k_{p,2} = 0.19$, $k_{p,3} = 0.35$ and $k_{p,4} = 0.55$; they express the total pressure loss in the hydrogen storage system and have been chosen to show the boundary limits according to the SAE TIR J2601 and two fuellings which are in-between the boundary conditions. Figure 6.3(c) shows the mass flow for different pressure losses in the hydrogen storage system. The figure shows that the peak mass flow is lower at high pressure losses; the total mass when fuelling to the same pressure is slightly less than fuelling with low pressure loss (not shown here). This is due to the temperature inside the hydrogen storage system tank shown in Figure 6.3(a) which increases relatively to the pressure loss increase shown in Figure 6.3(b). As the fuelling ends at the same pressure, the density of the warmer hydrogen will be lower, resulting in a lower total mass. The fuelling time is also increased with increased pressure loss in the hydrogen storage system. Intuitively, one would expect it to be the same because the APRR is the same. However, due to the increased pressure loss in the hydrogen storage system, the pressure rise in the tank is slower, as shown in Figure 6.3(b). The APRR is set at the nozzle and so the pressure loss in the hydrogen storage system will affect the pressure rise in the hydrogen storage system tank. Figure 6.3(d) shows the cooling demand as a function of the pressure loss, it is worth noting that the peak cooling demand is lower as the peak mass flow rate is lowered. In this example, the peak cooling demand becomes 35% lower for the highest pressure loss. Such change is significant, because it can lower the refrigeration requirements in a facility for high pressure loss vehicles (though it most likely will have to service vehicles with lower pressure loss as well). The pressure drop in the hydrogen fuelling station only affects the tank at the hydrogen fuelling station. The pressure and the volume of the tank at the hydrogen fuelling station have to be dimensioned so that the pressure is always higher before the reduction valve than after. The pressure at the end has to be high enough to overcome the back pressures in the system.

6.4 Effects of using cascade fuelling

This section describes how the model can be used for energy and time optimization for the fuelling of a hydrogen vehicle. The two systems which are used to show the optimization can be seen in Figure 6.1 and Figure 6.4. The only difference between the two systems is the number of tanks at the hydrogen fuelling station. In the system in Figure 6.1 there is one tank at $90MPa$, and in the fuelling station in Figure 6.4, there are three tanks at 45, 65 and 91 MPa, respectively. The second system is also generally known as a cascade filling.

The thermodynamics of the cascade filling system can be seen in Figure 6.5. Figure 6.5(b) shows the pressures in the system. The pressure out of the tanks at the hydrogen fuelling station is lower for the two first tanks in the cascade

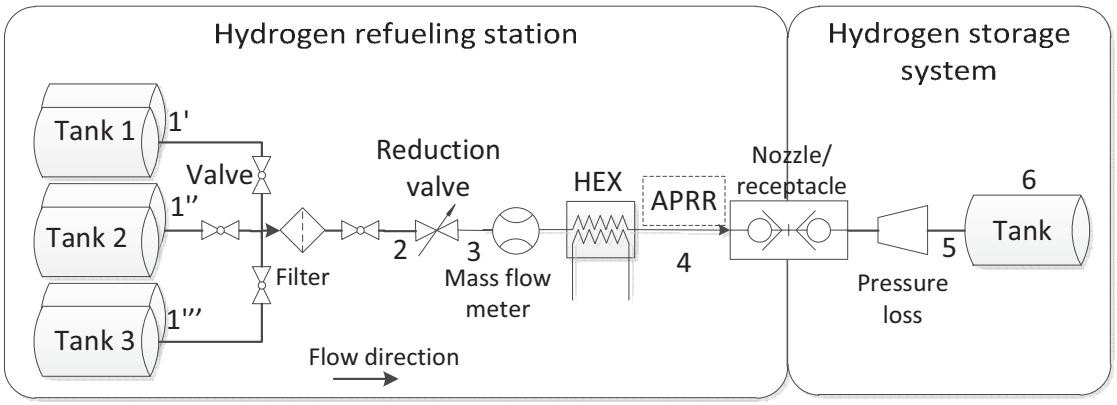

Figure 6.4: Cascade fuelling station.

filling, which naturally results in a lower pressure decrease across the reduction valve. Comparing to Figure 6.2(b), it can be seen that the pressures after the reduction valve are the same for both one tank and three tanks. As the pressure difference between the tank at the hydrogen fuelling station and the hydrogen storage system tank is lower, the heat up of the hydrogen due to the Joule-Thompson effect is lower. This is shown in Figure 6.5(a). Comparing the pressures, temperatures and mass flow in the hydrogen storage system with the ones in Figure 6.2, it can be seen that the cascade filling has no effect on the hydrogen storage system; this proves the point from Section 6.2 that the design of the hydrogen fuelling station does not influence the hydrogen storage system. Figure 6.5 generally shows the cascade filling and the thermodynamics; it can be seen that multiple tanks lower the pressure losses and the heat up of the hydrogen without compromising the fuelling of the tank in the hydrogen storage system. Figure 6.5(c) shows the mass flow and cooling demand for the cascade filling. Comparing to Figure 6.2(c), the size of the peak cooling demand is the same for both fillings, but for the cascade fuelling, it peaks much later than for the one tank filling, even though the mass flow is the same. The reason is that the pressure and the temperature when shifting to the last tank in the cascade filling are higher at that time than for the one tank filling. The enthalpy is therefore higher, and a higher cooling demand is needed at that time with three tanks than with one tank.

6.5 Optimization using cascade fuelling

Fuelling the high-pressure tanks at the hydrogen fuelling station is necessary; this is typically done from low-pressure tanks at $20MPa$ using a booster to reach the final pressure. Figures 6.6(a) and 6.6(b) show the two different scenarios. The fuelling of the tanks is done in order to receive the same mass as

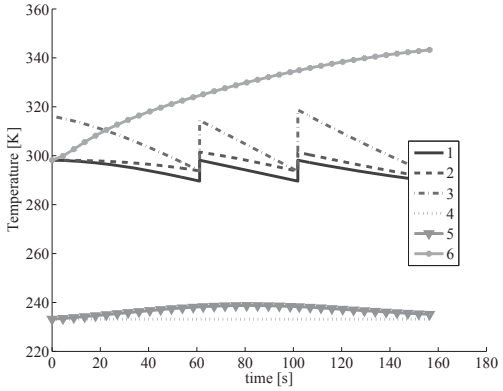

(a) Temperature development

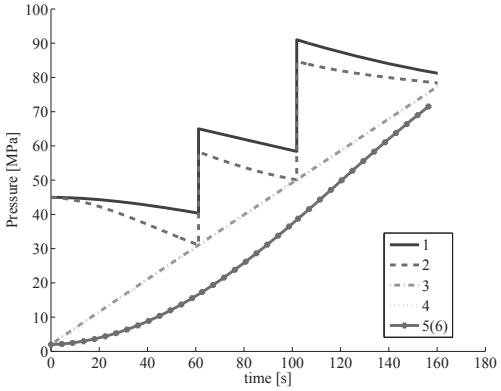

(b) Pressure development

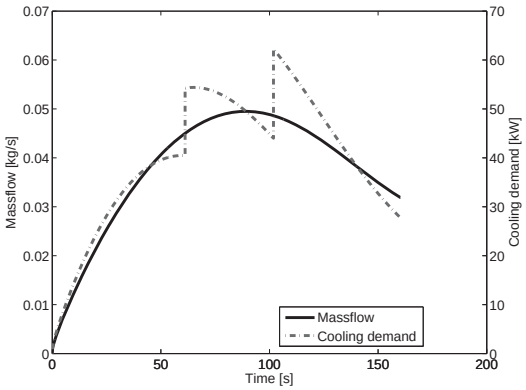

(c) Mass flow and cooling demand

Figure 6.5: The thermodynamics of a cascade filling.

before the fuelling of the vehicle started. So the total mass filled back into the three tanks and the one tank case is the same. The compared parameters are the energy consumption of the booster and the fuelling time. The fuelling of the tanks is started when the fuelling of the vehicle has finished. The total volume of stored hydrogen is the same for both systems, $3m^3$ distributed with $1m^3$ in each tank for the three tank system. Table 6.1 shows the difference in energy consumption of a booster (high-pressure compressor) and the running time of the compressor. The total mass which needs to be stored in order to do a 7 kg fuelling of a vehicle is 138.85 kg at 90 MPa or 112.3 kg distributed in three tanks of 45 MPa, 65 MPa and 91 MPa pressure, respectively. The fuelling only requires approximately 6 kg. This means that the rest of the hydrogen only has the function to keep the pressure up in the tanks and can therefore not be used for fuelling. The savings in the total hydrogen mass between one and three tanks at the hydrogen fuelling station is thus 26.6 kg, approximately

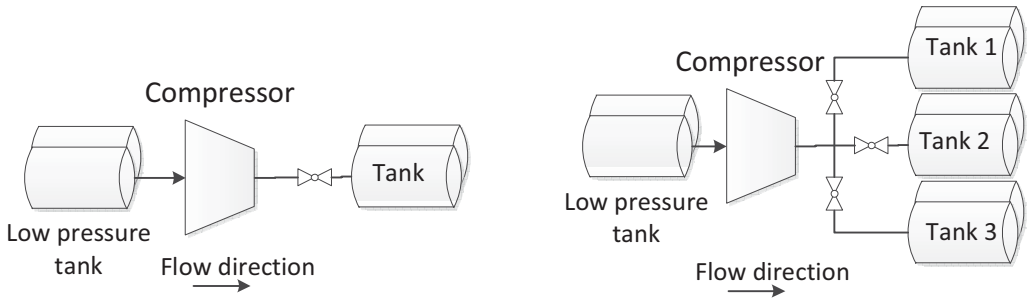

(a) Fuelling from low-pressure tanks at the hydrogen fuelling station to high-pressure tank.

(b) Fuelling from low-pressure tanks at the hydrogen fuelling station to three high-pressure tanks.

Figure 6.6: Sketch of the fuelling setups of the tanks at the hydrogen fuelling station.

Table 6.1: Comparison between energy and time consumption

	1 tank	3 tanks	Savings
Total mass [kg]	138.85	112.3	26.6
Power [kWh]	1.22	1.01	0.21
Time [s]	508	485	23
Total cooling [kWh]	1.93	1.70	0.23
Peak cooling [kW]	61.7	65.1	-3.1

20% of the total mass stored in the one tank system. The power needed to run the compressor for fuelling the three tanks instead of one is approximately 17% lower. The time difference of fuelling one or three banks is 23s corresponding to saving 5% time when fuelling the three-tank system. The refrigeration facility is also influenced by the number and the pressure in the tanks at the hydrogen fuelling station. Using three tanks gives a savings of 12% of the cooling capacity needed for one tank, though the peak cooling demand is approximately 5% higher using the cascade filling. From a cooling perspective it is worth noticing the lower total cooling capacity. The peak cooling demand is difficult to compare as it depends on the back-pressure in the hydrogen storage system as shown in Figure 6.3(d) and therefore depends on the vehicle.

6.6 Summary

A model of a fuelling station has been made with the hydrogen fuelling library for Dymola. The model has been used to show the thermodynamics of a simple system fuelling a vehicle. Pressure, temperature and mass flow have been

analysed, and it has been shown that the pressure loss in the hydrogen storage system has a significant impact on the hydrogen fuelling process in terms of mass flow, cooling demand and storage dimensioning. The cooling demand is 35% lower with a high pressure loss than with almost no pressure loss in the hydrogen storage system. The pressure losses and the design of the station do not influence the fuelling into the hydrogen storage system as long as the protocol J2601 is fulfilled by the station. The difference between fuelling from one tank and three tanks in a cascade setup at the hydrogen fuelling station has been shown from a thermodynamic point of view. The time used for a whole cycle at the fuelling station, fuelling a vehicle and afterwards fuelling of the high-pressure tanks at the hydrogen fuelling station, is 5% lower with the cascade filling. Furthermore the cascade filling used 12% less energy for cooling and 17% less energy for compression with the given compressor equations. Additional components can be added to the model, in order to simulate and predict a complete fuelling event (e.g., heat transfer and pressure losses from the interconnecting tubing and components). The current model can be used for design optimization of hydrogen fuelling stations. Dynamic models of the main components in a hydrogen fuelling station and the vehicle's storage system have been made in Dymola. The models can be connected in order to simulate a complete hydrogen fuelling station.

Chapter 7

Optimization of cascade fuelling systems

This chapter contains an analysis of cascade fuelling with respect to energy consumption. A parameter variation of the number of tanks in the cascade system is performed, including the volume of the tanks and the initial pressures. The energy reduction between the different parameter variations is analysed with respect to a reference system.

The presented results are also discussed in the conference paper from SEEP2013; Paper IV in Appendix, and in Rothuizen et al. [33]: Optimization of the overall energy consumption in cascade fueling stations for hydrogen vehicles.

7.1 Introduction

Hydrogen fuelling systems at the present time typically consist of a cascade system fuelling station where hydrogen is stored at different pressure levels. The number of tanks and the volumes of the tanks are typically designed for one vehicle fuelling, as high-pressure tanks have a high cost to volume ratio. Analysis of operational energy savings by adding more tanks to the system and analysis of the sizes and pressures of the tanks have not been conducted.

The first part of this chapter explains the principles of a full fuelling cycle.

This includes fuelling a vehicle from the cascade system with subsequent fuelling of the tanks in the cascade system from hydrogen storage at low pressure. This gives an understanding of the complete system in a hydrogen fuelling station. The primary focus is on the hydrogen storage system at the station, and less attention is paid to the fuelling process which was the primary focus in Chapter 6.

The second part explains the analyses that are conducted and shows the values used for the parameter variations. Furthermore, the section also considers the thermodynamics of a complete fuelling cycle.

An energy analysis is conducted on the basis of the parameter variation of the tanks. The first study contains an analysis of the effect of the number of tanks on the energy consumption for a whole fuelling cycle. The second study shows the additional energy savings by decreasing the tank volumes in the cascade system. The third analysis considers the pressures in the tanks at the cascade system. The pressures in the tanks are optimized by having the same pressure ratio between each tank. The energy savings is shown as additional energy savings in the study where the number of tanks were considered. This section shows the influence of the cascade systems tanks on the energy consumption of a whole fuelling cycle.

7.2 System design

The model used for simulation of hydrogen fuelling complies with the protocol by the Society of Automotive Engineers, TIR J2601. The fuelling system that is modelled is shown in Figure 7.1. The system is separated into two main sections, the fuelling station and the hydrogen vehicle. The hydrogen fuelling station is divided into two parts, the fuelling system used for fuelling the vehicle and the compressor system used to fuel the tanks at the station. The main fuelling system consists of a number of high-pressure tanks set up in a cascade system for fuelling the vehicle and the components used to assure the fuelling comply with J2601. The compressor system consists of a medium pressure bank of tanks, a compressor and a heat exchanger that removes the heat after the compression. A short walk-through of a fuelling follows. The vehicle pulls up to the station and is connected at the nozzle. The fuelling station measures the pressure of the hydrogen in the vehicle before it sends in a pulse where the mass is known, the pressure in the vehicle is measured again, by knowing the pressure rise and the mass which was in the pulse, the size of the tank can be determined. The pressure in the tank and the ambient temperature are then used to set the average pressure ramp rate that is to be used for the fuelling. The volume of the tank indicates how much the reduction valve should open when the fuelling starts, and during the fuelling a control system decides the

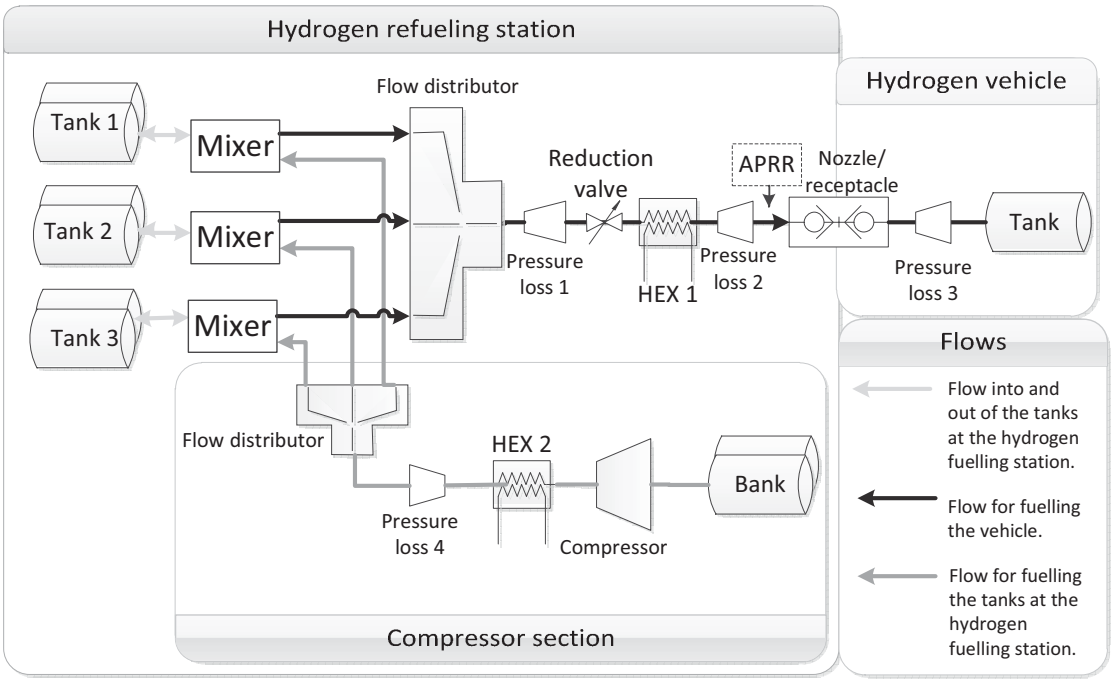

Figure 7.1: Sketch of a hydrogen fuelling station with three tanks in a cascade setup and a compressor section to fuel the station.

valve opening. The system now opens for tank 1 and lets the hydrogen flow to the vehicle tank. At the same time the compressor starts up and delivers hydrogen to the stream going from tank 1 to the vehicle. If the mass flow from the compressor is larger than needed for the fuelling, the excess hydrogen is stored in the tank. When the pressure across the reduction valve reaches a certain limit, the station changes to tank 2 which is at higher pressure than tank 1 and the fuelling continues. The compressor fills tank 1 back to starting mass/pressure before it starts filling tank 2. When the pressure in tank 2 becomes too low to keep up the average pressure ramp rate, the station changes to tank 3 which is at a higher pressure than tank 2. When the outlet of the station reaches the final pressure, the fuelling of the vehicle is aborted. The compressor keeps running until all the tanks at the station are back to starting mass/pressure. The process of fuelling the vehicle and bringing the tanks at the station back to starting pressure, is referred to as: a complete fuelling cycle. As one may have noticed, the pressure losses in the system are collected at four different strategically selected places. There is a pressure loss before the reduction valve (pressure loss 1) which takes into account the tubing and valves. This pressure loss influences the pressure into the reduction valve and thereby when to change tank in the cascade system. Decreasing the pressure loss before the reduction valve increases the time before shifting from the first tank. The second pressure loss (pressure loss 2) is between the reduction valve and the

average pressure ramp rate (APRR); this takes into account the pressure loss in the heat exchanger and some valves. This is the pressure loss the reduction valve needs to adjust for in order to have the average pressure ramp rate at the nozzle. The third pressure loss (pressure loss 3) is the pressure loss in the vehicle. Pressure loss 3 influences the mass flow of the fuelling; low pressure loss gives an earlier and higher peak in mass flow. When increasing the pressure loss in the vehicle, the peak mass flow rate is decreased and will peak later in the fuelling. This has a large influence on the station as an early mass flow peak results in more mass being drawn from the tanks at lower pressures, and with a late mass flow peak more mass is drawn from the tanks with higher pressure. The last pressure loss (pressure loss 4) accounts for the pressure losses between the compressor and the mixer. The compressor has to make up for this loss when delivering hydrogen. The mixers are ideal mixers where the flow from the compressor can mix with the mass flow for the fuelling of the vehicle. The flow distributor controls the flow; only one flow can pass through at a time. The heat exchanger at the outlet of the fuelling system cools the hydrogen to the desired temperature set by the fuelling protocol J2601. The heat exchanger after the compressor cools the hydrogen to the same temperature as ambient. For the model the station can have up to eight tanks in the cascade system. The extra tanks are connected like tank 1, 2, and 3 in Figure 7.1.

7.3 Analysis and discussion

The following section presents and discusses the results obtained from the energy optimization of the cascade system at the hydrogen fuelling station. Table 7.1 contains the volumes used for the tanks and Table 7.2 contains the pressures used. For the parameter variation of the tank sizes and pressures, the given volumes and pressures are the ones for which it was not possible to go further down in volume or pressure.

7.3.1 Simulation comparisons

The three different scenarios that are compared in this section are first, the effect of adding more tanks to the cascade system at the station. This analysis is done for both the maximum allowed pressure loss in the vehicle and for a low pressure loss in the vehicle. Second, the volume of the tanks is changed, decreasing the volume as the pressure increases. Third, there is a variation of the pressures in the tanks, lowering the pressures to a minimum in order for the fuelling to take place. The first parameter variation shows the effect of adding another tank to the cascade system, the second parameter variation shows the effect of decreasing the volume of the tanks, and the third parameter variation shows the gain by having the minimum required pressures in the tanks. The trade-off between power consumption, tank size and tank pressures

is interesting not only from an energy point of view, but also from an economical point of view, as the investment cost of the tanks increases with increasing volume and pressure. Though, it is up to the manufacturer to judge where the best trade-off is between energy consumption and investment costs of tanks. This paper shows the trends and can therefore not be used for the final sizing of fuelling stations in industry. The pressures and sizes reached in this paper are specific for the pressure losses at this station, and all stations should be evaluated individually to find the best tank size/pressure setup. However, the energy savings should be of the same magnitude for all stations with a similar layout. When adding more tanks to the fuelling station, the volume of each tank is 1 m^3 and the pressures are as follows: when only one tank is present, it is 950 bar; for two tanks it is 400 and 950 bar, and for more than two tanks, the pressure is distributed in between 400 and 950 bar with equal pressure difference between each tank; this is shown in Table 7.2. The parameter variation of the tank sizes allows four different sizes to be used 0.25 m^3, 0.50 m^3, 0.75 m^3 and 1 m^3. The variation is done by decreasing the tank volumes to a minimum starting with the highest pressure tank, then moving down gradually decreasing the volumes until the fuelling of the vehicle just can succeed. The final volumes can be seen in Table 7.1. The third parameter variation with constant volume of the tanks of 1 m^3 allows the pressures to be set between 350 and 950 bar. The main constraint is that the pressure, when the fuelling of the vehicle is finished, is between 10 and 20 bar across the reduction valve. Furthermore, all the tanks in the cascade system have to be used. The pressures for this variation were tested using both the same pressure difference between each tank and then using the same pressure ratio between each tank in the cascade system instead. Having the same pressure ratio gives a decreased pressure difference between each tank step in the cascade system. It was found that using the same pressure ratio between tanks next to each other, gave the lowest energy consumption. Therefore all results shown are with the equal pressure ratios.

Other system assumptions

The pressure loss in the vehicle is the highest allowed, according to the SAE TIR J2602, which peaks at 200 *bar* during the fuelling. This pressure loss gives the most demanding fuelling of the vehicle for the station in terms of pressures and sizes of the tanks. Using a lower pressure loss will fill a larger mass to the vehicle, but the mass flow will peak earlier and be lower towards the end of the fuelling. This results in more mass being drawn in the beginning of the fuelling from the tanks at lower stages in the cascade system; thereby the demand for hydrogen from high pressure tanks is lower, the decrease in pressure is less and hence less mass is drawn from these tanks. So if the station can fulfil this fuelling of a vehicle with high pressure loss, it can satisfy all fuellings. This will be explained further in Section 7.3.2. The two heat exchangers in the system

Number of tanks at station	Scenario	Tank 1 (m^3)	Tank 2 (m^3)	Tank 3 (m^3)	Tank 4 (m^3)	Tank 5 (m^3)	Tank 6 (m^3)	Tank 7 (m^3)	Tank 8 (m^3)
1	1, 3	1							
	2	1							
2	1, 3	1	1						
	2	1	0.75						
3	1, 3	1	1	1					
	2	1	0.75	0.50					
4	1, 3	1	1	1	1				
	2	1	1	0.75	0.5				
5	1, 3	1	1	1	1	1			
	2	1	1	0.75	0.25	0.25			
6	1, 3	1	1	1	1	1	1		
	2	1	0.50	0.25	0.25	0.25	0.25		
7	1, 3	1	1	1	1	1	1	1	
	2	0.25	0.25	0.25	0.25	0.25	0.25	0.25	
8	1, 3	1	1	1	1	1	1	1	1
	2	0.25	0.25	0.25	0.25	0.25	0.25	0.25	0.25

Table 7.1: Volumes of the tanks. Scenario 1 is increasing number of tanks, scenario 2 is decreasing tank volume and scenario 3 is decreasing the pressure of the tanks.

Number of tanks at station	Scenario	Tank 1 (bar)	Tank 2 (bar)	Tank 3 (bar)	Tank 4 (bar)	Tank 5 (bar)	Tank 6 (bar)	Tank 7 (bar)	Tank 8 (bar)
1	1, 2	950							
	3	925							
2	1, 2	400	950						
	3	550	925						
3	1, 2	400	675	950					
	3	350	650	875					
4	1, 2	400	583	767	950				
	3	350	551	712	840				
5	1, 2	400	538	675	813	950			
	3	350	503	630	737	825			
6	1, 2	400	510	620	730	840	950		
	3	350	475	582	674	753	820		
7	1, 2	400	492	583	675	767	858	950	
	3	350	455	548	629	699	761	815	
8	1, 2	400	479	557	635	714	793	871	950
	3	350	441	522	594	658	715	765	810

Table 7.2: The pressures used for the comparisons. Scenario 1 is increasing number of tanks, scenario 2 is decreasing tank volume and scenario 3 is decreasing the pressure of the tanks.

are connected to a refrigeration facility, which for the heat exchanger after the compressor (HEX2) has a $COP = 2$ and after the reduction valve (HEX1) has a $COP = 1.5$. The COPs have been conservatively chosen using the confidential work of J. Jensen [16]. The compressor has a peak mass flow capacity of 0.015 kg/s, which is obtained when the pressure ratio is close to one. The peak mass flow corresponds to the largest hydrogen compressors which are presently available.

7.3.2 General thermodynamics of the system

To explain the properties of the system further, a complete cycle for a three-tank cascade fuelling station is used as an example. Figure 7.2 shows the mass flows for a fuelling with a high pressure loss (HPL) and for a low pressure loss (LPL) fuelling. It is clear that the mass flow peaks later when a large pressure loss is present in the vehicle. Furthermore, the total mass fuelled is

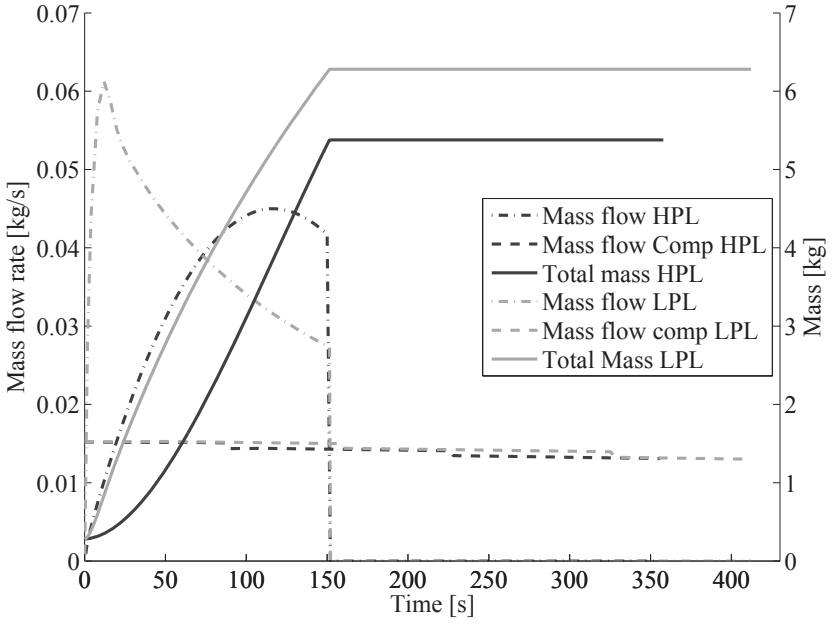

Figure 7.2: The mass flows and total mass for a fuelling of a vehicle with both low and high pressure losses.

less with a high pressure loss than with a low pressure loss; this is because the fuelling finishes when the pressure at the outlet of the station reaches a certain value. Therefore the pressure is higher in the tanks when the pressure loss in the vehicle is lower. The mass flow through the compressor decreases as it shifts the tank to fuel. For the station to recover after fuelling a low pressure loss vehicle, it takes longer time as more mass has been fuelled to the vehicle. It may seem contradictory to consider the high pressure loss fuelling as more mass is fuelled with low pressure loss, but when considering the pressures in the tanks at the station, it becomes clear why the higher pressure loss fuelling is of greater importance. Figure 7.3 shows the pressures in the system at the reduction valve, at the compressor outlet and at the nozzle (the average pressure ramp rate). The pressures into the reduction valve have two changes in pressure (the vertical parts of the lines); this is due to the change of tank in the cascade system. Considering the pressure into the reduction valve, the

low-pressure tank ends at lower pressure for fuelling a low-pressure vehicle compared to a high-pressure vehicle, and it changes to the medium-pressure tank earlier; hence, more mass has been drawn from the low-pressure tank. The medium-pressure tank delivers approximately the same amount of mass as

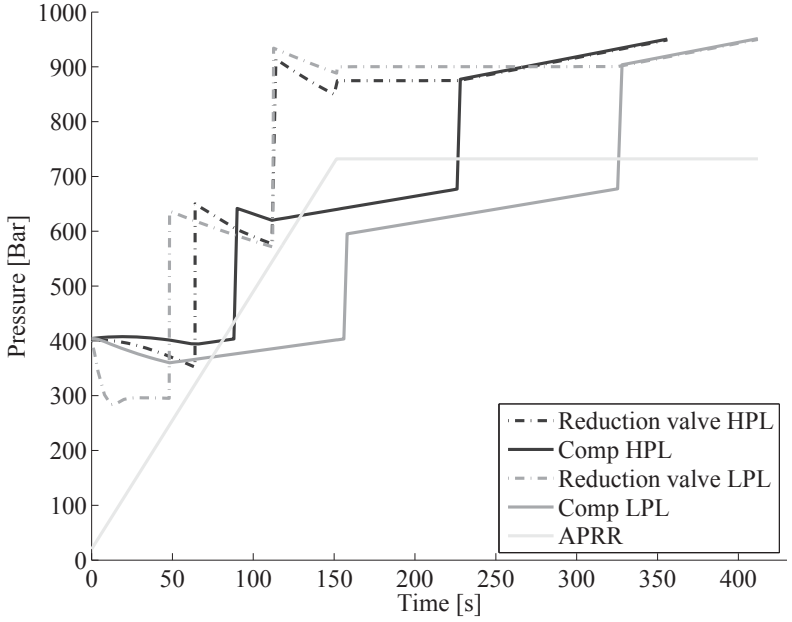

Figure 7.3: The pressures for a fuelling of a vehicle with both low and high pressure loss.

they end at the same pressure. The high-pressure tank for the low pressure loss vehicle ends at a higher pressure than for a high pressure loss vehicle fuelling; hence, less mass has been drawn from it. When deciding the pressures in the tanks at the fuelling station, it is most energy-efficient if the pressure into the reduction valve is close to the outlet of the reduction valve when the fuelling finishes; hence, the compressor has not used more work to compress hydrogen to a higher pressure than necessary. Figure 7.4 shows the pressure losses in the system with reference to Figure 7.1. The pressure loss, pressure loss 3 HPL, uses the second y-axis in Figure 7.4. The sudden changes in pressure loss 2 are due to the change of tank at the station for the fuelling. After 152 seconds the only place there is a pressure loss is between the compressor and the tank it is fuelling, as the fuelling of the vehicle has finished. The fuelling in Figure 7.3 is therefore not the most energy-effective, as there are more than 100 bar difference between the reduction valve and the average pressure ramp rate, and the pressure loss between the reduction valve and the nozzle is only 17 bar.

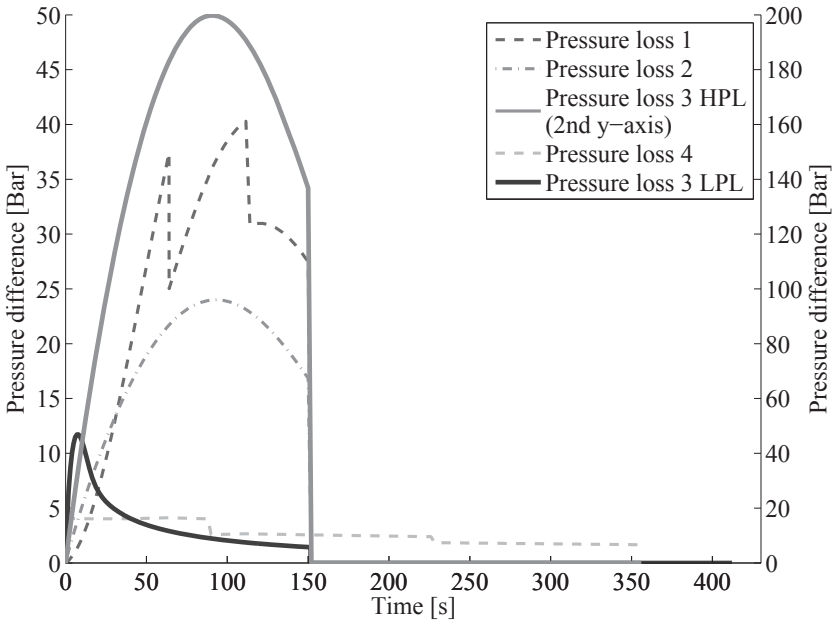

Figure 7.4: The pressure losses for a fuelling of a vehicle with high pressure loss and for a vehicle with low pressure loss.

7.3.3 Results

The first simulation has a constant volume of the tanks of 1 m^3 and the tanks vary in number from 1 to 8 tanks. This is the reference case for further comparisons with variable tank size and with variable pressure. The energy consumption of a complete cycle is shown in Figure 7.5(a) for fuelling of a vehicle with a low pressure loss and a high pressure loss. The energy consumption is decreasing, approaching an exponential function as one more tank is added to the fuelling station. It is clear that using a cascade system compared to one tank is favourable from an energy consumption point of view. The hydrogen which is fuelled to the vehicle has an energy content of approximately 240 kWh, and the largest amount of energy used for a full cycle with a high pressure loss vehicle is 5.97 kWh, which is 2.5 % of the energy fuelled. Figure 7.5(a) also shows that the energy consumption for a complete fuelling cycle with a low pressure loss vehicle changes from being more energy consuming at three tanks to being less at four tanks. This fact proves the point that even though more mass is fuelled for the lower pressure loss case, it is taken from the lower pressure tanks. The distribution of the energy consumption between the components is shown in Figure 7.5(b). The compressor accounts for more than 50 %, and the refrigeration facility for the heat exchanger after the compressor for approximately 30 %; the lowest energy consumption is for the cooling of

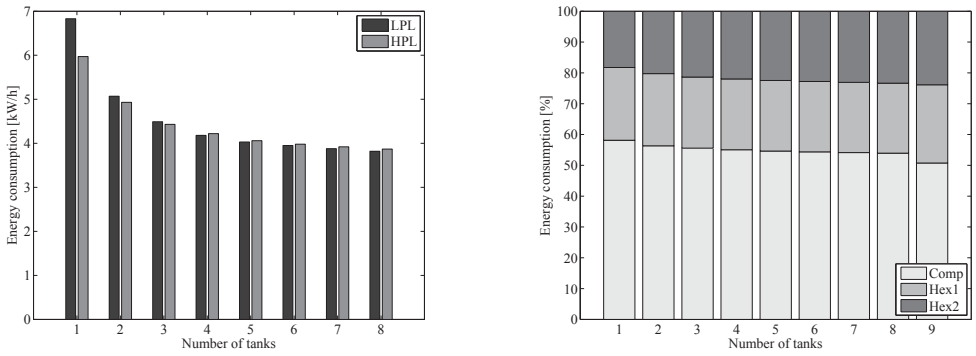

(a) Energy consumption as a function of tanks in the cascade system, shown for a low pressure loss (LPL) and a high pressure loss (HPL) in the vehicle.

(b) Energy distribution between the compressor and the cooling facilities.

Figure 7.5: The thermodynamics of hydrogen fuelling.

the hydrogen at the exit of the station accounting for approximately 20 %. Figure 7.6 shows the energy savings when adding more tanks to the cascade system; the savings are shown for each component as well as the total savings. The savings from going from one to two tanks is 18 %, and the savings for the compressor which accounts for more than 50 % of the total energy used is 20 %. The energy savings by adding another tank to the cascade system approaches an exponential equation. Figure 7.6 shows that the energy savings is significant until three tanks are reached in the cascade system. From four to five tanks the savings is approximately 5 %, and after going from four to five tanks the energy savings by adding an extra tank is less than 3 % for each extra tank. It should be noted that for the cascade system using 6, 7 and 8 tanks, the high-pressure tank of 950 bar was not in use for the vehicle fuelling, as the other tanks could satisfy the demand. This will be examined further when studying the effect of reducing the tank sizes and changing the pressures, so the pressure difference in the cascade system does not necessarily have an even pressure difference between them. Decreasing the sizes of the tanks will have an effect on the energy consumption of the fuelling. First, by lowering the volume, the final pressure in the tanks will be lower after having fuelled the vehicle, which gives a lower pressure ratio for the compressor at the beginning of refuelling the cascade system. Second, by decreasing the volume of the tanks and thereby decreasing the pressure faster during the fuelling of a vehicle, the cascade system will change tank earlier. This results in more mass being taken from the higher pressure tanks, which increases the energy consumption when the compressor has to fuel the station. The minimum size of tanks which can be obtained with the given pressures can be seen in Table 7.1. For four and five tanks, the second tank has to be 1 m^3 which might seem strange comparing to

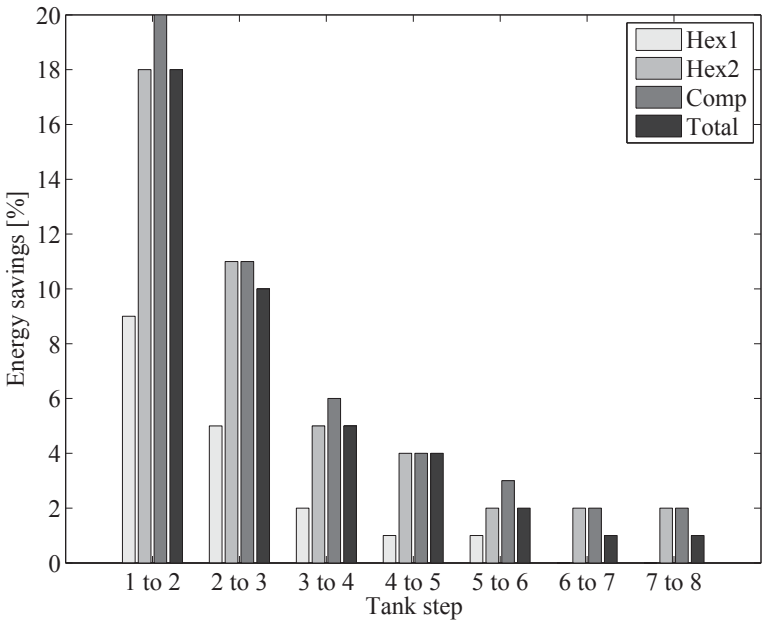

Figure 7.6: Energy savings by adding an extra tank to the fuelling station

three tanks where the medium-tank is 0.75 m^3, but that is because the pressure is lower in the medium range tank comparing with three tanks and the high-pressure tanks are smaller; see Tables 7.1 and 7.2. Figure 7.7 shows the energy savings compared to the corresponding system with 1 m^3 tanks. For cascade systems up to five tanks, the energy savings is between 1 % and 2.7 %; when having more than five tanks in the cascade system, the energy consumption increases. This is a result of not all of the tanks being used in the reference case with a constant volume and linear pressure distribution. The compressor never had to fuel up to 950 bar, but by decreasing the volumes, all the tanks are taken into use, which results in an energy increase between 1 % and 1.6 %. The third parameter variation is the pressure in the tanks. This is done for tanks with a constant volume of 1 m^3. Figure 7.8 shows the energy saving compared to the reference scenario. The energy savings are for all the cascade systems between 4 % and 5 %; for a single tank, the savings is lower than 2.5 %. It is obvious that the largest savings is gained from the compressor section; this is because the pressures have been lowered. It results in a lower compression ratio and a decreased temperature out of the compressor, meaning that less energy is required for compression and there is a lower cooling demand. The pressures in the tanks were both lowered using the same pressure difference between each tank, but with different boundary pressures and by having the same pressure ratio between each step with different boundary pressures. It was found that using 350 bar as the lower pressure when there are three tanks or more in the

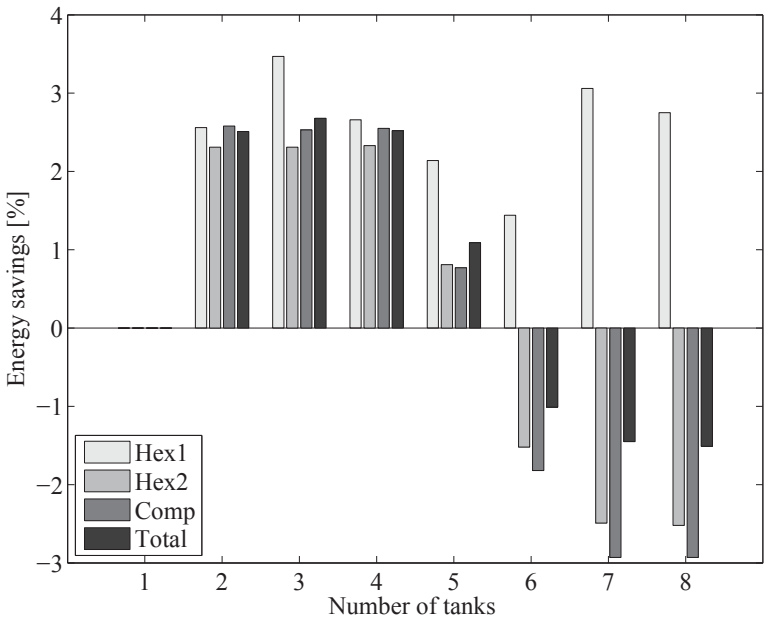

Figure 7.7: The energy difference for decreasing the tank volume.

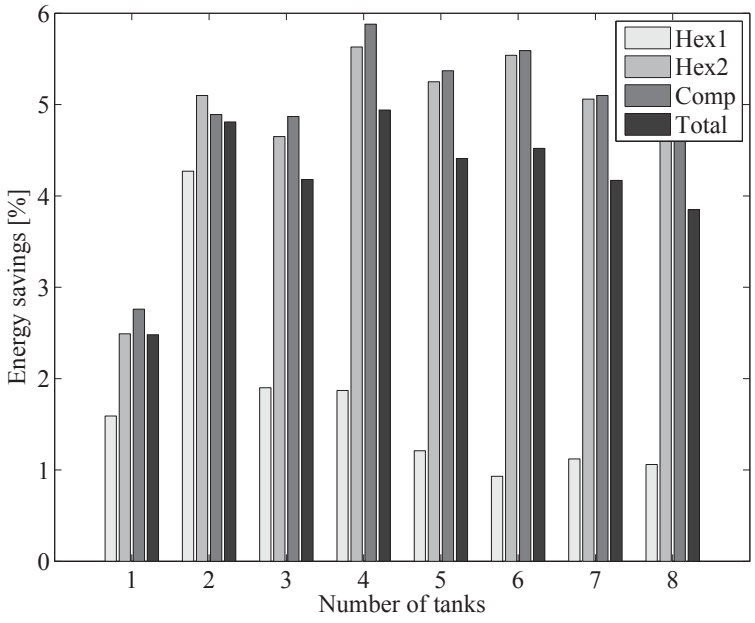

Figure 7.8: The energy difference when optimizing the pressure in the tanks.

cascade system and having the same pressure ratio between each step in the cascade system, gave the lowest energy consumption.

7.3.4 General considerations

The results show that the design of the hydrogen fuelling station influences the energy consumption, and thereby the operation costs, but it also influences the investment costs, as the high-pressure tanks are expensive and if the volume of the high-pressure tanks is decreased, the investment cost decreases. The trade-off between tank volumes, pressures and costs must be considered for the specific station taking into account the daily demand. With small tanks at the station, the mass stored is low and the possibility of doing another fuelling before the station has completed the cycle might not be possible. The larger tanks allow for more flexible use and the possibility to set the pressure in the tanks to cover more than one fuelling before recovery is necessary or the pressure can be lower in order to decrease energy consumption. The number of tanks at the station should be selected carefully, as the energy consumption approaches an exponential function. Too few will result in high energy consumption by the station, and too many does not have a significant energy savings compared to the investment costs of adding more tanks. It is therefore important to consider each station individually with respect to number of tanks, the volumes of the tanks and the pressure in the tanks. Having three or three tanks at the station in a cascade setup optimizing the pressures is probably the best solution. The energy savings by increasing the volume of the high-pressure tanks to 1 m^3 is approximately 2.5 %, but it also allows for more flexible use. Going from three to four tanks has an energy savings of 5 %, and it should be considered whether or not a fourth tank is worth it.

7.4 Summary

The thermodynamic models of the fuelling systems have been created using the hydrogen fuelling library. The models take into account the heat transfer from the tanks, the pressure losses in the system, the cooling demands and the compressor work, and the models comply with the protocol for fuelling hydrogen vehicles for personal transportation. The analysis was done in three steps, with first studying the effect of numbers of tanks in the cascade system with respect to the energy consumption of the individual component and the overall consumption. When going from one tank at the fuelling station to eight tanks, the energy consumption decreased, approaching an exponential function with the largest energy savings of 18 % per complete fuelling cycle going from one to two tanks at the station. The energy consumption starts levelling out when more than four tanks are present in the cascade system. The second analysis with varying tank volumes showed that decreasing the volume

of the tanks, with the largest decrease in the high-pressure tanks, gave a small reduction in the energy consumption when five tanks or fewer were used for the vehicle fuelling. By lowering the volume in the lower pressure tanks, more mass was drawn from the higher pressure tanks, which in principle mean a higher pressure ratio for the compressor, but because the volumes were decreased, the pressure ratio was decreased and the overall energy consumption lowered by 2.5 %. The third analysis showed that by having a constant volume of 1 m^3 in all the tanks and then changing the pressures in the tanks, starting from 350 bar and then increasing with an equal pressure ratio between consecutive tanks and ending at a pressure difference across the reduction valve between 10 and 20 bar, lowered the energy consumption by approximately 5 % compared to having fixed pressures between 400 and 950 bar. The analysis shows that an optimal number of tanks in a cascade fuelling system is three to four tanks and that it is important to consider the pressure loss in the station in order to determine the pressures that are used in the tanks. Furthermore, the hydrogen fuelling station should be designed according to filling a vehicle with a high pressure loss even though the mass fuelled is considerably lower than when fuelling a vehicle with a low pressure loss. This is because the mass flow curve is dependent on the vehicle's pressure loss. A lower pressure loss results in an earlier mass flow peak, and the extra mass which is fuelled is taken from the lower pressure tanks at the station. This results in every fuelling station that can handle a vehicle with a high pressure loss, being also able to handle a vehicle with a lower pressure loss. The results from this analysis can be applied to fuelling stations, but the values set as pressures and volumes are only valid with the pressure losses of this specific case. Therefore all hydrogen fuelling stations should be examined individually in order to obtain the optimal pressure and volumes of the tanks in the cascade system.

Chapter 8

Different fuelling station designs

This chapter analyses three different systems for fuelling hydrogen vehicles: a cascade fuelling system, a direct compression fuelling system and a direct compression system with a small buffer. The cascade system and the direct compression system with a buffer are following the fuelling protocol and the direct compression system is using an average mass flow instead. The cascade fuelling system and the direct compression system are both known technologies, but the direct compression with a small buffer is a new design.

8.1 Introduction

This chapter compares three different fuelling systems for fuelling hydrogen vehicles. The cascade system until now has been analysed in detail regarding thermodynamics, energy optimization and dimensioning of the tank volumes and pressures. In the literature, cascade systems are also the most common for the analysis of hydrogen fuelling systems [14] [9] [24] [29]. This is because it is the most common technology used by industry.

This chapter considers two alternative fuelling station designs to the cascade system. The two systems are direct compression and direct compression with a buffer. Each system, including the cascade system, is explained and advantages

and disadvantages are listed for each system with respect to the other two systems. This is done to outline the differences and similarities among the systems.

The thermodynamics of each system is explained and some repetition of the cascade system from Chapters 6 and 7 cannot be avoided. The thermodynamics of the two alternative systems is explained thoroughly, and similarities and differences to the cascade system are considered. Furthermore, the thermodynamics also explains how the fuelling is done with the specific system design.

The systems might work thermodynamically, but how do they perform from an energy point of view? The three systems are compared by first examining the energy consumed for a complete fuelling cycle and second by performing an exergy analysis to point out the components with the highest energy destruction.

8.2 System designs

The three systems considered are a normal cascade fuelling system that will be the reference case, a mixture between using a compressor directly and a small buffer tank, and a direct compressor fuelling. The cascade system and the direct compression system with a buffer both fuel according to the SAE J2601 [34]. The direct compression system uses an average mass flow rate. The analysis of the different designs has the goal of determining if other fuelling methods could be alternatives to cascade fuelling. The energy usage, the complexity of the systems and the complexity of the fuelling process are all considered.

8.2.1 Cascade fuelling

The fuelling process of a cascade fuelling system has been described in Chapter 7, but a short summary with respect to Figure 8.1 is described here. The vehicle is connected to the station, and the pressure and the size of the tank are registered by the fuelling station either mechanically by sending a mass flow into the tank and then measuring the pressure increase or by infra-red communication between the vehicle and the station. The fuelling of the vehicle proceeds by first opening between the bank and the vehicle until the pressure across the reduction has reached a certain value, e.g., 20 bar, then the station changes tank to tank 1 and proceeds the fuelling until the pressure across the reduction valve reaches its limit. The station then changes to tank 2 and proceeds the fuelling until the fuelling has finished. Either while the fuelling of the vehicle proceeds or afterwards, the compressor at the fuelling station fills up the tanks in the cascade system from the bank, before the next vehicle fuelling can be done. Typically the high-pressure tanks are limited in size and the "real" storage of the hydrogen is therefore in the lower pressure bank. The

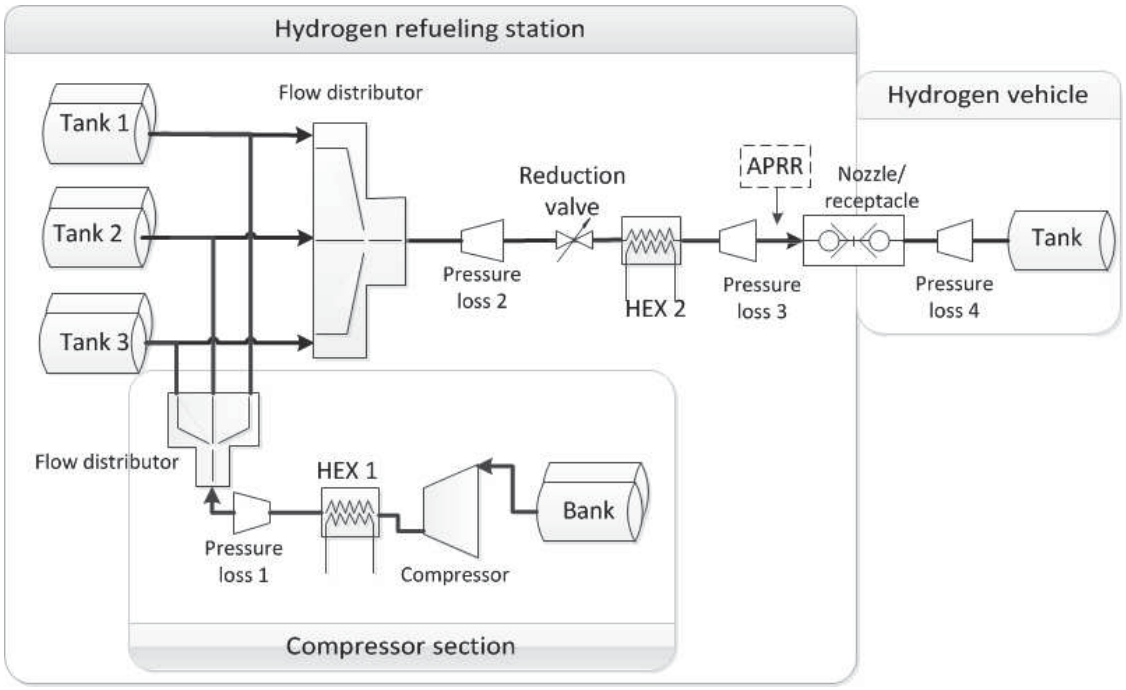

Figure 8.1: Sketch of a hydrogen fuelling station with three tanks in a cascade setup and a compressor section to fuel the station.

advantages of the cascade system are:

- Well known technology
- Simple operational strategy
- Continues availability of high-pressure hydrogen(operational during a power outage)
- Smaller compressor

The technology is at the moment used for all hydrogen fuelling stations being built and it has shown itself to work effectively. The operational strategy can be simple as the reduction valve controls the whole system, and the tanks at the station are changed according to the measurement from it. The cascaded system also has the benefit of having high-pressure hydrogen stored at all times, which means that if the electricity fails it is still operational to fuel a vehicle, though it should be done very slowly if no cooling is available. The compressor for fuelling the cascade system can be dimensioned according to a specified allowed recovery time. The downsides of cascade fuelling are:

- Compression of hydrogen to pressures higher than needed
- Complex system with many components

- Recovery time between fuellings
- Storage of high-pressure hydrogen

The compression of hydrogen to a higher pressure than needed results in an increased energy consumption. The concept of cascade fuelling is that the tank at the station filling the vehicle, always has a larger pressure than the vehicle and the pressure is thus reduced through a reduction. The pressure reduction in the valve represents the extra work of the compressor. The system is quite complex and requires multiple tanks at different pressures and many open/close valves for the control. The recovery time between each fuelling of a vehicle depends on the size of the tanks in the cascade system and the size of the compressor. If the tanks are dimensioned to do one fuelling before recovering and the compressor only delivers 25 % of the vehicle's fuelling mass flow, then the time before the next fuelling would correspond to the time of three to four fuellings depending on how the recovery of the station is done. Storage of high-pressure hydrogen has some safety issues, and the tanks for storing at high pressure, tank Type III and Type IV, are expensive compared to Type I and Type II.

The wide use of cascade systems is due to the simple operation and design. As the present hydrogen fuelling stations only serve small fleets of vehicles and the research and experience in building stations are still in a developing phase, the main goal until now has been to make stations that work.

8.2.2 Direct compression

The direct compression system consists of a bank with medium-pressure hydrogen (200-300 bar) and a compressor, as shown in Figure 8.2. The fuelling

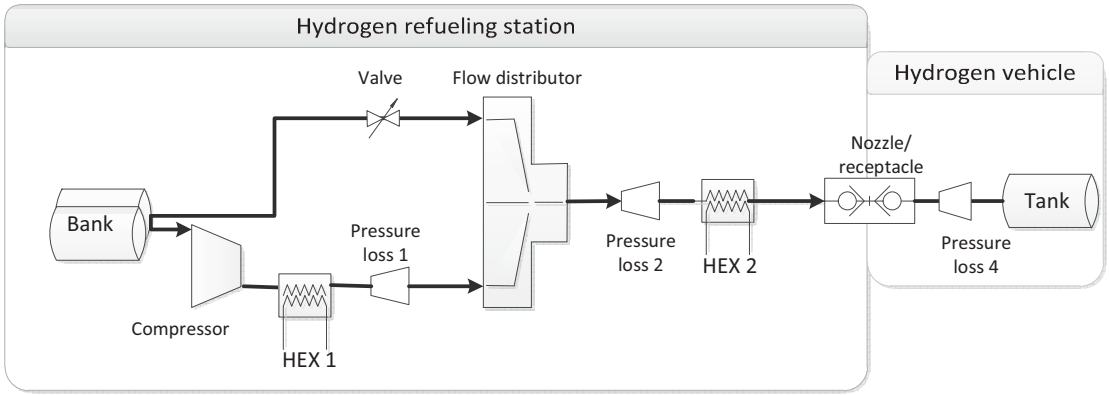

Figure 8.2: Sketch of a direct compression hydrogen fuelling station that does not follow the SAE J2601.

proceeds as follows. The vehicle connects to the station and the properties of the tank are measured, like for the cascade system. The fuelling starts by taking hydrogen from the bank through a valve to the vehicle tank. When the pressure drop across the valve reaches a lower level, the compressor starts. By knowing the pressure and the volume of the tank, the compressor regulates its rotation to deliver an average mass flow corresponding to the average mass flow of a fuelling with the average pressure ramp rate. The compressor then fills the vehicle until the desired pressure. When the fuelling has finished, the station is ready to commence a new vehicle fuelling immediately. The advantages of using a direct compression system are:

- No recovery time for the station between vehicle fuellings
- No need for high pressure storage or a cascade system
- Storage of hydrogen accomplished by Type I and Type II tanks
- Less complex system compared to a cascade fuelling station
- Compression of hydrogen by the compressor only to the needed pressure

No recovery time of the station enables continuous fuelling of vehicles, securing the station for future demand for a larger vehicle fleet. No high-pressure storage and no cascade system reduces the number of components and the complexity of the system. Compared to the cascade system, the three tanks are eliminated, but the compressor size has increased. The bank should be the same for both systems as it is where the large mass of hydrogen is stored. The pressure loss that is present when using a reduction valve in the cascade system is eliminated as the compressor delivers directly to the needed pressure. The disadvantages of the direct compression system are:

- Compressor with an average mass flow of approximately 40 g/s to fill a 7 kg tank from 20 to 700 bar in 156 seconds
- Complexity of the compressor control
- Cannot fuel a vehicle without power
- Does not follow the average pressure ramp rate

The compressor needs to be able to deliver the average mass flow for the fuelling, whereas the compressor in the cascade system can be smaller as the fuelling does not depend on it. Furthermore, this requires a high power usage during operation, but a lower operating time. The control of the compressor needs to be quite accurate so the mass flow is balanced with the vehicle tank size; hence, the compressor should have frequency control. If there is a power outage, the vehicle can only be fuelled to a maximum pressure corresponding to the bank pressure. The system by definition does not follow the average

pressure ramp rate, as the compressor delivers an average mass flow defined by the size of the vehicle tank.

The reason such a system has not been implemented is because the compressor is very expensive, the necessary control might be hard to achieve and the largest commercial hydrogen compressors on the market only deliver approximately 20 g/s. This means two compressors should be used.

8.2.3 Direct compression with a small buffer

The direct compression with a small buffer is very similar to the direct compression system, though there are two important differences. First, the system contains a small buffer tank after the compressor. Second, the fuelling is done using the average pressure ramp rate from the fuelling protocol. The system is shown in Figure 8.3 The fuelling proceeds in a similar manner to the di-

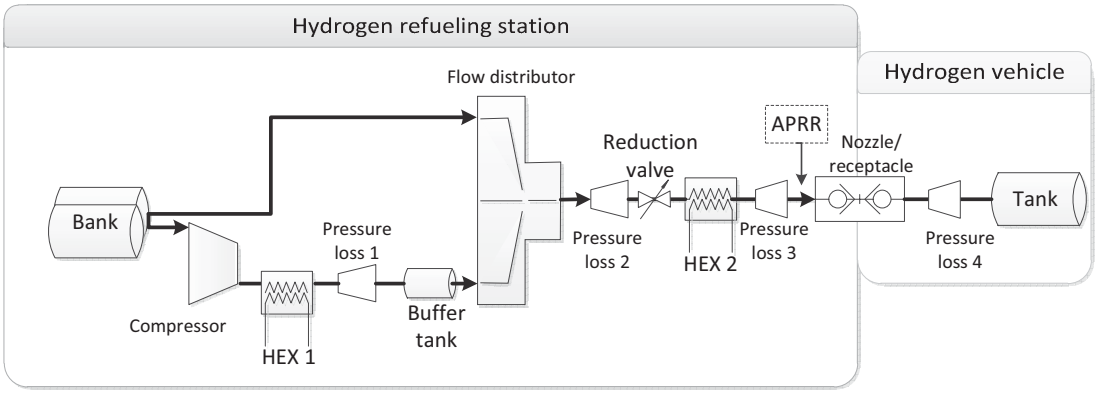

Figure 8.3: Sketch of a direct compression hydrogen fuelling station with a small buffer, fuelling according to SAE J2601.

rect compression system. First the bank fuels to the vehicle, but in this case through a reduction valve keeping the average pressure ramp rate. When the pressure across the reduction valve is too low to maintain the mass flow rate, it shuts off and starts drawing from the buffer tank. The buffer tank is at high-pressure. When the pressure difference across the reduction valve reaches a certain limit, the compressor starts filling into the buffer tank, securing that the pressure of the buffer tank is higher than needed out of the reduction valve. In this way the fuelling can be done in accordance with the fuelling protocol. The advantages of the system are:

- Fuelling according to the protocol with an average pressure ramp rate [34]
- No recovery time for the station between vehicle fuellings

- Only one very small high-pressure tank is needed
- The average pressure ratio across the compressor might be lower than for the cascade fuelling

The station complies with the fuelling protocol that secures a safe fuelling of the vehicle [34]. However, there are no guidelines for the buffer tank, though temperature and pressure limits are comparable to the vehicle's tank given by the SAE J2601. As the compression is direct, the system is ready for a new fuelling instantly, securing the station for larger hydrogen vehicle fleets. There is a reduction in the number of components needed as only one small high-pressure tank is used instead of the three larger tanks in the cascade system. The energy consumption of the system is unknown compared to the cascade system, but as energy is wasted across the reduction valve, this system must require more energy than direct compression fuelling. The disadvantages of the system are:

- Compressor with an average mass flow of approximately 40 g/s to fill a 7 kg tank from 20 to 700 bar to keep the average pressure ramp rate
- Complexity of the compressor control including the buffer
- Cannot fuel a vehicle without power

The arguments are the same as for the direct compression system. It requires a large compressor or two compressors. The mass flow of the compressor needs to be controlled precisely and a vehicle can only be fuelled to the bank's pressure during an electricity outrage.

The system has not yet been seen described in the literature, and it is therefore not known if it has been considered before.

8.3 Assumptions

When comparing the three different fuelling systems, they should be as identical as possible. The control of the different systems cannot be the pressure at the outlet of the station, because the direct compression does not follow the fuelling protocol. By using the pressure at the exit of the station one might risk different final masses in the vehicle which would give misleading results. Therefore the fuelling uses the density in the vehicle tank as the control, as this gives exactly the same fuelled mass for all the systems. The fuellings all proceed until a density of 40.2 kg/m^3 is reached. This is the target density of the fuelling protocol [34]. In reality this can only be reached for a fuelling with communication, and the normal procedure is to stop when the target pressure is reached at the exit of the station. Furthermore, for the cascade

system, tank 1, tank 2 and tank 3 are each 1 m^3 and the pressures in the tanks have the same pressure ratio between them, starting from the bank pressure at 300 bar and ending at 950 bar. In order to compare energy consumption and exergy destruction, the cascade system does a complete fuelling cycle, fuelling the vehicle and then recovering the tanks at the station. The bank in all three systems is infinite and 300 bar in order to make the systems comparable. The buffer tank in the direct compression system is 25 litres, and its starting pressure is between 850 and 950 bar. The volume of the vehicle tank is 0.172 m^3 which corresponds to approximately 7 kg of hydrogen at a density of 40.2 kg/m^3. The pressure losses in the system have the values shown in Table 8.1, and the tubes have a diameter of 0.0052 m. The heat transfer coefficient

Table 8.1: Pressure losses for the three systems. Pressure losses 2 and 3 have been added together in the direct compression system's "pressure loss 2". "Pressure loss 4" is given for both a low pressure loss (LPL) vehicle and a high pressure loss (HPL) vehicle

Pressure loss	Type of loss and values
Pressure loss 1	Tube L=25, k=22.5
Pressure loss 2	Tube L=10, k=15
Pressure loss 3	Tube L=25, k=22.5
Pressure loss 4	Valve kv=0.60 and kv=0.06
Valve	Valve kv=0.2 (only direct compression)

for the tank charging is $h = 350W/(m^3K)$, and for the discharging, Daney's correlation has been used. The compressor in the cascade fuelling system has a maximum mass flow rate of 15 g/s, and for the direct compression and direct compression with buffer, the compressor has a nominal mass flow of 40 g/s but can be frequency-controlled to deliver between 30 and 50 g/s.

8.4 Thermodynamic analysis of the three systems

The following section compares the three systems. The first analysis is of the cascade system. A similar analysis can be found in Chapter 6, though this one is more complex. Second is the thermodynamic analysis of the direct compression system, and last is the analysis of the direct compression system with a buffer tank. The thermodynamic analysis is done for a high pressure loss (HPL) vehicle and a low pressure loss (LPL) vehicle. The pressure loss of the HPL vehicle is 200 bar and for the LPL vehicle, the pressure loss corresponds to a maximum mass flow of 0.06 kg/s, as given as maximum pressure loss and mass flow rate by the SAE J2601 [34]. The figures in this section can be related to Figure 8.1, Figure 8.2 and Figure 8.3 as the components have the same names

Table 8.2: Abbreviations used in figures

Name	Abbreviation
Compressor	Comp
Pressure loss 1	PL1
Pressure loss 2	PL2
Pressure loss 3	PL3
Pressure loss 4	PL4
Reduction valve	RV
High pressure loss	HPL
Low pressure loss	LPL

in the system sketches and in the thermodynamic figures. Note that some of the names are long and abbreviations have been used. The abbreviations and original names are shown in Table 8.2 together with two other abbreviations used in the figures to explain the type of the vehicle pressure loss. In the analysis a vehicle with a low pressure loss is abbreviated to "LPL" and a vehicle with a high pressure loss is abbreviated to "HPL". This is done in order not to confuse the fuelling analysed with what is going on in the explanation of the thermodynamics.

8.4.1 Cascade system

The explanation of the thermodynamics of a hydrogen fuelling using a cascade system can be found in Chapter 6. The system also consists of a compressor which fuels the tanks in cascade at the station. The compressor starts filling when tank 1 in the system has finished fuelling the vehicle; hence, the mass flow from the compressor does not mix with the flow for the fuelling. The mass flow of the fuelling and the compressor can be seen in Figure 8.4. The fuelling of a HPL vehicle takes a longer time than for a LPL vehicle. Furthermore, the compressor needs more time for the cascade system to recover. This can be explained considering the pressures during the fuelling. As the average pressure ramp rate is set at the outlet of the station, the HPL vehicle fuelling has a higher outlet pressure at the reduction valve than the LPL vehicle fuelling. With a higher pressure loss in the vehicle, more mass is drawn from the higher pressure tanks; see Chapter 6 for further explanation. The compressor therefore needs to fill more mass to a higher pressure, and due to the volumetric efficiency it takes a longer time. When using the target density for fuelling, it was found that the highest pressure tank in the cascade system needed to be 1000 bar in order for the system to complete a fuelling of a HPL vehicle. The pressures of the cascade system during the vehicle fuelling are shown in Figure 8.5; the labels correspond to Figure 8.1. It is shown that in fuelling a LPL vehicle, the tanks in the cascade system change later than for

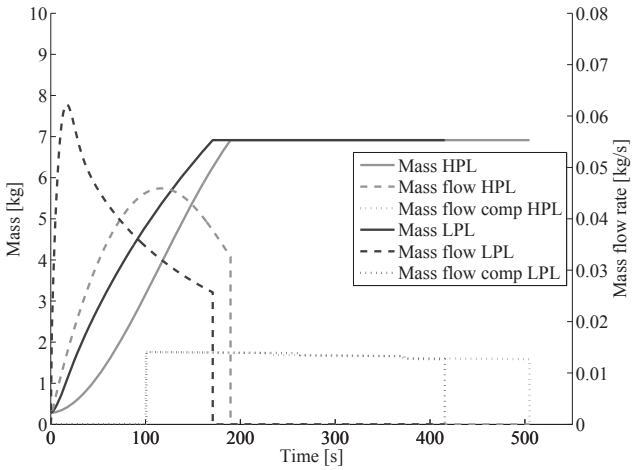

Figure 8.4: Mass flow rate and total mass in vehicle storage for a cascade fuelling.

a HPL vehicle fuelling. This combined with the mass flow rate shown in Figure 8.4, results in less use of the tanks at the highest pressure in the cascade system. The pressures of the cascade system and the compressor are shown

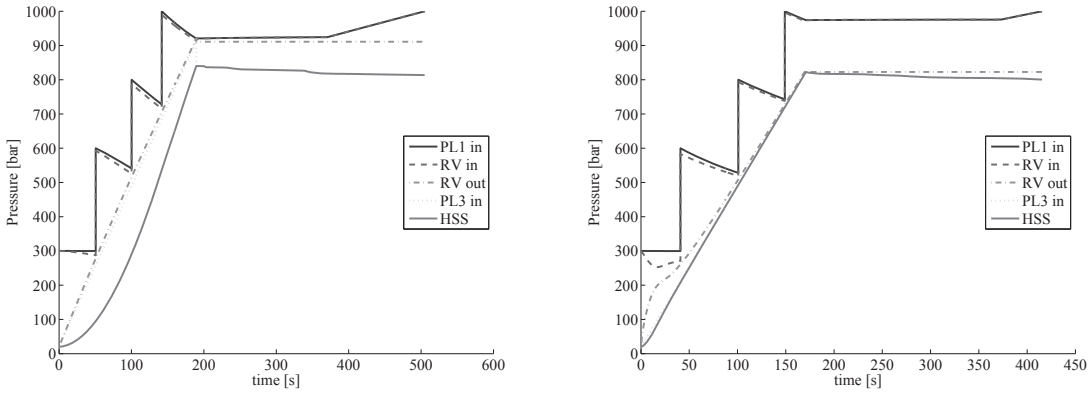

(a) High pressure loss

(b) Low pressure loss

Figure 8.5: The pressures of a cascade fuelling for a high and low pressure loss vehicle. Pressures are shown at strategical places (PL = pressure loss, RV = reduction valve).

in Figure 8.6 for both a LPL vehicle fuelling and a HPL vehicle fuelling. As expected the pressures in the cascade system decrease during the fuelling of the vehicle and increases as they are filled by the compressor. The bank at the

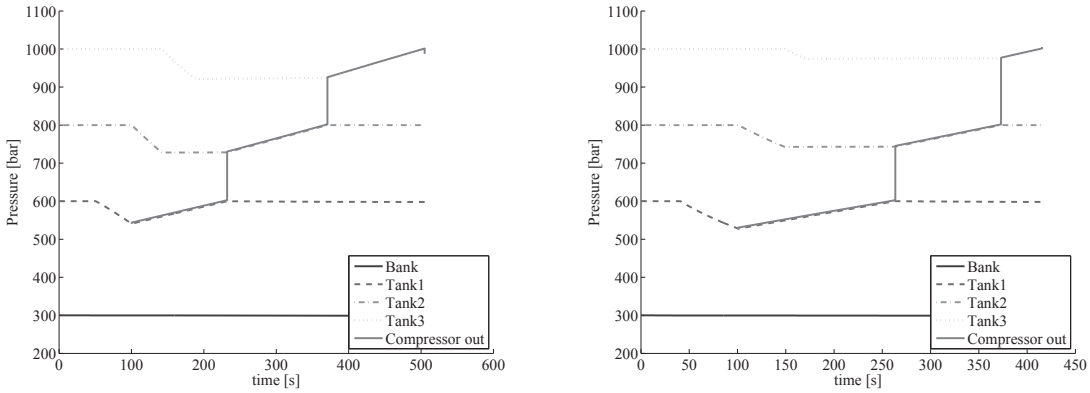

(a) High pressure loss.

(b) Low pressure loss.

Figure 8.6: The pressures related to filling the tanks in a cascade system shown for a high and a low pressure loss vehicle.

station is not visibly influenced by the fuelling, but with consecutive fuellings the pressure will decrease. The corresponding temperatures for Figure 8.5 and Figure 8.6 are shown in Figure 8.7 and Figure 8.8. It is worth noticing that the temperature of the tank in the vehicle in Figure 8.7 does not exceed 85 $°C$, which is the safety limit, and that a LPL vehicle fuelling has a lower ending temperature. Figure 8.8 shows that the tanks in the cascade system start and end, at the same temperature. Furthermore, the temperature out of the compressor is between 100 $°C$ and 160 $°C$. The pressure losses in the system

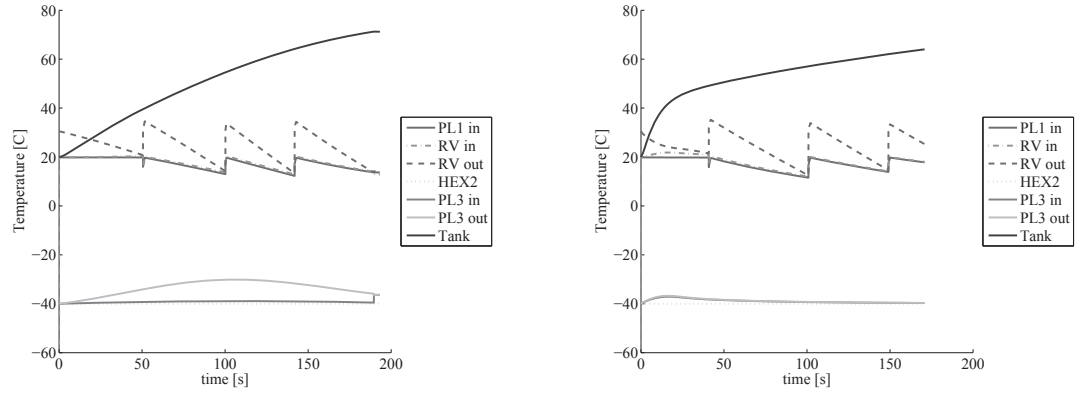

(a) High pressure loss.

(b) Low pressure loss.

Figure 8.7: The temperatures of a cascade fuelling for a high and a low pressure loss vehicle.

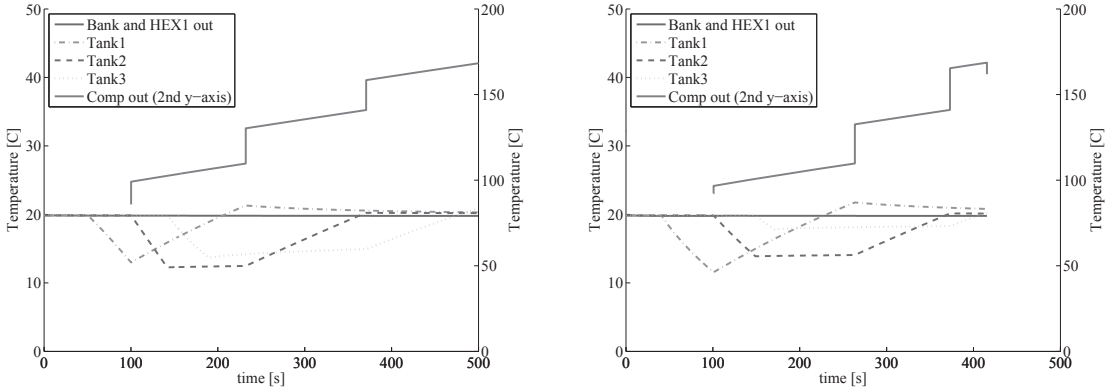

(a) High pressure loss (b) Low pressure loss

Figure 8.8: The temperatures of the tanks and compressor in a cascade system during a vehicle fuelling with subsequent fuelling of the tank in the cascade system.

are shown in Figure 8.9 for the fuelling of a HPL vehicle and a LPL vehicle, respectively. The pressure reduction in the reduction valve is very similar for

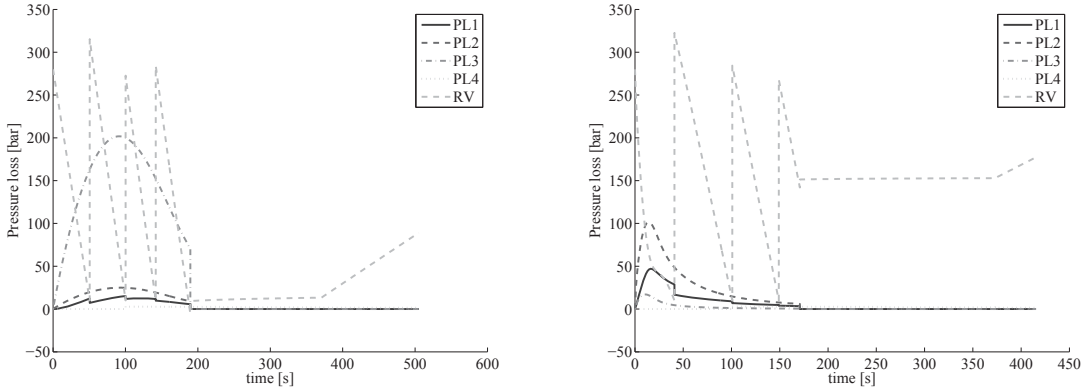

(a) High pressure loss (b) Low pressure loss

Figure 8.9: The pressure losses in the tubes and valves in the system.

the high pressure and the low pressure vehicle fuelling. The pressure losses in the system follow the mass flow rate shown in Figure 8.4. The vehicle's peak pressure loss is quite high for a LPL fuelling; this is due to the high mass flow rate that peaks higher than for an HPL vehicle fuelling. The pressure loss in a HPL vehicle is above 100 bar during most of the fuelling, whereas the low pressure loss vehicle's pressure loss is beneath 100 bar at all times and 2/3 of

the time lower than 50 bar.

8.4.2 Direct compression fuelling

The thermodynamics of the direct compression fuelling are interesting as the fuelling cannot follow the average pressure ramp rate, and the behaviour of a fuelling might not correspond to the analysis shown in Chapter 6. The mass flow rate of the fuelling, first through the valve and afterwards from the compressor, is shown in Figure 8.10 together with the total mass in the vehicle tank. The large difference in the mass flow rate between a HPL vehicle and

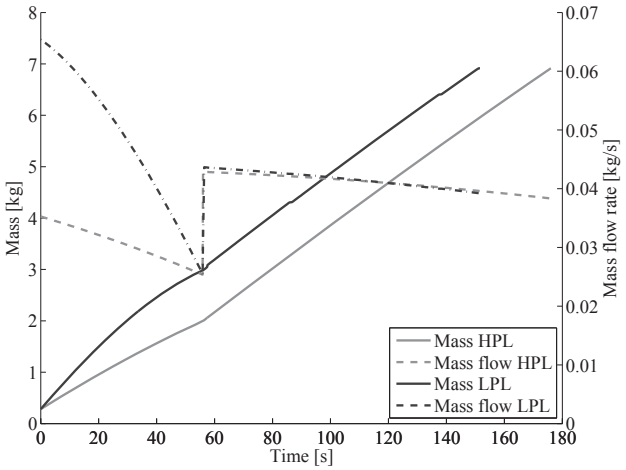

Figure 8.10: Mass flow rate and total mass in vehicle storage for a direct compression fuelling.

a LPL vehicle fuelling is due to the difference in pressure loss in the vehicle system. For the LPL there is a higher pressure drop across the valve when fuelling from the bank, resulting in a higher mass flow rate than for the HPL vehicle. The shorter fuelling time for the LPL vehicle is also because of the higher mass flow rate in the beginning. Furthermore, the compressor has to compress more hydrogen during the HPL vehicle fuelling, due to the lower mass flow rate when fuelling from the bank. The pressures of the direct compression system are shown in Figure 8.11. The most noticeable pressure differences between the HPL and the LPL vehicle fuelling are the reduction across the valve when fuelling from the bank and the pressure loss of the vehicle. The pressure reduction across the valve is higher for the LPL vehicle fuelling because the pressure loss in the vehicle is lower. For the HPL vehicle fuelling the pressure loss in the valve is small, because the pressure loss of the vehicle is high. Furthermore, the pressure out of the compressor is lower for the LPL vehicle fuelling because it does not have to compensate as much for the pressure

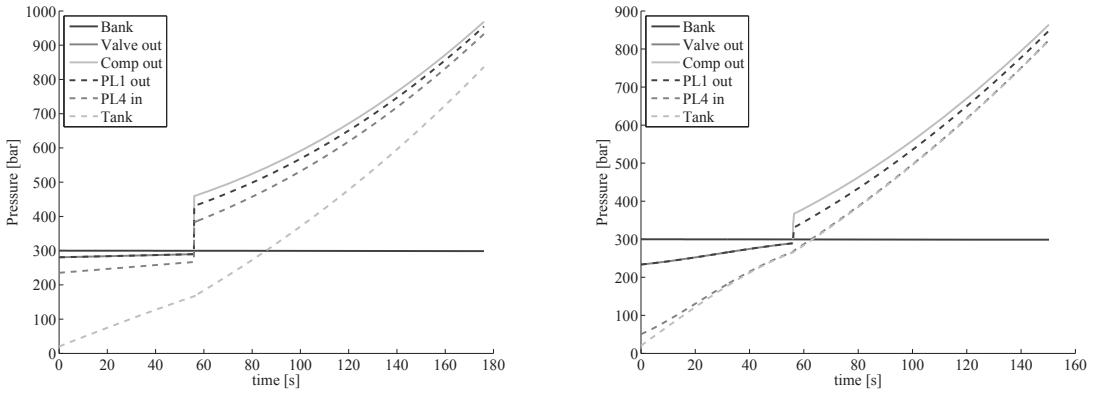

(a) High pressure loss

(b) Low pressure loss

Figure 8.11: The pressures through a direct compression fuelling of both a high pressure loss and the low pressure loss vehicle.

loss in the vehicle. This corresponds to the HPL and the LPL vehicle cascade fuelling, as shown in Figure 8.5 where the pressure into the reduction valve is close to the LPL vehicle pressure. The pressure at the exit of the direct compression station does not follow the average pressure ramp rate, though the pressure increase in the vehicle tank does not differ much compared to the pressure in the vehicle of the cascade fuelling. The direct compression system's pressure losses in the components are shown in Figure 8.12 The pressure loss

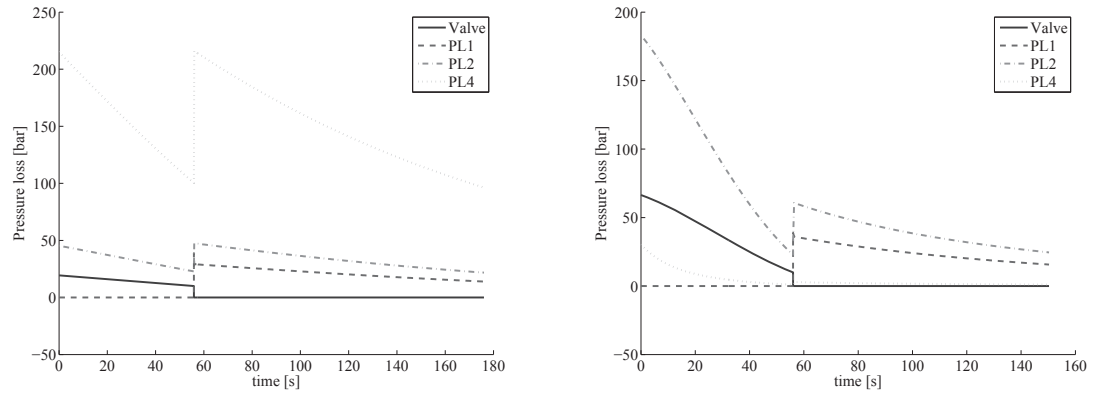

(a) High pressure loss

(b) Low pressure loss

Figure 8.12: The pressure losses of the components in a direct compression fuelling of both a high pressure loss and the low pressure loss vehicle.

in the HPL vehicle exceeds 200 bar; where for a cascade fuelling with the same

vehicle pressure loss, it is just under 200 bar. This is because the compressor has a higher mass flow rate than obtained using the average pressure ramp rate. The same pressure loss constant is used to simulate the vehicle pressure loss in both systems. For the LPL vehicle fuelling, the largest pressure loss is in the station after the compressor (pressure loss 1). The temperatures of the direct compression fuelling system are shown in Figure 8.13. The temperatures

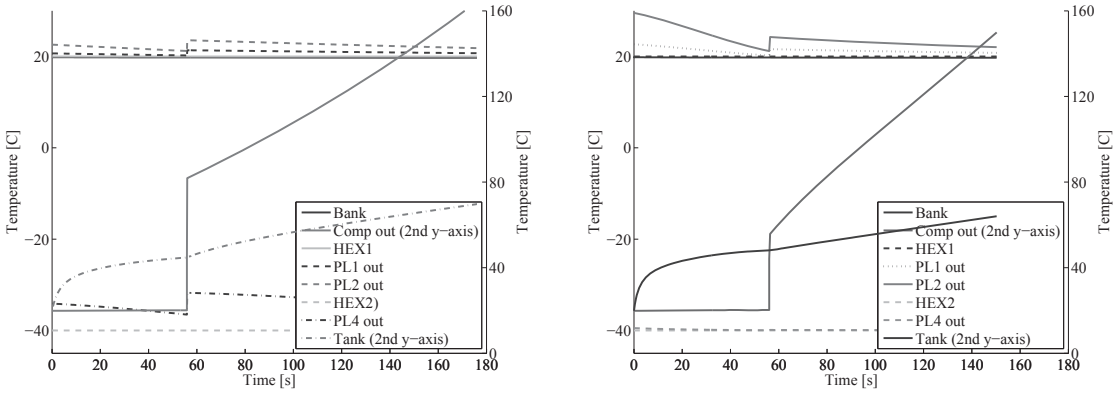

(a) High pressure loss

(b) Low pressure loss

Figure 8.13: Temperatures across the direct compression fuelling system.

during a fuelling are similar to the ones in the cascade system. The temperature of the vehicle does not exceed 80 °C, though the temperature curve has a small increase when the compressor starts filling. The temperature out of the compressor is as expected and very similar to the cascade fuelling. The temperature difference in the vehicle tank between a LPL and a HPL vehicle fuelling is also present in the direct compression fuelling system, even though the temperature difference is smaller than for the cascade system.

8.4.3 Direct compression with a small buffer

The direct compression system with a buffer is a mixture between the direct compression system and the cascade system. It eliminates the pressure tanks from the cascade system and uses a large compressor with a small high-pressure buffer tank instead. In addition, the system is able to fuel according to the fuelling protocol SAE J2601. The mass flows of the system are shown in Figure 8.14; there are two mass flows present: one from the compressor to the buffer tank and one for the fuelling of the vehicle first from the bank and later from the buffer tank. The mass flow rate to the vehicle is the same as in the cascade system, as they both fuel according to the protocol and have the same pressure losses. This is also explained in Chapter 6. The thermodynamics of the fuelling proceeds in the same way for the direct compression system with

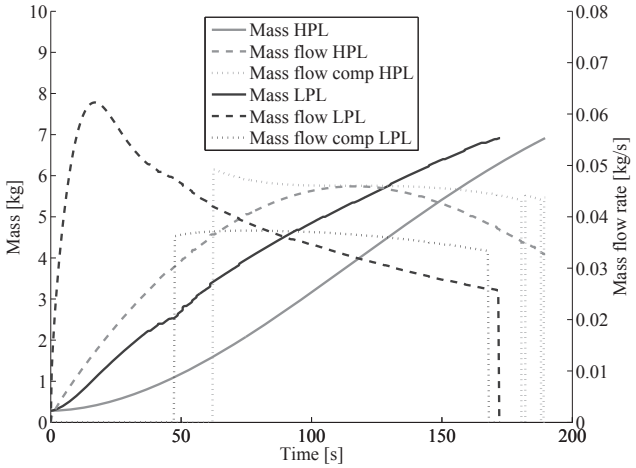

Figure 8.14: Mass flow rate and total mass in vehicle storage for a direct compression fuelling.

the buffer as for a cascade system, from the vehicles point of view. The mass flow of the compressor varies with the pressure of the buffer tank, as shown in Figure 8.15. The reason that the compressor's mass flow is not steady as

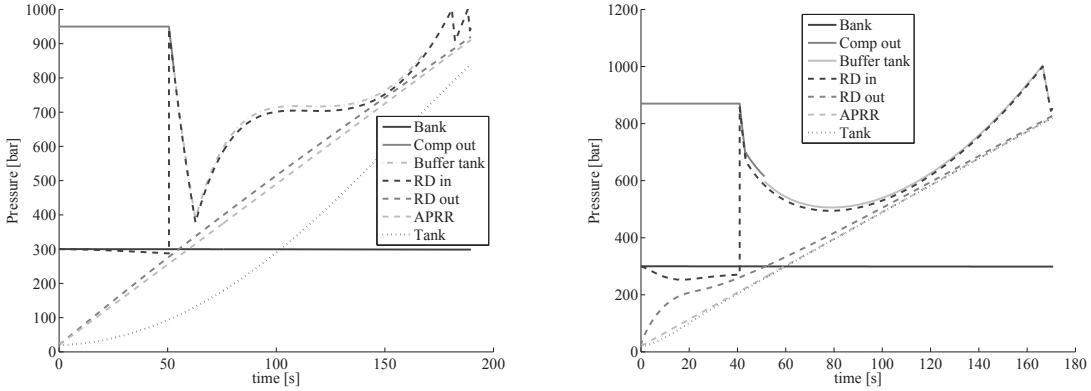

(a) High pressure loss.

(b) Low pressure loss.

Figure 8.15: The pressures through a direct compression system with a buffer for both a high pressure loss and a low pressure loss vehicle fuelling.

in the direct compression fuelling is that the buffer tank fluctuates in pressure and the compressor's mass flow is a function of the volumetric efficiency and thereby the pressure ratio. Considering the HPL vehicle fuelling, the compressor starts when there is a 20 bar pressure difference across the reduction valve.

The compressor fills into the buffer tank which increases in pressure as the mass flow rate into it is higher than the mass flow rate out of it. At some point the pressure of the buffer tank is almost constant; this is because the mass flow rate of the vehicle fuelling increases to the same as the compressor's mass flow rate. The pressure in the buffer tank then increase as the mass flow rate of the vehicle fuelling decreases. At the end the pressure in the buffer tank reaches 1000 bar which is the maximum pressure allowed. The compressor therefore turns off. When the pressure across the reduction valve reaches 20 bar, the compressor starts up. Considering the thermodynamics after the reduction valve, the fuelling of the vehicle proceeds exactly as for the cascade system. For the LPL vehicle fuelling, the pressure development in the buffer tank can be explained similarly to the HPL vehicle fuelling,; However, in this case the compressor delivers less mass flow than needed for the vehicle fuelling in the beginning, and the pressure of the buffer tank decreases. At some point the mass flow rate for the vehicle fuelling becomes lower than the mass flow rate of the compressor, and the pressure in the buffer tank increases. When the pressure in the buffer tank reaches 1000 bar the compressor turns off, and the last mass for the fuelling is drawn from the buffer tank. The buffer tank starts at 950 bar in the HPL vehicle fuelling and 870 bar in the LPL vehicle fuelling. This does not matter for the fuelling, as long as the pressure in the buffer tank is above 800 bar, the fuelling will proceed as shown. The buffer tank will always have a pressure above 800 bar as the pressure out of the reduction will exceed 800 bar at the end of the fuelling. The pressure losses in the components are shown in Figure 8.16. The pressure losses in the components after the reduction

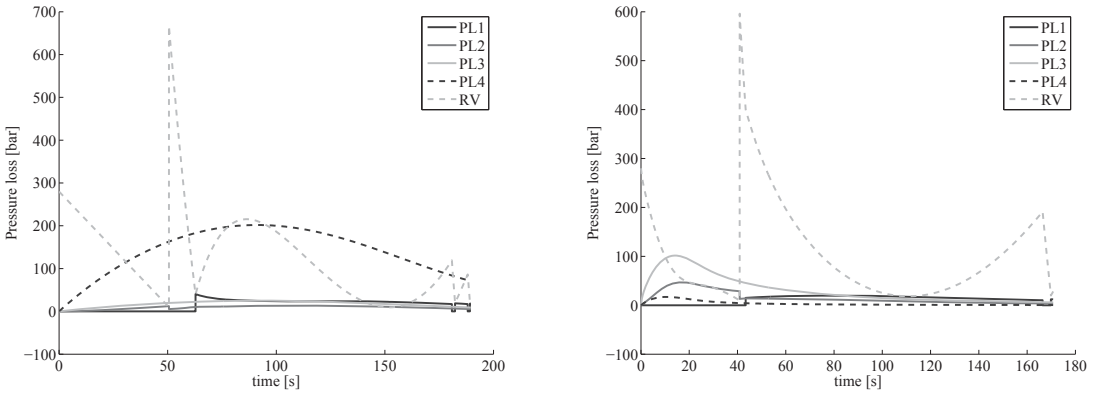

(a) High pressure loss.

(b) Low pressure loss.

Figure 8.16: The pressure losses in the components for a direct compressor system with buffer.

valve are the same as in a cascade fuelling with the same vehicle pressure loss, proving the statement that the thermodynamics of the vehicle is independent

of the station design, as long as the fuelling complies with the SAE J2601. The pressure loss across the reduction valve is very high when the system changes from fuelling from the bank to the buffer tank. This is due to the very high initial pressure in the buffer tank. The temperatures of the system are shown in Figure 8.17. It is worth noticing the temperature of the buffer tank which

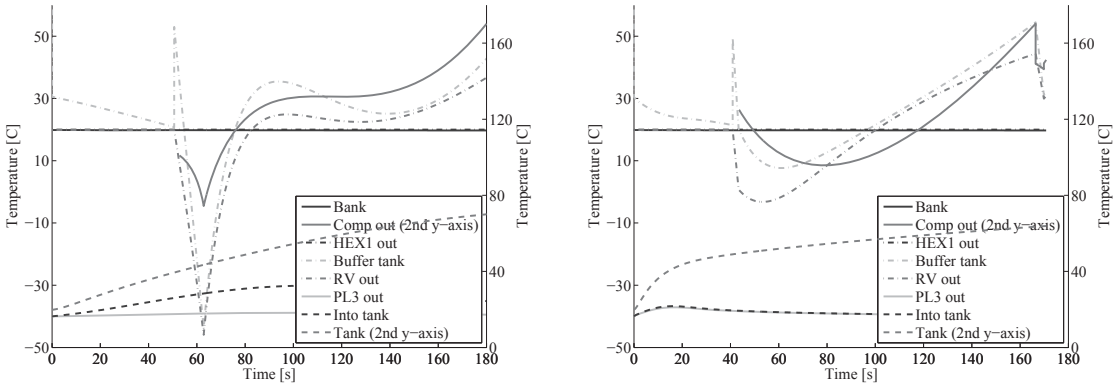

(a) High pressure loss.

(b) Low pressure loss.

Figure 8.17: The temperatures in a direct compressor system with buffer when fuelling a vehicle.

fluctuates between 20 $°C$ and -50 $°C$. The sudden decrease in temperature is a result of the decrease of pressure when the buffer tank is used for the fuelling of the vehicle. The hydrogen temperature actually exceeds the lower safety limit of -40$°C$. The temperature out of the compressor follows the pressure out and peaks at the end with just over 160 $°C$. The temperatures after heat exchanger 2 are the same as for the cascade system.

8.5 Energy analysis of the different fuelling systems

An energy analysis of the three different systems is done showing the energy consumption of each system and the exergy destruction. The exergy analysis is used to point out the most exergy destructive components in each system from a thermodynamic point of view.

8.5.1 Energy consumption of the three systems

The energy consumption for the three different systems includes the compressor, the heat exchanger after the compressor (HEX1) and the heat exchanger

Table 8.3: Energy consumption of the components in the three different fuelling station designs. All values are given in kilo watt hours [kWh].

System	Comp	HEX1	HEX2	Total
Cascade HPL	3.13	1.31	1.17	5.61
Cascade LPL	2.23	0.94	1.17	4.34
Direct compression HPL	2.40	1.02	1.14	4.56
Direct compression LPL	1.59	0.68	1.16	3.44
Direct comp w. buffer HPL	3.30	1.38	1.23	5.91
Direct comp w. buffer LPL	2.14	0.91	1.17	4.22

at the exit of the station (HEX2). The temperatures of the heat exchangers are the same for HEX1 in all three systems and HEX2 in all three systems. The energy consumption used to cool the hydrogen in the heat exchangers has been found using a $COP = 2$ for the heat exchanger after the compressor and $COP = 1.5$ for the heat at the exit of the station. The results are partly comparable to the results in Chapter 7, as the coefficients of performances are the same and the heat exchanger temperatures are the same. The difference is the control of the fuelling; as the fuellings in Chapter 7 stop when the pressure at the exit of the station reaches the target pressure, and in this analysis the fuelling stops when the target density is reached in the tank. The difference in the fuelling control can be seen when considering the total mass in the vehicle tank, shown in Figure 7.2 when the fuelling is pressure-controlled and in Figure 8.4 for a density-controlled fuelling. The energy consumed by the refrigeration facilities and the compressor are shown in Table 8.3. The consumption is shown for fuelling a HPL and a LPL vehicle. The energy consumption of the cascade system and the direct compression system with a buffer tank is very similar though the cascade system is better at HPL vehicle fuelling and the direct compression with a buffer tank is better for LPL vehicle fuelling. The direct compression system uses much less energy than the two other systems. The energy reduction using a direct compression system compared to one of the two others is for a HPL vehicle fuelling approximately 18 % and for a LPL vehicle fuelling approximately 18 % too. The large difference in energy usage is directly related to the compressor. The compressor consumes 23 % less energy for a direct compression system, and the energy needed to cool the hydrogen after the compression is significantly lower with a reduction of 22 %. The reason for this is found in the design differences and thermodynamics of the systems. The cascade system and the direct compression system with a buffer tank both need a "hydrogen storage" at higher pressure than needed for the fuelling, in order to satisfy the mass flow demand. The direct compression system delivers hydrogen at the needed pressure only. It compensates for the pressure losses between itself and the vehicle tank, but it does not compress the hydrogen to a higher pressure than needed. This can be seen in Figure 8.11.

The compressor in the cascade system and the direct compression system with buffer therefore require more energy as the hydrogen is compressed to a higher pressure. This also results in a higher hydrogen temperature out of the compressor, which explains that the energy for cooling after the compressor is less for the direct compression system. The direct compression system is one of the most energy-effective systems that can be designed for fuelling hydrogen vehicles as the compressor only delivers the hydrogen at the required pressure. An exergy analysis is conducted to identify the components where the ability to perform work is lost. This will help to understand the differences in energy consumption.

8.5.2 Exergy Analysis

The exergy analysis is done in three parts, one for each system considered. The results for the cascade system, the direct compression and the direct compression with a buffer tank are shown in Tables 8.4, 8.5 and 8.6, respectively. Each part consists of two steps. First, the components with the largest exergy destructions are pointed out and suggestions for improvements are considered. Second, the systems are considered in relation to the cascade system to point out the differences in the systems from an exergy destruction point of view.

Cascade system

The exergy destruction and percentage of total exergy destruction in each component for the cascade system are shown in Table 8.4 for a HPL and a LPL vehicle fuelling, respectively. The components with the largest exergy destruction in the HPL vehicle fuelling are the vehicle pressure loss (PL4) with almost 20 % of the total exergy destruction, the heat exchanger after the compressor (HEX1) with 14.6 % of the total exergy destruction, the destruction inside the vehicle tank with 12 % of the total destruction and the reduction valve (RV) with 11.1 % of the total destruction. Considering the bank and the tanks in the cascade system at the station, the exergy destruction corresponds to approximately 30 % of the total exergy destruction. The compressor's exergy destruction is 6.3 % of the total destruction. The pressure losses and mixers at the station all have exergy destruction of less than 3 % of the total destruction. The exergy destruction in the vehicle tank and pressure loss 4 which is also in the vehicle, cannot directly be improved from a station point of view. The exergy destruction in all the tanks in the station are due to the pressure and temperature fluctuation related to the fuelling of the vehicle and the recovery afterwards of the cascade system. The exergy destruction could be minimized by adding more tanks with pressures between the already existing tanks. This would not only reduce the exergy destruction in the tanks, but also affect the compressor and the heat exchanger after the compressor. The compressor's exergy destruction is directly related to the pressure ratio and

Table 8.4: Exergy destruction in the components of the hydrogen cascade fuelling system.

fuelling	HPL	LPL
Component	$[kWh]([\%])$	$[kWh]([\%])$
Bank	0.41 (5.5)	0.41 (7.8)
Tank 1	0.46 (6.2)	0.55 (10.4)
Tank 2	0.62 (8.4)	0.50 (9.5)
Tank 3	0.75 (10.1)	0.25 (4.64)
Tank	0.89 (12.0)	0.91 (17.1)
Compressor	0.47 (6.3)	0.37 (7.0)
HEX 1	1.09 (14.6)	0.76 (14.3)
HEX 2	0.22 (3.0)	0.22 (4.1)
RV	0.83 (11.1)	0.91 (17.2)
PL1	0.01 (0.1)	0.01 (0.1)
PL2	0.05 (0.7)	0.14 (2.7)
PL3	0.13 (1.8)	0.06 (1.0)
PL4	1.43 (19.3)	0.12 (2.2)
Mixer 1	0.05 (0.6)	0.03 (0.6)
Mixer 2	0.03 (0.4)	0.03 (0.6)
Mixer 3	0.01 (0.2)	0.03 (0.6)
Total	5.95 (100)	5.31 (100)

the mass the compressor needs to move. Adding more tanks in the cascade system would cause the compressor to deliver mass at lower pressure ratios. The heat exchanger after the compressor (HEX1) would also reduce the exergy destruction, as the temperature out of the compressor would be reduced due to lower compression ratios; hence, considering eq. 3.46, it can be seen how the cooling demand and the temperature are directly influencing the exergy destruction of the components in terms of heat flow. The reduction valve of the system has increasing exergy destruction as the pressure ratio across the valve increases. There are two ways of decreasing the exergy destruction in the valve. Adding more tanks in the cascade system or installing a work producing expander. Adding one more tank to the cascade system (total of four) results in a reduction in exergy destruction in the tanks in the cascade system for a HPL fuelling of 0.06 kWh in total, the compressor decreases with 0.02 kWh and the exergy destruction in the heat exchanger after the compressor decreases with 0.06 kWh. The reduction valve exergy destruction decreases with 0.09 kWh. This gives a total exergy savings on these components of 0.22 kWh or 3.7 % compared to the reference system.

Considering the LPL vehicle fuelling, the overall exergy destruction is 11 % lower compared to the high pressure loss vehicle fuelling. The critical compo-

nents considering exergy destruction are in general the same as for the high pressure loss vehicle fuelling, though there are two components which stand out: the exergy destruction of the pressure loss in the vehicle (PL4) and the reduction valve. The exergy destruction in the vehicle is only 8 % of the exergy destruction in the HPL vehicle fuelling; this is due to the much lower pressure loss in the vehicle. The exergy destruction in the reduction valve is higher for the LPL vehicle fuelling. This is because the pressure loss is lower in the vehicle, so the reduction valve does a higher pressure reduction. The exergy destruction in the vehicle tank is higher in the LPL vehicle fuelling; this is because of the lower pressure loss in the vehicle, compared to the HPL fuelling. For the LPL vehicle fuelling the hydrogen is colder than for the HPL vehicle fuelling as the pressure drop between the heat exchanger and the vehicle tank is lower; the heat up of hydrogen due to the Joule-Thomson effect is lower. The density of the hydrogen entering the tank is therefore higher for a LPL vehicle fuelling. In the HPL vehicle fuelling, a part of the heat up of the hydrogen has already happened in the vehicle pressure loss, resulting in a lower density difference between the hydrogen stream into the tank and the density in the tank. As the total mass removed from the cascade system to the vehicle is the same for both fuellings, one might wonder why there are exergy differences in the tanks in the cascade system between the high and the low pressure loss vehicle fuelling. This is because the low pressure loss fuelling takes most of the mass from the lower tanks (bank and tank 1) and less from the upper tanks (tank 2 and tank 3), and therefore the exergy destruction in these tanks is larger compared to a high pressure loss vehicle fuelling. Considering the high-pressure tank (tank 3), the exergy destruction is larger for the high pressure loss system as more mass is removed and then filled to it. In order to reduce the exergy destruction in the low pressure loss vehicle fuelling, the same initiatives as for the high pressure loss vehicles are valid.

Direct compression

The exergy destruction and the percentage of the total destruction in each component in the direct compression system is shown in table 8.5 for both a HPL and a LPL vehicle fuelling. Considering the exergy destruction for a HPL vehicle fuelling, the components with the largest exergy destructions are the vehicle pressure loss with 32 % of the total exergy destruction, the vehicle tank with 19 % of the total destruction, the heat exchanger after the compressor with 18 % of the total destruction, the bank at the station with 9 % of the total destruction and the compressor with 9 % of the overall exergy destruction. The exergy destruction in the vehicle is independent of the fuelling stations design, and can therefore not directly be improved by changing the station. The only way the station can directly influence the vehicle is by increasing or decreasing the fuelling time, though improvement with respect to exergy of the station also indirectly decreases the exergy destruction in the vehicle.

Table 8.5: Exergy destruction in the components of the direct compression system

Fuelling Component	HPL $[kWh]([\%])$	LPL $[kWh]([\%])$
Bank	0.42 (9.2)	0.42 (11.6)
Tank	0.91 (19.4)	0.91 (25.1)
Compressor	0.42 (9.1)	0.33 (9.1)
HEX 1	0.81 (17.8)	0.53 (14.6)
HEX 2	0.23 (5.0)	0.22 (6.2)
Valve	0.03 (0.8)	0.17 (4.6)
PL1	1.48 (1.8)	0.14 (2.4)
PL2	0.22 (4.8)	0.81 (22.4)
PL4	1.48 (32.3)	0.14 (4.0)
Total	4.59 (100)	3.44 (100)

By increasing the fuelling time, the exergy destruction in the vehicle tank will decrease, and by decreasing the fuelling time, the exergy destruction increases since the temperature inside the tank would be lower with increased fuelling time as more heat would dissipate to the surroundings. The exergy destruction in the heat exchanger after the compressor is a result of the pressure and the temperature out of the compressor. The exergy destruction in the bank is unavoidable without changing the design of the system to consist of more than one tank at the station.

The fuelling for a LPL vehicle has a 25 % lower overall exergy destruction compared to the HPL vehicle fuelling. The components that are noticeably affected by the LPL vehicle compared to the HPL vehicle are the pressure loss in the vehicle (PL4) and the pressure loss at the exit of the station (PL2). The pressure loss in the vehicle is lower which results in a lower exergy destruction. The exergy destruction at the outlet of the station is 75 % higher for the LPL vehicle fuelling than for the HPL vehicle fuelling. This is a result of the lower pressure loss in the vehicle, creating a much higher mass flow when fuelling from the bank; see Figure 8.10. The higher mass flow results in a larger pressure loss (see fig.8.12) and a higher increased temperature due to the Joule-Thomson effect. That is what causes the increases in exergy destruction in the pressure loss (PL2) at the exit of the station. Another point worth noting is that the exergy destruction in the vehicle tank is not influenced by the kind of vehicle being fuelled;both have an exergy destruction of 0.91 kWh per fuelling.

Comparing the direct compression system to the cascade system, one must first note the use of considerably fewer components, reducing the number of potential places for exergy destruction. The second point to be aware of is

that the cascade system has a reduction valve which is used during the whole fuelling, and the direct compression system only has a valve when using the bank for fuelling. The exergy destruction in the reduction valve (RV) is more than four times larger than for the valve in the direct compression system. Furthermore, the compressor for the direct compression system has an exergy destruction that is 25 % lower than for the cascade system. This is because the compressor does not have to compress to a higher pressure than needed for the fuelling. In relation to the compressor, the heat exchanger after the compressor has a 25 % lower exergy destruction for the direct compression system compared to the cascade system. This can be directly related to the lower temperature out of the compressor. The exergy destruction in the vehicle tank is approximately the same. This is because the the total mass filled to the tank is the same resulting in the same heat up of the hydrogen. Thus, the temperature difference between the ambient and the hydrogen is the same. If the tank in the vehicle was adiabatic, the heat up of the hydrogen would be independent of time and only a result of the mass being filled to it, though the tank is not adiabatic, resulting in heat dissipating through the wall lowering the temperature. Therefore, by increasing fuelling time, the exergy destruction could be decreased. The tank is made of carbon fibre to withstand the high pressures, and carbon fibre has very low conductivity; the time should therefore increase a lot in order to lower the exergy destruction. This would compromise the time set for a customer-acceptable fuelling according to the fuelling procedure [34]. The reduction in exergy destruction going from a fuelling time of 176 s to 440 s (time ratio of 2.5) is 2.5 %. Considering the difference in energy usage in Table 8.3, the differences in exergy destruction can be related to the energy usage of the component. It can be seen that the direct compression system uses approximately 20 % less energy for a fuelling than the cascade system, and the exergy destruction is approximately 23 % lower.

Direct compression system with a buffer tank

The exergy destruction and the percentage of the total destruction in each component in the direct compression system with a buffer are shown in Table 8.6 for a HPL and a LPL vehicle fuelling. For the HPL vehicle fuelling the largest exergy destruction is in the pressure loss in the vehicle (PL4) which accounts for 25 % of the total exergy destruction; the heat exchanger after the compressor (HEX1) accounts for 20 % of the destruction, the tank in the vehicle accounts for 16 %, and the reduction valve accounts for 13 % of the total exergy destruction. Furthermore, the exergy destruction in the compressor is approximately 9 % of the total destruction. The exergy destruction in the vehicle can be indirectly improved by improving the fuelling station. The exergy destruction in the heat exchanger after the compressor is a result of the temperature out of the compressor which depends on the pressure inside the buffer tank. Considering Figure 8.15 the pressure of the buffer tank has a large

Table 8.6: Exergy destruction in the components of the hydrogen fuelling systems, fuelling a high pressure loss vehicle.

Fuelling Component	HPL $[kWh]([\%])$	LPL $[kWh]([\%])$
Bank	0.42 (7.5)	0.42 (9.9)
Buffer	0.02 (0.3)	0.00 (0)
Tank	0.89 (15.7)	0.91 (21.3)
Compressor	0.48 (8.6)	0.38 (8.9)
HEX 1	1.15 (20.3)	0.72 (17.0)
HEX 2	0.21 (3.7)	0.20(4.8)
RV	0.76 (13.4)	0.75 (17.7)
PL1	0.09 (1.7)	0.06 (1.4)
PL2	0.05 (0.9)	0.14 (3.4)
PL3	0.13 (2.4)	0.55 (13.0)
PL4	1.43 (25.46)	0.12 (2.7)
Total	5.63 (100)	4.22 (100)

difference down to the pressure out of the reduction valve, resulting in a larger pressure reduction than needed across the reduction valve. The compressor does not stop during a fuelling before the pressure in the buffer tank reaches 1000 bar. If a different approach was taken, limiting the pressure difference between the buffer tank and the outlet of the reduction valve to 80 bar, then the compressor would stop and wait for the pressure in the buffer tank to decrease to a pressure difference of, e.g., 20 bar across the reduction valve before starting again. This operational strategy results in a lower exergy destruction of the whole system of 0.44 kWh, where the largest decreases in exergy destruction are found in the reduction valve (0.34 kWh), and the heat exchanger after the compressor (0.15 kWh) though the exergy destruction in the pressure losses increases with 0.04 kWh. In addition, the total energy consumption of the compressor decreases with 0.37 kWh. This operation of the fuelling station has not been analysed further, as it would not be very effective in reality to have a compressor that constantly starts and stops.

Considering the low pressure loss vehicle fuelling, the exergy destructions that are different from the high pressure loss vehicle fuelling are the exergy destruction in the heat exchanger after the compressor, the exergy destruction in the compressor and the exergy destruction in the pressure loss at the outlet of the station. The difference in exergy destruction in the compressor and in the heat exchanger for the two systems is caused by two different effects. First, the mass flow rate of the low pressure loss system reveals that more is filled from the bank to the vehicle tank, which means that the compressor has less mass to pressurize for the fuelling. Second, the buffer tank has a lower pressure

during the fuelling of a low pressure vehicle, decreasing the pressure out of the compressor. Though it the might seem strange that the exergy destruction in the reduction valve is the same, this is caused by the lower pressure loss in the vehicle, resulting in the reduction valve reducing the pressure further down than it would for a high pressure loss vehicle fuelling.

The total exergy destruction of the direct compression system with a buffer is 4 % lower for a HPL vehicle fuelling and 20 % lower for a LPL vehicle fuelling, compared to the exergy destruction of the cascade system. The exergy destruction in each component for the two systems is almost identical. This could indicate that the exergy destruction in the components is related to the fuelling method, since both use the average pressure ramp rate. The reason for the overall lower exergy destruction in the direct compression system with a buffer can be found when comparing the high-pressure tank of the cascade system to the buffer tank. The buffer tank has an exergy destruction of 0.02 kWh where the three tanks in the cascade system have an overall exergy destruction of more than 1.3 kWh. This shows that the buffer tank is an improvement over the cascade system as the exergy destruction of the bank and the compressor are the same for the two systems.

8.6 Summary

A comparison of the three different hydrogen fuelling systems, the cascade system, the direct compression system and the direct compression system with a buffer, has been carried out. Then a thermodynamic analysis for each system, and an energy and exergy analysis considering the performance of each station was performed and the different station compared by their energy usage and destruction. The thermodynamic analysis showed that when fuelling hydrogen according to the average pressure ramp rate, the thermodynamics and variation in state of the hydrogen after the reduction valve, are the same for the cascade system and the direct compression system with a buffer. The direct compression system with a buffer also showed that it is possible to do a fuelling according to the fuelling protocol without using a cascade system, reducing the overall number of components. However, the control of the system needs to be very accurate, and in reality, tests should be made to see if the direct compression system with buffer is possible. Furthermore, at some point during the fuelling of a high pressure loss vehicle, the temperature exceeded the lower safety limit of -40 $^{\circ}C$ in the buffer tank by 7 $^{\circ}C$. The thermodynamics of the direct compression system showed that it is possible to make a system eliminating the average pressure ramp rate and instead use the mass flow out of the compressor directly. The system was at all times within the safety limits of the fuelling protocol, and the pressure increase in the tank did not deviate

much from an average pressure ramp rate. In addition, the direct compression system requires the least components of the three systems, and the highest pressure tank needed is the bank at 300 bar. A practical challenge is that the compressor needs to be able to deliver the average mass flow needed for the fuelling. One large difference between the cascade system and the two other systems is the recovery time of the station after a fuelling. The direct compression and the direct compression with a buffer can continuously fuel vehicles, whereas the cascade system needs recovery time depending on the size of the compressor.

The energy analysis of the three systems showed that the direct compression system with a buffer and the cascade system consumed almost the same amount of energy to perform a complete fuelling cycle. For the cascade system the energy consumption was 5.61 and 4.34 kWh for the high and the low pressure loss vehicle fuelling respectively. For the direct compression system with a buffer, the energy consumption for the low and the high pressure loss vehicle fuelling were 5.91 and 4.22 kWh, respectively. The direct compression system used 18 % less energy than the cascade system for both kinds of fuellings, showing itself to be the least energy-requiring system for fuelling a hydrogen vehicle. For all the systems the largest energy consumer was the compressor.

The exergy analysis showed that the largest exergy destruction occurred in the vehicle's pressure loss and the vehicle tank. For all systems the exergy destruction in the vehicle tank was approximately 0.9 kWh. This is because the same mass is filled over approximately the same period of time resulting in identical heat up of the tanks. In general the vehicle's exergy destruction cannot be reduced directly by the station manufacturers, though improvement of the station might cause less exergy destruction in the vehicle. Furthermore, the compressor and the heat exchanger after the compressor also have high exergy destruction in all three systems. The destruction varies from 6 to 9 % of the total exergy destruction of each system for the compressor and between 12 and 20 % for the heat exchanger in the systems. For the direct compression system with a buffer tank, a different control of the compressor or a different size of the buffer tank, could reduce the exergy destruction in the compressor and heat exchanger after the compressor. For the cascade system the exergy destruction of the compressor and heat exchanger after the compressor could be reduced further by introducing more tanks at different pressures in the cascade system. In general more tanks in the cascade system would reduce the exergy destruction, lowering the energy demand as shown in Chapter 7.

The analysis of the three systems showed that considering energy usage and exergy destruction of the station, the direct compression system has an 18 % lower energy consumption and a 23 % lower exergy destruction, compared to the cascade and the direct fuelling system with a buffer. Furthermore, the

direct compression requires the smallest number of tanks and the control is quite simple compared to the direct compression with a buffer. Although the ramp rate is not followed, the deviation is within the allowance of the average pressure ramp rate which will be published when the fuelling protocol SAE TIR J2601 becomes a standard (expected in the spring of 2014).

Chapter 9

Concluding remarks

The aim of this study is to contribute to the understanding of hydrogen fuelling systems for fuelling hydrogen vehicles for personal transportation. This includes exploring the thermodynamics of a complete system and the optimization of fuelling systems. The work deals with hydrogen fuelling in general with respect to the fuelling protocol and the energy optimization of the fuelling process. Specific focus is kept on a cascade fuelling system as that is the most common technology used.

9.1 Summary of findings

Based on a literature review, the area of hydrogen fuelling had not been explored from a system perspective. However, there are several papers with more thorough studies of tanks for hydrogen storage and the thermodynamics of filling them, as well as experiments and numerical and CFD calculations of the temperature distribution inside the tank. During the time of this study, there has been attention to energy and exergy considerations of simple fuelling systems, though the systems studied do not comply with the fuelling protocol.

A thermodynamic library is made in Dymola, a dynamic simulation software based on the Modelica language. The library is built up by separate component models that all receive and pass on mass flow, enthalpy and pressure. In this way all the components can be connected together in any unspecified order to design different systems. The library is able to include components made by

other developers using the same information as input and output. The models from the library have successfully been compared to models made by industry. Furthermore, the model has been compared to experimental data of a hydrogen fuelling station showing the same trends.

Using the library for hydrogen fuelling, two different models were made. The first model fuels a hydrogen vehicle using only one high-pressure tank. The second model fuels a hydrogen vehicle from a cascade system consisting of three tanks at different pressures. To analyse the thermodynamics of hydrogen fuelling, the first model was used due to its simplicity. The analysis shows the temperature, pressure and mass flow development during a fuelling at strategic places in the system. A parameter variation of the vehicle's pressure loss shows that the mass flow rate of the fuelling changes as the pressure loss in the vehicle changes. A low pressure loss results in a high early peak of mass flow, whereas a high pressure loss results in a lower peak later on in the fuelling. Following the non-communicative protocol, a higher pressure loss in the vehicle results in less mass fuelled, a lower cooling demand of up to 35 % and a higher ending temperature in the vehicle tank. Comparing the one-tank system to the system with three-tanks in cascade, one sees that the fuelling of the vehicle is independent of the station design as the outlet pressure and the temperature are the same for both system designs. The vehicle fuelling is not influenced by the station design, but the station and the fuelling process are influenced by the pressure loss in the vehicle. Furthermore, the comparison shows that in general the cascade system performs better than the single-tank fuelling station, in that it has a lower amount of total mass stored, lower energy consumption and a faster recovery time. However, the peak cooling demand in the pre-cooler in the dispenser is higher using the cascade system.

Considering the analysis comparing a single-tank fuelling station and the cascade system fuelling station, it was clear that more research should be done to optimise the station design. A more general and detailed compressor model was therefore implemented in the library along with the concept of *stream* which enables the mass flows in the system to be zero. With this improvement, the model is able to do a simulation of a complete fuelling cycle; hence, the vehicle fuelling section and the storage system of the station are in the same model unlike previous studies (e.g. [32]) where they are calculated separately.

The library for hydrogen fuelling was used to build a model of a complete fuelling station, including the storage section, a compressor and the cascade fuelling system. The system was then used to perform three different parameter variations of the cascade system. First, there are simulations increasing the number of tanks in the cascade system from one to eight. Second, for each simulation done in the tank variation, an optimization of the volume of each tank was done. The volumes were specified by decreasing the size of the

highest pressure tank to a minimum, and then the volume of the tank with the second highest pressure was decreased and so on. Third, keeping the volume of the tanks in the first analysis constant at 1 m^3 each, the pressure in the tanks was reduced by reducing the pressure of the highest pressure tank to a minimum, keeping the lowest pressure tank constant. The other tanks were distributed with an equal pressure ratio between them. The study shows that by increasing the number of tanks, the energy consumption decreases approaching an exponential function. By going from a single tank to two tanks in the cascade system, the energy consumption would be reduced by 18 %, and when increasing the number of tanks to more than four, the energy savings becomes less than 5 % for each extra tank. Furthermore, the study shows that the compressor accounts for more than 50 % of the total energy consumption. Decreasing the volumes of the tanks shows that the additional energy savings would be less than 3 %. Though smaller tanks would also decrease the investment costs, even though the energy savings are low, the overall cost could be reduced significantly. The third analysis reducing the pressure in the tanks for each of the systems from the tank variation, shows an additional energy savings of around 4-5 % for each system. In general, the analysis shows that the design of the cascade system has a great influence on the energy consumption of a complete fuelling cycle. Especially with less than four tanks in the cascade system, additional energy savings can be made by an extra tank.

The high-pressure tanks in the cascade system are expensive, and other alternative fuelling systems could be considered in order to reduce the number of tanks. From a system design perspective, fuelling directly from a compressor is potentially the simplest fuelling and should require less energy as the hydrogen is only compressed to the needed pressure for the fuelling of the vehicle. However, by using a compressor directly, the average pressure ramp cannot be satisfied as the system becomes controlled by the mass flow of the compressor instead of the pressure rise at the exit. An alternative system has therefore been proposed, where the compressor instead of fuelling directly into the vehicle, fuels into a small (0.025 m^3) high-pressure buffer tank. The buffer tank then delivers hydrogen for the vehicle fuelling enabling the average pressure ramp rate to be satisfied at the exit of the station, while the compressor runs at constant speed. The direct compression system and the direct compression system with a buffer are compared to a cascade system with four tanks. First, a thermodynamic analysis of each system is performed for vehicles with a high and a low pressure loss. The analysis of the direct compression system shows that it does not compress hydrogen to a higher pressure than needed, and the temperature inside the vehicle tank does not exceed 85 %. The thermodynamic analysis of the direct compression system with a buffer shows that it is possible to perform a fuelling according to the SAE J2601, without using a cascade system. The compressor can run at a constant speed throughout the fuelling, and the buffer tank secures that the average pressure ramp rate

is satisfied. In addition, the thermodynamic properties of the hydrogen in the vehicle are the same for the cascade fuelling and for the direct compression with a buffer fuelling. This emphasizes the point from Chapter 6, that the station does not influence the fuelling of the vehicle, but the vehicle influences the station. Furthermore, the thermodynamic study reveals that it is possible to do two alternative systems where large high pressure tanks are eliminated.

The energy analysis comparing the direct compression system, the direct compression system with a buffer and the cascade system shows that there is not a large difference in energy usage between the direct compression system with a buffer and the cascade system. The reason the direct compression system with a buffer uses the same amount of energy as the cascade system is because the compressor needs to compress to the pressure of the buffer tank, which is at a higher pressure than needed for the fuelling. The direct compression system has an energy savings of 18 % compared to the two other systems. The energy savings of the compressor is more than 23 %, as the pressure out is generally lower than for the two other systems, and the temperature out is also lower resulting in an energy savings of 22 % for the cooling needed after the compression. In order to see which components in the three different fuelling systems have the largest influence on the energy consumption, an exergy analysis is performed for each system, showing the exergy destruction in each component. The exergy analysis shows that the largest exergy destruction for all the systems is in the vehicle's pressure loss and tank. The destruction in the vehicle tank is for all three systems approximately 0.9 kWh. This indicates that the destruction is related to the mass filled and heat of compression, and therefore hard to improve. The compressor and the heat exchanger after the compressor also have high exergy destructions with a total of between 20-29 % for each system. Furthermore, for the direct compression system with a buffer tank, a more intelligent control could be implemented with more starts and stops of the compressors assuring that the pressure reduction across the reduction valve is minimized. Considering the reduction valve in the cascade system and the direct compression system with a buffer, it accounts for 10-17 % of the total exergy destruction. This exergy destruction is not present in the direct compression system as a result of using the mass flow rate directly from the compressor for fuelling instead of an average pressure ramp rate. The most energy-efficient system is without doubt the direct compression system, which has an overall lower energy consumption and exergy destruction.

9.2 Recommendations for further work

The results in this study are based on numerical calculations. Even though the models have been verified with another model and compared to test data from a hydrogen fuelling station, further work lies in an extensive validation of the

model. This could involve using an experimental setup where each component can be tested separately with controlled mass flow and pressures. Validation of the heat transfer model could be done by placing thermocouples inside and on the outside of a hydrogen cylinder in a controlled environment. The hydrogen and wall temperatures should be measured over time to estimate the heat stored in the thermal mass of the tank and the heat transfer to the environment.

Furthermore, it could be interesting to extend the component library to include fuel cell and electrolysis equations and solid storage. In this way the library could be a universal hydrogen library and be able to consider not only fuelling stations, but also complete vehicle systems and solid storage technology.

For research within hydrogen fuelling stations, it could be interesting to investigate systems other than cascade fuelling systems and do life-time cost analysis, to see which one is the best investment.

Another issue would be to optimize the fuelling stations according to the improved fuelling protocol that is to be released soon (end 2013). The new protocol has new temperature intervals for pre-cooling, and there has been discussion about raising the temperature limit inside the vehicle tank.

Having multiple compressors at the station enables the possibility of different operation strategies when fuelling the tanks in the cascade system. There could be one compressor filling the lower pressure tanks and then one which fuels from the lower pressure tanks to the high-pressure tanks, using the tanks in the cascade system as an intermediate step, similar to a two-stage compressor.

Bibliography

[1] Abhilash S, Kim H, Setoguchi T. Three dimensional numerical computations on the fast filling of a hydrogen tank under different conditions. Int J Hydrogen Energy 2012;37:7600–7611.

[2] Bejan A, Tsatsaronis G, Moran M. Thermal design and optimization 1 ed. New York John Wiley & Sons; 1996, p. 113–163.

[3] Bell I, Quoilin S, Wronski J, Lemort V. CoolProp: An open-source reference-quality thermophysical property library. ASME-ORC 2013 – 2nd International Seminar on ORC Power Systems 2013.

[4] Burkert. Data Sheet. 2013. *http* : *//www.burkert.dk/products*$_d$*ata/datasheets/DS*2836 − *Standard* − *EU* − *EN.pdf*. 1, The 10th of June 2013.

[5] Cengel Y, Cimbala J. Fluid mechanics: fundamentals and applications. 1 ed. New York McGraw-Hill; 2006, p. 321–354.

[6] Daney DE. Turbulent natural convection of liquid deuterium hydrogen and nitrogen within enclosed vessels. Int J Heat Mass Tran 1976;19:431–441.

[7] Dicken CBJ, Mérida W. Measured effects of filling time and initial mass on the temperature distribution within a hydrogen cylinder during refueling. J Power Sources 2006;165:324–336.

[8] Dixon S. Fluid dynamics and thermodynamics of turbomachinery. 4 ed. Butterworth-Heinemann; 1998, p. 15–17.

[9] Farzaneh-Gord M, Deymi-Dashtebayaz M, Rahbari H, Niazmand H. Effects of storage types and conditions on compressed hydrogen fuelling stations performance. Int J Hydrogen Energy 2012;37:3500–3509.

[10] Farzaneh-Gord M, Deymi-Dashtebayaz M, Rahbari H, Niazmand H. Effects of geometry and inconsistent mass flow rate on temperature within a pressurized cylinder during refueling. Int J Hydrogen Energy 2012;37:6043–6052.

[11] Fritzson P. Principles of object oriented Modelling and simulation with modelica 2.1. Wiley-IEEE Press; 2004.

[12] Galassi C, Baraldi D, Iborra BA, Moretto P. CFD analysis of fast filling scenarios for 70 mpa hydrogen type 4 tanks. Int J Hydrogen Energy 2012;37:6886–6892.

[13] Heitsch M, Baraldi D, Moretto P. Numerical investigations on the fast filling hydrogen tanks. Int J Hydrogen Energy 2010;36:2606–2612.

[14] Hosseini M, Dincer I, Naterer G, Rosen MA. Thermodynamic analysis of filling compressed gaseous hydrogen storage tanks. Int J Hydrogen Energy 2012;37:5063–5071.

[15] Incropera F, DeWitt D, Theodore B,Lavine A. Introduction to heat transfer. 5 ed. New York John Wiley & Sons; 2007.

[16] Jensen J. Thermodynamic and Thermoeconomic Analysis of Refrigeration Systems for Hydrogen Refueling Stations. Master thesis; The Technical University of Denmark; 2012.

[17] Kaern MR. Analysis of flow maldistribution in fin-and-tube evaporators. Ph.D. thesis; The Technical University of Denmark; 2011. DCAMM special report no. S132.

[18] Kaviany M. Principles of Heat Transfer. 1 ed. New York John Wiley & Sons; 2002, p. 294–296.

[19] Kim SC, Lee SH, Yoon KB. Thermal characteristics during hydrogen fueling process of type 4 cylinder. Int J Hydrogen Energy 2010;35:6830–6835.

[20] Krex H. Maskin staabi. 9 ed. Copenhagen Nyt Teknisk Forlag; 2004, p. 143–151.

[21] Kumer S, Raju M, Kumar V. System simulation models for on-board hydrogen storage systems. Int J Hydrogen Energy 2011;37:2862–2873.

[22] Lemmon E, Huber M, McLinden. NIST standard reference database 23: Reference fluid thermodynamics and transport properties-REFPROP. 9.1. National institute of standards and technology, standard reference library; 2013.

[23] Li Q, Zhou J, Chang Q, Xing W. Effects of geometry and inconsistent mass flow rate on temperature within a pressurized cylinder during refueling. Int J Hydrogen Energy 2012;37:6043–6052.

[24] Maus S, Hapke J, Ranong C, Wuchner E, Friedlmeier G, Wenger D. Filling procedure for vehicles with compressed hydrogen tanks. Int J Hydrogen Energy 2008;33:4612–4621.

[25] Modelica. Modelica- A unified object-oriented language for physical system modeling. 3.2 ed.; 2010.

[26] Monde M, Mitsutake Y, Woodfield P, Maruyama S. Characteristics of heat transfer and temperature rise of hydrogen during rapid hydrogen filling at high pressure. Heat Transfer - Asian Research 2007;36:13–27.

[27] Monde M, Woodfield P, Takano T, Kosaka M. Estimation of temperature change in practical hydrogen pressure tanks being filled at high pressure of 35 and 70 mpa. Int J Hydrogen Energy 2012;37:5723–5734.

[28] Mori D, Haraikawa N, Takiguchi T, Shinozawa T,Matsunaga T,Toh K,Fujita K,Kumano A,Kubo H,. High-pressure Metal Hydride Tank for Fuel Cell Vehicles. SAE-2007 – Society of Automotive Engineers 2007.

[29] Ozsaban M, Midilli A, Setoguchi T. Exergy analysis of a high pressure multistage hydrogen gas storage system. Int J Hydrogen Energy 2011;36:11440–11450.

[30] Raju M, Ortmann J, Kumar S. System simulation model for high-pressure metal hydride hydrogen storage systems. Int J Hydrogen Energy 2010;35:8742–8754.

[31] Richter C. Proposal of New Object-Oriented Equation-Based Model Libraries for Thermodynamic Systems. Ph.D. thesis; Technical University Carolo-Wilhelmina of Braunschweig; 2008.

[32] Rothuizen E, Merida W, Rokni M, Wistoft-Ibsen M. Optimization of hydrogen vehicle refueling via dynamic simulation. Int J Hydrogen Energy 2013;38:4221–4231.

[33] Rothuizen E, Rokni M. Optimization of the overall energy consumption in cascade fueling stations for hydrogen vehicles. Int J Hydrogen Energy 2014;98:582–592.

[34] Society of Automotive Engineers. Fuelling protocols for light duty gaseous hydrogen surface vehicle. Technical Information Report J2601; 2010.

[35] Society of Automotive Engineers. Compressed hydrogen vehicle fueling connection devices. Technical Information Report J2600; 2008.

[36] Smith R. Chemical Process. 1 ed. New York John Wiley & Sons; 2005, p. 273–275.

[37] Woodfield P, Monde M, Takano T. Heat transfer characteristics for practical hydrogen pressure vessels being filled at high pressure. J Therm Sci Tech-JPN 2008;3:214–253.

[38] Woodfield P, Monde M, Mitsutake Y. Measurement of averaged heat transfer coefficient in high-pressure vessel during charging with hydrogen nitrogen and argon gas. J Therm Sci Tech-JPN 2007;2:180–191.

[39] Yang J. A thermodynamic analysis of refueling of a hydrogen tank. Int J Hydrogen Energy 2009;34:6712–6721.

[40] Zhao L, Liu Y, Yang J, Zhao Y, Zheng J, Bie H, et al. Numerical simulation of temperature rise within hydrogen vehicle cylinder during refueling. Int J Hydrogen Energy 2010;35:8092–8100.

[41] Zhao Y, Liu G, Liu Y, Zheng J, Chen Y, Zhao L, et al. Numerical study on fast filling of 70 MPa type III cylinder for hydrogen vehicle. Int J Hydrogen Energy 2012;37:17517–17522.

Appendix A

Appendix

This appendix contains additional information on the components modeled in Dymola. The primary intent is to give the reader an understanding of how the models are composed.

A.1 System structure

The predefined component models in the library can be dragged and dropped into the templates or a new model. It is possible to connect the component models by dragging a line between them. Each model has a user interface that allows the user to change parameters. Changing the parameters in the new system model allows each component to have different values in different system models, hence the parameters are changed locally and specific for the model in that system. This allows the same component model to be reused with different parameters in the same or different systems, eliminating the need for multiple models of the same component in the library. Figure A.1 shows the parameter window for a tank.

A.1.1 Templates

Hydrogen fuelling is a complex process both with regards to the control of the station but also when taking into account SAE J2601 [34]. A template, in which larger systems can be made, containing global variables is therefore necessary. *Template* retrieves the global variables from the *control* model and the information about the fuelling process from the *HRSInfo*. Therefore both

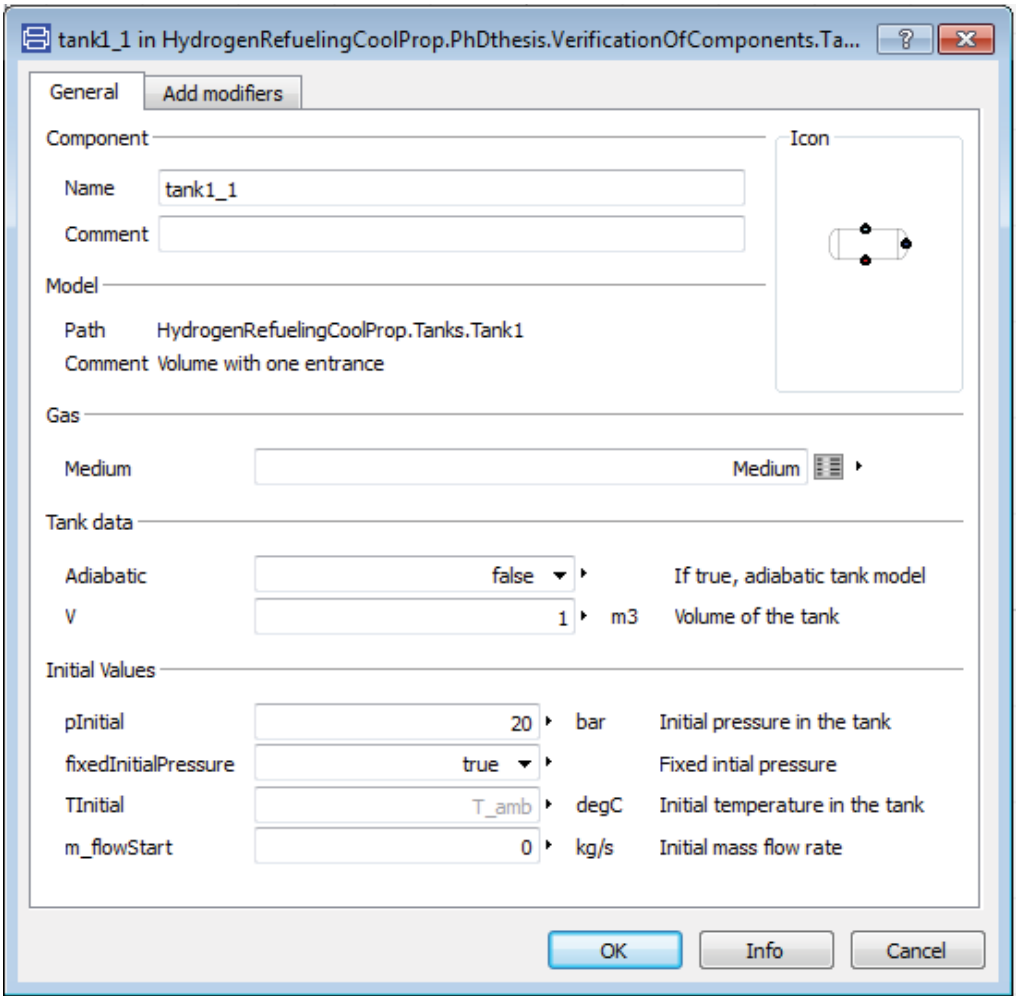

Figure A.1: The user interface of the tank models

a control model and the *HRSInfo* needs to be present, *HRSInfo* comes as standard in *Template*. The global variables which are accessible through the template are for the *HRSInfo*; Ambient temperature (T_amb), Ambient pressure (P_amb) and starting pressure in vehicle (P_start). Parameters from the fuelling protocol are; Average pressure ramp rate (APRR), reference pressure for fuelling (P_ref), target state of charge (SOC_target), ending pressure for fuelling (P_end) and hydrogen temperature out of the station (T_cool). These are all parameters which are found in *HRSInfo* depending on the user input (see information about *HRSInfo* for further explanation). The parameters which are made global from the control models is; z1, z2, z3 and z4. They are integers that, when triggered by an event, can change. The models that need control are depending on these values. Figure A.2 shows a template with a control model, the *HRSInfo* and a whole fuelling system. The template is the white background on top of which the components lie. The principle of connecting

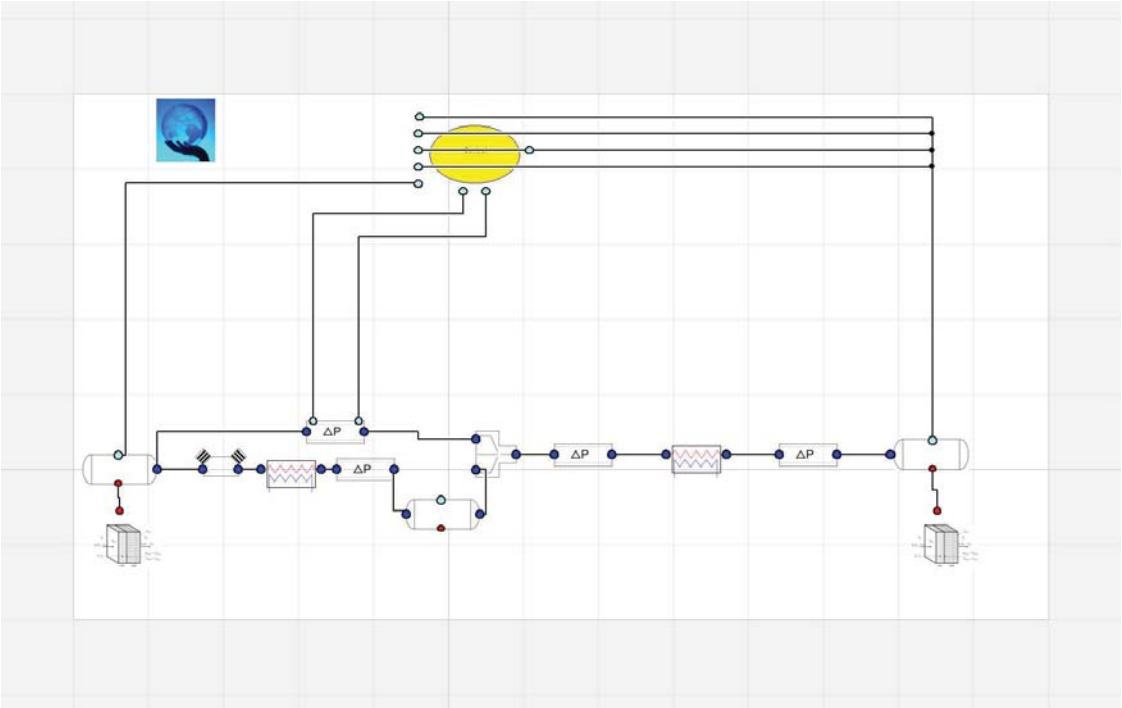

Figure A.2: The template with the HRSInfo, a control model and ta whole fuelling system

the components is also shown. *Template2* is a template where the connections to the control model have been eliminated, it can be used for simple systems which do not require controls. The *HRSInfo* is integrated in the template in a way which means it can be present without being used, unlike the control models. If no models are added in *Template2* it can lookup values from the fuelling protocol J2601, based on the user's inputs in *HRSInfo*.

A.1.2 Fueling protocol

The fuelling of hydrogen can be done according to the technical information report from the society of automotive engineers J2601; Fueling protocol for light duty gaseous hydrogen surface vehicle [34]. The model *HRSInfo* has integrated the protocol and by typing the ambient temperature (T_amb), the starting pressure in the vehicle tank (P_start) and choosing the fuelling protocol, the model returns target pressure for the vehicle tank (P_end), target state of charge (SOC_target), average pressure ramp rate (APRR), reference pressure (P_ref) and temperature of hydrogen out of the station (T_cool). Another parameter which can also be typed in by the user is ambient pressure which is not used for the lookup, but by having it here it can be made accessible for other models through the templates. The model can be used as a stand-alone

for calling parameters, but it is integrated into both the templates so all returns from the call are available for the models of other components..

A.1.3 Connectors

A connector is the outside link to a model that assures that data can be passed on into or out of the model. For the hydrogen fuelling library there are three different connectors that are used; *FlowPort*, *PressurePort* and *HeatFlow* which has 4 derivations. The ports have no user based options for changes and they are designed for minimizing the number of different ports needed in the library. The *FlowPort* is the general port passing on information between the components. All models have at least one *FlowPort* port. It passes on mass flow, enthalpy and pressure. The flow port uses the concepts of *flow* and *stream* for the mass flow and enthalpy, repectively. The *HeatFlow* port passes on information between the heat transfer models. It passes on information of temperature, pressure, area and heat flow. There are four different heat ports with minor differences in which data is passed on. *HeatFlow2* also passes on mass flow, *HeatFlowTube* is specifically designed for heat transfer through a tube wall and *TemperaturePort* only passes on temperature. The *PressurePort* port passes on information about pressure in the component, this is used for passing on information from the component to the control model. The ports are collected in the folder called Ports i the library and their symbol are shown in figure A.3.

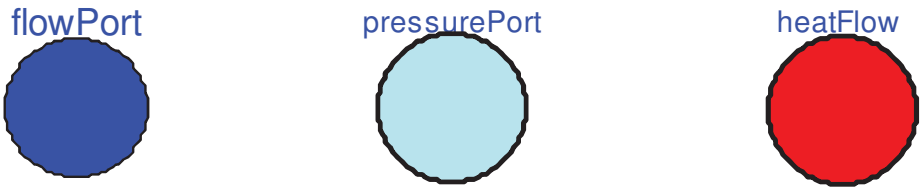

Figure A.3: The ports as they appear in Dymola. From left: flowport, pressureport and heatflow

A.1.4 Tanks

The folder *Tanks* in the library includes 2 models. One for a tank with one entrance and one for a tank with two entrances.

- Tanks
  - *Tank1* - Tank model with one entrance
  - *Tank2* - Tank model with two entrances

The most common kind of tank for hydrogen storage has one entrance, but in some systems 2 entrances are useful. The tank models are made with the equations from section 3.4 using enthalpy. The tank models have the user defined parameters and choices:

- Parameters
  - Volume (V) - Volume of the tank
  - Initial pressure ($pInitial$)
  - Initial temperature ($TInitial$)
  - Guess start mass flow rate ($m\_flowStart$)
- Choices
  - Adiabatic fuelling ($Adiabatic$) - true for adiabatic fuelling
  - Fixed initial pressure ($FixedInitialPressure$) - True for fixed pressure

The possibility of choosing an adiabatic tank enables the user to easily switch between a tank with or without heat transfer without deleting models. The option of fixing the pressure or only using it as a guess value is useful when a tank is placed between two other volumes, with unknown pressure losses in-between, as the initial pressure in such case is unknown. The output of the Tank models are the changes in thermodynamic properties such as pressure, enthalpy, internal energy, entropy, exergy, temperature, density, thermal conductivity, heat flow rate etc. Other properties that can be seen are the change of total mass, the mass flow rate and the state of charge of the tank. For a tank used as a vehicle tank, the state of charge is related to the protocol and for a storage tank at the station the state of charge is related to the initial mass in the tank. Figure A.4 shows the symbol of the tank in the library. The tank models have

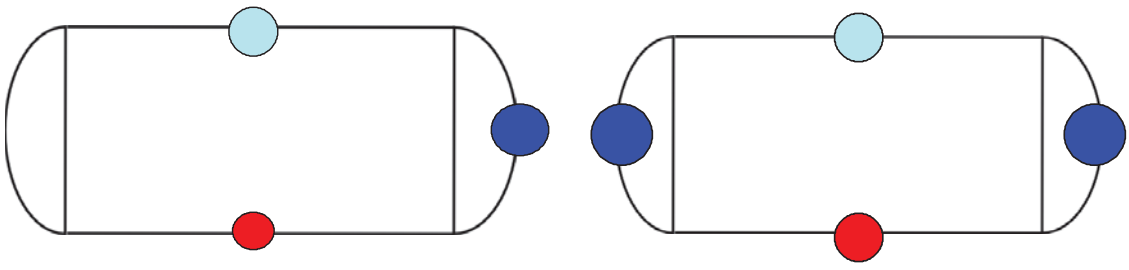

Figure A.4: Tank1 to the left and tank2 to the right

besides the *FlowPorts* one *HeatFlow* and one *PressurePort*. The *HeatFlow* and *PressurePort* are optional ports and if no connections are present the model will still function. The *PressurePort* passes on the pressure to the control model

and the *HeatFlow* port exchanges data with the heat transfer model, by not connecting to a heat transfer model, the tank is per definition adiabatic.

A.1.5 Heat transfer

The heat transfer model is the the only model that uses sub models. The heat transfer model is created by connecting several cells together. The structure in the library is as follows:

- HeatTransfer
  - *HeatTranferTank* - Heat transfer model for a tank
  - *HeatTranferTube* - Heat transfer model for a tube
  - *WallPieces* - Folder containing sub models
    - InnerWallCell
    - OuterWallCell
    - LinerCell
    - TankCell
    - TubeCell
    - Liner5Pieces
    - Tank10Pieces
    - Tube5Pieces

The two models which is used for simulations is *HeatTranferTank* and *HeatTranferTube*. The folder *WallPieces* contains submodels that are used in the two main models in order to get unsteady 1-dimensional transient heat transfer for the tank and tube walls as well as changing gas temperature in the length dimension of the tube. The models named liner represent the first layer of material in a tank and the models named tank represent the wrapping around the liner. The models named tube are specifically made for calculation of heat transfer in a tube with a non-uniform temperature distribution of the hydrogen. The sub-models named "Cell" at the end represent one volume of the wall and the sub-models named "Pieces" in the end contains a number of cells in serial connection. The predefined numbers of liner cells in a tank is 5 and for tank cells it is 10 cells. The number of cells is chosen iteratively using several simulations with different numbers of liner and tank cells. It was found that using more than 5 liner cells and 10 tank cells did not change the results but increased the calculation time. For the tube there are 3 volumes through the wall and 30 pieces, each containing the 3 volumes of the wall, in the lengthwise direction of the wall.

Tanks

The parameters that are user defined for *HeatTranferTank* are:

- Parameters
  - Charging heat transfer coefficient (*h_charging*)
  - Dicharging heat transfer coefficient (*h_discharging*)
  - Heat transfer coefficient outside the tank (*h_o*)
  - Thickness of liner (*xLiner*)
  - Thickness of wrapping (*xTank*)
  - Inside diameter of the tank (*dInner*)
  - Inside length of the tank (*LInner*)
  - Inside area of tank walls (*AInner*)
- Choices
  - Tank type (*tank*) - Decides the tank type for property calls
  - Calculation of area used (*Area*) - true for using the given tank dimension to calculate area, false to type own area

The choice of tank type is between the 4 different tank types used for pressurized hydrogen; Type I, Type II, Type III and Type IV. Table A.1 shows the main properties of the different tank types used in the heat transfer model. This enables the same model to be used for all the different tank types. Further

Property/Tank	Type I	Type II	Type III	Type IV
Tank	Steel	Alumina	Composite	Composite
Specific heat $[kJ/(kgK)]$	481	896	1075	1075
Thermal conductivity $[W/(mK)]$	15	236	1.14	1.14
Density $[kg/m^3]$	8050	2700	1374	1374
Liner	-	-	Alumina	Plastic
Specific heat $[kJ/(kgK)]$	-	-	896	1578
Thermal conductivity $[W/(mK)]$	-	-	180	1.17
Density $[kg/m^3]$	-	-	2700	1287

Table A.1: Properties of the four different tank types for storing of hydrogen

the geometry of the tank is user defined, it is therefore possible to model most hydrogen tanks within a good estimate. The properties of the tank materials are predefined by standard, but it is possible to change them by changing the external text document "Heatransferporperties.txt". The inside area of the tank can either be calculated by the user defined geometrical parameters or given directly by the user. The area will in both cases increase throughout the

wall with the thickness of the walls using radial coordinates. The model considers the mass flow rate in the tank to decide which heat transfer coefficient to use, the tank can therefore both be charged and discharged within the same simulation. A.5. The output of the model is the heat flow rate through the

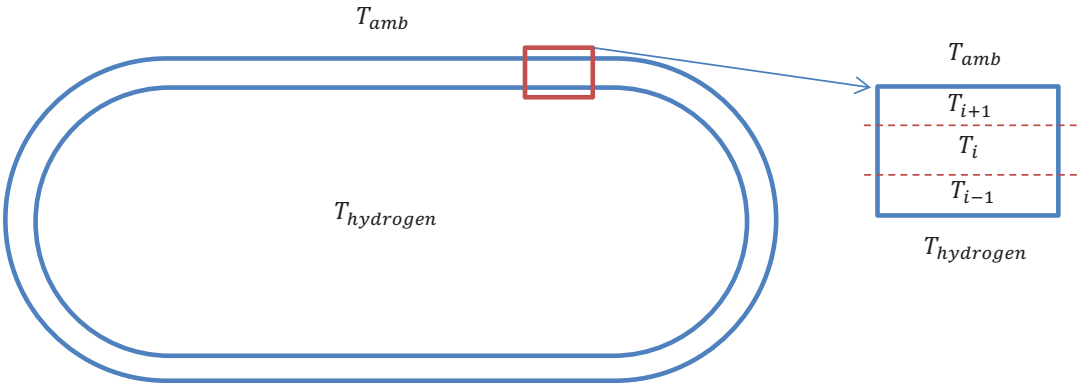

Figure A.5: Sketch of the principal of the model in Dymola

wall which is used in the energy balance of the hydrogen inside the tank. The change in thermodynamic properties of hydrogen in the tank is interdependent with the heat flow through the wall. Other outputs are the temperature distribution in the wall, the heat flow through each layer etc. The principle of the heat transfer through the wall in the tank is shown in fig. A.5. The temperature distribution of the hydrogen inside the tank is uniform that results in a uniform temperature distribution in the wall.

Tubes

For the tube model the parameters and choices that are user defined in *HeatTranferTube* are:

- Parameters
  - The inner diameter of the tube (d_i)
  - The outer diameter of the tube (d_o)
  - The Length of the tube (*Length*)
  - The heat transfer coefficient outside the tube h_o

The tube properties are the same as for stainless steel in table A.1. The change of the hydrogen temperature through the tube is calculated in 30 steps in the flow direction. The output of the heat transfer model of the tube is the temperature out. Though the temperature into, out of and through the wall of each wall piece can be found. The principal of the heat transfer through a

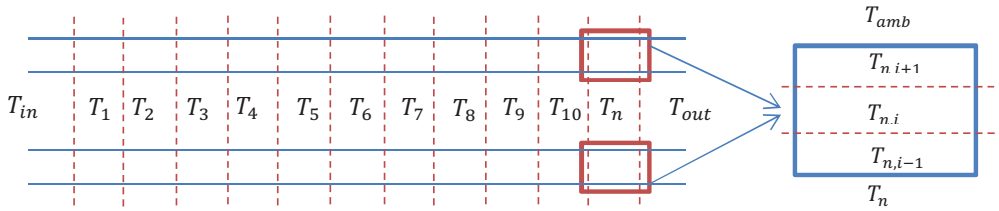

Figure A.6: The principal of the tube in Dymola

tube is shown in figure A.6. The tube consists of 30 pieces that each contain a uniform temperature distribution of the hydrogen. Though, the hydrogen temperature changes between each piece. Each tube piece can be considered as a 1-dimensional unsteady heat flow model. Though, between each piece the temperature of the hydrogen changes, so the heat transfer is 2-dimensional as the temperature both changes through the wall but also in the flow direction.

A.1.6 Pressure losses

The pressure loss folder consists of 4 models with different functions.

- PressureLosses
  - *ReductionValve* - Reduction valve model
  - *AveragePressureRampRate* - Sets an average pressure ramp rate
  - *PressureLoss* - Pressure loss model containing 3 different presure losses
  - *TubeWithHeatTransfer* - Tube model with heat transfer connections

All the pressure loss components consist of two flow ports where one acts as an entrance and the other as an exit, though the ports are not dedicated and the flow can go both ways through the model due to the flow and stream concept. The model symbols are shown in figure A.7. For all the flow components the

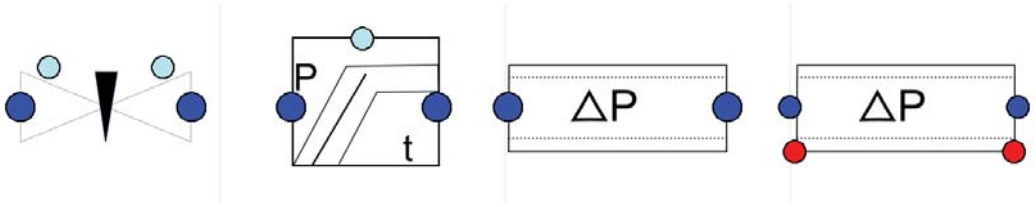

Figure A.7: From the left. ReductionValve, AveragePressureRampRate, PressureLoss and TubeWithHeatTransfer

pressure loss is formulated as a function of the volume flow. This result in the pressure loss is found as a square root. In order to avoid problems when the volume flow approaches or is equal to zero a square root function is used, linearising the pressure drop when it becomes less than 10 Pa. The outputs that can be studied are the thermodynamic properties; the pressure drop, enthalpy, exergy, temperature etc.

Reduction valve and average pressure ramp rate

The reduction valve and the average pressure ramp rate are closely connected and if one is used the other one needs to be present. The average pressure ramp rate sets the ramp rate in a system at the placement of it. This is the only the place where the ramp rate is set and therefore not necessarily the same place as where the pressure is regulated. The reduction valve regulates the pressure so that the average pressure ramp rate is maintained in the average pressure ramp rate model, thus compensating for pressure losoes that might occur between them. The reduction valve has two pressure ports to measure the pressures at the inlet and exit; these are used in the control for changing tanks. The average pressure ramp rate has one pressure port which is also used to measure the pressure. The reduction valve and the average pressure ramp rate components have the following parameter inputs:

- Reduction valve
  - Initial temperature in (*TinitialIn*)
  - Initial pressure in (*pIntialIn*)
  - Initial pressure out (*pInitialOut*)
- Average pressure ramp rate
  - Initial temperature (*TInitial*)
  - Initial pressure (*pInitial*)
  - Alternative ramp rate (*APRR2*)
  - Choice between which ramp rate to use (*SAEJ2601*)

The initial values are guess values and an approximate guess is enough. For the reduction valve both the pressure into and out of it should be guessed as the pressure difference often can be of significant magnitude. For the average pressure ramp rate, there is the possibility of using a user defined ramp rate instead of the predefined ramp rates from the protocol SAE J2601 [34]. If *SAEJ2601* is false then the *APRR2* is enabled. The output of the average pressure ramp rate is a pressure rise equal to the ramp rate and for the reduction valve the pressure out is decided to maintain the average pressure ramp rate.

Pressure losses

The pressure loss model consists of the option to choose between the three different pressure losses described in chapter 3.6. the options are; pressure loss through a valve with a given pressure loss constant (k_v), pressure loss through a mass flow meter or a filter with a given pressure loss constant k_p and pressure loss through a tube including length equivalent pressure losses. The inputs that are given to the *PressureLoss* model are:

- Tube
  - Inside diameter (*Diameter*)
  - Length in flow direction (*Length*)
  - Roughness of tube (*Roughness*)
  - Length equivalent (*K_length*)
- Valve
  - Pressure loss constant (*kv*)
- Filter and mass flow meter
  - Pressure loss constant (*kp*)
- Common parameters for all pressure losses
  - Initial temperature (*TInitial*)
  - Initial pressure (*pInitial*)

When one of the three different pressure loss calculations is chosen the parameters that need to be filled in become accessible in the software and it is not possible to put in values for other parameters than the ones related to the pressure loss. The initial state parameters are stating guess values and do not need to be accurate.

Tube with heat transfer

The tube model with heat transfer consists of the same parameters as the tube model in the *PressureLoss* model for deciding the pressure loss, but in addition it has the outer diameter of the tube for calculation of the Biot number. Further it has two heat transfer ports, which should be connected to the tube heat transfer model. It also has more outputs as the coefficient of heat transfer for the hydrogen is calculated. The heat transfer ports pass on the relevant information for calculating the temperature out to the heat transfer model and it then receives the temperature out of the tube.

A.1.7 Compressors

The *Compressors* folder contains one master compressor *Compressor* model and a number of variations, made for specific systems, e.g. different control, volume instead of mass flow based. The variations are not considered here as they only deviate a little from the master compressor model and they do not change the core compressor equations from 3.7. The inputs for the compressor model are:

- Choice of efficiency calculation *CompressorType*
- Number of strokes per minute *Strokes*
- The volume of the cylinder

The output is the work done, the efficiency, the enthalpy, pressure and temperature out. The compressor is modelled without cooling, but a heat exchanger can be placed after it in a system to obtain an estimate of the cooling demand needed in the compressor for a specific outlet temperature. The symbol of the compressor model is shown in fig. A.8 There is a maximum pressure ratio of 5

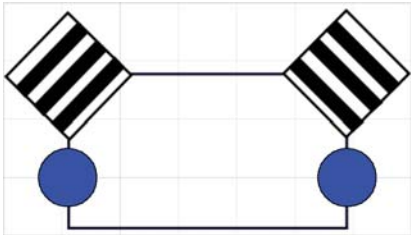

Figure A.8: The compressor symbol in Dymola

limitation to the compressor model, see chapter 3.7.2

A.1.8 Heat exchangers

The *HeatEchangers* folder contains one model of a simple heat exchanger according to chapter 3.8. The model has the option of using the outlet temperature set by the protocol SAE J2601 [34] or to use a user defined outlet temperature. The heat exchanger works with flow from either direction and gives the outlet temperature set. The output is the cooling demand. Figure A.9 shows the symbol of the heat exchanger model.

A.1.9 Mixers

The folder *Mixers* contains two models of mixers. One with a volume *VolumeMixer* and one without *IdealMixing*, see chapter 3.8 for further theoretical explanation.

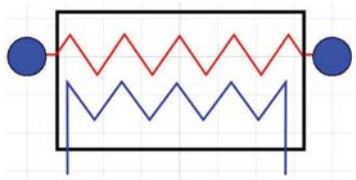

Figure A.9: The heat exchanger symbol in Dymola

- Mixers
  - *VolumeMixer* -Mixer with a volume
  - *IdelaMixer* - Mixer without a volume

The ideal mixing without a volume has no inputs. The mixer with a volume has the following inputs:

- Volume of the mixer (V)
- Fixing the pressure (*FixedIntitalPressure*)
- Initial pressure (*pInital*)
- Initial temperature (*TInitial*)

For the volume mixer the volume should be small so it does not influence the system, if it is too large it will act as a tank with 3 entrances. The Fixed initial pressure is an important parameter as the initial pressure either is fixed or just a guess value. With other volumes connected directly to the mixer one of them has to be fixed and the other one free. Both the *VolumeMixer* and the *IdelMixer* models have a confusing way to show results. In the model when simulated all the ports have the same pressure and enthalpy, even though the flows going into the mixer have different enthalpies. This is because the connectors are considered to be just inside the mixer and therefore take the same values as the mixed flow. For the energy balance the correctly values for enthalpies are used through the stream concept. The mass flow entering or leaving the mixer is shown correct in the ports. The symbol of the mixer component model is shown in fig. A.10

A.1.10 Switches

The switch is used to choose which flow to pass on to the rest of the system choosing from more than one flow. The switches folder contains switches with entrances of between 2 to 10 flows. The switches are components without any mathematical description, as it they do not influence the properties of the flow. The switches are controlled by the control model and receive a signal through

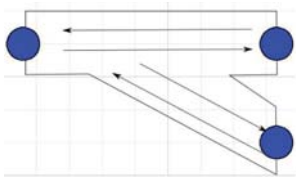

Figure A.10: The mixer symbol in Dymola

a global variable which it then uses to direct the flows. There are two different kinds of switches, one with a stop (*WithStop*) and one without (*WithOutStop*). The parameters of the model are:

- Switch control - compressor or vehicle (*control*)
- Stop control - Station or vehicle decided - only available in models with stop)(*control2*)

The Stop function terminates the simulation when either the vehicle tank is filled up or when the tanks at the hydrogen fuelling station are filled up. Both type of switches are controlled by either the pressure difference across the reduction valve or the pressure in the tank at the station. The option of controlling it by the pressure across the reduction valve is used to direct the flow of fuelling a hydrogen vehicle. the option controlling it by the pressure in the tanks at the station are used to direct the flow from the compressor. The symbol for the *Switches* is shown in fig. A.11.

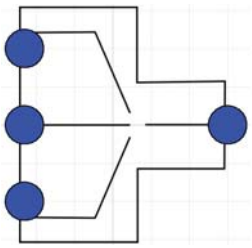

Figure A.11: The switch symbol in Dymola, for a switch choosing between 3 flows

Appendix B

Verification of listed component models

This appendix contains additional information on the components modeled in Dymola. The primary intent is to show the the behavior of the thermodynamic component models.

Tank

The following figures show the temperature, pressure and mass development in two tanks. One tank which is discharging through a valve into a charging tank, see fig. B.1. The volume of both tanks are $1m^3$ and they are adiabatic. The valve is isenthalpic and does not influence the tanks but it assures a slower mass flow between the tanks in order to see the thermodynamics of the tanks better. Figure B.2 shows the pressure and temperature development in the two tanks.

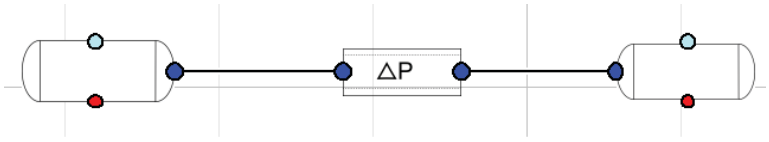

Figure B.1: The system considered for the verification. Two tanks with a valve in-between to lower the mass flow rate between them (from left to right)

The pressure decreases in the tank that in discharged and increases in the tank

charging. The final pressure in the two tanks are the same. The temperature

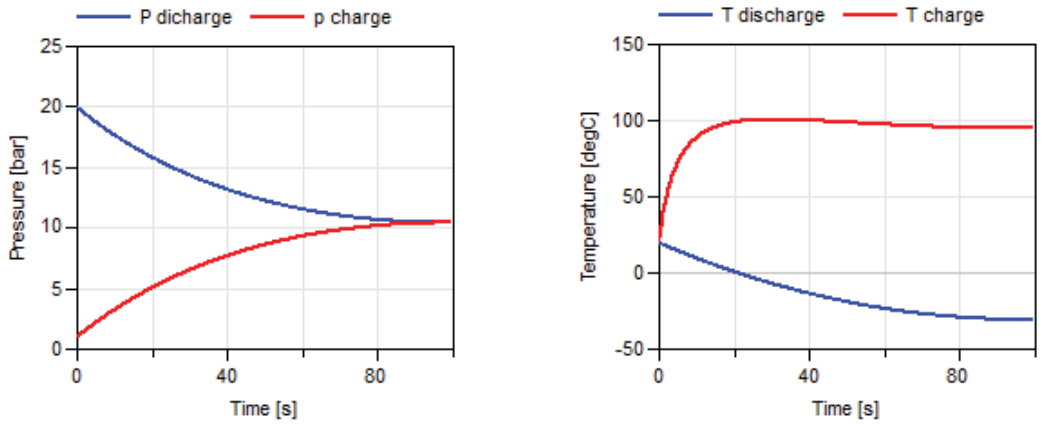

Figure B.2: Temperature (right) and pressure (left) development in the tanks. Tank1 is discharging and tank2 charging

decreases in the tank discharging due to mass leaving the tank and increases rapidly in the first 10 seconds of the tank being charged, this was expected as the temperature increase depends on the ratio of the pressure increase in the tank and it is largest in the first period of time, hence heat of compression. The temperature then levels out and in the end decreases. The decrease in temperature is due to the lower temperature of the hydrogen entering the tank, and expected when considering the temperature difference between the tanks. Considering the internal energy of the two tanks in fig. B.3 it decreases in the tank discharging and increases equivalent in the charging tank, this was expected as there should be energy balance in the system. Further the internal energy of the two tanks added together is constant, proving the energy balance. The right side of figure B.3 shows the mass in the two tanks, here the mass decreases in the tank being discharged and it increases equivalent in the tank charging, as expected there is mass balance in the system. The Total mass in the system is constant proving the mass balance. As the tanks are $1m^3$ each, the mass is equal to the density. The density in the tank discharging decreases as mass is flowing out of the tank and the density increases equivalent in the tank charging as mass flows in to it. This is very much as expected. Even though the two tanks have the same pressure in the end, there is a density difference, this is due to the large temperature differences between the tanks. Hot gas has a lower density than cold gas, the density development of the tanks therefore seem reasonable compared to each other. Figure B.4 shows the enthalpy in the two tanks. The charging tank has an increase in enthalpy while the discharging tanks enthalpy decreases.

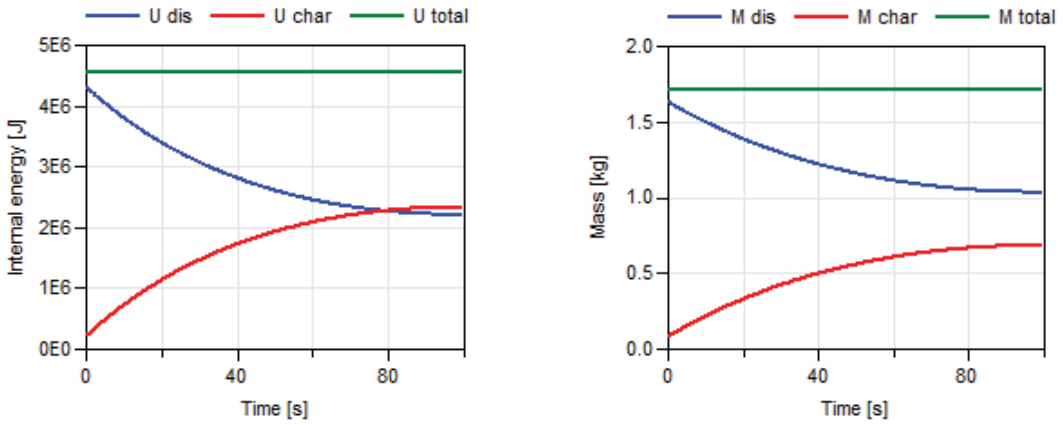

Figure B.3: Internal Energy (left) and mass development with energy including total energy and mass in the system. Tank1 is discharging and tank2 charging

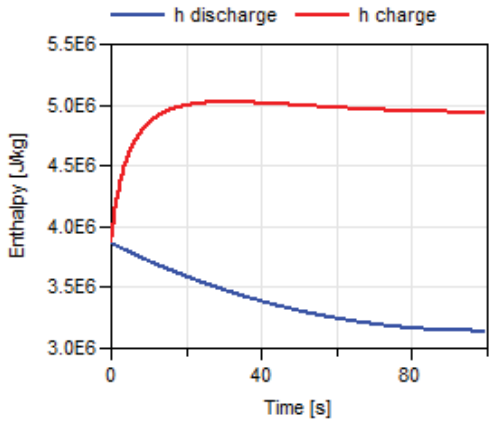

Figure B.4: Enthalpy development in the tanks. Tank1 is discharging and tank2 charging

Heat transfer

This section contains simulations to show the behavior of the heat transfer models. It is used for verification of the tank and the tube. heat transfer models.

Heat transfer for tank model

The results when simulating the tank model of the heat transfer is shown for both a charging and discharging tank. The system used is the same as for the tank verification, but with heat transfer added to the two tanks. Figure B.5 shows the system with mass flow from left to right. The heat flow between the

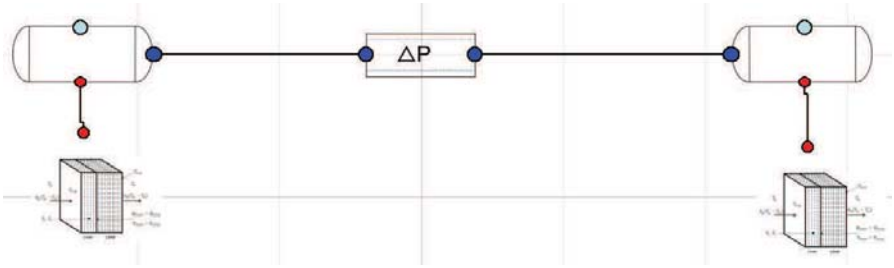

Figure B.5: Model used to for verification of the tank heat transfer model

hydrogen and the wall and the temperature of the hydrogen in the tank for the four different tank types are shown in figure B.6 and B.7 for discharging and charging, respectively.
The heat flow from the hydrogen to the tank wall depends on the material of the wall. It is shown that Tank II and Tank III which have alumina as the contact surface with the hydrogen have the highest heat flow in the beginning. The Type I tank made of steel has similar properties of the type III, but does not absorb the heat as fast. Considering the properties of the tanks shown in table A.1 this was expected, as the conductivity of aluminum is the highest, followed by steel, the plastic liner and carbon fiber wrapping. The temperature of the hydrogen inside the tanks are noticeably different comparing a tank with heat transfer and an adiabatic tank. This was expected as energy is either absorbed by the tank when charging or desorbed when discharging. The discharging tank has the largest variation in temperature and heat flow among the different tank types. This is because the heat transfer number is larger using Daney's correlation which increases influence of the tank materials on the heat transfer. Considering the wall of the a charging tank fig B.8 and B.9 shows the temperature for the different wall cells in the simulation with heat transfer coefficients of $h = 150W/(m^2K)$ and $h = 500W/(m^2K)$, respectively. Figure B.8 shows that the aluminum liner almost has the same temperature all the way through it and that the carbon fiber wrapping has a large temperature gradient. This is due to the conductivity of the carbon fiber, which is low compared to the aluminum conductivity. Further fig. B.9 shows a comparison between the heat transfer coefficient, the temperature of the hydrogen and the temperature of the liner. The heat transfer numbers compared are $h = 150W/(m^2K)$ and $h = 5000W/(m^2K)$. It can be seen that with the high heat transfer number the hydrogen is considerably colder and the temperature of the liner is almost

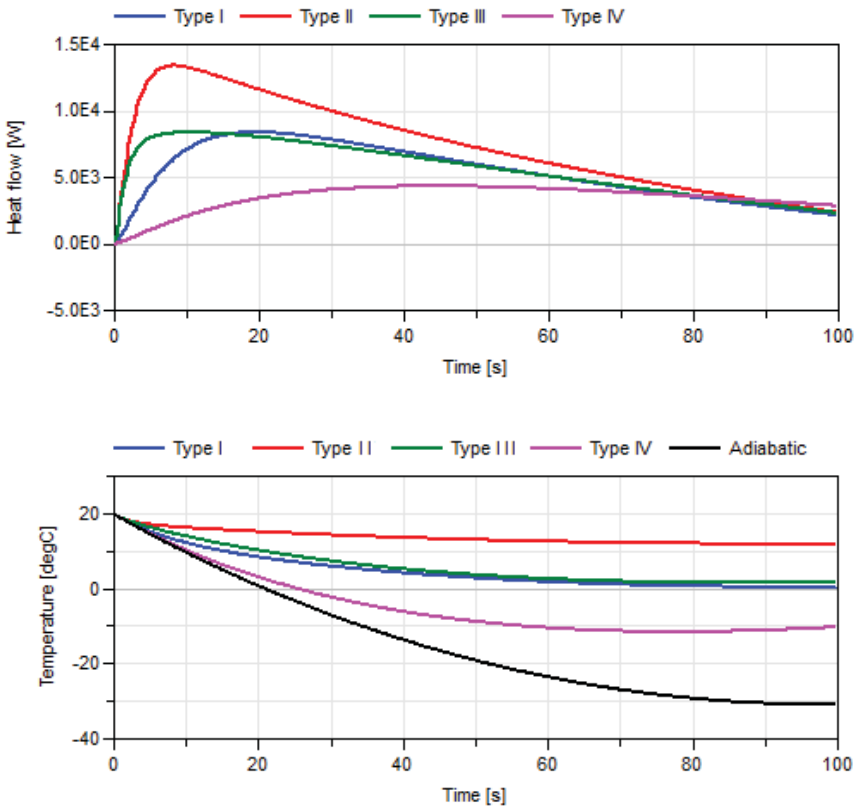

Figure B.6: The heat transfer and temperature difference between the different tank types for a discharging tank. Top: The heat transfer between the hydrogen and the wall. Bottom: The temperature of the hydrogen

the same. This shows that the limiting factor is the heat transfer number and considering the fig. B.8 also the carbon fiber wrapping. The heat flow through the tank wall corresponding to the temperatures in fig B.8 is shown in fig B.10. The heat flow is largest at the beginning where the hydrogen is rapidly increasing in temperature, hence the largest temperature difference between the hydrogen and the wall. The heat flow from the hydrogen to the walls results in a decreasing hydrogen temperature and thereby a lower heat flow. For discharging the temperature distribution and the heat flow through the wall are shown in fig. B.11 and B.12, respectively. The heat flow shows the same relation to the temperature difference, the higher the temperature difference the higher the heat flow. This is as expected as the heat transfer is a function of the temperature difference.

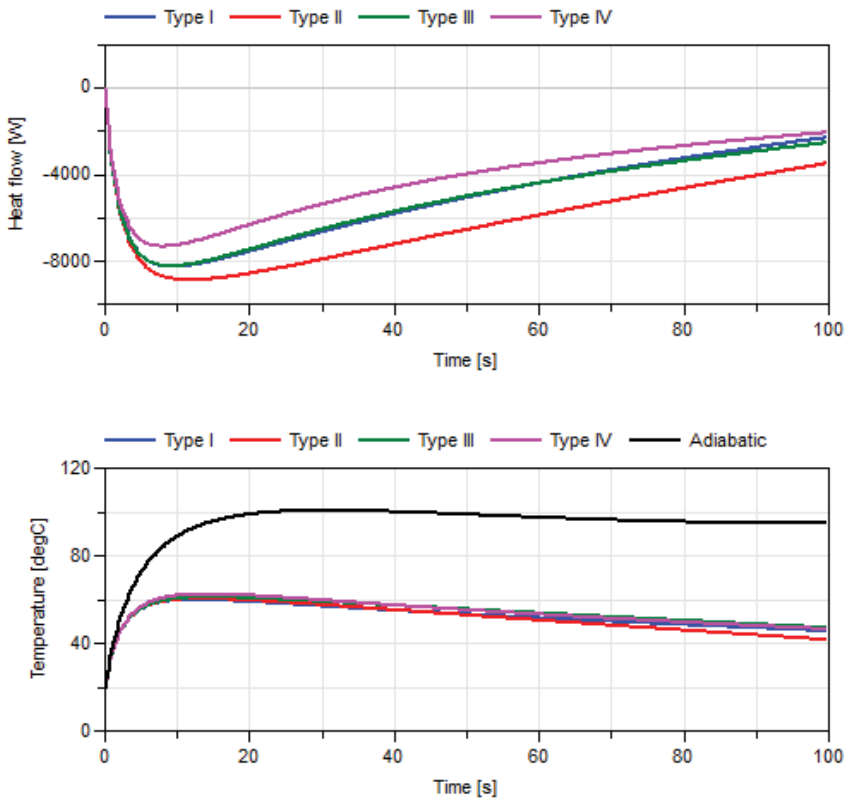

Figure B.7: The heat transfer and temperature difference between the different tank types for a charging tank. Top: The heat transfer between the hydrogen and the wall. Bottom: The temperature of the hydrogen

Heat transfer for tube model

The system simulated for heat transfer in tubes is shown in fig B.13. The system is similar to the one used for the verification of the tank model, but a piece of 12 meter tube has been added between the discharging tank and the valve. The mass flow in fig B.13 goes from the right to the left. The tube heat transfer model has similarities to the tank heat transfer model as the heat transfer through the wall is calculated in the same way, although the wall is build up by 3 wall pieces through the wall and 30 pieces in the flow direction that consist of 3 walls cells each. The temperature change of the hydrogen flowing through a tube is shown in figure B.14. The temperature is shown for the entrance, the exit and for each 5 pieces of wall (each 1 meter of tube). The temperature of the hydrogen into the tube is decreasing and is beneath the ambient temperature, which is also the initial temperature of the tube. When the hydrogen flows through the tube it heats up as the tube is warmer than the hydrogen. The heat up is dependent on the hydrogen and the thermal mass

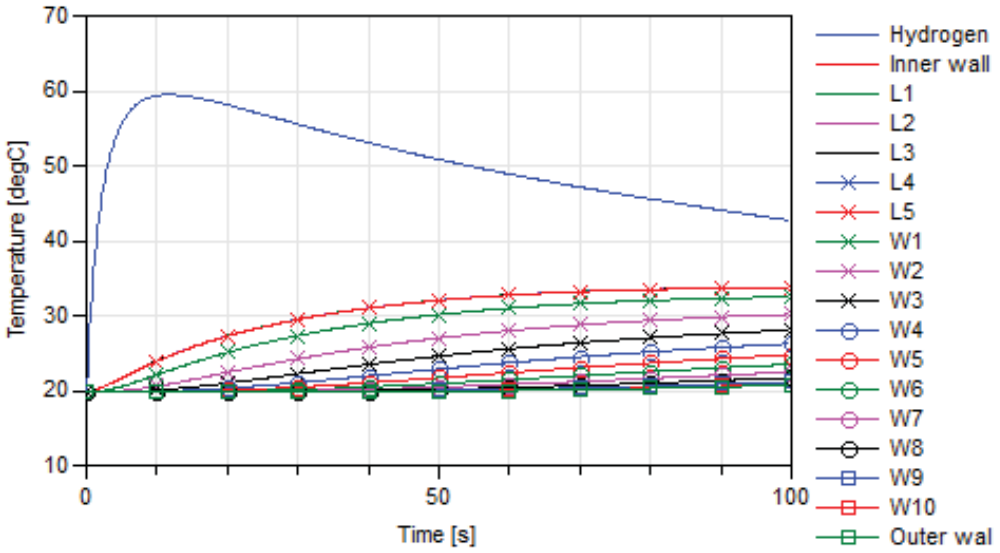

Figure B.8: Temperature distribution in the wall of a tank Type III with $h = 150W/(m^2K)$

of the tube. Considering the tube at the entrance, the middle and at the exit. The temperature of the hydrogen, the inner wall of the tube and the outer wall of the tube is shown in fig. B.15. The hydrogen temperature increases through the tube and so also does the wall temperature of the tube. The wall inside and outside temperatures are almost the same. The walls are cooled down to a temperature close to the hydrogen and stays only a couple of degrees warmer than the hydrogen through out the tube even though there is a temperature difference to the ambient of $30°C$. The reason for this can be found in the heat transfer coefficients, to the ambient there is natural convection and inside the tube the flow is turbulent causing forced convection. It is therefore as expected that the tube has a temperature close to the hydrogen temperature. This point is stated when considering the heat flow for the middle piece of the tube, shown in fig. B.16. The heat transfer "inside the wall", is between the hydrogen and the wall, the heat transfer in "tube wall" is heat transfer between the control volumes of the wall and "out side tube wall" from the wall to the ambient. The heat transfer from the hydrogen to the wall is much larger than from the wall to the ambient which is consistent with the temperature of the tube walls.

Pressure losses

Considering the pressure losses the system shown in in figure B.17 has been used. The system consists of two tanks, one discharging into the other one,

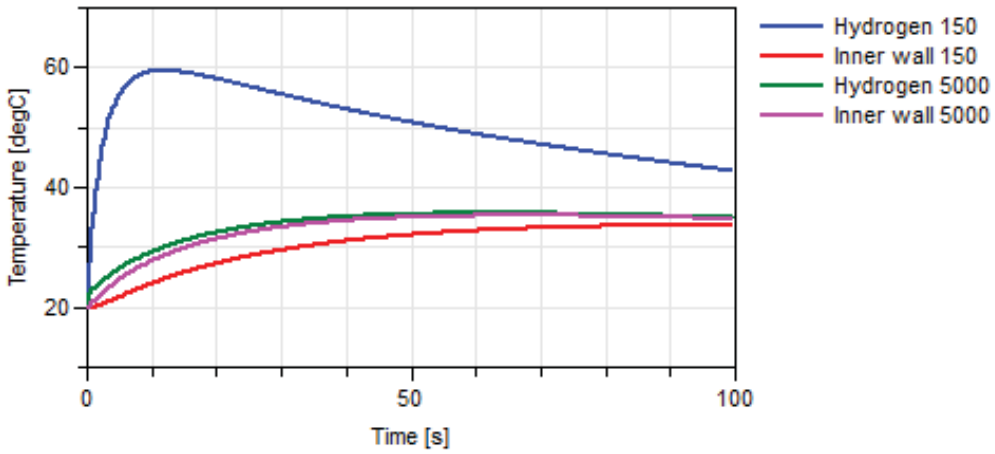

Figure B.9: Temperature of the gas and the inner wall of a tank Type III for $h = 150W/(m^2K)$ and $h = 5000W/(m^2K)$

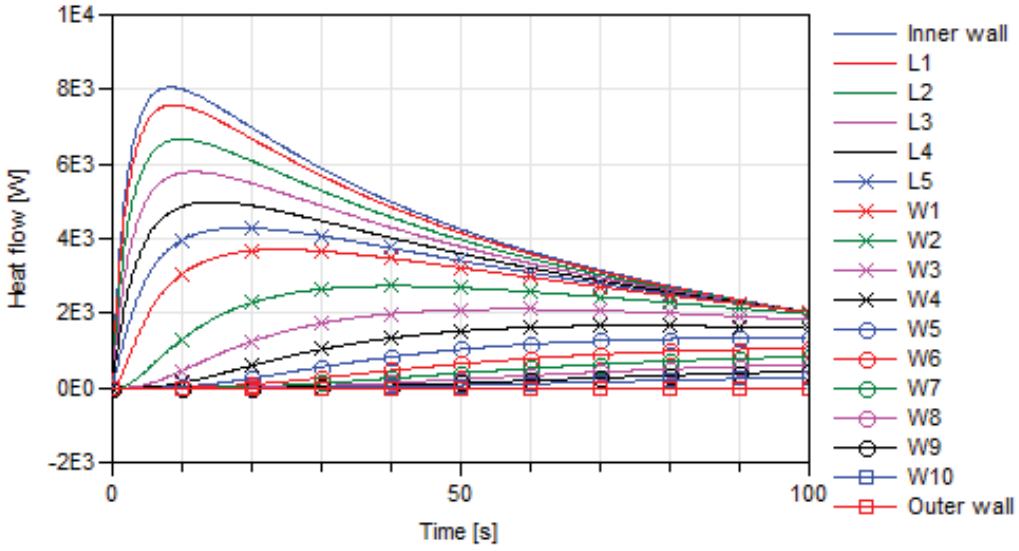

Figure B.10: Heat flow through the cells in the tank wall of a Type III tank using $h = 150W/(m^2K)$

the pressure loss component model, a reduction valve and an average pressure ramp rate. The reduction valve and average pressure ramp rate has been used for all the pressure loss models, as the ramp rate secures the same volume flow, hence the volume flow is independent of the pressure loss model considered, see chapter 6. The analysis can therefore be made with basis of the same volume

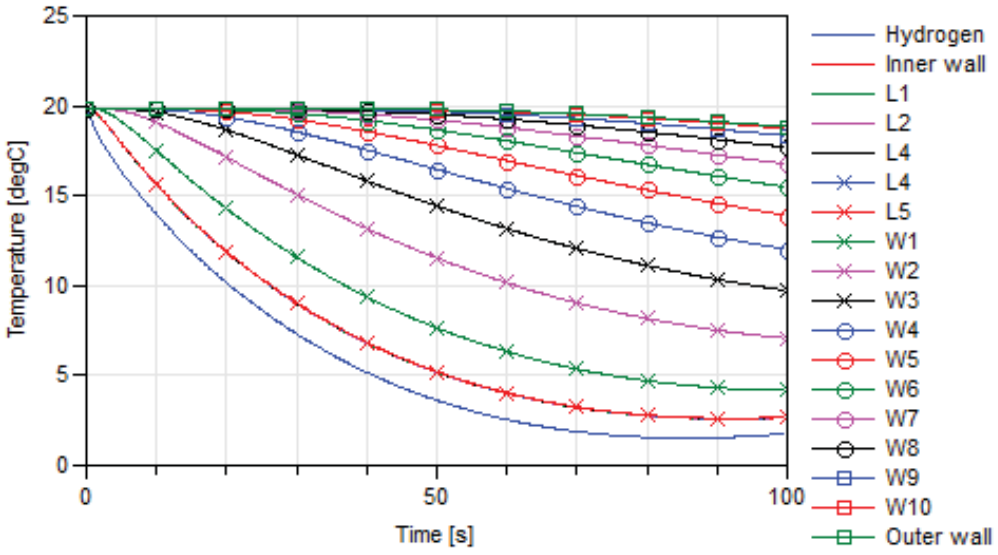

Figure B.11: Temperature distribution in the wall of a tank Type III when discharging

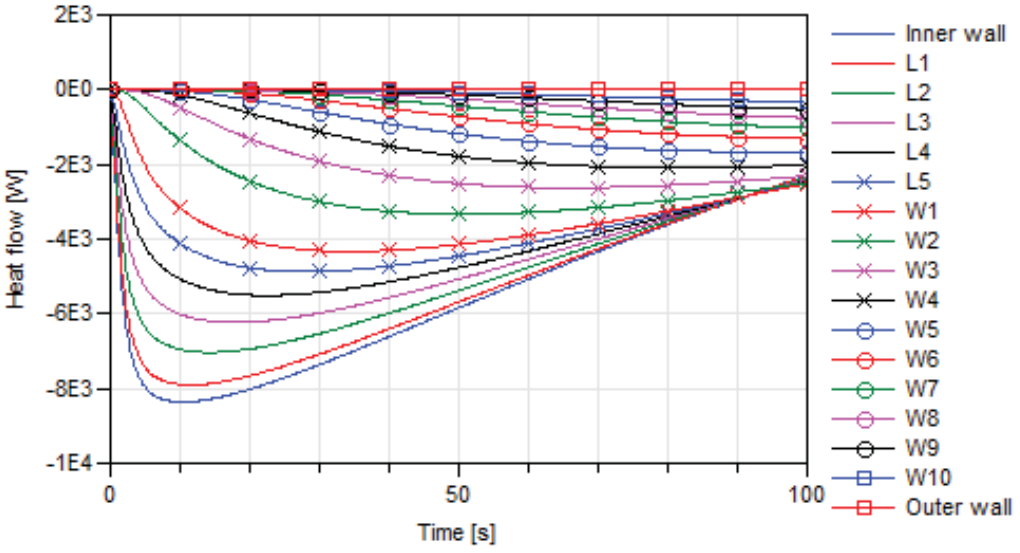

Figure B.12: heat flow through the cells in the tank wall of a discharging tank

flow which is an important parameter for the pressure losses.

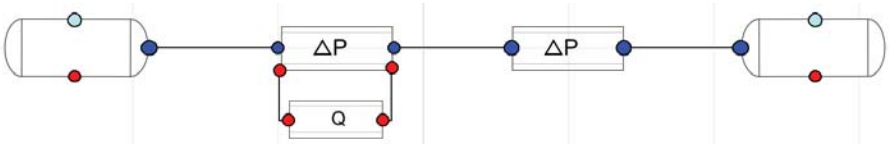

Figure B.13: Model used to for verification of the tube heat transfer model

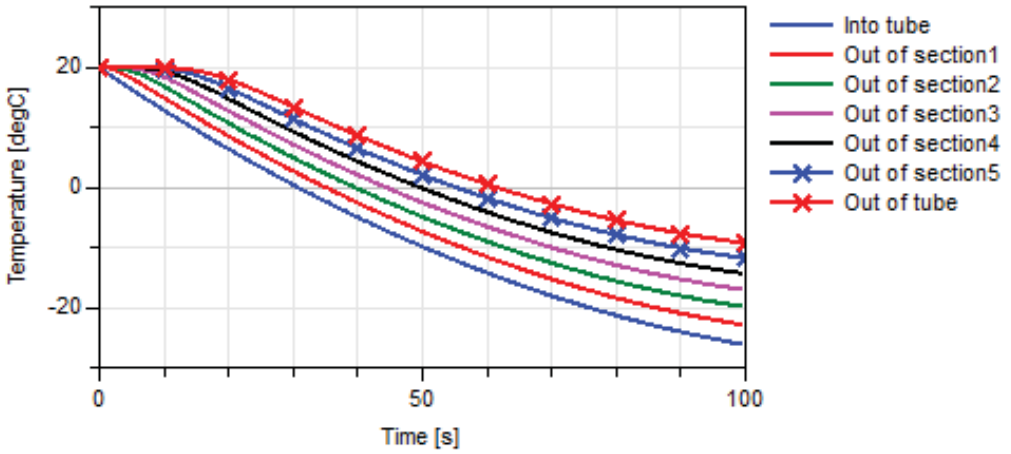

Figure B.14: Hydrogen temperature through a tube

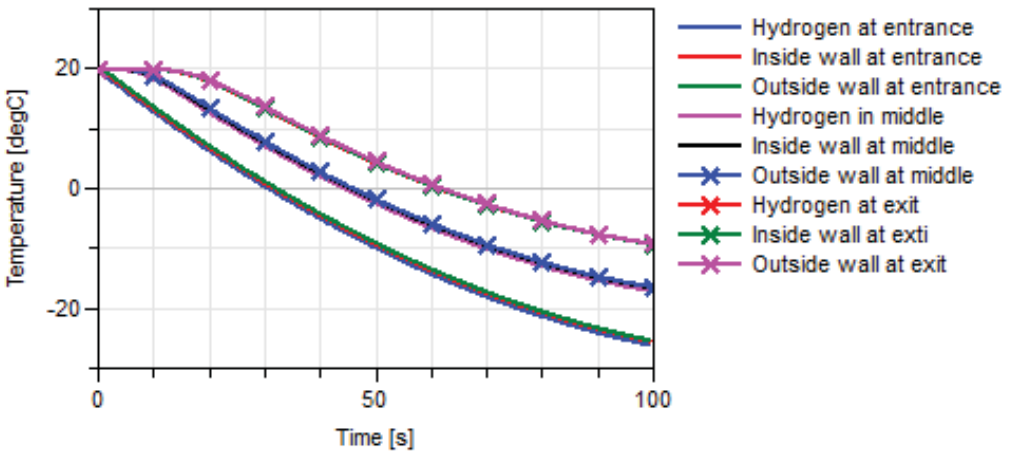

Figure B.15: Hydrogen and tube temperature through a tube at 3 strategical points; entrance, middle and exit. The ambient temperature is the straight line

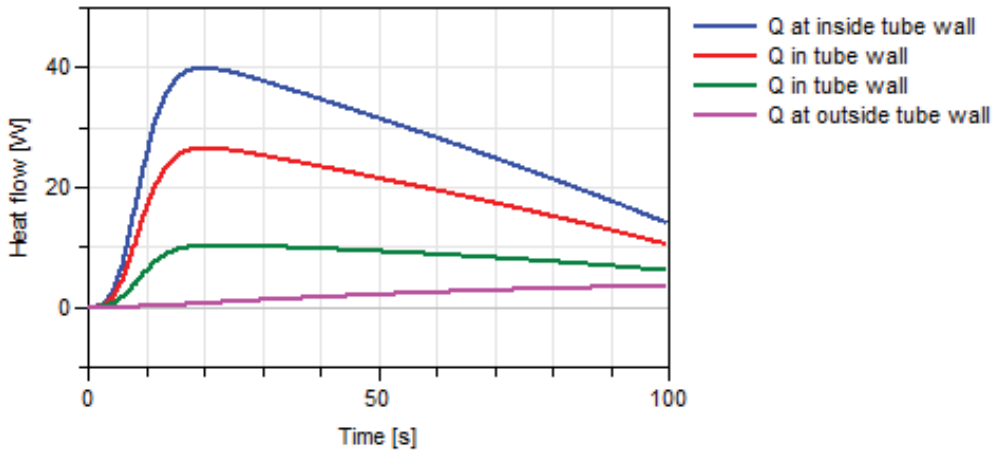

Figure B.16: Hydrogen and tube temperature through a tube at 3 strategical points; entrance, middle and exit. The ambient temperature is the straight line

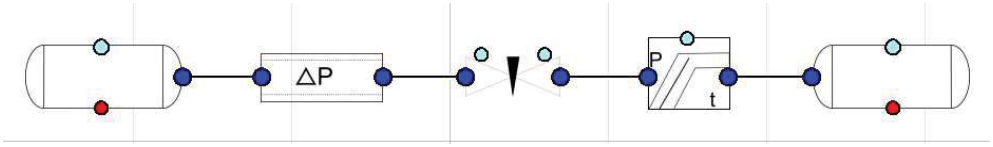

Figure B.17: The system used to analyse the pressure losses

Reduction valve and average pressure ramp rate

First the reduction valve and average pressure ramp rate are considered. The two components are closely connected as one cannot function without the other. The average pressure ramp rate, the pressure into and out of the reduction valve are shown in fig. B.18. As there are no pressure losses between the reduction valve and the average pressure ramp rate in B.18 left side, the pressure out of the reduction valve is the same as the average pressure ramp rate. The right side of fig. B.18 shows the pressures into and out of the reduction valve and the average pressure ramp, when there is a pressure loss between the average pressure ramp rate and the reduction valve. It is shown that the reduction valve compensates for the pressure loss between the two components. The hydrogen heats up when throttled through the reduction valve due to the Joule-Thomson effect. The rise in temperature is shown in fig. B.19 for a throttling like B.18 left side. It can be seen when comparing the two figures that the temperature increase is direct related to the pressure difference across the reduction valve.

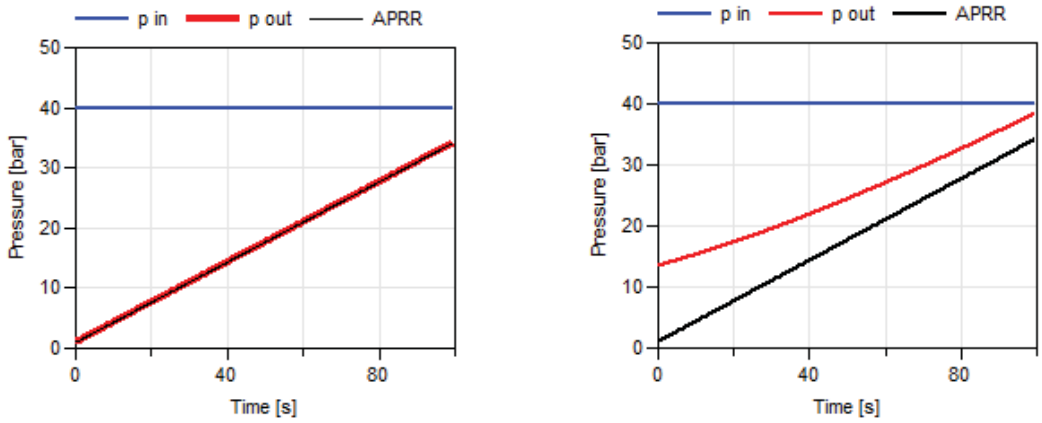

Figure B.18: Pressures into and out of the reduction valve and the average pressure ramp rate. Left: No pressure losses between reduction valve and ramp rate. Right: With a pressure loss between the reduction valve and the ramp rate

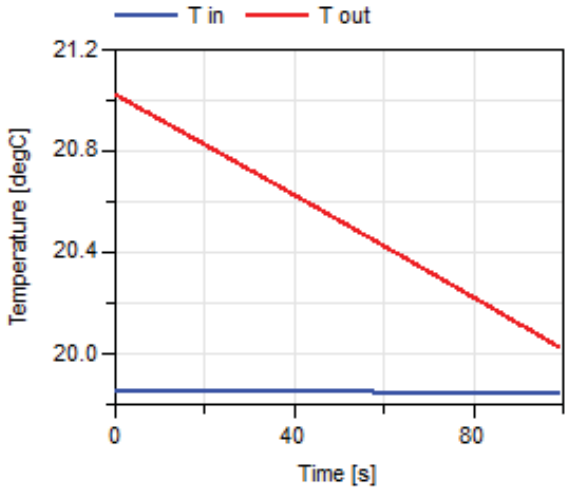

Figure B.19: The temperature increase due to the Joule-Thomson effect when throttling hydrogen

Valve model

To show the functioning of the valve model, a parameter variation of the pressure loss constant kv has been done. The different values of the pressure loss constant are $kv = 0.15$, $kv = 0.25$ and $kv = 0.4$. Figure B.18 shows the pressures into and out of the valve with a slightly decreasing volume flow rate,

that is shown in fig. B.21. When the pressure loss constant increases the

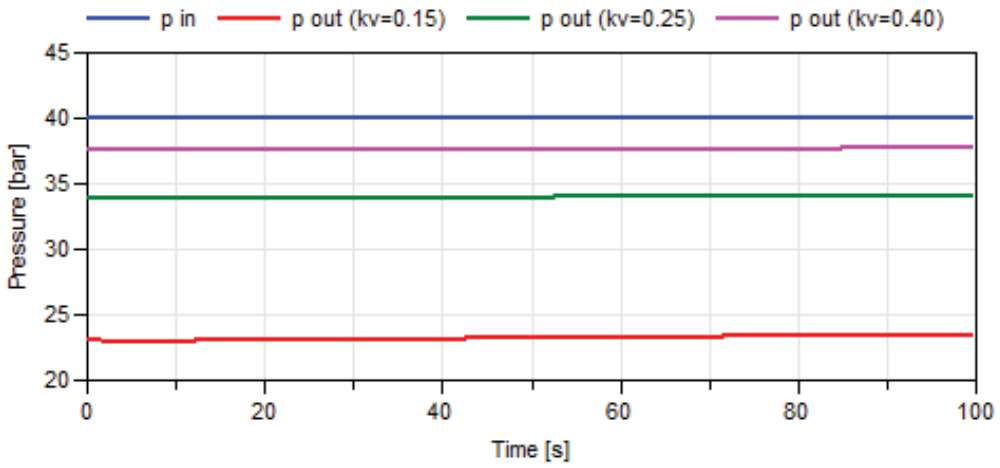

Figure B.20: The pressure into the valve and out of the valve for different pressure loss constants

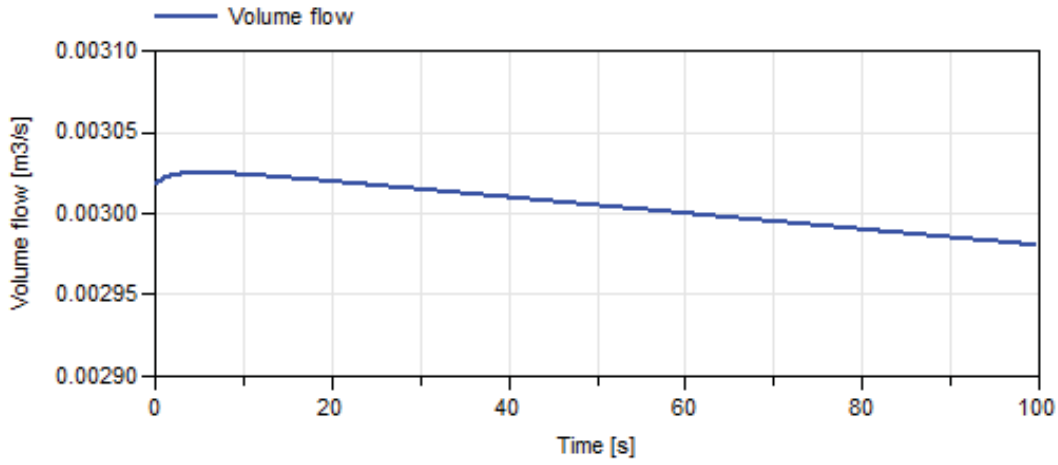

Figure B.21: The volume flow through the valve is slightly decreasing

pressure loss decreases. This is as expected. Further there is a small decrease in the volume flow, which results in a higher pressure out of the valve, hence a lower pressure loss. The pressure loss decreases as the flow decreases, this corresponds to eq. 3.30 in chapter 3.

Mass flow meter and filter model

The mass flow meter and the filter model is shown by a parameter variation of the pressure loss constant kp. The values used are $kp = 0.01 =$, $kp = 0.02$ and $kp = 0.1$. The model for the filter and mass flow meters pressure losses have a pressure loss constant that influences the volume flow inverted of the valve model. An increase in the pressure loss constant results in an increase in the pressure loss. Further a decrease in the volume flow results in a decrease in the pressure loss and an increase in the volume flow results in a increased pressure loss. Figure B.22 shows the pressures into and out of the component. Figure

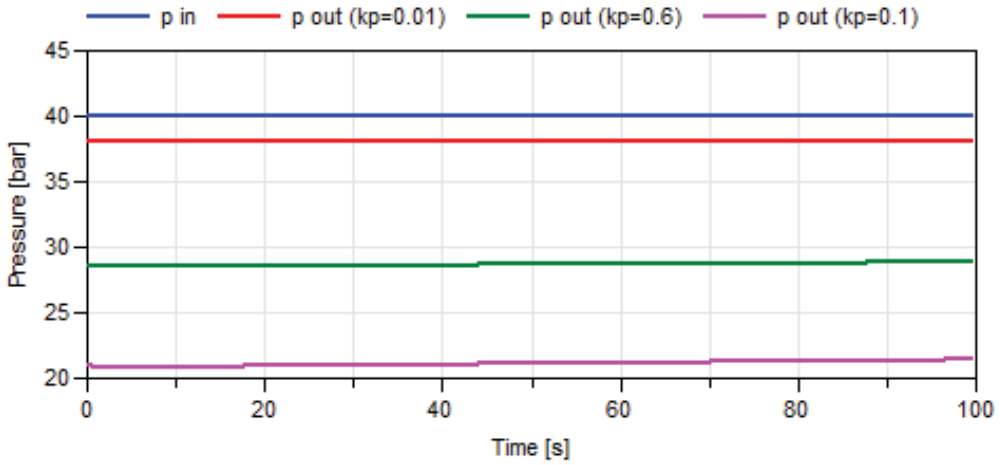

Figure B.22: The pressure into and out of the mass flow meter or filter as a function of the pressure loss constant

B.23 shows the volume flow.

Tube model

The tube model is a function of the tube material, the diameter and the length of the tube. The influence of the roughness of the tube is not shown, but the pressure loss as a function of diameter and length is shown. Figure B.24 shows the pressure into and out of the tube with a diameter of 0.005 meters and 3 different tube lengths (25, 50 and 75 meters). It shows that the increase in pressure loss is proportional to the increase in length. Figure B.25 shows the influence of the diameter of the tube. The length of the tube is 50 meters and the diameters are $d = 0.005$, $d = 0.0075$ and $d = 0.01$ meters. Figure B.25 shows that by increasing the diameter with 50% the pressure drop is decreased with with 80% and by doubling the diameter the pressure loss decreases with 95%. This is as expected considering the relation between diameter, cross sectional area and pressure loss in equation 3.32 in chapter 3.6.

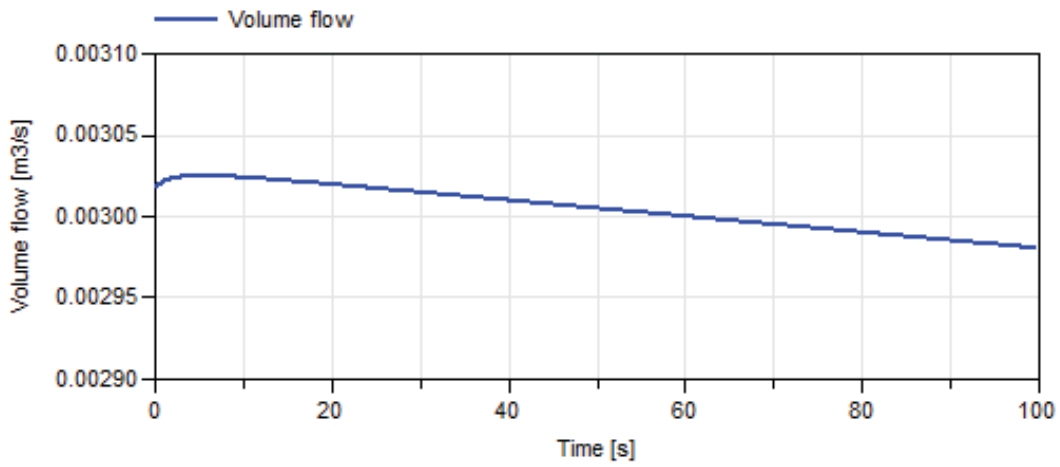

Figure B.23: The volume flow as a function of the pressure loss constant

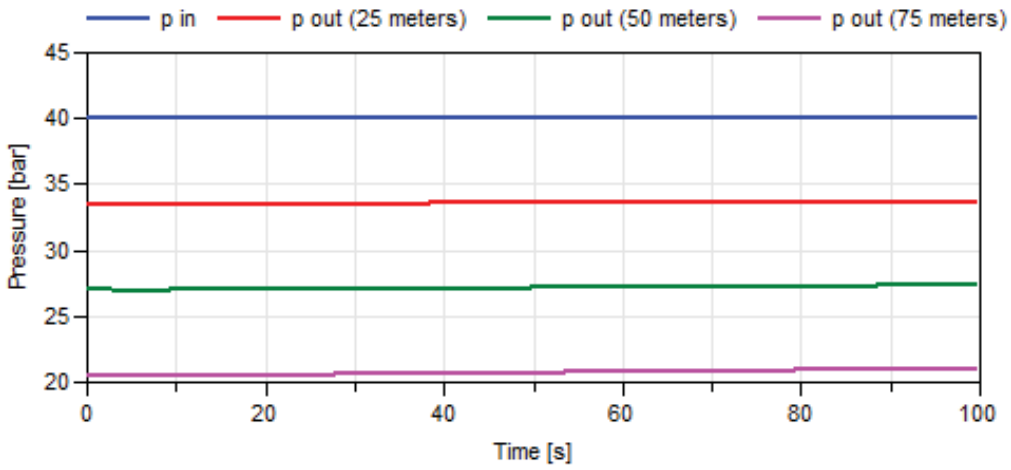

Figure B.24: The pressure drop across the tube as a function of the length

Mixers

The system used to see how the mixer performs is shown in figure B.26: The mixer system consists of three tanks at different pressures (1, 15 and 20 bars) and three pressure losses with different kv values in order to isolate the mixer from the tanks.

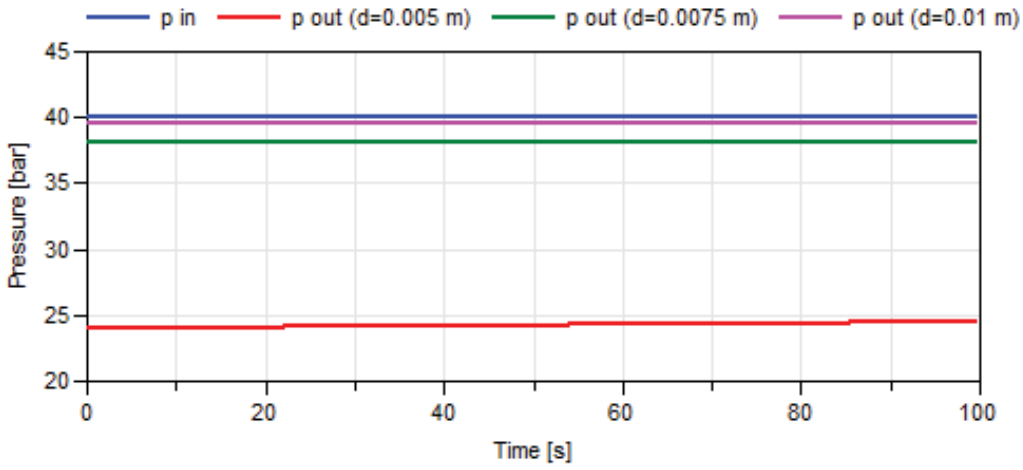

Figure B.25: The pressure drop across the tube as a function of the diameter

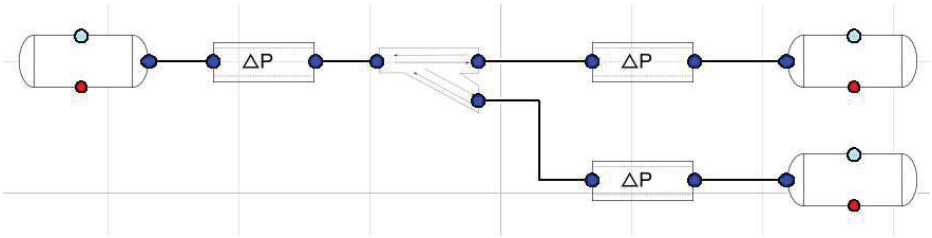

Figure B.26: The system used to show the function of the mixers

Volume Mixer

The pressures of the tanks and the mixer are shown in fig. B.27 together with the mass flows to/from the mixer . The pressure of tank 1 is at the beginning larger than both tank 2 and tank 3, the mass flow is therefore going from tank 1 to tank 2 and tank 3. At some point the pressure of tank 3 levels out with the pressure in tank 1 and both are now filling into tank 1. The reason that the pressures are not the same is because there is a pressure loss between them and the mixer. It is clear that tank 2 changes direction of the mass flow into the mixer considering fig. B.27. Figure B.28 shows the enthalpies into and out of the mixer including the enthalpy of the mixed stream in the mixer. The energy and mass balance of the system are shown in fig. B.29. It is shown in fig B.29 that there is both energy and mass balance in the system. The internal energy is shown for the three tanks, the mixer and the sum of the internal energies. The sum is to show the energy balance of the adiabatic system. The mass of the tanks, in the mixer and the total mass is shown. The total mass of the closed system is constant proving mass balance.

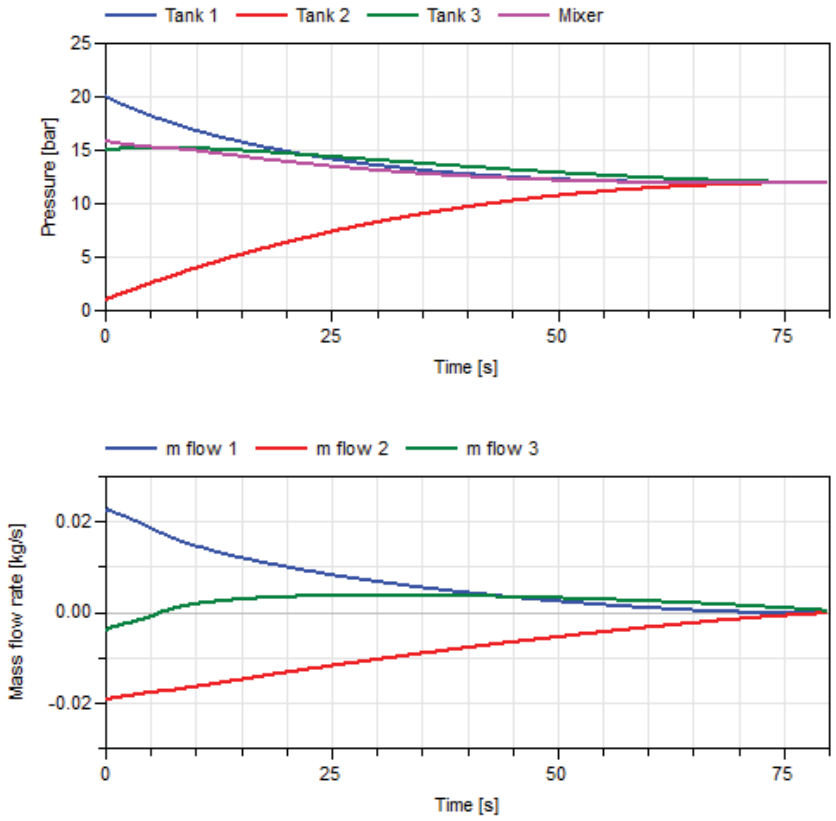

Figure B.27: Top: The pressures of the tanks and the mixer. Bottom: The mass flows to/from the mixer.

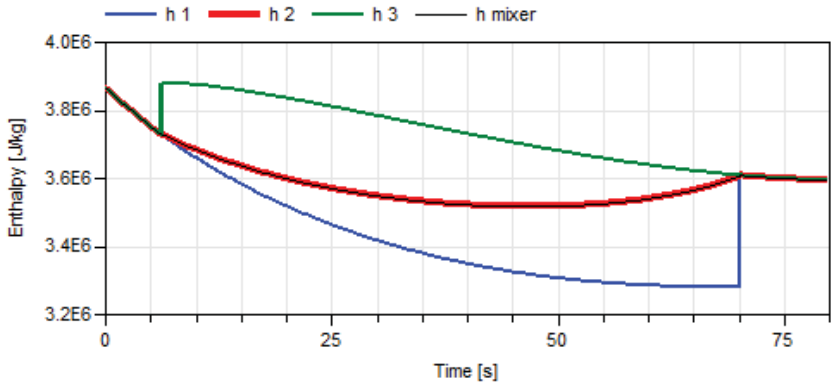

Figure B.28: Top: The enthalpies at the entrances to the mixer and inside the mixer. Bottom: Enthalpy shown in ports

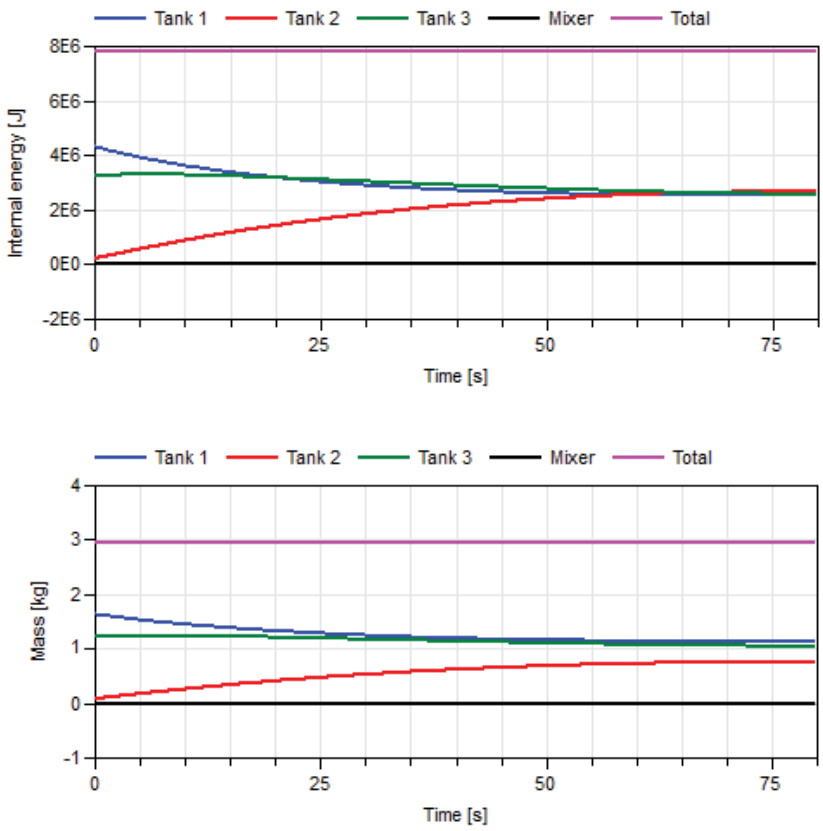

Figure B.29: Top: The internal energy of the tanks and the mixer. Bottom: The masses of the tanks and the mixer.

Ideal mixer

For the *IdealMixer* the thermodynamics are very much like for the volume mixer and the change in enthalpy, mass flow, pressure etc are almost identical. Therefore only the pressures and enthalpies into the mixer are shown here to show that the ideal mixer acts in the same way as the volume mixer. The pressure and enthalpies into/out of the mixer are shown in fig. B.30

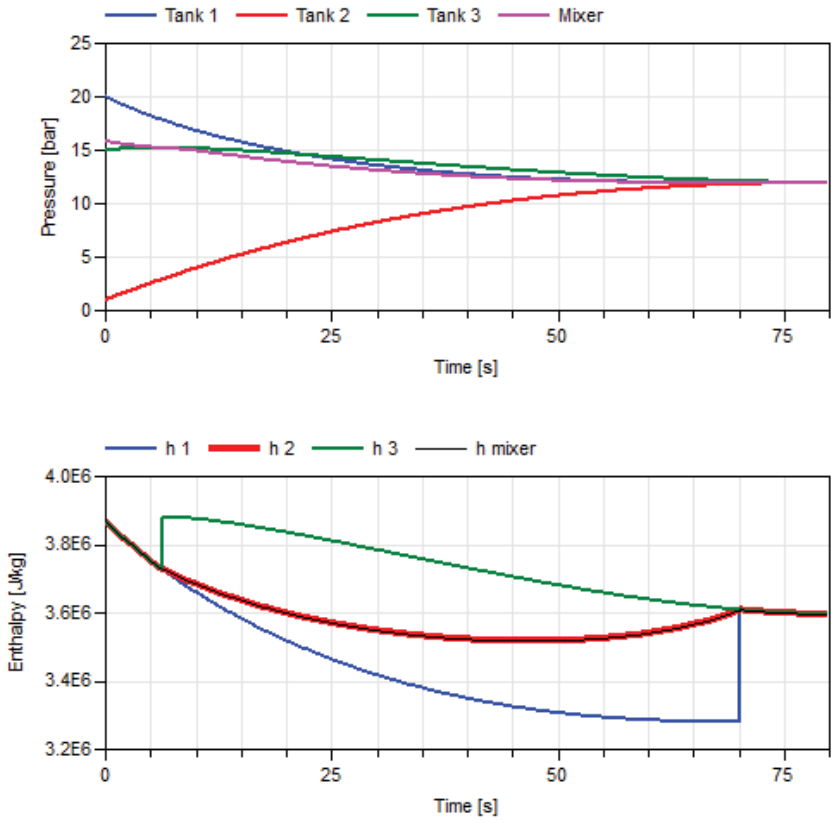

Figure B.30: Left: The pressures of the tanks and the mixer. Right: The enthalpies into/out of the mixer.

Compressor

The compressor is considered in a system with one tank at 1 bar and another smaller tank at 1.1 bar. The compressor then draws mass from the 1 bar tank to the 1.1 bar tank which then increase in pressure. The system used can be seen in fig. B.31. The inlet and outlet pressure and the mass flow

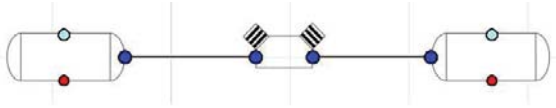

Figure B.31: The volume flow as a function of the pressure loss constant

through the compressor are shown in fig. B.32. As the pressure increase the mass flow decreases proportional, this is due to the volumetric efficiency. The temperature and enthalpy into and out of the compressor is shown in fig. B.33.

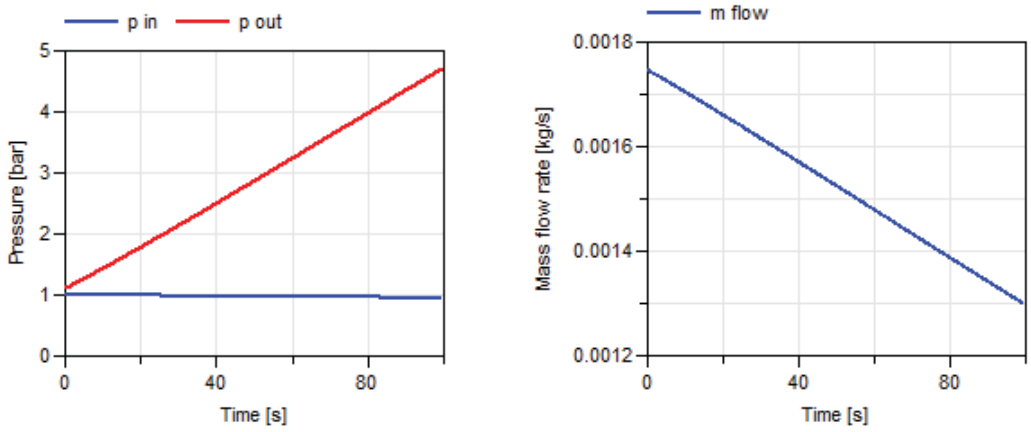

Figure B.32: Pressure into and out of the compressor (left) and the corresponding mass flow rate (right)

Both the temperature and enthalpy increases, the slope of the figures are largest in the beginning this is due to the isentropic efficiency, which can be seen in figure B.33 together with the volumetric effciency and the work required for the compression. The work required for the compression is depending on both

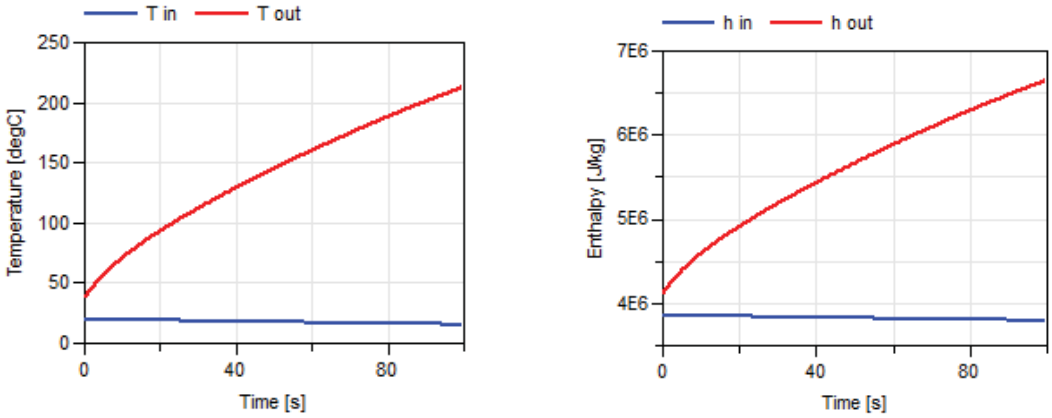

Figure B.33: The temperature (left) and enthalpy (right) into and out of the compressor

the volumetric and isotropic efficiency. The work is increasing as the pressure ratio increases. This is expected as it requires more work for a larger pressure lift done by the compressor.

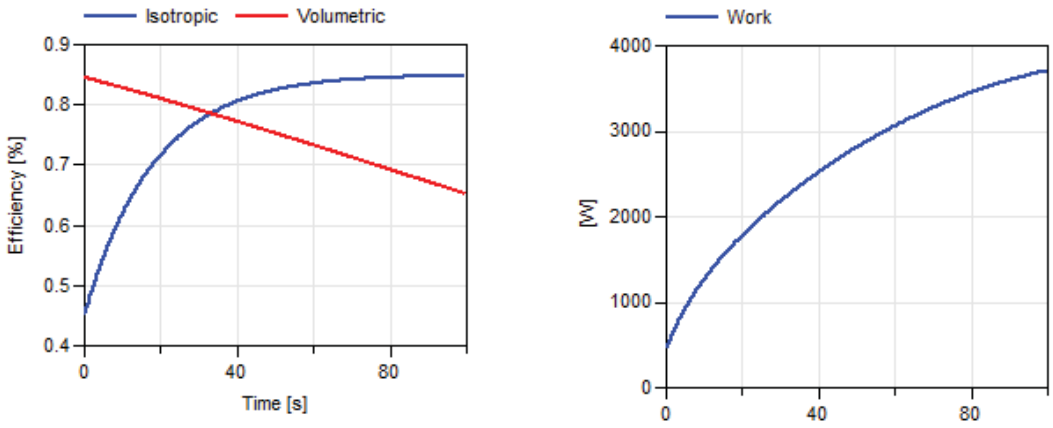

Figure B.34: The efficiencies of the compressor (Left) and the work required for the specific mass flow rate (Right)

Heat exchanger

The heat exchanger only calculates the required cooling for a given exit temperature. The system which has been used can be seen in fig. B.35. It consists of two tanks and a pressure loss to slow down the mass flow between the two tanks. The temperature out of the heat exchanger is fixed to $-40°C$. The tem-

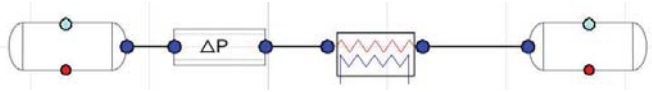

Figure B.35: The system used to see the performance of the heat exchanger

perature into and out of the heat exchanger is shown in fig. B.36 together with the mass flow rate. The corresponding cooling demand and total energy usage is shown in figure B.37. The cooling demand decreases with as the temperature difference between inlet and outlet decreases and the mass flow decreases. the total energy consumption is the sum of the cooling demand over the period of time.

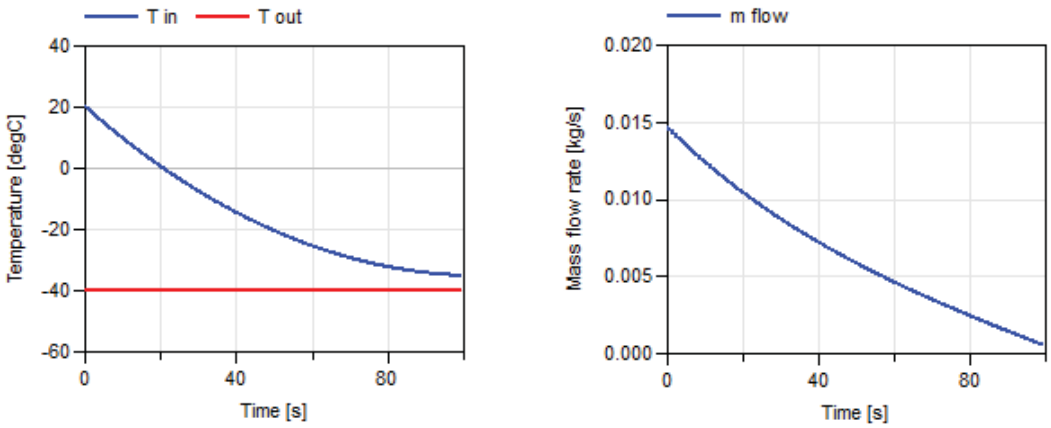

Figure B.36: The temperatures into and out of the heat exchanger (Left) and the mass flow rate (Right)

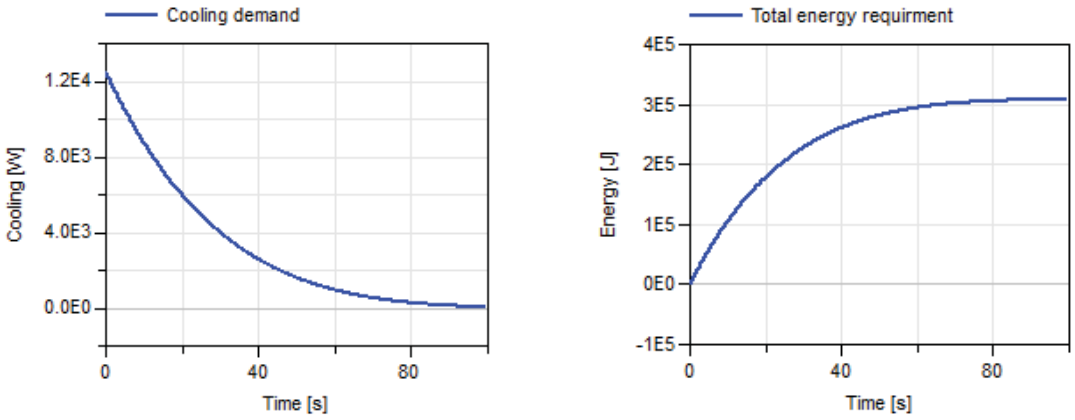

Figure B.37: The instant cooling demand (Left) and the total amount of energy required (Right)

Appendix C

Component model listing

This appendix contains additional information on all the codes for the different models. The models are very similar in structure and for most models, text comments explaining the data are added. Further the the SI unit options have been used. From that all data can be determined. The components are shown in the same structure as the in the library.

HRSInfo

```
model HRSInfo "Sets the parameters for the fueling based on J2601"
//Decideds the average pressure ramp rate, final pressure in HSS,
//final state of charge and temperature out of the fueling station based on J2601
//using ambient temperature, starting pressure in HSS and refueling protocol as input
import SI =
         Modelica.SIunits;
  /*************************************************/
  /*General parameters*/
  /*************************************************/
parameter Integer Fueling_protocol=1 "Fueling protocol" a;
parameter SI.Temperature T_amb=293 "Ambient temperature";
parameter SI.Pressure P_amb=101000 "Ambient pressure";
parameter SI.Pressure P_start=2e6 "Start pressure i the HSS";
  /*************************************************/
  /*APRR*/
  /*************************************************/

  Real T=T_amb;
  Real P=P_start;
  Real  T_cool;
  Real APRR;

  SI.Pressure FP;
  Real SOC;
  SI.Pressure P_ref;
  Real APRR_1;
  SI.Pressure FP_1;
  Real SOC_1;
  Real APRR_2;
  SI.Pressure FP_2;
  Real SOC_2;
  Real APRR_3;
  SI.Pressure FP_3;
  Real SOC_3;
  Real APRR_4;
  SI.Pressure FP_4;
  Real SOC_4;
  Real APRR_5;
  SI.Pressure FP_5;
  Real SOC_5;
  Real APRR_6;
  SI.Pressure FP_6;
  Real SOC_6;
  Real APRR_7;
  SI.Pressure FP_7;
  Real SOC_7;
  Real APRR_8;
  SI.Pressure FP_8;
  Real SOC_8;

  /*************************************************/
  /*Consstants from SAE*/
  /*************************************************/
constant SI.Temperature T1=273.15-40;
constant SI.Temperature T2=273.15-20;
constant SI.Temperature T3=273.15;

constant SI.Pressure P_ref1=70e6;
constant SI.Pressure P_ref2=35e6;

  /*************************************************/
  /*Look up tables for SAE*/
  /*************************************************/
  // A70 1-7 kg
  // For the APRR (Average pressure ramprate)
  Modelica.Blocks.Tables.CombiTable1Ds APRR1(
```

```
  tableOnFile=true,
  smoothness=Modelica.Blocks.Types.Smoothness.ContinuousDerivative,
  tableName="APRR_A1",
  fileName="C:/Users/edro/Documents/Dymola/External files/Lookuptables/APRR.txt")
  a;

// For FP (final pressure)
Modelica.Blocks.Tables.CombiTable2D FP1(
  tableOnFile=true,
  tableName="FP_A1",
  smoothness=Modelica.Blocks.Types.Smoothness.ContinuousDerivative,
  fileName=
      "C:/Users/edro/Documents/Dymola/External files/Lookuptables/FP.mat")
  a;

//For SOC (state of charge)
Modelica.Blocks.Tables.CombiTable2D SOC1(
  tableOnFile=true,
  tableName="SOC_A1",
  smoothness=Modelica.Blocks.Types.Smoothness.ContinuousDerivative,
  fileName=
      "C:/Users/edro/Documents/Dymola/External files/Lookuptables/SOC.mat")
  annotation (Placement(transformation(extent={{-10,-50},{10,-30}})));

// A70 7-10 kg
// For the APRR (Average pressure ramprate)
Modelica.Blocks.Tables.CombiTable1Ds APRR2(
  tableOnFile=true,
  smoothness=Modelica.Blocks.Types.Smoothness.ContinuousDerivative,
  tableName="APRR_A2",
  fileName="C:/Users/edro/Documents/Dymola/External files/Lookuptables/APRR.mat");

// For FP (final pressure)
Modelica.Blocks.Tables.CombiTable2D FP2(
  tableOnFile=true,
  tableName="FP_A2",
  fileName="C:/Users/edro/Documents/Dymola/External files/Lookuptables/FP.mat",
  smoothness=Modelica.Blocks.Types.Smoothness.ContinuousDerivative);

//For SOC (state of charge)
Modelica.Blocks.Tables.CombiTable2D SOC2(
  tableOnFile=true,
  tableName="SOC_A2",
  fileName="C:/Users/edro/Documents/Dymola/External files/Lookuptables/SOC.mat",
  smoothness=Modelica.Blocks.Types.Smoothness.ContinuousDerivative);

// A35
// For the APRR (Average pressure ramprate)
Modelica.Blocks.Tables.CombiTable1Ds APRR3(
  tableOnFile=true,
  smoothness=Modelica.Blocks.Types.Smoothness.ContinuousDerivative,
  tableName="APRR_A3",
  fileName="C:/Users/edro/Documents/Dymola/External files/Lookuptables/APRR.mat");

// For FP (final pressure)
Modelica.Blocks.Tables.CombiTable2D FP3(
  tableOnFile=true,
  tableName="FP_A3",
  fileName="C:/Users/edro/Documents/Dymola/External files/Lookuptables/FP.mat",
  smoothness=Modelica.Blocks.Types.Smoothness.ContinuousDerivative);

//For SOC (state of charge)
Modelica.Blocks.Tables.CombiTable2D SOC3(
  tableOnFile=true,
  tableName="SOC_A3",
  fileName="C:/Users/edro/Documents/Dymola/External files/Lookuptables/SOC.mat",
```

```
  smoothness=Modelica.Blocks.Types.Smoothness.ContinuousDerivative);

// B70 1-7kg
// For the APRR (Average pressure ramprate)
Modelica.Blocks.Tables.CombiTable1Ds APRR4(
  tableOnFile=true,
  smoothness=Modelica.Blocks.Types.Smoothness.ContinuousDerivative,
  tableName="APRR_B1",
  fileName="C:/Users/edro/Documents/Dymola/External files/Lookuptables/APRR.mat");

// For FP (final pressure)
Modelica.Blocks.Tables.CombiTable2D FP4(
  tableOnFile=true,
  tableName="FP_B1",
  fileName="C:/Users/edro/Documents/Dymola/External files/Lookuptables/FP.mat",
  smoothness=Modelica.Blocks.Types.Smoothness.ContinuousDerivative);

//For SOC (state of charge)
Modelica.Blocks.Tables.CombiTable2D SOC4(
  tableOnFile=true,
  tableName="SOC_B1",
  fileName="C:/Users/edro/Documents/Dymola/External files/Lookuptables/SOC.mat",
  smoothness=Modelica.Blocks.Types.Smoothness.ContinuousDerivative);

// B70 7-10kg
// For the APRR (Average pressure ramprate)
Modelica.Blocks.Tables.CombiTable1Ds APRR5(
  tableOnFile=true,
  smoothness=Modelica.Blocks.Types.Smoothness.ContinuousDerivative,
  tableName="APRR_B2",
  fileName="C:/Users/edro/Documents/Dymola/External files/Lookuptables/APRR.mat");

// For FP (final pressure)
Modelica.Blocks.Tables.CombiTable2D FP5(
  tableOnFile=true,
  tableName="FP_B2",
  fileName="C:/Users/edro/Documents/Dymola/External files/Lookuptables/FP.mat",
  smoothness=Modelica.Blocks.Types.Smoothness.ContinuousDerivative);

//For SOC (state of charge)
Modelica.Blocks.Tables.CombiTable2D SOC5(
  tableOnFile=true,
  tableName="SOC_B2",
  fileName="C:/Users/edro/Documents/Dymola/External files/Lookuptables/SOC.mat",
  smoothness=Modelica.Blocks.Types.Smoothness.ContinuousDerivative);

// B35
// For the APRR (Average pressure ramprate)
Modelica.Blocks.Tables.CombiTable1Ds APRR6(
  tableOnFile=true,
  smoothness=Modelica.Blocks.Types.Smoothness.ContinuousDerivative,
  tableName="APRR_B3",
  fileName="C:/Users/edro/Documents/Dymola/External files/Lookuptables/APRR.mat");

// For FP (final pressure)
Modelica.Blocks.Tables.CombiTable2D FP6(
  tableOnFile=true,
  tableName="FP_B3",
  fileName="C:/Users/edro/Documents/Dymola/External files/Lookuptables/FP.mat",
  smoothness=Modelica.Blocks.Types.Smoothness.ContinuousDerivative);

//For SOC (state of charge)
Modelica.Blocks.Tables.CombiTable2D SOC6(
  tableOnFile=true,
  tableName="SOC_B3",
  fileName="C:/Users/edro/Documents/Dymola/External files/Lookuptables/SOC.mat",
```

```
    smoothness=Modelica.Blocks.Types.Smoothness.ContinuousDerivative);

  // C35
  // For the APRR (Average pressure ramprate)
  Modelica.Blocks.Tables.CombiTable1Ds APRR7(
    tableOnFile=true,
    smoothness=Modelica.Blocks.Types.Smoothness.ContinuousDerivative,
    tableName="APRR_C1",
    fileName="C:/Users/edro/Documents/Dymola/External files/Lookuptables/APRR.mat");

  // For FP (final pressure)
  Modelica.Blocks.Tables.CombiTable2D FP7(
    tableOnFile=true,
    tableName="FP_C1",
    fileName="C:/Users/edro/Documents/Dymola/External files/Lookuptables/FP.mat",
    smoothness=Modelica.Blocks.Types.Smoothness.ContinuousDerivative);

  //For SOC (state of charge)
  Modelica.Blocks.Tables.CombiTable2D SOC7(
    tableOnFile=true,
    tableName="SOC_C1",
    fileName="C:/Users/edro/Documents/Dymola/External files/Lookuptables/SOC.mat",
    smoothness=Modelica.Blocks.Types.Smoothness.ContinuousDerivative);

  // D35
  // For the APRR (Average pressure ramprate)
  Modelica.Blocks.Tables.CombiTable1Ds APRR8(
    tableOnFile=true,
    smoothness=Modelica.Blocks.Types.Smoothness.ContinuousDerivative,
    tableName="APRR_D1",
    fileName="C:/Users/edro/Documents/Dymola/External files/Lookuptables/APRR.mat");

  // For FP (final pressure)
  Modelica.Blocks.Tables.CombiTable2D FP8(
    tableOnFile=true,
    tableName="FP_D1",
    fileName="C:/Users/edro/Documents/Dymola/External files/Lookuptables/FP.mat",
    smoothness=Modelica.Blocks.Types.Smoothness.ContinuousDerivative);

  //For SOC (state of charge)
  Modelica.Blocks.Tables.CombiTable2D SOC8(
    tableOnFile=true,
    tableName="SOC_D1",
    fileName="C:/Users/edro/Documents/Dymola/External files/Lookuptables/SOC.mat",
    smoothness=Modelica.Blocks.Types.Smoothness.ContinuousDerivative);

  /************************************************/
  /*Equations*/
  /************************************************/
equation
  FP1.u1 = T;
  FP1.u2 = P;
  FP1.y = FP_1;
  SOC1.u1 = T;
  SOC1.u2 = P;
  SOC1.y = SOC_1;
  APRR1.u = T;
  APRR1.y[1] = APRR_1;

  FP2.u1 = T;
  FP2.u2 = P;
  FP2.y = FP_2;
  SOC2.u1 = T;
  SOC2.u2 = P;
  SOC2.y = SOC_2;
  APRR2.u = T;
```

```
APRR2.y[1] = APRR_2;

FP3.u1 = T;
FP3.u2 = P;
FP3.y = FP_3;
SOC3.u1 = T;
SOC3.u2 = P;
SOC3.y = SOC_3;
APRR3.u = T;
APRR3.y[1] = APRR_3;

FP4.u1 = T;
FP4.u2 = P;
FP4.y = FP_4;
SOC4.u1 = T;
SOC4.u2 = P;
SOC4.y = SOC_4;
APRR4.u = T;
APRR4.y[1] = APRR_4;

FP5.u1 = T;
FP5.u2 = P;
FP5.y = FP_5;
SOC5.u1 = T;
SOC5.u2 = P;
SOC5.y = SOC_5;
APRR5.u = T;
APRR5.y[1] = APRR_5;

FP6.u1 = T;
FP6.u2 = P;
FP6.y = FP_6;
SOC6.u1 = T;
SOC6.u2 = P;
SOC6.y = SOC_6;
APRR6.u = T;
APRR6.y[1] = APRR_6;

FP7.u1 = T;
FP7.u2 = P;
FP7.y = FP_7;
SOC7.u1 = T;
SOC7.u2 = P;
SOC7.y = SOC_7;
APRR7.u = T;
APRR7.y[1] = APRR_7;

FP8.u1 = T;
FP8.u2 = P;
FP8.y = FP_8;
SOC8.u1 = T;
SOC8.u2 = P;
SOC8.y = SOC_8;
APRR8.u = T;
APRR8.y[1] = APRR_8;

/************************************************/
/*Deciding output values*/
/************************************************/

if Fueling_protocol == 1 then //A70 1-7 kg
  APRR = APRR_1;
  FP = FP_1;
  SOC = SOC_1;
  T_cool=T1;
  P_ref=P_ref1;
```

```
  elseif Fueling_protocol == 2 then //A70 7-10 kg
    APRR = APRR_2;
    FP = FP_2;
    SOC= SOC_2;
    T_cool=T1;
    P_ref=P_ref1;
  elseif Fueling_protocol == 3 then //A35
    APRR = APRR_3;
    FP = FP_3;
    SOC = SOC_3;
    T_cool=T1;
    P_ref=P_ref2;
  elseif Fueling_protocol == 4 then //B70 1-7 kg
    APRR = APRR_4;
    FP = FP_4;
    SOC = SOC_4;
    T_cool=T2;
    P_ref=P_ref1;
  elseif Fueling_protocol == 5 then //B70 7-10 kg
    APRR = APRR_5;
    FP = FP_5;
    SOC = SOC_5;
    T_cool=T2;
    P_ref=P_ref1;
  elseif Fueling_protocol == 6 then //B35
    APRR = APRR_6;
    FP = FP_6;
    SOC = SOC_6;
    T_cool=T2;
    P_ref=P_ref2;
  elseif Fueling_protocol == 7 then //C35
    APRR = APRR_7;
    FP = FP_7;
    SOC = SOC_7;
    T_cool=T3;
    P_ref=P_ref2;
  elseif Fueling_protocol == 8 then //D35
    APRR = APRR_8;
    FP = FP_8;
    SOC = SOC_8;
    T_cool=T;
    P_ref=P_ref2;
  else
    APRR = 0;
    FP = 0;
    SOC = 0;
    T_cool=0;
    P_ref=0;
  end if;

  /*************************************************/
  /*Checking input values*/
  /*************************************************/

algorithm
  assert(Fueling_protocol < 9, "Not a valid fueling procedure. Choose one between 1 and
  1: A70 1-7 kg,
  2: A70 7-10 kg,
  3: A35,
  4: B70 1-7 kg,
  5: B70 7-10 kg,
  6: B35,
  7: C35,
  8: D35");
  assert(if Fueling_protocol == 3 or Fueling_protocol == 6 or
  Fueling_protocol == 7 or Fueling_protocol == 8 then P <= 35e6
```

```
      else P <= 70e6,
     "The initial HSS pressure is above allowance of fuelling procedure -
      No need for refilling, HSS is already full!");

  a;
end HRSInfo;
```

Ports

All 6 ports are shown below, separated with *connector* and *end*.

```
connector FlowPort
  "Flow port passing on mass flow, pressure and enthalpy"
 import SI = Modelica.SIunits;
 SI.AbsolutePressure p "Pressure";
 flow SI.MassFlowRate m_flow "Mass flow rate";
 stream SI.SpecificEnthalpy h_outflow "Specific enthalpy";

  a;
end FlowPort;

connector PressurePort "Passes on pressure"
  import SI = Modelica.SIunits;
  SI.Pressure p "Pressure";
  a;
end PressurePort;

connector HeatFlow
  "Heat flow port passing on temperature, heat flow, pressure and area"
  import SI = Modelica.SIunits;
  SI.Temperature T "Temperature";
  flow SI.HeatFlowRate Q "Heat flow";
  SI.Pressure P "Pressure";
  Real Counter "Count pieces of walls";

  a;
end HeatFlow;

connector HeatFlow2
  "Heat flow port passing on temperature, heat flow, pressure and area"
  import SI = Modelica.SIunits;
  SI.Temperature T "Temperature";
  flow SI.HeatFlowRate Q "Heat flow";
  SI.Pressure P "Pressure";
  Real Counter "Count pieces of walls";
  SI.MassFlowRate m_flow;
  a;
end HeatFlow2;

connector TemperaturePort
  import SI = Modelica.SIunits;
  SI.Temperature T;

  a;
end TemperaturePort;

connector HeatFlowTube
  import SI = Modelica.SIunits;
 SI.Temperature T;
 flow SI.MassFlowRate m_flow;
 SI.SpecificHeatCapacity cp;
 SI.CoefficientOfHeatTransfer h;
  a;
end HeatFlowTube;
```

Tank1

```
model Tank1 "Volume with one entrance"
import SI =
          Modelica.SIunits;

 /****************** Thermodynamic property call *************************/
    replaceable package Medium =
     CoolProp2Modelica.Interfaces.ExternalTwoPhaseMedium ;

       Medium.ThermodynamicState medium;

 /******************** Connectors ****************************/

  Ports.FlowPort portA "port connection component to other components"
    ;
//( m_flow(final start=m_flowStart))
  Ports.HeatFlow2 heatFlow "connection to heat transfer model"
    ;
  Ports.PressurePort pp "Connection for control of system"
    ;

 /****************** General parameters ******************/
  parameter Boolean Adiabatic = false "If true, adiabatic tank model" ;
  parameter SI.Volume V=1 "Volume of the tank" ;

 /******************  Initial and start values ******************/

  parameter SI.Pressure pInitial=1.013e5 "Initial pressure in the tank"
    ;
  parameter Boolean fixedInitialPressure = true "Fixed intial pressure"
                            ;

  parameter SI.Temperature TInitial=T_amb "Initial temperature in the tank"
    ;

  parameter SI.MassFlowRate m_flowStart=0 "Initial mass flow rate"
    ;

  outer parameter SI.Temperature T_amb "Ambient temperature";

 /****************** variables ******************/

  SI.Mass M "Gas mass in control volume";
  Real drhodt;
  SI.Heat Q;
  SI.InternalEnergy U;
  SI.Pressure p(start=pInitial, fixed=fixedInitialPressure);
  SI.SpecificEnthalpy h;
  Real HeatOfCompression "heat of compression";
  constant Real Counter=0;

/****************** Initial equations ******************/
initial equation
h=Medium.specificEnthalpy_pT(pInitial, TInitial);

/****************** equations ******************/
equation

medium=Medium.setState_ph(p, h);
U=(h-p*1/medium.d)*M;
HeatOfCompression=V*der(p);

if Adiabatic == false then
der(Q)=heatFlow.Q;
else
der(Q)=0;
end if;
```

```
 der(h) = 1/M*(noEvent(actualStream(portA.h_outflow))*portA.m_flow - portA.m_flow*h
 + V*der(p)+der(Q)) "Energy balance";

  p = portA.p;

  portA.h_outflow = h;

  M = V*medium.d "Mass in cv";
 drhodt = Medium.density_derp_h(medium)*der(p)+Medium.density_derh_p(medium)*der(h)
    "Derivative of density";

 drhodt*V = portA.m_flow "Mass balance";

//heatFlow.Q=der(Q);
heatFlow.m_flow=portA.m_flow;
heatFlow.T=medium.T;
heatFlow.P=p;
heatFlow.Counter=Counter;

pp.p=p;

  a;
end Tank1;
```

Tank2

```
model Tank2 "Volume with two entrances"

 /****************** Gas ************************/
    replaceable package Medium =
     CoolProp2Modelica.Interfaces.ExternalTwoPhaseMedium a;

       Medium.ThermodynamicState medium;

 /******************** Connectors ****************************/

  Ports.FlowPort portB(
                       m_flow(final start=m_flowStart))
    "port connection component to other components"
    a;

  Ports.HeatFlow2 heatFlow "connection to heat transfer model"
    a;
  Ports.PressurePort pp "Connection for control of system"
    a;
  Ports.FlowPort portA(m_flow(final start=m_flowStart))
    "port connection component to other components"
    a;
 /******************* General parameters ******************/
  parameter Boolean Adiabatic = false "If true, adiabatic tank model" a;
  parameter Modelica.SIunits.Volume V=1 "Volume of the tank" a;

 /******************  Initial and start values ******************/

  parameter Modelica.SIunits.Pressure pInitial=1.013e5
    "Initial pressure in the tank"
    a;
  parameter Boolean fixedInitialPressure = true "Fixed intial pressure"
                            a;

  parameter Modelica.SIunits.Temperature TInitial=T_amb
    "Initial temperature in the tank"
    a;

  parameter Modelica.SIunits.MassFlowRate m_flowStart=0
    "Initial mass flow rate"
    a;

 outer parameter Modelica.SIunits.Temperature T_amb "Ambient temperature";

 /****************** variables ******************/

  Modelica.SIunits.Mass M "Gas mass in control volume";
  Real drhodt;
  Modelica.SIunits.HeatFlowRate Q;

  Modelica.SIunits.Pressure p(start=pInitial, fixed=fixedInitialPressure);
  Modelica.SIunits.SpecificEnthalpy h;
  Real HeatOfCompression "heat of compression";
  constant Real Counter=0;

/****************** Initial equations ******************/
initial equation
h=Medium.specificEnthalpy_pT(pInitial, TInitial);

/****************** equations ******************/
equation

medium=Medium.setState_ph(p, h);

HeatOfCompression=V*der(p);
```

```
if Adiabatic == false then
der(Q)=heatFlow.Q;
else
der(Q)=0;
end if;

der(h) = 1/M*(noEvent(actualStream(portA.h_outflow))*portA.m_flow - portA.m_flow*h
 + noEvent(actualStream(portB.h_outflow))*portB.m_flow - portB.m_flow*h
 + V*der(p)+der(Q));

  p = portA.p;

  portA.h_outflow = h;

  M = V*medium.d "Mass in cv";
 drhodt = Medium.density_derp_h(medium)*der(p)+Medium.density_derh_p(medium)*der(h)
    "Derivative of density";

drhodt*V = portA.m_flow + portB.m_flow "Mass balance";

//heatFlow.Q=der(Q);
heatFlow.m_flow=portA.m_flow-portB.m_flow;
heatFlow.T=medium.T;
heatFlow.P=p;
heatFlow.Counter=Counter;

pp.p=p;

  a;
end Tank2;
```

Heat Transfer

Heat Transfer Tank

```
model HeatTransferTank

import SI =
          Modelica.SIunits;

/******************** Connectors ****************************/
  Ports.HeatFlow2 heatFlow
    a;

/****************** General parameters ******************/
parameter Integer tank=4 "Tank type" a;

  inner parameter Boolean Charging = true
    "If true, tank is charging with given heat transfer coefficient" a;
  parameter SI.CoefficientOfHeatTransfer  h_charging=150 "Charging, Heat transfer
  coefficient inside HSS tank 150 w/m2K - 500w/m2K
    according to monde (0 is adiabatic fuelling)"

  parameter SI.CoefficientOfHeatTransfer  h_discharging=-1 "Discharging heat transfer
  coefficient, if <0 then Daney relation
     is used, if >0 then the given number is used "
  inner parameter SI.CoefficientOfHeatTransfer  h_o=8
    "Heat transfer coefficient outside the tanks (typical natural convection)" a;
 // inner parameter Real  T_amb=273;

 inner parameter SI.Length xLiner=0.003 "Thickness of liner" a;
 inner parameter SI.Length  xCFRP=0.022 "Thickness of wrapping/tank" a;
 parameter SI.Length dInner=0.4 "Inside diameter of cylinder" a;
 parameter SI.Length LInner = 1 "Inside length of tank" a;
 parameter Boolean Area = true
    "If true, area is calcualted from length and diameter" a;
 parameter SI.Area AInner= 1 "Inside tank area "
                              a;

protected
 inner parameter SI.Length x1=xLiner/(t1-0.5);
 inner parameter SI.Length x2=xCFRP/(t2-0.5);
 inner constant Real t1=5.5;
 inner constant Real t2=10.5;
 inner Real y1;
 inner Real y2;

public
 inner SI.CoefficientOfHeatTransfer  h_i = (if Charging == true
 then h_charging else h_discharging);
 inner SI.Length   d = (if Area == false then AInner/(Modelica.Constants.pi)
 else dInner);
 inner SI.Length   L= (if Area == false then 0.8 else LInner);
 inner SI.Area   A = (if Area == false then AInner else 2*
 Modelica.Constants.pi*d/2*L+2*(d/2)^2*Modelica.Constants.pi);

  WallPieces.InnerWallCell
                        wallCell_discharging
    a;
  WallPieces.OuterWallCell
                        outer_wall
    a;
  WallPieces.Liner5Pieces wall_liner
    a;
  WallPieces.Tank10Pieces wall_CFRP
    a;

/***************** equations ******************/
equation
//Deciding which calls to make in lookup tables in wallpieces for tank properties
 if tank==1 then
```

```
    y1=1;
    y2=1;
  elseif tank==2 then
    y1=2;
    y2=2;
  elseif tank==3 then
    y1=2;
    y2=4;
  elseif tank==4 then
    y1=3;
    y2=4;
  else
    y1=3;
    y2=4;
    end if;

   connect(wall_CFRP.heatFlow, wall_liner.heatFlow1) ;
   connect(wall_liner.heatFlow, wallCell_discharging.portB) ;
   connect(wall_CFRP.heatFlow1, outer_wall.portA) ;
   connect(wallCell_discharging.portA, heatFlow) ;
   ;
end HeatTransferTank;
```

Heat Transfer Tube

```
model HeatTransferTube

  import SI = Modelica.SIunits;

/******************** Connectors ******************************/
    Ports.HeatFlowTube HTIn
    a;
  Ports.TemperaturePort
                     HT2
    a;

protected
  Ports.TemperaturePort                      HT1
    a;

/****************** General parameters ********************/
public
inner SI.MassFlowRate m_flow;
inner SI.SpecificHeatCapacity cp_h2;
inner SI.CoefficientOfHeatTransfer h;
inner parameter SI.Length d_i=0.0052;
inner parameter SI.Length d_o=0.00952;
parameter SI.Length Length=6;
parameter SI.CoefficientOfHeatTransfer h_o=8;
protected
inner parameter SI.CoefficientOfHeatTransfer h_amb=h_o;
inner SI.Length L=Length/30;

  WallPieces.Tube5Pieces                              steel5Cells
    a;
  WallPieces.Tube5Pieces                              steel5Cells1
    a;
  WallPieces.Tube5Pieces                              steel5Cells2
    a;
  WallPieces.Tube5Pieces                              steel5Cells3
    a;
  WallPieces.Tube5Pieces                              steel5Cells4
    a;
  WallPieces.Tube5Pieces                              steel5Cells5
    a;
/****************** equations ********************/
equation
HTIn.m_flow=m_flow;
HTIn.cp=cp_h2;
HTIn.h=h;
HT1.T=HTIn.T;

  connect(steel5Cells.HT1, HT1) a;
  connect(steel5Cells.HT2, steel5Cells1.HT1) a;
  connect(steel5Cells1.HT2, steel5Cells2.HT1) a;
  connect(steel5Cells2.HT2, steel5Cells3.HT1) a;
  connect(steel5Cells3.HT2, steel5Cells4.HT1) a;
  connect(steel5Cells4.HT2, steel5Cells5.HT1) a;
  connect(steel5Cells5.HT2, HT2) a;
  a;
end HeatTransferTube;
```

Inner Wall Cell

```
model InnerWallCell

  import SI = Modelica.SIunits;
/*********************** Thermodynamic property call ***********************

              replaceable package Medium = CoolProp2Modelica.Media.Hydrogen (
        onePhase=true) constrainedby Modelica.Media.Interfaces.PartialMedium ;
Medium.ThermodynamicState medium;

/******************** Connectors ****************************/
  Ports.HeatFlow2 portA "Heat flow is pos when added to the wall"
    ;
  Ports.HeatFlow portB "Heat flow is pos when subtracted from the wall"
    ;

/****************** variables ******************/
  SI.Temperature T "Temperature of the wall element";
  SI.Pressure p "Pressure of the hydrogen";
  SI.ThermalResistance R "Thermal resistance of liner";
  SI.CoefficientOfHeatTransfer h "Heat transfer coefficient";
  SI.ThermalConductivity k "Thermal conductivity of liner";
  SI.SpecificHeatCapacity cp "Specific heat capacity of liner";
  SI.Density rho "Density of liner";
  Real Tau "Dimenasionless time";
  Real Ra "Dimensionless hydrogen properties number";
  Real beta "Thermal expansion coefficient";
  Real v "kinematic viscosity";
  Real a "thermal diffusivity of hydrogen";
  Real Nu "Dimensionless heat transfer number";

/****************** General parameters ******************/
  constant Real g=9.82 "accelaration due to gravity";
  SI.Length dx=x1/2;

      outer SI.Length d "inside diameter of cylinder";
      outer SI.Temperature T_amb "Ambient temperature";
      outer Real y1;
      outer SI.CoefficientOfHeatTransfer  h_i;
      outer SI.Area A;
      outer SI.Length x1;
/******************* Tables ******************/
  Modelica.Blocks.Tables.CombiTable1Ds tank_prop(
    tableName="properties",
    tableOnFile=true,
    table=[1,850,15,481; 2,2700,236,900; 3,1286,1.17,1578; 4,1374,1.14,1075],
    fileName="C:/Users/edro/Documents/Dymola/External files/Lookuptables/heat_trans_prop
    ;

/****************** Initial equations ******************/
initial equation
  T=T_amb;

/****************** equations ******************/
equation
medium=Medium.setState_pT(p, T);
tank_prop.u=y1;
tank_prop.y[1]=rho;
tank_prop.y[2]=k;
tank_prop.y[3]=cp;

portA.P=p;

 Medium.thermalConductivity(medium)=a;
 Medium.dynamicViscosity(medium)/Medium.density(medium)=v;

//calculation of rayleighs number taken from 'Natural convection cooling of
```

```
//rectangular and cylindrical containers' by Wenxian Lin, S.W. Armfield
Ra=g*beta*d^3*Medium.specificHeatCapacityCp(medium)*
Medium.density(medium)^2*abs(portA.T-T)/(v*k);
beta=1/portA.T;
Tau=time/(d^2/(a*Ra^(1/2)));
Nu=0.104*Ra^(0.352);

if portA.m_flow < 0.00 then
  h=Nu*k/d;
elseif portA.m_flow > 0.00 then
  h=h_i;
else
  h=50;
end if;

R = dx / (A*k);

  portA.Q = (portA.T-T) / (1/(h*A));
  portB.Q = (portB.T-T) / (R/2);

  A*dx*rho*cp*der(T) = portA.Q + portB.Q;

portA.P=portB.P;
portA.Counter+1=portB.Counter;
  a
end InnerWallCell;
```

Outer Wall Cell

```
model OuterWallCell "Outer wall with natural convection given by h_o"
  import SI = Modelica.SIunits;

/******************** Connectors ****************************/
 Ports.HeatFlow portA "Heat flow is pos when added to the wall"
   a;

/****************** variables ******************/
 SI.Temperature T "Temperature of the wall element";
 SI.ThermalResistance R;
 SI.ThermalConductivity k;
 SI.SpecificHeatCapacity cp;
 SI.Density rho;
 SI.Area  A "heat flow surface area, dz*dy";
 SI.Length dx=x2/2;
 SI.HeatFlowRate Q;

/****************** General parameters ******************/
      outer parameter SI.CoefficientOfHeatTransfer h_o;
      outer SI.Temperature T_amb;
      outer Real y1;
      outer Real x2;
      outer SI.Length d;
      outer SI.Length xLiner;
      outer SI.Length  xCFRP;
      outer SI.Length L;

/****************** Tables ******************/
 Modelica.Blocks.Tables.CombiTable1Ds tank_prop(
    tableName="properties",
    tableOnFile=true,
    table=[1,850,15,481; 2,2700,236,900; 3,1286,1.17,1578; 4,1374,1.14,1075],
    fileName="C:/Users/edro/Documents/Dymola/External files/
    Lookuptables/heat_trans_prop.mat")
    a;
/****************** Initial equations ******************/
initial equation
 T=T_amb;
/****************** equations ******************/
equation
A=(d/2+xLiner+xCFRP)*2*Modelica.Constants.pi*L+2*
(d/2+xLiner+xCFRP)^2*Modelica.Constants.pi;

tank_prop.u=y1;
tank_prop.y[1]=rho;
tank_prop.y[2]=k;
tank_prop.y[3]=cp;

 R = dx / (A*k);

portA.Q = (portA.T-T) / (R/2);
Q=h_o*(T_amb-T)*A;

 A*dx*rho*cp*der(T) = portA.Q+Q;

 a;
end OuterWallCell;
```

Liner Cell

```
model LinerCell
  import SI = Modelica.SIunits;

  /******************** Connectors ****************************/
 Ports.HeatFlow portA "Heat flow is pos when added to the wall"
    ;
  Ports.HeatFlow portB "Heat flow is pos when subtracted from the wall"
    ;

/****************** variables ******************/
  SI.Temperature T "Temperature of the wall element";
  SI.ThermalResistance R;
  SI.ThermalConductivity k;
  SI.SpecificHeatCapacity cp;
  SI.Density rho;
  SI.Area A "heat flow surface area, dz*dy";
  SI.Length dx=x1;

/****************** General parameters ******************/
 outer SI.Temperature T_amb;
 outer Real x1;
 outer Real y1;
 outer Real t1;
 outer SI.Length d;
 outer SI.Length L;

/****************** Tables ******************/
Modelica.Blocks.Tables.CombiTable1Ds tank_prop(
    tableName="properties",
    table=[1,850,15,481; 2,2700,167,1106; 3,1286,1.17,1578; 4,1374,1.14,
        1075],
    fileName=
        "C:/Users/edro/Documents/Dymola/External files/Lookuptables/
        HeatTransferProperties.txt",
    tableOnFile=true)
    ;

/****************** Initial equations ******************/
initial equation
  T=T_amb;
/****************** equations ******************/
equation
A=((portA.Counter-0.5)*x1+d/2)*Modelica.Constants.pi*2*L+2*
((portA.Counter-0.5)*x1+d/2)^2*Modelica.Constants.pi;

tank_prop.u=y1;
tank_prop.y[1]=rho;
tank_prop.y[2]=k;
tank_prop.y[3]=cp;

  R = dx / (A*k);
  portA.Q = (portA.T-T) / (R/2);
  portB.Q = (portB.T-T) / (R/2);

  A*dx*rho*cp*der(T) = portA.Q + portB.Q;

if portA.Counter>=t1+0.5 then
  portB.Counter =0;
  else
portA.Counter+1=portB.Counter;
end if;

portA.P=portB.P;
  ;
end LinerCell;
```

Tank Cell

```
model TankCell
  import SI = Modelica.SIunits;

  /******************** Connectors ****************************/
 Ports.HeatFlow portA "Heat flow is pos when added to the wall"
    a;
 Ports.HeatFlow portB "Heat flow is pos when subtracted from the wall"
    a;

  /****************** variables ******************/
 SI.Temperature T "Temperature of the wall element";
 SI.ThermalResistance R;
 SI.ThermalConductivity k;
 SI.SpecificHeatCapacity cp;
 SI.Density rho;

  SI.Area A "heat flow surface area, dz*dy";

  SI.Length dx=x2;

  /****************** General parameters ******************/
  outer SI.Temperature T_amb;
  outer SI.Length x2;
  outer SI.Length x1;
  outer Real y2;
  outer SI.Length d;
  outer SI.Length L;
  outer Real t1;
  outer Real t2;

/****************** Tables ******************/
Modelica.Blocks.Tables.CombiTable1Ds tank_prop(
    tableName="properties",
    fileName="C:/Users/edro/Documents/Dymola/External files/
    Lookuptables/heat_trans_prop.mat",
    smoothness=Modelica.Blocks.Types.Smoothness.LinearSegments,
    table=[1,850,15,481; 2,2700,236,900; 3,1286,1.17,1578; 4,1500,0.5,940],
    tableOnFile=true)
    a;
  /****************** Initial equations ******************/
initial equation
  T=T_amb;
  /****************** equations ******************/
equation
A=((portA.Counter-0.5)*x2+x1*t1+d/2)*Modelica.Constants.pi*2*L+2*
((portA.Counter-0.5)*x2+x1*t1+d/2)^2*Modelica.Constants.pi;

tank_prop.u=y2;
tank_prop.y[1]=rho;
tank_prop.y[2]=k;
tank_prop.y[3]=cp;

  R = dx / (A*k);
  portA.Q = (portA.T-T) / (R/2);
  portB.Q = (portB.T-T) / (R/2);

A*dx*rho*cp*der(T) = portA.Q + portB.Q;
portA.P=portB.P;
if portA.Counter>=t2-0.5 then
  portB.Counter =0;
  else
portA.Counter+1=portB.Counter;
end if;
  a;
end TankCell;
```

Tube Cell

```
model TubeCell
  import SI = Modelica.SIunits;
  import C = Modelica.Constants;

/******************** Connectors ******************************/
    Ports.TemperaturePort                    HT1
    a¡
  Ports.TemperaturePort                     HT2
    a¡

/****************** General parameters ******************/
 outer SI.MassFlowRate m_flow;
 outer SI.SpecificHeatCapacity cp_h2;
 outer SI.CoefficientOfHeatTransfer h;
 outer SI.CoefficientOfHeatTransfer h_amb;
 outer parameter SI.Length d_i;
 outer parameter SI.Length d_o;
 outer parameter SI.Temperature T_amb;
 outer SI.Length L;
parameter SI.Length dx=(d_o-d_i)/12;

/****************** variables ******************/
flow SI.HeatFlowRate[8] Q;
SI.Temperature[7] T;
Real R;
SI.SpecificHeatCapacity cp;
SI.Density rho;
SI.Conductivity k;

/****************** Tables ******************/
Modelica.Blocks.Tables.CombiTable1Ds tank_prop(
    tableName="properties",
    table=[1,850,15,481; 2,2700,167,1106; 3,1286,1.17,1578; 4,1374,1.14,
        1075],
    tableOnFile=true,
    fileName=
        "C:/Users/edro/Documents/Dymola/External files/
        Lookuptables/HeatTransferProperties.txt")
    a¡
/******************** Initial equations ******************/
initial equation
  T[1]=T_amb;
  T[3]=T_amb;
  T[5]=T_amb;
  T[7]=T_amb;

/****************** equations ******************/
equation

  tank_prop.u=1;
  tank_prop.y[1]=rho;
  tank_prop.y[2]=k;
  tank_prop.y[3]=cp;

  R=dx/((d_i*C.pi*L)*k);
//Between hydrogen and inner wall
  Q[1]=(HT1.T-T[1])/(1/(h*(d_i*C.pi*L)));
  Q[2]=(T[2]-T[1])/(R/2);
  (d_i*C.pi*L)*dx*rho*cp*der(T[1]) = Q[1] + Q[2];
//Between two wall volumes
  -Q[2]=Q[3];
  Q[3]=(T[2]-T[3])/(R/2);
  Q[4]=(T[4]-T[3])/(R/2);
  ((d_i/2+dx*2)*2*C.pi*L)*2*dx*rho*cp*der(T[3]) = Q[3] + Q[4];
//Between two wall volumes
  -Q[4]=Q[5];
```

```
  Q[5]=(T[4]-T[5])/(R/2);
  Q[6]=(T[6]-T[5])/(R/2);
  ((d_i/2+dx*4)*2*C.pi*L)*2*dx*rho*cp*der(T[5]) = Q[5] + Q[6];
//Between outer wall volume and ambient
  -Q[6]=Q[7];
  Q[7]=(T[6]-T[7])/(R/2);
  Q[8]=h_amb*(T_amb-T[7])*((d_i/2+dx*6)*2*C.pi*L);
  ((d_i/2+dx*6)*2*C.pi*L)*dx*rho*cp*der(T[7]) = Q[7] + Q[8];

  -Q[1]=cp_h2*m_flow*(HT1.T-HT2.T);

  a;
end TubeCell;
```

Liner 10 Pieces

```
model Liner5Pieces
//Import of models
  LinerCell
        liner
    a;
  LinerCell
        liner1
    a;
  LinerCell
        liner2
    a;
  LinerCell
        liner3
    a;
  LinerCell
        liner4
    a;
  Ports.HeatFlow heatFlow
    a;
 Ports.HeatFlow heatFlow1
    a;
equation
  connect(liner.portB, liner1.portA) a;
  connect(liner1.portB, liner2.portA) a;
  connect(liner2.portB, liner3.portA) a;
  connect(liner3.portB, liner4.portA) a;
  connect(liner.portA, heatFlow) a;
  connect(liner4.portB, heatFlow1) a;
  a;
end Liner5Pieces;
```

Tank 10 Pieces

```
model Tank10Pieces
//import models
  TankCell
       cFRP
    a;
  TankCell
       cFRP1
    a;
  TankCell
       cFRP2
    a;
  TankCell
       cFRP3
    a;
  TankCell
       cFRP4
    a;
  TankCell
       cFRP5
    a;
  TankCell
       cFRP6
    a;
  TankCell
       cFRP7
    a;
  TankCell
       cFRP8
    a;
  TankCell
       cFRP9
    a;
  Ports.HeatFlow heatFlow
    a;
  Ports.HeatFlow heatFlow1
    a;
equation
  connect(cFRP.portA, heatFlow) a;
  connect(cFRP.portB, cFRP1.portA) a;
  connect(cFRP1.portB, cFRP2.portA) a;
  connect(cFRP2.portB, cFRP3.portA) a;
  connect(cFRP3.portB, cFRP4.portA) a;
  connect(cFRP4.portB, cFRP5.portA) a;
  connect(cFRP5.portB, cFRP6.portA) a;
  connect(cFRP6.portB, cFRP7.portA) a;
  connect(cFRP7.portB, cFRP8.portA) a;
  connect(cFRP8.portB, cFRP9.portA) a;
  connect(cFRP9.portB, heatFlow1) a;
  a;
end Tank10Pieces;
```

Tube 5 Pieces

```
model Tube5Pieces

  TubeCell   tubeHeatTransfer3Testing
    a;
  TubeCell   tubeHeatTransfer3Testing1
    a;
  TubeCell   tubeHeatTransfer3Testing2
    a;
  TubeCell  tubeHeatTransfer3Testing3
    a;
  TubeCell  tubeHeatTransfer3Testing4
    a;

  Ports.TemperaturePort                    HT1
    a;

  Ports.TemperaturePort                    HT2
    a;
equation
  connect(HT1,tubeHeatTransfer3Testing. HT1) a;
  connect(tubeHeatTransfer3Testing1.HT2,tubeHeatTransfer3Testing2. HT1)
    a;
  connect(tubeHeatTransfer3Testing2.HT2,tubeHeatTransfer3Testing3. HT1)
    a;
  connect(tubeHeatTransfer3Testing3.HT2,tubeHeatTransfer3Testing4. HT1)
    a;
  connect(tubeHeatTransfer3Testing4.HT2, HT2) a;
  connect(tubeHeatTransfer3Testing1.HT1, tubeHeatTransfer3Testing.HT2)
    a;
  a;
end Tube5Pieces;
```

Pressure Losses

Reduction Valve

```
model ReductionValve
  import SI = Modelica.SIunits;
/*********************** Thermodynamic properties ***********************************/
     replaceable package Medium =
       CoolProp2Modelica.Interfaces.ExternalTwoPhaseMedium ;
//
        Medium.ThermodynamicState mediumA;
       Medium.ThermodynamicState mediumB;

/******************** Connectors ****************************/
public
  Ports.FlowPort portA(
 p(final start=pInitialIn),
  h_outflow(final start=hInitial),
 m_flow(final start=m_flowInitial))
    ;

  Ports.FlowPort portB(
  p(final start=pInitialOut),
   h_outflow(final start=hInitial))
    ;

   Ports.PressurePort pp1 ;
   Ports.PressurePort pp2 ;
 /****************** parameters ******************/
  SI.Pressure pressureDrop "calculated pressure drop";
  parameter SI.Pressure pInitialIn = 1.013e5  ;
  parameter SI.Temperature TInitialIn = T_amb  ;
  parameter SI.Pressure pInitialOut=20e5 ;
  outer parameter SI.Temperature T_amb;

 /****************** Start values ******************/
//
protected
  parameter SI.SpecificEnthalpy hInitial=Medium.specificEnthalpy_pT(T=TInitialIn,
  p=pInitialIn) ;
  parameter SI.MassFlowRate m_flowInitial = 0 ;

equation
  //Passing on enthalpy between the ports
  portB.h_outflow = inStream(portA.h_outflow);
  portA.h_outflow = inStream(portB.h_outflow);

  portA.m_flow + portB.m_flow = 0 "mass balance";

  pressureDrop = portA.p - portB.p "Momentum balance";

//Deciding propeties depending on the flow direction
   if portA.p > portB.p then
       mediumA=Medium.setState_ph(portA.p, actualStream(portA.h_outflow));
       mediumB=Medium.setState_ph(portB.p, portB.h_outflow);
   else
     mediumA=Medium.setState_ph(portB.p, actualStream(portB.h_outflow));
     mediumB=Medium.setState_ph(portA.p,portA.h_outflow);
   end if;

 pp1.p=portA.p;
 pp2.p=portB.p;

  ;
end ReductionValve;
```

Reduction Valve

```
model AveragePressureRampRate
  import SI = Modelica.SIunits;
/************************ Thermodynamic properties ***********************************/
     replaceable package Medium =
      CoolProp2Modelica.Interfaces.ExternalTwoPhaseMedium a;

/******************** Connectors ****************************/
public
   Ports.FlowPort portA(
     p(final start=pInitial),
     h_outflow(final start=hInitial),
     m_flow(final start=m_flowInitial))
    a;

  Ports.FlowPort portB(
    p(final start=pInitial),
    h_outflow(final start=hInitial))
       a;
   Ports.PressurePort pp1
     a;

 /****************** parameters ******************/

  parameter Boolean SAEJ2601 = true
    "If true, the ramp rate is retrieved from J2601"                                    a;
  parameter SI.Pressure APRR2=28e6 "MPa/min - Alternative refueling rate" a;

   parameter SI.Pressure pInitial = 1.013e5  a;
   parameter SI.Temperature TInitial = 298  a;

  outer SI.Pressure APRR "MPa/min";
  outer Integer z3;
  Real APRR_used;
  SI.Pressure dp;

 /****************** Start values ******************/
protected
   parameter SI.SpecificEnthalpy hInitial=Medium.specificEnthalpy_pT(T=TInitial,
    p=pInitial) a;
   parameter SI.MassFlowRate m_flowInitial = 0.0000 a;

equation
  portB.h_outflow =inStream(portA.h_outflow);
  portA.h_outflow= inStream(portB.h_outflow);
//Deciding which ramp rate to be used
if SAEJ2601==true then
  APRR=APRR_used;
else
  APRR_used=APRR2;
end if;

portA.p-portB.p=dp "Momentum balance";
//Deciding APRR for controls and mass balances
if z3==0 then
  der(portA.p) = APRR_used/60;
  dp=0;
  portA.m_flow + portB.m_flow = 0;
else
der(portA.p) = 0;
portB.m_flow=0;
portA.m_flow=0;
 end if;
   pp1.p=portA.p;
  a;
end AveragePressureRampRate;
```

Pressure Loss

```
model PressureLoss

  import SI = Modelica.SIunits;
/*********************** Thermodynamic properties ***********************************/
    replaceable package Medium =
      CoolProp2Modelica.Interfaces.ExternalTwoPhaseMedium
    "The library called to obtain properties for the fluid";
//Modelica.Media.Interfaces.PartialMedium
       Medium.ThermodynamicState mediumA;
       Medium.ThermodynamicState mediumB;
     //  Medium.BaseProperties medium;

/******************** Connectors ****************************/

public
  Ports.FlowPort portA(
    p(final start=pInitial),
    h_outflow(final start=hInitial),
    m_flow(final start=m_flowStart))
    a;
  Ports.FlowPort portB(
    p(final start=pInitial),
    h_outflow(final start=hInitial))
    a;

 /****************** parameters ******************/

  parameter String inputChoice = "Tube" "|Input|"
  annotation(choices(choice = "Tube", choice="Valve",
  choice="Filter and Mass flow meter"));

  parameter Real kv = 1 "pressure loss coefficient"
                                    a;

 parameter Real kp = 1 "pressure loss coefficient"
                                    a;
 inner parameter SI.Diameter Diameter = 0.0052
    "represented inner diameter of tube"   a;

 inner parameter SI.Length  Length = 1 "represented Length"
                                      a;
  parameter Real Roughness = 0.000007 "Roughness of pipe"   a;

  parameter Real K_length = 0
    "Pressure loss from bends given in equivalent length"

  SI.Pressure pressureDrop "calculated pressure drop";

  parameter SI.Pressure pInitial = 1.013e5  a;
  parameter SI.Temperature TInitial = T_amb  a;

  outer parameter SI.Temperature  T_amb;

 /****************** Start values ******************/
protected
  parameter SI.SpecificEnthalpy  hInitial=
  Medium.specificEnthalpy_pTX(T=TInitial, p=pInitial, X=X) a;
  constant Real X[1]={1};
  parameter SI.MassFlowRate m_flowStart = 0.000 a;
/******************** Variables *****************************/

public
  SI.Area A "Area";
  SI.Velocity w "Velocity";
  SI.VolumeFlowRate Vdot "Volume flow rate";
  SI.Density d_in "density";
```

```
  SI.DynamicViscosity mu_in "Dynamic viscosity";
  Real ReynoldsNumber "ReynoldsNumber";
  Real FrictionFactor "Friction factor";
  constant SI.Density rho_w = 1000 "Density for water at 0 C and 1.0314 bars";

/******************** Equatuions ****************************/
equation
  A=Diameter*Diameter*Modelica.Constants.pi/4 "Cross sectional area";
  Vdot=portA.m_flow/d_in "Volume flow";
  w=Vdot/A "Velocity";

//Setting thermodynamic properties
mediumA=Medium.setState_phX(portA.p,inStream(portA.h_outflow),X);
mediumB=Medium.setState_phX(portB.p,inStream(portB.h_outflow),X);

// Setting the enthalpies in the connectors
  portB.h_outflow = inStream(portA.h_outflow);
  portA.h_outflow = inStream(portB.h_outflow);

// mass and momentum balance
  portA.m_flow + portB.m_flow = 0;
  pressureDrop = portA.p - portB.p;

//Giving reynolds number if mass flow = 0
    if Vdot <> 0 then
    ReynoldsNumber=d_in*abs(Vdot/A)*Diameter/mu_in;
    else
     ReynoldsNumber=1;
    end if;

// Calculation of the friction factor
   FrictionFactor=(1/(-1.8*log((6.9/ReynoldsNumber)+
   ((Roughness/Diameter)/3.7)^1.11)))^2;

//Deciding properties dendent on the flow direction
  if portA.p > portB.p then
    d_in = mediumA.d;
    mu_in=Medium.dynamicViscosity(mediumA);
  else
    d_in = mediumB.d;
    mu_in=Medium.dynamicViscosity(mediumB);
  end if;

//Pressure loss equations
if inputChoice == "Tube" then
  Vdot=A*Functions.squareRootFunction(pressureDrop, 10)/
  sqrt(0.5*d_in*(K_length+FrictionFactor*Length/Diameter));
elseif inputChoice == "Valve" then
 Vdot=sqrt(rho_w)*(kv/3600)/sqrt(d_in)*Functions.squareRootFunction(pressureDrop/
 10^5, 1e-3);
 //abs(Vdot)=sqrt(rho_w)*(kv/3600)/sqrt(d_in)*sqrt(max(pressureDrop/10^5,1));
else
    Vdot=Functions.squareRootFunction(pressureDrop/10^5, 1e-3)/sqrt(0.5*kp*d_in)/3600;
end if;

  a;
end PressureLoss;
```

Tube With Heat Transfer

```
model TubeWithheatTransfer
  import SI = Modelica.SIunits;
  import Constant = Modelica.Constants;

/*********************** Thermodynamic property call ***********************************
 replaceable package Medium = CoolProp2Modelica.Media.Hydrogen
                                                    a;

Medium.ThermodynamicState mediumA;
Medium.ThermodynamicState mediumB;

/******************* Connectors ****************************/
  Ports.FlowPort portA(
    p(final start=pInitial),
    h_outflow(final start=hInitial),
    m_flow(final start=m_flowStart))
    a;
  Ports.FlowPort portB(p(final start=pInitial), h_outflow(
        final start=hInitial))
    a;
  Ports.TemperaturePort                      HTIn
    a;
  Ports.HeatFlowTube                        HTOut
    a;

/****************** General parameters *******************/
 parameter SI.Diameter DiameterInner = 0.0052
    "represented hydraulic inner diameter of tube"   a;

      parameter SI.Diameter DiameterOuter = 0.0095 "Outer diameter of tube"
                                  a;

 parameter SI.Length  Length = 1 "represented Length"
                                  a;
  parameter Real Roughness = 0.000007 "Roughness of pipe"   a;

protected
 parameter SI.MassFlowRate m_flowStart = 0.000 a;
 parameter SI.SpecificEnthalpy  hInitial=
 Medium.specificEnthalpy_pT(T=TInitial, p=pInitial) a;

//Initial values
public
 parameter SI.Pressure pInitial = 1.013e5  a;
 parameter SI.Temperature TInitial = T_amb  a;
 outer parameter SI.Temperature  T_amb;

/****************** variables ******************/
SI.Area A_cross=(DiameterInner/2)^2*Constant.pi;
SI.Area A_surface=DiameterInner*Constant.pi*Length;
SI.Temperature T_in;
//SI.Temperature T_b;
SI.Temperature T_out(start=T_amb);
SI.Density d_in;
SI.VolumeFlowRate Vdot;
SI.Pressure pressureDrop;

//Heat Transfer unknowns
SI.CoefficientOfHeatTransfer h;
  SI.DynamicViscosity mu_in;
  Real ReynoldsNumber;
  Real FrictionFactor;
  Real Pr;
  Real Nu;
  Real BiotNumber;
  SI.SpecificHeatCapacity cp;
```

```
  SI.HeatFlowRate Q_new;
   SI.SpecificEnthalpy dh;

/****************** equations ******************/
equation
portA.m_flow+portB.m_flow=0;
T_in=HTOut.T;

Vdot=portA.m_flow/d_in;

//Heat transfer equations
    if Vdot<>0 then
    ReynoldsNumber=d_in*abs(Vdot/A_cross)*DiameterInner/mu_in;
    else
    ReynoldsNumber=0.1;
    end if;

   BiotNumber=h*((DiameterOuter-DiameterInner)/2)/14;
   FrictionFactor=(1/(-1.8*log((6.9/ReynoldsNumber)+
   ((Roughness/DiameterInner)/3.7)^1.11)))^2;

   Nu=0.023*ReynoldsNumber^(4/5)*Pr^(0.3);

if Vdot>=0 then
 mediumA = Medium.setState_ph(portA.p, inStream(portA.h_outflow));
 mediumB = Medium.setState_pT(portB.p,HTIn.T);
 mediumA.T=T_in;
 d_in=mediumA.d;
 mu_in=Medium.dynamicViscosity(mediumA);
 Pr=mediumA.cp*mu_in/mediumA.lambda;
 h=Nu*mediumA.lambda/DiameterInner;
 cp=mediumA.cp;
   else
mediumB = Medium.setState_ph(portB.p, inStream(portB.h_outflow));
mediumA = Medium.setState_pT(portA.p, HTIn.T);
mediumB.T=T_in;
d_in=mediumB.d;
mu_in=Medium.dynamicViscosity(mediumB);
Pr=mediumB.cp*mu_in/mediumB.lambda;
 h=Nu*mediumB.lambda/DiameterInner;
cp=mediumB.cp;
   end if;

//inStream(portA.h_outflow)*portA.m_flow+portB.h_outflow*portA.m_flow+Q_new=0;
inStream(portB.h_outflow)=portA.h_outflow+dh;
inStream(portA.h_outflow)=portB.h_outflow+dh;

dh=Medium.specificEnthalpy(mediumA)-Medium.specificEnthalpy(mediumB);
actualStream(portA.h_outflow)*portA.m_flow+
actualStream(portB.h_outflow)*portA.m_flow+Q_new=0;

 Vdot = A_cross*sqrt(2*DiameterInner/(FrictionFactor*d_in*Length))*
 TIL_Hydrogen_CoolProp.Functions.squareRootFunction(pressureDrop, 10);
pressureDrop = portA.p - portB.p;
HTIn.T=T_out;
HTOut.cp=cp;
HTOut.h=h;
HTOut.m_flow=portA.m_flow;

  a
end TubeWithheatTransfer;
```

Compressor

```
model Compressor
  import SI = Modelica.SIunits;

/******************** Thermodynamic properties*****************************/
    replaceable package Medium =
       CoolProp2Modelica.Interfaces.ExternalTwoPhaseMedium ;

       Medium.ThermodynamicState mediumA;
       Medium.ThermodynamicState mediumB;
       Medium.ThermodynamicState mediumIS;

/******************** Ports ****************************/
  Ports.FlowPort                       portA
    ;
  Ports.FlowPort                       portB
    ;

/******************** parameters ****************************/
parameter String CompressorType = "Isentropic" "|Input|" ;

parameter Integer Strokes=500 "Strokes pr. minut" ;
parameter SI.Volume V=0.0001 "Volume of cylinder" ;

/******************** variables ****************************/
SI.Efficiency eta_is "Isentropic efficiency";
SI.Efficiency eta_poly "polytropic efficiency";
SI.Efficiency eta "Efficiency of compression, either isentropic or polytropic";
Real r "Pressure ratio";
SI.Heat W "Work added to the compression";
SI.Efficiency VolumetricEfficiency "Volumetric efficiency";
SI.VolumeFlowRate Vdot "volume flow";
SI.SpecificEnthalpy dh "Change of enthalpy across the compressor";

SI.SpecificEnthalpy h_out "Discharge enthalpy of the compressor";

/******************** Equations ****************************/
equation
//Dimensioning the compressor and finding the mass and volume flow
VolumetricEfficiency=-0.05*(r)+0.9 "Volumetric efficiency";
portA.m_flow=V*mediumA.d*VolumetricEfficiency*Strokes/60 "Mass flow rate";
Vdot=portA.m_flow/mediumA.d "Volume flowrate";

// Chooses between isentropic and polytropic efficiency
//depending users input choice
if CompressorType == "Isentropic" then
  eta=eta_is;
else
  eta=eta_poly;
end if;

//Compressor equations, the isentropic efficiency
  eta_is=0.1091*(log(r))^3-0.5247*(log(r))^2+0.8577*log(r)+0.3727
    "Valid in the range of 1.1<r<5";
//Compressor equations, the polytropic efficiency
     eta_poly=0.017*log(Vdot)+0.7;

  r=portB.p/portA.p "Pressure ratio";

//Finding the properties of the hydrogen in and out of the compressor
  mediumA=Medium.setState_ph(portA.p, inStream(portA.h_outflow));
  mediumIS=Medium.setState_ps(portB.p, Medium.specificEntropy(mediumA));
  mediumB=Medium.setState_ph(portB.p, h_out);

//Calculating the discharge enthalpy
  h_out=Medium.specificEnthalpy(mediumA)+(mediumIS.h
  -Medium.specificEnthalpy(mediumA))/eta;
```

Heat Exchanger

```
model HeatExchangerFixedTemperature
  "Simple heat exchanger setting the outlet temperature"

 import SI = Modelica.SIunits
    "Renemaing the path to the SI units in modelica library";

/******************** thermodynamic properties ****************************/
    replaceable package Medium =
       CoolProp2Modelica.Interfaces.ExternalTwoPhaseMedium ;
       Medium.ThermodynamicState mediumB;
       Medium.ThermodynamicState mediumA;

/******************** Connectors ****************************/

  Ports.FlowPort portA
    ;
  Ports.FlowPort portB
    ;

/******************** parameters ****************************/
 Boolean SAEJ2601=true "Use SAE's outlet temperature" ;
 outer SI.Temperature   T_cool;
 parameter SI.Temperature T_hex = 273.15
    "Temperature out of the heat exchanger"   ;
 SI.Temperature THEX = (if SAEJ2601 == true then T_cool else T_hex);

/******************** Variables ****************************/
SI.Heat Q "Heat transfer";
SI.Pressure dp "Change in pressure";
SI.SpecificEnthalpy dh "Change in enthalpy";

/******************** Equations ****************************/
equation

  dp=0 "Pressure loss";
inStream(portB.h_outflow)=portA.h_outflow+dh "Enthalpy definition";
inStream(portA.h_outflow)=portB.h_outflow+dh "Enthalpy definition";

if portA.m_flow>=0 then
  mediumB = Medium.setState_pT(portB.p, THEX);
  mediumA= Medium.setState_ph(portA.p, inStream(portA.h_outflow));
  portA.h_outflow*portA.m_flow + inStream(portB.h_outflow)*portB.m_flow
  +der(Q) =0.0 "Energy balance";
  dh=Medium.specificEnthalpy(mediumA)-Medium.specificEnthalpy(mediumB)
      "Change in enthalpy";
else
  mediumA = Medium.setState_pT(portB.p, THEX);
  mediumB= Medium.setState_ph(portA.p, inStream(portA.h_outflow));
  inStream(portA.h_outflow)*portA.m_flow + portB.h_outflow*portB.m_flow
  +der(Q) =0.0 "Energy balance";
  dh=Medium.specificEnthalpy(mediumB)-Medium.specificEnthalpy(mediumA)
      "Change in enthalpy";
end if;

  portA.m_flow+portB.m_flow=0 "Mass balance";
  dp=portB.p-portA.p "momentum balance";

  ;
end HeatExchangerFixedTemperature;
```

Mixers

Volume Mixer

```
model VolumeMixer "Mixes 2 flows into one or splits 1 flow into two"
  import SI = Modelica.SIunits;

/****************** Call to gas properties ******************/
    replaceable package Medium =
          CoolProp2Modelica.Interfaces.ExternalTwoPhaseMedium ;
    Medium.ThermodynamicState medium;

  /*********************Connectors*****************************/

  Ports.FlowPort portA(
                      m_flow(final start=m_flowInitial)) "port A"
    ;
  Ports.FlowPort portB(
                      m_flow(final start=m_flowInitial)) "port B"
    ;
  Ports.FlowPort portC(
                      m_flow(final start=-m_flowInitial)) "port C"
    ;

  /*******************Geometry*******************************/
  parameter SI.Volume V=1e-9 "Volume of mixer" ;

  /*********************Initial conditions*********************/
public
  parameter Boolean fixedInitialPressure = true
    "if true, initial pressure is fixed";

  parameter SI.Pressure pInitial=1.013e5 "Initial value for air pressure"
    ;

  parameter SI.Temperature TInitial=T_amb "Initial value for air temperature"
    ;

outer parameter SI.Temperature T_amb;

protected
  parameter SI.SpecificEnthalpy hInitial=
      Medium.specificEnthalpy_pT(T=TInitial, p=pInitial) "Initial enthalpy" ;

  parameter SI.MassFlowRate m_flowInitial=0 "Start value for mass flow rate"
     ;

  /*******************Variables******************************/

public
  SI.SpecificEnthalpy h "Specific enthalpy";
  SI.Pressure p(final start=pInitial, fixed=fixedInitialPressure);
  SI.Mass M "mass of gas in mixer";
  Real drhodt "derivative of density";
  SI.InternalEnergy U;
/*********************Equations*****************************/

initial equation
  h=hInitial;

equation
medium=Medium.setState_ph(p,h);
U=(h-p*1/medium.d)*M;

if portA.m_flow >=0 then
  inStream(portA.h_outflow) = h1;
else
  h1=h;
end if;
```

```
if portB.m_flow >=0 then
  inStream(portB.h_outflow) = h2;
else
  h2=h;
end if;

if portC.m_flow >=0 then
  inStream(portC.h_outflow) = h3;
else
  h3=h;
end if;

  portA.p = p;

//Energy balance
    der(h) = 1/M*(portA.m_flow*noEvent(actualStream(portA.h_outflow) - h) +
      portB.m_flow*(actualStream(portB.h_outflow) - h) +
      portC.m_flow*(actualStream(portC.h_outflow) - h)
      + V*der(p)) "Energy balance";

    M = V*medium.d "Mass in control volume";

 drhodt = Medium.density_derp_h(medium)*der(p)
 + Medium.density_derh_p(medium)*der(h) "Derivative of density";

  drhodt*V   = portA.m_flow + portB.m_flow + portC.m_flow "Mass balance";

    portA.p - portB.p = 0 "Momentum balance";
    portA.p - portC.p = 0 "Momentum balance";

    ;
end VolumeMixer;
```

Ideal Mixer

```
model IdealMixing
import SI = Modelica.SIunits;

  /********************Thermodynamic properties*****************************/
replaceable package Medium =
      CoolProp2Modelica.Interfaces.ExternalTwoPhaseMedium ;
    Medium.ThermodynamicState medium;

/********************Connectors*****************************/
  Ports.FlowPort portA
    ;
  Ports.FlowPort portB
    ;
  Ports.FlowPort portC
    ;

/********************Variables*****************************/
  SI.Pressure p;
  SI.SpecificEnthalpy h;
  SI.SpecificEnthalpy hA;
  SI.SpecificEnthalpy hB;
  SI.SpecificEnthalpy hC;

equation
// property call
medium = Medium.setState_ph(p,h);
if portA.m_flow >=0 then
  inStream(portA.h_outflow) = hA;
else
  hA=h;
end if;

if portB.m_flow >=0 then
  inStream(portB.h_outflow) = hB;
else
  hB=h;
end if;

if portC.m_flow >=0 then
  inStream(portC.h_outflow) = hC;
else
  hC=h;
end if;

// Mass Balance
portA.m_flow+portB.m_flow+portC.m_flow=0;

//Momentum equations
portA.p=p;
p-portB.p=0;
p-portC.p=0;

 portA.h_outflow=h;
 portB.h_outflow=h;
 portC.h_outflow=h;

//Energy balance
    0 = portA.m_flow*(actualStream(portA.h_outflow) - h) +
      portB.m_flow*(actualStream(portB.h_outflow) - h) +
      portC.m_flow*(actualStream(portC.h_outflow) - h);

  ;
end IdealMixing;
```

Control

```
model ControlMultiplebanks
  import SI = Modelica.SIunits;

/******************** Connectors ****************************/

  Ports.PressurePort pp1
    a;
  Ports.PressurePort pp2
    a;
  Ports.PressurePort pp3
    a;
  Ports.PressurePort pp4
    a;
  Ports.PressurePort pp5
    a;
  Ports.PressurePort pp6
    a;

  Ports.PressurePort pp7
    a;
  Ports.PressurePort pp8
    a;
  Ports.PressurePort pp9
    a;
  Ports.PressurePort pp10
    a;
  Ports.PressurePort pp11
    a;
  Ports.PressurePort pp12
    a;
  Ports.PressurePort pp13
    a;

/****************** General parameters *******************/
outer SI.Pressure  P_end;
parameter SI.Pressure Switch_pressure=10e5 "Pressure across
reduction valve" a;
//parameter SI.Pressure Switch_pressure2( start=10e5);

 parameter SI.Pressure Tank1= 45e6 "Tank1" a;
 parameter SI.Pressure Tank2 = 65e6 "Tank2" a;
 parameter SI.Pressure Tank3 = 95e6 "Tank3" a;
 parameter SI.Pressure Tank4 = 95e6 "Tank4" a;
 parameter SI.Pressure Tank5 = 95e6 "Tank5" a;
 parameter SI.Pressure Tank6 = 95e6 "Tank6" a;
 parameter SI.Pressure Tank7 = 95e6 "Tank7" a;
 parameter SI.Pressure Tank8 = 95e6 "Tank8" a;
 parameter SI.Pressure Tank9 = 95e6 "Tank9" a;
 parameter SI.Pressure Tank10 = 95e6 "Tank10" a;

/****************** variables ******************/
Integer z1(start=0);
Integer z2(start=0);
Integer z3(start=0);
Integer z4=0;

/****************** equations ******************/
algorithm
// controlling tank shifts (up to 5 tanks)
  when pp1.p-pp2.p <= Switch_pressure and z1==0 then
  z1 :=1;
  elsewhen pp1.p-pp2.p <= Switch_pressure and z1==1 then
  z1 :=2;
  elsewhen pp1.p-pp2.p <= Switch_pressure and z1==2 then
  z1 :=3;
  elsewhen pp1.p-pp2.p <= Switch_pressure and z1==3 then
```

Templates

Template 1

```
model Template
  import SI = Modelica.SIunits;

/*********************** Thermodynamic property call ***********************************
 replaceable package Medium = CoolProp2Modelica.Media.Hydrogen (onePhase=true)
   constrainedby Modelica.Media.Interfaces.PartialMedium
                                                    a;

/****************** General parameters *******************/
inner parameter SI.Temperature T_amb=HRSinfo.T_amb;
inner SI.Temperature  T_cool=HRSinfo.T_cool;
inner SI.Pressure  P_amb;
inner SI.Pressure P_start;
inner Real SOC_target;
inner SI.Pressure P_end;
inner SI.Pressure P_ref;
inner Real APRR;
parameter Boolean control_valve=true;
inner Integer z1;
inner Integer z2;
inner Integer z3;
inner Integer z4;

  HRSInfo HRSinfo
    a;
/****************** equations ******************/
equation
  control.z1=z1;
  control.z2=z2;
  control.z3=z3;
  control.z4=z4;

HRSinfo.P_amb=P_amb;
HRSinfo.P_start=P_start;
HRSinfo.FP=P_end;
HRSinfo.SOC=SOC_target;
HRSinfo.APRR=APRR;
HRSinfo.P_ref=P_ref;

  a;
end Template;
```

Template 2

```
model Template2
  import SI = Modelica.SIunits;

/*********************** Thermodynamic property call ***********************************
  replaceable package Medium = CoolProp2Modelica.Media.Hydrogen (onePhase=true)
   constrainedby Modelica.Media.Interfaces.PartialMedium
                                                    a;

/****************** General parameters *******************/
inner parameter SI.Temperature T_amb=HRSinfo.T_amb;
inner SI.Temperature  T_cool=HRSinfo.T_cool;
inner SI.Pressure  P_amb;
inner SI.Pressure P_start;
inner Real SOC_target;
inner SI.Pressure P_end;
inner SI.Pressure P_ref;
inner Real APRR;

parameter Boolean control_valve=true;

  HRSInfo HRSinfo
    a;

/****************** equations *******************/
equation
HRSinfo.P_amb=P_amb;
HRSinfo.P_start=P_start;
HRSinfo.FP=P_end;
HRSinfo.SOC=SOC_target;
HRSinfo.APRR=APRR;
HRSinfo.P_ref=P_ref;

  a;
end Template2;
```

Appendix D

Paper I

Erasmus Rothuizen, Walter Mérida, Masoud Rokni and Morten Wistoft-Ibsen

Optimization of hydrogen vehicle refuelling via dynamic simulation

International Journal of Hydrogen 38, 4221-4231. (2013)

INTERNATIONAL JOURNAL OF HYDROGEN ENERGY 38 (2013) 4221–4231

Available online at www.sciencedirect.com

SciVerse ScienceDirect

journal homepage: www.elsevier.com/locate/he

Optimization of hydrogen vehicle refueling via dynamic simulation

E. Rothuizen [a,*], W. Mérida [b], M. Rokni [a], M. Wistoft-Ibsen [c]

[a] Section for Thermal Energy Systems, The Technical University of Denmark, 2800 Kgs. Lyngby, Denmark
[b] Clean Energy Research Center, University of British Columbia, Vancouver, British Columbia, Canada
[c] H2Logic, Herning, Denmark

ARTICLE INFO

Article history:
Received 6 November 2012
Received in revised form
17 January 2013
Accepted 21 January 2013
Available online xxx

Keywords:
Hydrogen refueling
Optimization
Design
SAE TIR J2601
Dynamic simulation

ABSTRACT

A dynamic model has been developed to analyze and optimize the thermodynamics and design of hydrogen refueling stations. The model is based on Dymola software and incorporates discrete components. Two refueling station designs were simulated and compared. The modeling results indicate that pressure loss in the vehicle's storage system is one of the main factors determining the mass flow and peak cooling requirements of the refueling process. The design of the refueling station does not influence the refueling of the vehicle when the requirements of the technical information report J2601 from Society of Automotive Engineers are met. However, by using multiple pressure stages in the tanks at the refueling station (instead of a single high-pressure tank), the total energy demand for cooling can be reduced by 12%, and the compressor power consumption can be reduced by 17%. The time between refueling is reduced by 5%, and the total amount of stored hydrogen at high pressure is reduced by 20%.

1. Introduction

During the last decade, technologies required to transition the transportation sector from fossil-based fuels towards renewable energies, such as hydrogen, have emerged. In 2010, there were 79 pilot projects for hydrogen refueling stations in Europe, and today, there are more than 500 stations in use worldwide. Moreover, commercial hydrogen refueling stations are available on the market from suppliers, including H2Logic, Linde and Powertech Labs. Many of these stations are limited to specialized suppliers because there were no performance guidelines when the stations were built. In 2010, the Society of Automotive Engineers (SAE) released the first Technical Information Report (TIR) describing fast hydrogen vehicle refueling without exceeding storage-tank safety limits [1]. Additionally, the SAE has created a TIR for on-board vehicle systems. This procedure is used by all major car manufacturers, including Hyundai, Honda, and Daimler-Chrysler. The TIRs are compatible: if car manufacturers build their vehicles according to SAE TIR J2600 [2] and if the fueling stations are built according to SAE TIR J2601, it will be possible to refuel any car at any refueling station worldwide. Other initiatives towards standardizing hydrogen refueling include the "H_2 Mobility" program in Europe, which incorporates guidelines for rating refueling stations with respect to their capacity. H2 Mobility and SAE TIR J2601 are complementary and consistent. The SAE TIR J2601 primarily describes the process with respect to safety, while H_2 Mobility categorizes refueling stations according to capacity requirements (e.g., kg of H_2 per day and time between refuels).

* *Corresponding author*. Tel.: +45 4525 4329; fax: +45 4588 4325.
E-mail address: edro@mek.dtu.dk (E. Rothuizen).
0360-3199/$ – see front matter
http://dx.doi.org/10.1016/j.ijhydene.2013.01.161

The main research focus has been on describing the behavior of the compressed hydrogen on board and the heat transfer through both type-3 and type-4 tanks, which consist of a carbon outer shell wrapped around an aluminum or plastic liner, respectively. Some of the first comprehensive studies on compressed hydrogen refueling were performed by Dicken and Mérida, who placed 63 thermocouples in a type-3 tank while refueling to 350 bars [3]. The study showed a non-uniform temperature distribution with a temperature variation of up to 6 °C. Furthermore the study showed that the main contributor to heat development in the tank was compression, rather than the Joule-Thomson effect. Although the study showed a non-uniform temperature distribution during refueling, it is generally accepted that the temperature can be assumed uniform in mathematical models (new tanks have a distributor at the inlet to ensure a more uniform temperature distribution) [4–6]. Different analytical and numerical models have been developed to study transient heat transfer from the hydrogen through the tank wall to the ambient air. Depending on the nozzle design in the tank (e.g., advanced or straight nozzles), the average local hydrogen heat transfer number inside the tank during a refueling can vary between 150 and 500 W/(m^2K) [4] [7]. For discharging vessels, Daney's relation has been shown to be valid for a large range of Rayleigh numbers [7]. The thermodynamics of filling a hydrogen tank has been investigated through exergy analysis, and it has been shown that increasing the initial pressure increases the exergy efficiency and lowers the final temperature in the hydrogen tank [8].

In this study, we concentrated on the overall process of hydrogen refueling through a hydrogen refueling station. The effect of pressure losses on the system is analyzed, and an optimization of a system is shown. Table 1 briefly summarizes the work performed by other research groups and the differences from the work presented here.

1.1. *Safety when refueling hydrogen*

The refueling protocol SAE TIR J2601 has been developed from various tests of refueling conditions at PowerTech Labs in British Columbia, Canada. The German engineering company Wenger Engineering has performed simulations using these tests to verify and validate their models. The work by PowerTech Labs and Wenger has been collected and synthesized into the protocol SAE TIR J2601 [1]. The main safety consideration is that the hydrogen temperature inside the tank to be maintained above −40 °C and below 85 °C to avoid thermal stress damage to the tanks. The protocol prescribes the temperature at which the hydrogen should leave the refueling station, and there are 4 possible temperature ratings (A, B, C and D) and two pressure ratings 35 MPa and 70 MPa. The ratings are are shown in Table 2. Rating A corresponds to cooling to −40 °C, B to −20 °C, C to 0 °C and D has no cooling. Furthemore the protocol describes refueling for both 35 MPa and 70 MPa tanks. Refueling stations are rated in order of their cooling and highest possible fueling pressure, e.g., an A70 station cools to −40 °C and delivers at 70 MPa. The goal when refueling is to reach the target density of 40.2 kg/m^3 inside the tank when refueling is finished (corresponding to a pressure of 700 bars at 15 °C). The relationship between the target density and the real density is referred to as the tanks state of charge (SOC). The lower limits are given by the protocol SAE TIR J2601. Refueling is controlled by an average pressure ramp rate (APRR), which is determined using the ambient temperature and the initial pressure in the tank. The average pressure ramp rates are designed so that if the cooling demand is satisfied, then the temperature of the hydrogen inside the tank during filling will not exceed 85 °C. Refueling is aborted at a given pressure inside the tank that depends on initial pressure and ambient temperature, so the SOC is not necessarily 100% when the refueling cycle is completed. All the relevant data can be found in SAE TIR J2601 with tables for final pressure, minimum SOC and APRR depending on the ambient temperature, initial pressure and the temperature of the hydrogen when it leaves the station. The protocol is in the process of being evaluated to become a standard. With such a standard, all vehicle manufacturers will be able to produce hydrogen vehicles following the corresponding protocols to enable refueling at any station worldwide.

2. Theory

2.1. *Governing equations for thermodynamic model*

With reference to Fig. 1, the system for hydrogen refueling of a tank can be divided into three main components: the tank at the station, the tank in the vehicle, and the control valve.

Table 1 – Work comparison.

Authors	Work	Current study
Dicken and Mérida [3]	Comprehensive study of temperature distribution inside a type-3 tank	
Woodfield and Monde [4–7]	Thorough study of heat transfer in hydrogen tanks during refueling; Suggested heat transfer number for the hydrogen in the tank while refueling; Conductivity study of the materials used for liner and wrapping	Thermodynamic analysis of a whole refueling system; from tank at refueling station to tank in vehicle taking SAE TIR J2601 into account; Analyzing and optimizing the cooling demand; Analyzing the effect of pressure losses in the system on mass flow
Sung Chan kim; Lei Zhao; M. Cristina Galassi [9–11]	CFD modeling and numerical modeling of temperature distribution fueling of a hydrogen tank; the effect of mass flow on temperature rise in tank was analyzed	
M. Hosseini [8]	Thermodynamics analyses inside the tank using exergy analysis	

Table 2 – Hydrogen refueling station ratings.

Type	Pressure [bar]	Temperature [C]
A70	700	−40
A35	350	−40
B70	700	−20
B35	350	−20
C35	350	0
D35	350	Ambient

These components determine how the refueling process will take place. The tank at the fueling station has mass leaving from it while the vehicle tank is receiving mass. Due to mass conservation, the mass leaving is the same as the mass received. The thermodynamics of the tanks can be determined from the first law of thermodynamics for an open system without any work added:

$$\frac{dU}{dt} = h\frac{dm}{dt} + \frac{dQ}{dt} \tag{1}$$

where dU/dt is the change in internal energy of the system, h is the enthalpy leaving or entering the tank, dm/dt is the mass flow rate and dQ/dt is the heat rate entering or leaving the system. Introducing $u = h - pv$, the internal energy inside the tank can be described through the derivatives of enthalpy and pressure [12]:

$$\frac{dU}{dt} = v\left(\rho\frac{dh}{dt} + h\frac{d\rho}{dt} - \frac{dP}{dt}\right) \tag{2}$$

where h and P are the enthalpy and the pressure in the tank, ρ is the gas density and v is the volume of the tank. The time derivative of ρ can be expressed through the derivative of enthalpy and pressure:

$$\frac{d\rho}{dt} = \frac{\partial\rho}{\partial P}\Big|_h \cdot \frac{dP}{dt} + \frac{\partial\rho}{\partial h}\Big|_P \cdot \frac{dh}{dt} \tag{3}$$

The controlling equation of the system can either be defined as a function of the mass flow change or a function of the pressure change. The two different possibilities can be described as

$$\frac{dP}{dt} = f(P) \tag{4}$$

$$\frac{dm}{dt} = g(\dot{m}) \tag{5}$$

For an adiabatic thermodynamic model, eqs. (1) and (2) and either 4 or 5 need to be present; hence, only the mass leaving or entering the tank influences the temperature and pressure. Heat transfer equations can be added to the system to create a more detailed model.

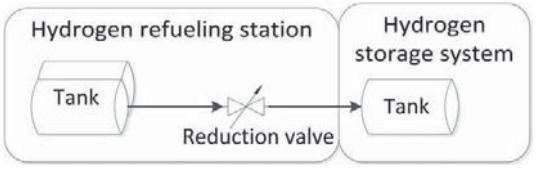

Fig. 1 – The 3 main components; the tank (s) at the refueling station, the reduction valve and the tank (s) in the vehicle.

2.2. *Heat transfer equations*

The heat transfer through the tank is assumed to be 1-dimensional unsteady heat conduction (the temperature of the gas changes when gas is leaving or entering the tank). The general heat equation and the boundary conditions are given in eqs. (6)–(8):

$$\frac{\partial^2 T_s}{\partial x^2} = \frac{1}{a}\frac{\partial T_s}{\partial t} \tag{6}$$

$$k\frac{dT_w}{dx}\Big|_{x=0} = \alpha_g\left(T_g - T_w|_{x=0}\right) \tag{7}$$

$$k\frac{dT_w}{dx}\Big|_{x=L} = \alpha_a\left(T_w|_{x=L} - T_a\right) \tag{8}$$

where T_w is the wall temperature, T_g is the gas temperature in the tank and T_a is the air temperature outside the tank, k is the thermal conductivity, and α_g and α_a are the heat transfer coefficients of the gas inside and outside the tank, respectively.

A numerical solution to eq. (6) can be obtained with the capacitance resistance method, which corresponds to a finite small-volume analysis [13]. A node system can be defined with "i" as the subscript identifying a node where the heat transfer occurs (see Fig. 2). Assuming a uniform temperature distribution and that the wall acts like a plain wall, the resistance capacitance method can be applied to the hydrogen tank using eqs. (9) and (10):

$$Q_{A,i} = \sum_j Q_{k,i-j} = (Q_k)_{i,i-1} + (Q_k)_{i,i+1} \tag{9}$$

and

$$Q_{A,i} = (\rho c \Delta V)_i \frac{dT_i}{dt} + \dot{s}_i \Delta V_i \tag{10}$$

where the subscript "i" is the node where the temperature is calculated and $\dot{s}_i$ is the rate of surface energy conversion. The resistance capacitance method simplifies the partial differential equation eq. (6) into the ordinary differential equation

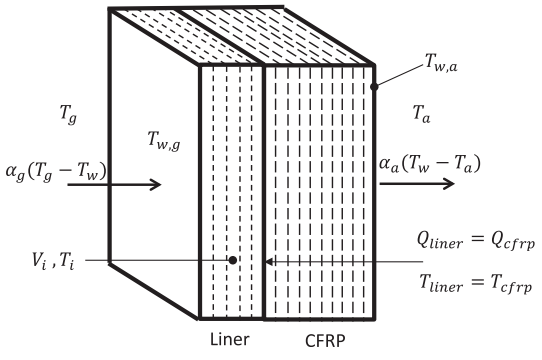

Fig. 2 – Diagram of heat transfer through wall piece.

eq. (10). The heat transfers $Q_{k,i-1}$ and $Q_{k,i+1}$ can be found from eqs. (11) and (12).

$$Q_{k,i-1} = \frac{T_i - T_{i-1}}{R_{i,i-1}} \tag{11}$$

$$Q_{k,i+1} = \frac{T_i - T_{i+1}}{R_{i,i+1}} \tag{12}$$

The boundary conditions in eqs. (9) and (10) are given by

$$\left.\frac{dT_i}{dx}\right|_{x=0} = \frac{\alpha_g}{k}\left(T_g - T_i|_{x=0}\right) \tag{13}$$

$$\left.\frac{dT_i}{dx}\right|_{x=L} = \frac{\alpha_a}{k}\left(T_i|_{x=L} - T_a\right) \tag{14}$$

The heat transfer coefficient α_g depends on the tank design and varies between 150 W/(m^{2}K) and 500 W/(m^{2}K) when increasing pressure in a tank [4] [7]. For decreasing pressure in a tank, Daney's correlation is used for the Nusselt's number, as shown in eq. (15) [14]

$$Nu = 0.104Ra^{0.352} \tag{15}$$

The Rayleigh number is given by eq. (16)

$$Ra = \frac{g\beta d^3 c\rho^2\left(T_w - T_g\right)}{\mu k} \tag{16}$$

where g is gravity, β is the thermal expansion coefficient, d is the inside diameter of the tank, c is the specific heat capacity at constant pressure, and μ is the dynamic viscosity of the gas.

2.3. Pressure losses

Other pressure losses in the system can be calculated using real gas equations. For valves, the pressure at the exit of the valve is found from eq. (17)

$$P_{out} = \frac{-P_{in} - \sqrt{P_{in}^2 - 4K}}{-2} \tag{17}$$

where K is

$$K = \frac{\rho T_{in}}{\left(514 k_v/\dot{v}\right)^2} \tag{18}$$

k_v is a pressure loss constant given by the manufacturer and $\dot{v}$ is the volume flow rate of the gas through the valve. The pressure loss in the mass flow meter, the filter and the hydrogen storage system is given by eq. (19):

$$P_{loss} = 0.5 k_p \rho\left(\frac{\dot{m}}{A\rho}\right)^2 \tag{19}$$

where k_p is a dimensionless pressure loss coefficient given by the component manufacturer.

2.4. Other equations

The cooling demand for the hydrogen in the heat exchanger is found from eq. (20):

$$Q = \dot{m}(h_{in} - h_{out}) \tag{20}$$

where h_{in} and h_{out} are the enthalpies into and out of the heat exchanger, respectively.

2.5. Software used for model

The simulation software used for deployment of the model is Dymola, which is a front–end interface for the free simulation software Modelica. The language is a unified object-oriented language for physical system modeling. The approach is non-causal and uses true ordinary differential and algebraic equations. The software is capable of solving large complex systems using different solvers such as a Dassl, Euler, Lsoder or one of the many other solvers included.

2.6. Limitations of the model

The model does not take into account the thermal mass in the system between the two vessels. High pressure tubing will have an effect on the hydrogen temperature in the station before the heat exchanger. The hydrogen will be cooler when it enters the heat exchanger, which will lower the cooling capacity and decrease the peak demand. The model has not yet been validated with real data; such validation is the focus of current efforts. The pressure losses throughout the system have to be revised for every station and new k_v and k_p values should be obtained for the different components.

2.7. Combination of thermodynamic and heat transfer equations into a model

The model of the refueling station is built by objects (each component in the system is treated as an individual object, including the tanks, valves, etc.) The objects can be connected in any order because all of them receive and convey on information about the current states (mass flow, temperature, pressure and enthalpy). The state properties needed in each component, such as density, specific heat capacity, and viscosity are retrieved for each object using the Refprop library from the US National Institute of Standards and Technology (NIST). The object uses the input and the equations given for changes in pressure, temperature or enthalpy to evaluate the property states at the exit. Exergy calculations are performed for each object to calculate its exergy efficiency. Such object-oriented language with standardized inputs and outputs makes it possible to change the placement of objects and immediately observe the effects on the overall system.

3. Analysis and discussion

This section will analyze the thermodynamics of the hydrogen refueling station and the on board hydrogen storage system. Refueling is simulated in accordance with SAE TIR J2601. An optimization analysis using multiple tanks at the hydrogen refueling station is compared to implementations that use only a single tank. Information about all parameters for the different simulations can be found in A.1. The most important parameters are given here. The vessel has a volume of 0.172 m^3, corresponding to a 7 kg tank. The ambient temperature is assumed to be 25 °C, and the initial pressure in the

tank is 2 MPa. The APRR for these conditions is 28.2 MPa/min, and it decreases as the ambient temperature increases from 25 °C.

3.1. *Thermodynamics of the system*

A hydrogen refueling station is a high-pressure system in which the pressure and temperature of the hydrogen changes over time in the different components. A diagram for a conceptual hydrogen refueling station is shown in Fig. 3. It is a simplified model designed to show the thermodynamic evolution over time.

The model has one hydrogen tank with a pressure of 90 MPa at the hydrogen refueling station. The APRR is controlled at the station outlet. However, the pressure reduction valve is placed before the heat exchanger; hence, the reduction valve compensates for the pressure losses between itself and the nozzle. The pressure loss in the hydrogen storage system is given by the same equation as the pressure loss in the mass flow meter, eq. (19). Because pressure loss in the hydrogen storage system is different for different vehicle models, it is impossible to predict it in general, though it is not allowed to exceed 20 MPa at any time [1]. The thermodynamics of a full refueling event according to SAE TIR J2601 are shown in Fig. 4. The temperature and pressure at different locations are plotted and correspond to the numbers in Fig. 3: the tank outlet of the hydrogen refueling station (1), before and after the reduction valve (2 and 3), after the heat exchanger (4), at the inlet to the tank in the hydrogen storage system (5) and in the tank in the hydrogen storage system (6). These points were identified as critical locations in the overall system.

Fig. 4 (a) shows the temperatures throughout the system. The temperature at the outlet of the tank (1) at the hydrogen refueling station decreases as mass is removed. The temperature increases across components where there are pressure losses present these increases are due to the negative Joule-Thomson coefficient of hydrogen and are especially significant across the reduction valve (point 2-3). The temperature rise (point 4–5) is parabolic because the pressure drop is a function of the mass flow; the temperature rise is therefore due to the Joule-Thomson coefficient. The hydrogen gas temperature coming into the tank at the hydrogen storage system is much lower than the hydrogen gas temperature inside the tank; this is due to the heat of compression inside the tank. Fig. 4 (b) shows the pressures through the system. The pressure out of the tank at the hydrogen refueling station decreases as mass leaves the tank. Conversely, the pressure increases in the hydrogen storage system tank due to mass being transferred to it. Fig. 4 (c) shows the mass flow of the hydrogen and the demand for cooling the hydrogen to −40 °C. Because the system is fueled with an APRR, the mass flow varies depending on the back pressure in the hydrogen storage system; this will be explained in more detail in section 3.2. The cooling demand is a function of the mass flow and enthalpy. It is very similar to the mass flow curve, although it peaks earlier due to a higher enthalpy. The enthalpy is highest at the start and decreases during the refueling because mass is leaving the tank at the hydrogen refueling station, reducing the pressure and decreasing the temperature. Fig. 4 shows the gas temperature development in both the tank at the hydrogen refueling station and the tank in the hydrogen storage system over a period of an hour, starting with a refueling. The temperature either increases or decreases rapidly during the refueling. The thermal conductivity of the carbon fiber wrapping is low [4], and therefore, it takes a long time before the tanks come back to ambient conditions after refueling (with no mass leaving or entering).

3.2. *Effect of pressure loss in hydrogen storage system on the hydrogen refueling station*

As shown in Fig. 3, the system consists of the hydrogen refueling station and the hydrogen storage system. SAE TIR J2601 prescribes the outlet conditions of the hydrogen at the hydrogen refueling station: the pressure increase should be the APRR, 28.2 MPa/min and the temperature should be −40 °C for an A70 station at an ambient temperature of 25 °C filling from 2 MPa to 70 MPa. This means that the pressure losses in the hydrogen refueling station do not influence the refueling of the hydrogen storage system. The pressure losses of the hydrogen storage system, however, do have an influence on the hydrogen refueling station.

The tank in the vehicle and the pressure losses between the hydrogen refueling station and the tank in the hydrogen storage system determine the mass flow rate and the fueling time. Fig. 5 shows the pressure, temperature, mass flow and cooling demand for 4 different pressure losses in the hydrogen storage system. The pressure loss is calculated from eq. (19), where k_p values have been chosen to show almost no pressure loss across the components ($k_{p,1}$) and to illustrate the highest allowed pressure loss of 20 MPa ($k_{p,4}$) in the hydrogen storage system (according to SAE TIR J2601). The values are $k_{p,1} = 25$, $k_{p,2} = 100$, $k_{p,3} = 200$, and $k_{p,4} = 300$. Fig. 5

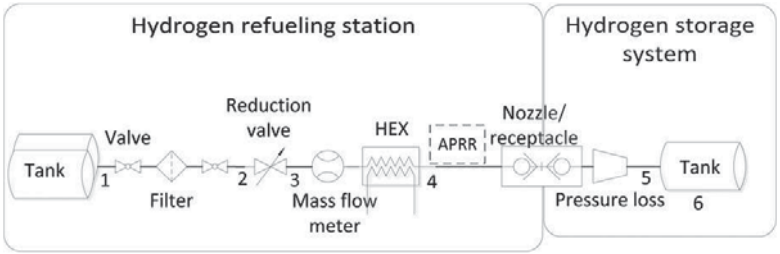

Fig. 3 – Simple hydrogen refueling station, reference model.

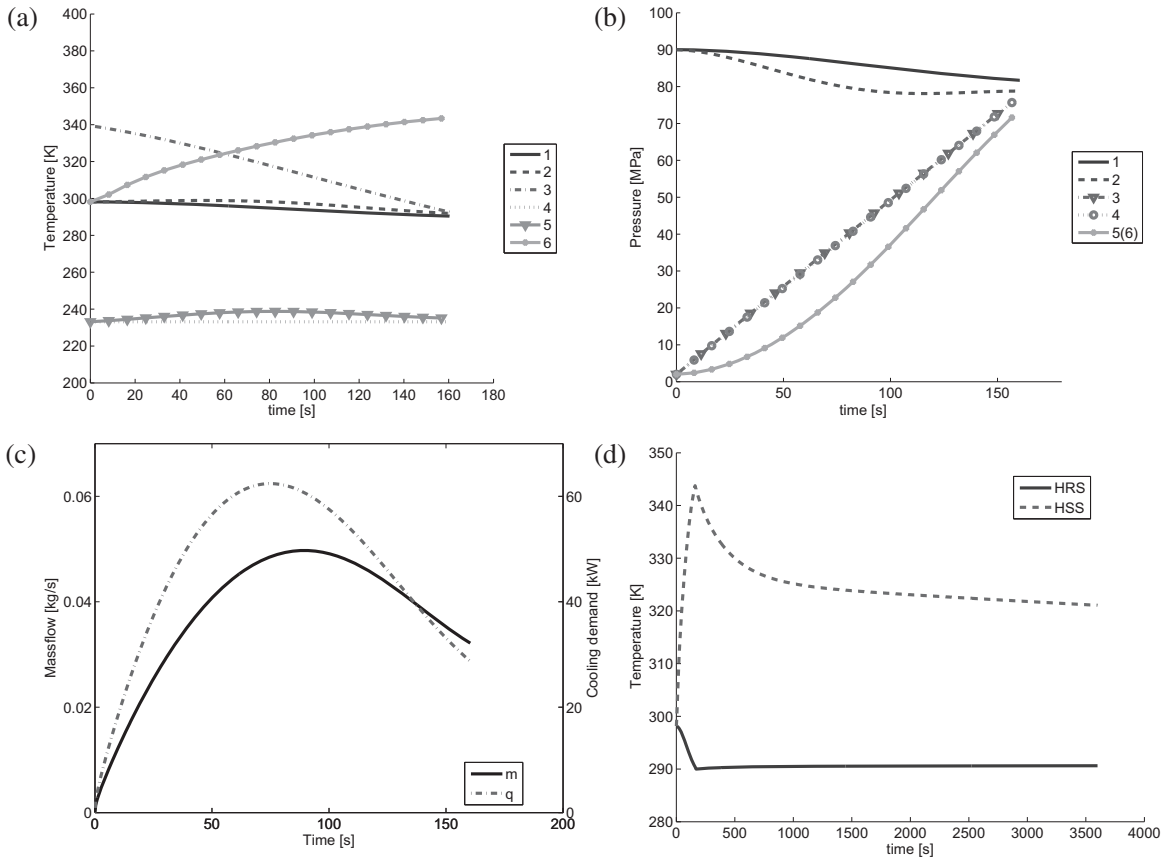

Fig. 4 – The thermodynamics of hydrogen refueling. (a) Temperatures in the system. (b) Pressures in the system. (c) Mass flow and cooling demand. (d) Temperature development in tanks with a refueling and 1 h afterwards.

(c) shows the mass flow for different pressure losses in the hydrogen storage system. The figure shows that the peak mass flow is lower at high pressure losses, and the total mass when fueling to the same pressure is slightly less than refueling with low pressure loss (not shown here). This is because of the temperature inside the hydrogen storage system tank, as shown in Fig. 5 (a); it increases relative to the pressure loss increase shown in Fig. 5 (b). Because fueling ends at the same pressure, the density of the warmer hydrogen will be lower, resulting in a lower total mass. The fueling time also increases with increased pressure loss in the hydrogen storage system. Intuitively, this should be the same because the APRR is the same. However, due to the increased pressure loss in the hydrogen storage system, the pressure rise in the tank is lower, as shown in Fig. 5 (d). The APRR is set at the nozzle, so the pressure loss in the hydrogen storage system will affect the pressure rise in the hydrogen storage system tank. Fig. 5 shows the cooling demand as a function of the pressure loss; it is worth noting that the peak cooling demand is lower as the peak mass flow rate decreases. In this example, the peak cooling demand is 35% lower for the highest pressure loss. Such a change is significant because it can lower the refrigeration requirements in a facility for high pressure loss vehicles (though it most likely will also service vehicles with lower pressure losses as well). The pressure drop in the hydrogen refueling station only affects the tank at the hydrogen refueling station. The pressure and the volume of the tank at the hydrogen refueling station have to be dimensioned so that the pressure is always higher before the reduction valve. The pressure at the end of a refueling has to be high enough to overcome the back pressures in the system.

3.3. *Effects of using cascade filling*

The following section will describe how the model can be used for energy and time optimization for refueling a hydrogen vehicle. The two systems that are used to show the optimization can be observed in Figs. 3 and 6. The only difference between the two systems is the number of tanks at the hydrogen refueling station. In the system in Fig. 3, there is a single tank at 90 MPa; in the refueling station in Fig. 6, there are three tanks at 45, 65 and 91 MPa. The second system is generally known as a cascade filling system.

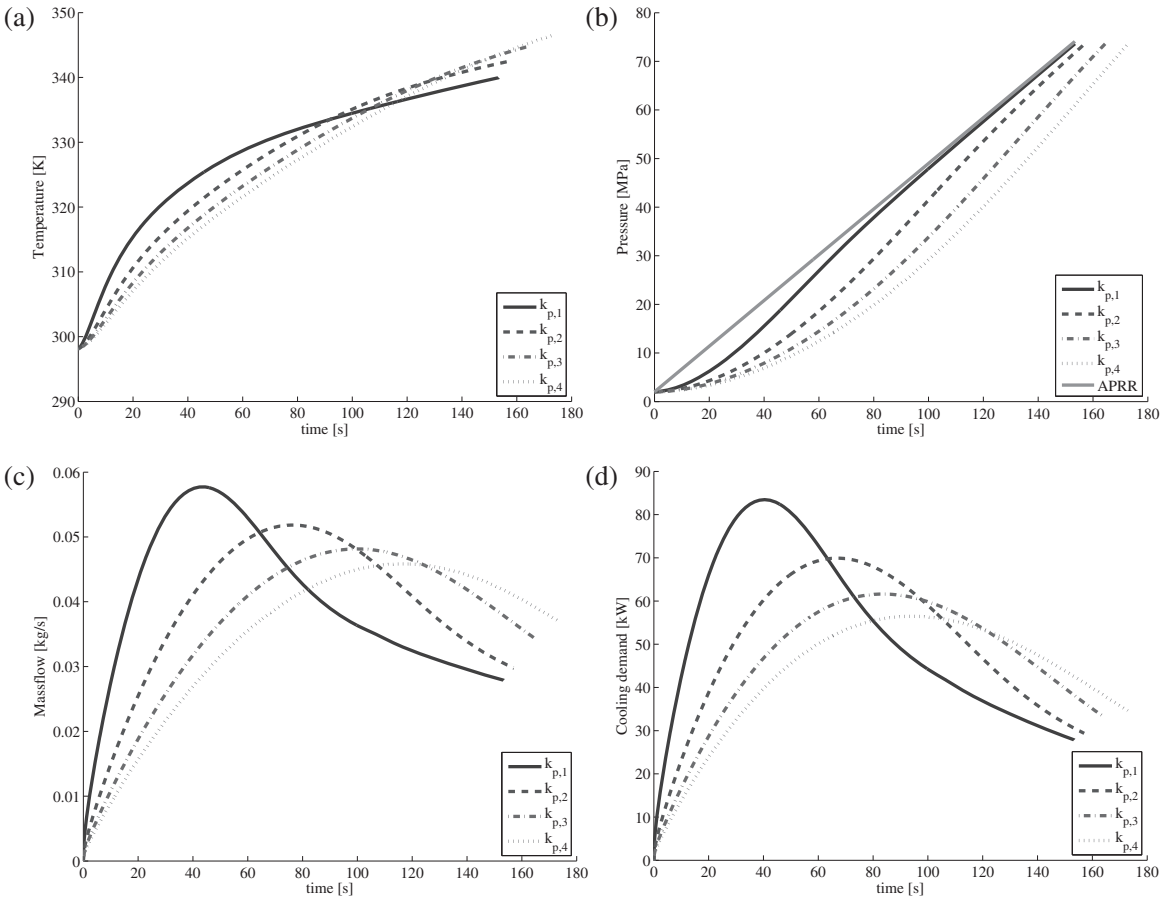

Fig. 5 – Effects of the pressure loss in the hydrogen storage system on the hydrogen refueling. (a) Higher k_p results in a larger temperature rise in the hydrogen storage system tank. (b) Higher k_p results in longer filling times before the pressure has reached the target pressure in the tank. (c) Higher k_p results in lower peak mass flow and the mass flow peaks later. (d) Higher k_p values results in lower peak cooling demand.

The thermodynamics of the cascade filling system can be observed in Fig. 7. Fig. 7 (b) shows the pressures in the system. The pressures out of the tanks at the hydrogen refueling station are lower for the two first tanks in the cascade filling, which naturally results in a lower pressure decrease across the reduction valve. Compared to Fig. 4 (b), it can be observed that the pressures after the reduction valve are the same for both a single tank and three tanks. Because the pressure difference between the tank at the hydrogen refueling station and the hydrogen storage system tank is lower, the heating up of the hydrogen due to the Joule-Thompson effect is lower (shown in Fig. 7 (a)). By comparing the pressures, temperatures and mass flows in the hydrogen storage system with the ones in Fig. 4, it can be observed that cascade filling has no effect on the hydrogen storage system, which proves the point from section 3.1 that the design of the hydrogen refueling station does not influence the hydrogen storage system. Fig. 7 generally shows cascade filling and its thermodynamics, demonstrating that multiple tanks lower the pressure losses and the heating up of the hydrogen without compromising the refueling of the tank in the hydrogen storage system.

Fig. 7 (c) shows the mass flow and cooling demand for the cascade filling. Compared to Fig. 4 (c), the size of the peak cooling demand is the same for both fillings, but peaks later for the cascade fueling than for the single tank filling, even though the mass flow is the same. The reason is that the pressure and temperature when shifting to the last tank in the cascade filling are higher at that time than for the single tank. The enthalpy is therefore higher, and a higher cooling demand is required.

3.4. *Optimization using cascade filling*

Replenishing the high-pressure tanks at the hydrogen refueling station is typical achieved using a booster drawing from low-pressure tanks at 20 MPa. Fig. 8 (a) and (b) show the two different scenarios.

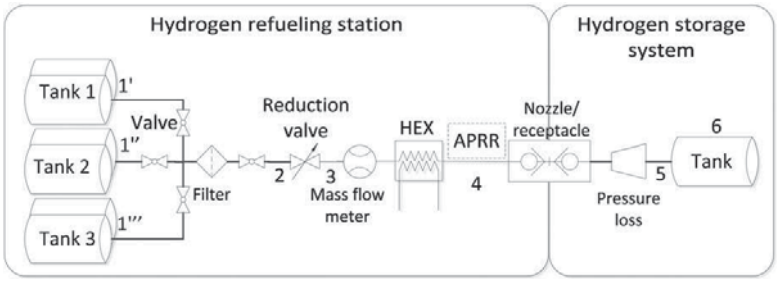

Fig. 6 – Cascade fueling station.

The replenishing of the tanks implies receiving the same mass as the refueling required, so the total mass filled back into the three tanks and the single tank are the same. The compared parameters are the energy consumption of the booster and the refueling time. The refueling of the tanks begins when the refueling of the vehicle has finished. The total volume of stored hydrogen is the same for both systems as 3 m^3 is distributed with 1 m^3 in each tank for the three tank system. Table 3 shows the differences in energy consumption of a booster (high-pressure compressor), the running time of the compressor and the cooling demand.

The total mass that needs to be stored to perform a 7-kg refueling of a vehicle is 138.85 kg in a single tank at 90 MPa or 112.3 kg distributed across three tanks of 45 MPa, 65 MPa and 91 MPa. Thus, the fueling only requires approximately 6 kg which means that the rest of the hydrogen only has the

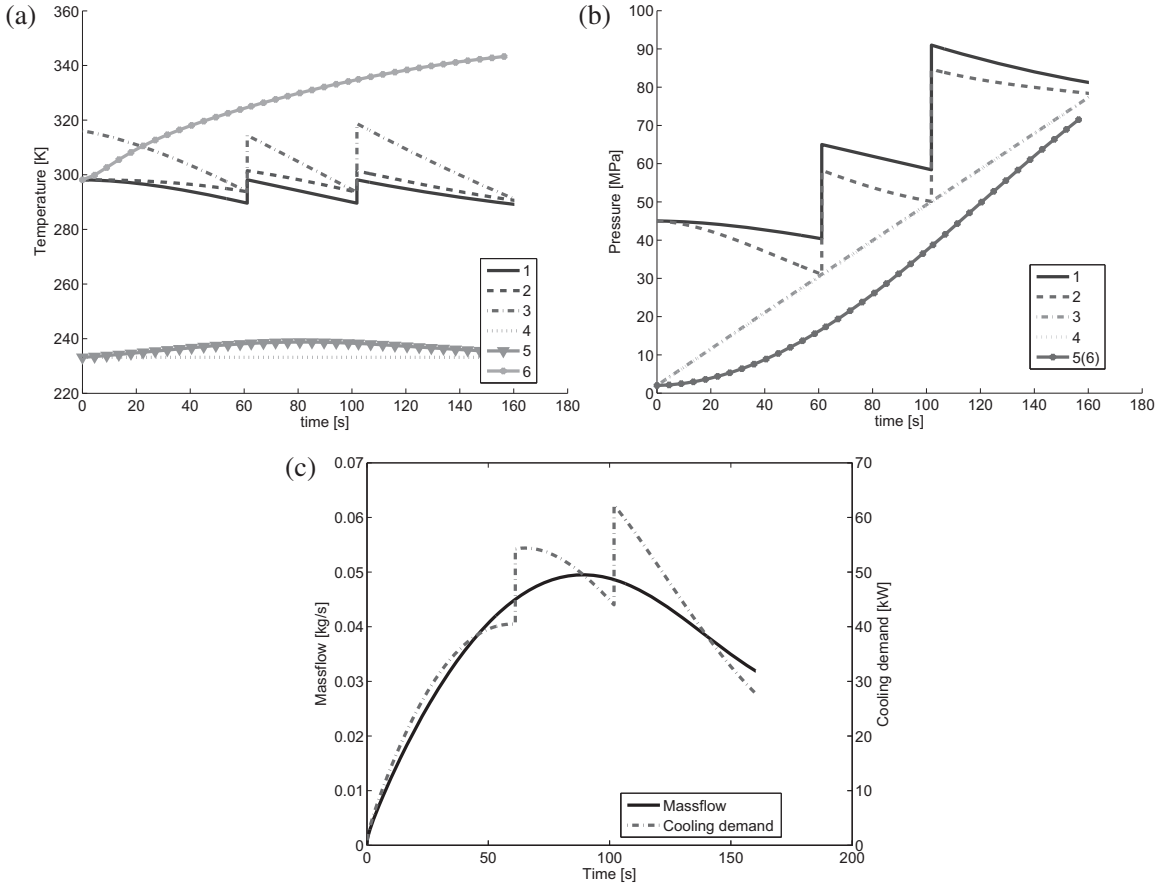

Fig. 7 – The thermodynamics of a cascade filling. (a) Temperature development. (b) Pressure development. (c) Mass flow and cooling demand.

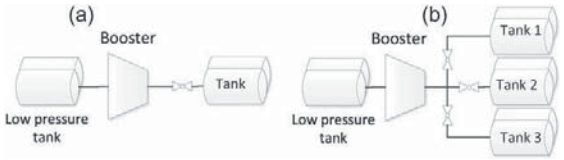

Fig. 8 – Sketch of the refueling set ups of the tanks at the hydrogen refueling station. (a) Refueling from low pressure tanks at the hydrogen refueling station to a single high pressure tank. (b) Refueling from low pressure tanks at the hydrogen refueling station to the three high pressure tanks.

Table 3 – Comparison between energy and time consumption.

	1 Tank	3 Tanks	Savings
Total mass [kg]	138.85	112.3	26.6
Power [kWh]	1.22	1.01	0.21
Time [s]	508	485	23
Total Cooling [kWh]	1.93	1.70	0.23
Peak cooling [kW]	61.7	65.1	−3.1

function of keeping the pressure up in the tanks and can therefore not be used for refueling. The savings in the total hydrogen mass between a single and three tanks at the hydrogen refueling station is 26.6 kg, approximately 20% of the total mass stored in the single tank system. The power needed to run the compressor for refueling the three tanks instead of a single tank is approximately 17% lower. The time difference for refueling a single tank or three tanks is 23s, corresponding to a 5% saving when refueling using the three tank system. The refrigeration facility is also influenced by the number of and pressure in the tanks at the hydrogen refueling station. Using three tanks gives a savings of 12% of the cooling capacity needed for the single tank system, though the peak cooling demand is approximately 5% higher using the cascade filling. From a cooling perspective, the lower total cooling capacity is notable. It is difficult to compare the peak cooling demand because this demand depends on the back pressure in the hydrogen storage system (as shown in Fig. 5 (d)) and therefore depends on the vehicle.

4. Conclusion

Dynamic models of the main components of a hydrogen refueling station and a vehicle storage system have been created using Dymola software. The models can be connected to simulate a complete hydrogen refueling station. The model has been used to show the thermodynamics of a simple system for refueling a vehicle. Pressure, temperature and mass flow have been analyzed, and it has been shown that the pressure loss in the hydrogen storage system has a significant impact on the hydrogen refueling process in terms of mass flow, cooling demand and storage dimensioning. The cooling demand is 35% lower for a high pressure loss hydrogen storage system than for a system with almost no pressure loss. The pressure losses and the design of the station do not influence refueling into the hydrogen storage system as long as the station fulfills the SAE TIR J2601. The differences between refueling from the single tank and three tanks designs at the hydrogen refueling station have been shown from a thermodynamic perspective. The time required for a whole cycle at the refueling station, i.e., refueling a vehicle and then refueling the high-pressure tanks at the hydrogen refueling station, is 5% lower under a cascade filling system. Furthermore, cascade filling used 12% less energy for cooling and 17% less energy for compression according to the given compressor equations. Additional components can be added to the model to simulate and predict a complete refueling event (e.g., heat transfer and pressure losses from the interconnecting tubing and components). The current model can be used for design optimization of hydrogen refueling stations.

Acknowledgments

The authors would like to thank the Danish Energy Agency for financial support and our industrial partner, H2Logic, for their collaboration and technical support.

Nomenclature

A	Area of tank, m^2
c	Specific heat capacity, J/(kgK)
e	Exergy, J/kg
g	Gravity, m/s^2
h	Enthalpy, J/kg
k	Conductivity, W/(mK)
k_v	Pressure loss constant, m^3/h
k_p	Pressure loss constant
$\dot{m}$	Mass flow rate, kg/s
M	Mass, kg
Nu	Nusselt number
P	Pressure, Pa
Q	Heat loss, J
R	Resistance, J/K
Ra	Rayleigh number
$\dot{s}$	Surface energy conversion, J
s	Entropy, J/kg
T	Temperature, K or °C
t	Time, s
U	Internal energy, J
V	Volume, m^3
x	Thickness, m

Greek

α	Heat transfer coefficient, $W/(m^2K)$
β	Thermal expansion coefficient, T^{-1}
μ	Dynamic viscosity, kg/(sm)
ρ	Density, kg/m^3

Subscript

0	Reference properties
a	Ambient

g	Gas
i	Node number
in	Into component
k	Conductivity
L	Total thickness
out	Out of component
P	Pressure
s	Solid
T	Temperature
w	Wall

Abbreviations

APRR	Average pressure ramp rate
SAE	Society of Automotive Engineers
SOC	State of charge
TIR	Technical information report

Appendix A. Input data used for the simulations.

Appendix A.1. Reference system

General settings	
APRR	28.2 MPa/min
T ambient	25 °C
P ambient	0.101 MPa
Hydrogen refueling station inputs	
V of tank	3 m^3
A of inside tank wall	4 m^2
α_g	150 W/(m^2K)
α_a	8 W/(m^2K)
x liner	0.003 m
x cfrp	0.022 m
P initial tank	90 Mpa
T initial tank	25 °C
k_v of valves	0.75 m^3/h
k_p of filter	100 m^3/h
k_p of mass flow meter	2.8 m^3/h
T heat exchanger	−40 °C
Hydrogen storage system inputs	
V of tank	0.173 m^3
A of inside tank wall	2 m^2
α_g	150 W/(m^2K)
α_a	8 W/(m^2K)
x liner	0.003 m
x cfrp	0.022 m
P initial	2 Mpa
P target	72 MPa

Appendix A.2. Cascade system

General settings	
APRR	28.2 MPa/min
T ambient	25 °C
P ambient	0.101 MPa
Hydrogen refueling station inputs	
Tank 1	
V of tank	1 m^3
A of inside tank wall	2 m^2
α_g	150 W/(m^2K)
α_a	8 W/(m^2K)
x liner	0.003 m
x cfrp	0.022 m
P initial tank	45 Mpa
Tank 2	
V of tank	1 m^3
A of inside tank wall	2 m^2
α_g	150 W/(m^2K)
α_a	8 W/(m^2K)
x liner	0.003 m
x cfrp	0.022 m
P initial tank	65 Mpa
Tank 3	
V of tank	1 m^3
A of inside tank wall	2 m^2
α_g	150 W/(m^2K)
α_a	8 W/(m^2K)
x liner	0.003 m
x cfrp	0.022 m
P initial tank	90 Mpa
Other values	
T initial tank	25 °C
k_v of valves	0.75 m^3/h
k_p of filter	100 m^3/h
k_p of mass flow meter	2.8 m^3/h
T heat exchanger	−40 °C
Hydrogen storage system inputs	
V of tank	0.173 m^3
A of inside tank wall	2 m^2
α_g	150 W/(m^2K)
α_a	8 W/(m^2K)
x liner	0.003 m
x cfrp	0.022 m
P initial	2 Mpa
P target	72 MPa
Low pressure tank	
V of tank	100 m^3
P initial	20 Mpa
T initial	25 °C

Appendix A.3. Compressor equation

Mass flow equation for the compressor. Made from experimental results delivered by the manufacture. The valid range is varying between an inlet pressure of 150–200 bar and an outlet pressure between 200 and 1000 bar.

$$\dot{m} = \frac{P_{out}}{10^4} \cdot \left(c1 - \frac{P_2 - P_{in}}{P_2 - P_1}(c1 - c2) \right) \cdot exp\left(\left(d1 - \frac{P_2 - P_{in}}{P_2 - P_1}(d1 - d2) \right) \right) \quad \text{(A1)}$$

Where $P_1 = 15 \cdot 10^6$ Pa and $P_1 = 20 \cdot 10^6$ Pa and the coefficients are $c1 = 0.013834957$, $c2 = 0.010681871$, $d1 = -0.000174506$ and $d2 = -0.000236707$.

REFERENCES

[1] Society of Automotive Engineers. Fueling protocols for light duty gaseous hydrogen surface vehicle. Technical information report J2601; 2010.

[2] Society of Automotive Engineers. Compressed hydrogen vehicle fueling connection devices. Technical information report J2600; 2008.
[3] Dicken CBJ, Mérida W. Measured effects of filling time and initial mass ont he temperature distribution within a hydrogen cylinder during refueling. J Power Sources 2006;165:324–36.
[4] Monde M, Woodfield P, Takano T, Kosaka M. Estimation of temperature change in practical hydrogen pressure tanks being filled at high pressure of 35 and 70 mpa. Int J Hydrogen Energy 2012;37:5723–34.
[5] Monde M, Mitsutake Y, Woodfield P, Maruyama S. Characteristics of heat transfer and temperature rise of hydrogen during rapid hydrogen filling at high pressure. Heat Transfer - Asian Res 2007;36:13–27.
[6] Woodfield P, Monde M, Takano T. Heat transfer charecteristics for practical hydrogen pressure vessels being filled at high pressure. J Therm Sci Tech-JPN 2008;3:214–53.
[7] Woodfield P, Monde M, Mitsutake Y. Measurement of averaged heat transfer coefficient in high-pressure vessel during charging with hydrogen nitrogen and argon gas. J Therm Sci Tech-JPN 2007;2:180–91.
[8] Hosseini M, Dincer I, Naterer GF, Rosen MA. Thermodynamic analysis of filling compressed gaseous hydrogen storage tanks. Int J Hydrogen Energy 2012;37:5063–71.
[9] Kim SC, Lee SH, Yoon KB. Thermal characteristics during hydrogen fueling process of type 4 cylinder. Int J Hydrogen Energy 2010;35:6830–5.
[10] Zhao L, Liu Y, Yang J, Zhao Y, Zheng J, Bie H, et al. Numerical simulation of temperature rise within hydrogen vehicle cylinder during refueling. Int J Hydrogen Energy 2010;35: 8092–100.
[11] Galassi C, Baraldi D, Iborra BA, Moretto P. CFD analysis of fast filling scenarios for 70 mpa hydrogen type 4 tanks. Int J Hydrogen Energy 2012;37:6886–92.
[12] Kaern MR. Analysis of flow maldistribution in fin-and-tube evaporators. Ph.D. thesis, The Technical University of Denmark; 2011. DCAMM special report no. S132.
[13] Kaviany M. Principles of heat transfer. 1 ed. New York: John Wiley & Sons; 2002. p. 294–6.
[14] Daney DE. Turbulent natural convection of liquid deuterium hydrogen and nitrogen within enclosed vessels. Int J Heat Mass Tran 1976;19:431–41.

Appendix E

Paper II

Erasmus Rothuizen, Masoud Rokni

Optimization of the overall energy consumption in cascade fueling stations for hydrogen vehicles

Submitted to: *International Journal of Hydrogen.* (2013)

INTERNATIONAL JOURNAL OF HYDROGEN ENERGY 39 (2014) 582–592

Available online at www.sciencedirect.com

ScienceDirect

journal homepage: www.elsevier.com/locate/he

Optimization of the overall energy consumption in cascade fueling stations for hydrogen vehicles

*E. Rothuizen**, *M. Rokni*

Section for Thermal Energy Systems, The Technical University of Denmark, 2800 Kgs. Lyngby, Denmark

ARTICLE INFO

Article history:
Received 6 September 2013
Accepted 13 October 2013
Available online 9 November 2013

Keywords:
Hydrogen refueling
Energy consumption
Optimization
Dimensioning
Dynamic simulation

ABSTRACT

Hydrogen fueling stations are emerging around and in larger cities in Europe and United States together with a number of hydrogen vehicles. The most stations comply with the refueling protocol made by society of automotive engineers and they use a cascade fueling system on-site for filling the vehicles. The cascade system at the station has to be refueled as the tank sizes are limited by the high pressures. The process of filling a vehicle and afterward bringing the tanks in refueling station back to same pressures, are called a complete refueling cycle. This study analyzes power consumption of refueling stations as a function of number of tanks, volume of the tanks and the pressure in the tanks. This is done for a complete refueling cycle. It is found that the energy consumption decreases with the number of tanks approaching an exponential function. The compressor accounts for app. 50% of the energy consumption. Going from one tank to three tanks gives an energy saving of app. 30%. Adding more than four tanks the energy saving per extra added tank is less than 4%. The optimal numbers of tanks in the cascade system are three or four.

1. Introduction

Hydrogen refueling stations are emerging in and around the larger cities in Europe and The United States. The investors in Europe are primarily municipals or public funding who buys the stations to run with a set of hydrogen vehicles in the municipal service department. The latest example is Copenhagen municipality who bought a H2Logic 700 bar station to run with 15 Hyundai hydrogen vehicles. The reason to spend such huge investment was to promote hydrogen in the transport sector. In order for the public to accept hydrogen vehicles they need to be introduced into the market at platforms where they are highly visible and people slowly get used to the idea and the sight of them. Even though many stations are bought by municipalities to use with a number of hydrogen vehicles, the stations are often public and placed like any other common petrol station with public access. The new stations follows the protocol from society of automotive engineers for high speed hydrogen refueling within the safety limits of the storage tank in the vehicle, SAE J2601 [1]. In addition, the society of automotive engineers has made a protocol for an on-board vehicle system, SAE J2600 [2]. The two protocols allows the vehicle manufactures to build vehicles which can be refueled at any station and station manufactures to build station that can refuel any vehicle, as long as both complies with SAE J2600 and SAE J2601. The two protocols are developed in close cooperation with both vehicle and refueling station manufactures in order to secure a high implementation rate from the start. This is seen as the same vehicles are used in demonstrations worldwide with different refueling stations. The refueling procedure of vehicles is stated in the protocol, where the stated parameters are the

* *Corresponding author*. Tel.: +45 4525 4329; fax: +45 4588 4325.
E-mail address: edro@mek.dtu.dk (E. Rothuizen).
0360-3199/$ – see front matter
http://dx.doi.org/10.1016/j.ijhydene.2013.10.066

outlet temperature, the pressure ramp rate and the final pressure at which the refueling should end. These conditions depend on the ambient conditions and the type of tank in the vehicle. The protocol does not dictate or suggest how to reach the outlet conditions of the refueling station or what should happen after the refueling. Therefore the different hydrogen refueling station manufactures have different station designs. Though there are some similarities in the design of the refueling stations. First, they all cool the hydrogen before the exit. Second, the refueling is done using a cascade tank setup at the station. The cascade system consist of two to four different pressure levels, with the lowest starting from 350–500 bar the medium 500–700 bar and the highest typically above 900 bar. Third, there is a low pressure hydrogen bank at the station, 200–350 bar that can be used for recovering of the tanks in the cascade system. The pressures are typically chosen by the physical limitations of the tanks and the price. The high pressure tanks usually have a smaller volume than the low pressure tanks and a larger price tag. It is therefore beneficial with small high pressure tanks from an investment cost perspective, but the energy consumption of refueling the tanks in the cascade system is not known. The refueling of the cascade system at the refueling station is done using compressors. Different types of compressors used in the system are reciprocating compressors which also is the most common one, as well as ionic liquid compressors and membrane compressors. They are typically compressing in two or more stages and the hydrogen needs to be cooled down during, or after the compression. The whole process of refueling a vehicle and afterward bringing the used tanks in the cascade system back to starting pressure for a new refueling, is referred to as a complete refueling cycle. A complete refueling cycle is yet unexplored with regards to deciding number of tanks in the cascade system and the pressure and sizes of them. Farzaneh-Gord et al. have done research in entropy generation and entropy optimization between using on buffer tank and a three tank cascade system and found that a cascade fueling had the least exergy destruction but it also had the longest fueling time [3]. Hosseini et al. have done a similar exergy analysis of using one buffer tank for refueling compared to a cascade system, they also concluded that the cascade system had the least exergy destruction [4]. This paper considers the trade-off between number of tanks, sizes of the tanks and the pressure levels in the tanks, from an energy consumption point of view. It includes the total energy consumption from all the major components in a refueling station, the compressor and the refrigeration facilities. The thermodynamic model used for simulation of the refuelings uses first law equations and the tanks are modeled accounting for heat loss. The hydrogen gas is considered as a real gas and the compression is adiabatic, giving the worst case scenario with regards to the temperature development of hydrogen due to the compression.

2. Theory

The following section describes the theory used for the model of a hydrogen refueling station. The section consist of four parts; Governing equations for the tanks, governing equations for isotropic adiabatic compression, heat transfer and pressure loss equations and at the end a model description. The theory which is different from the previous paper on "Optimization of hydrogen vehicle refueling via dynamic simulation" [5] is mainly the two first parts about the tank and the compression. The third part covers; heat transfer equations, pressure loss equations and calculation of cooling demand.

2.1. Governing equation for the tanks

Moving hydrogen from a low pressure tank to a higher pressure requires mechanical work which in this case is a piston compressor. Further two tanks in which the hydrogen is stored needs to be present. The system can be split up into three main components; the compressor, the tank at the suction side and the tank at the discharge side. For deciding the properties inside the tanks during a complete cycle, both discharging and charging, the energy balance is done using first law analysis and using the equations for enthalpy instead of internal energy. This is necessary for the model to be able to both discharge and charge the tank within the same simulation. The energy balance in terms of internal energy for the tanks is:

$$\frac{dU}{dt} = h\frac{dm}{dt} + \frac{dQ}{dt} \tag{1}$$

where dU/dt is the change in internal energy, h is the enthalpy, dm/dt is the change in mass and dQ/dt is the heat rate entering or leaving the tank. The internal energy is $U = H - pV$ which is the enthalpy (H), the pressure (p) and the volume (V). Rewriting and substituting internal energy with enthalpy into eq. (1) gives:

$$\frac{dh}{dt} = \frac{1}{M}\cdot\left(h_{out}\cdot\dot{m} - h\cdot\dot{m} + V*\frac{dP}{dt} + \frac{dQ}{dt}\right) \tag{2}$$

This gives the energy balance expressed through change in enthalpy. The mass flow is expressed through the change in density in the volume, eq. (3).

$$\frac{dm}{dt} = \frac{d\rho}{dt}*V \tag{3}$$

where $d\rho/dt$ is expressed through differentials of enthalpy and pressure [6].

$$\frac{d\rho}{dt} = \left.\frac{\partial\rho}{dP}\right|_h\cdot\frac{dP}{dt} + \left.\frac{\partial\rho}{dh}\right|_p\cdot\frac{dh}{dt} \tag{4}$$

The total mass in the system can be found from

$$M = V\cdot\rho \tag{5}$$

For an adiabatic thermodynamic model of a tank which describes the energy change through enthalpy, eqs. (2)–(5) are needed to be in present. The heat leaving or entering the tank is not necessary, but it is of importance as it influences the properties of the hydrogen in the tank. A more detailed model with the heat transfer is thus preferred. For the system to be dynamic a controlling equation describing the flows between the tanks should also be present. The controlling equation can either be a function of mass flow change or pressure change.

$$\frac{dP}{dt} = f(P) \tag{6}$$

$$\frac{dm}{dt} = g(\dot{m}) \tag{7}$$

For hydrogen refueling systems following the protocol SAE J2601 the mass flow rate to the vehicle tank is described through a pressure ramp rate found from the tables of SAE J2601, eq. (6) must therefore be used. The mass flow from the compressor is described through a mass flow equation, hence eq. (7).

2.2. Governing equations for an isotropic adiabatic compressor

The mass flow of the compressor is calculated defining the volume of the cylinders (V_{cyl}), piston strokes pr. second (n) and a defined function for the volumetric efficiency η_v.

$$\dot{m} = V_{cyl} \cdot \rho_{in} \cdot \eta_v \cdot n \tag{8}$$

The volumetric efficiency is highest at a low pressure ratio in the compressor and decreases almost proportionally as the pressure ratio increases. For this model the volumetric efficiency has the highest possible efficiency of 90% and is decreasing with 5% pr. pressure ratio. The energy balance of the compressor is the energy flow into the compressor, the energy flow out of the compressor and the work added in the compressor.

$$\dot{m} \cdot h_{in} - \dot{m} \cdot h_{out} + W = 0 \tag{9}$$

The enthalpy out of the compressor is found using the isentropic efficiency. The compressor is assumed to be a reciprocating compressor where an estimate of the isentropic efficiency can be found using eq. (10) [7]:

$$\eta_{is} = 0.1091 \cdot \log\left(\frac{P_{out}}{P_{in}}\right)^3 - 0.5247 \cdot \log\left(\frac{P_{out}}{P_{in}}\right)^2 + 0.8577 \cdot \log\left(\frac{P_{out}}{P_{in}}\right) + 0.3727 \tag{10}$$

where P_{in} is the suction pressure and P_{out} is the discharge pressure. Equation (10) is valid in the range $1.1 < P_{out}/P_{in} < 5$. The enthalpy at the discharge of the compressor found by eq. (11)

$$h_{out} = \frac{h_{out,is} - h_{in}}{\eta_{is}} - h_{in} \tag{11}$$

For simulating the refueling of the tanks at the station, the outlet temperature of the compressor is important as temperatures over 85 °C should be avoided for safety reasons. The temperature out of the compressor is found using state equations were $T(p,h)$. Is has been assumed that there is no heat loss from the compressor as this is a worst case scenario of the energy transferred to the hydrogen during compression.

2.3. Other components

The equations for the other components used in the model can be found in Tables 1 and 2. The equations have partly been described in Ref. [5]. Some new equation for calculation of pressure loss have been added, though they are general equations which can be found in any teaching book and has no critical influence on the model, therefore they are only shown in Table 2.

2.3.1. Heat transfer

The heat transfer equations are explained in detail by Kaviany [8], the equations is listed in Table 1 and cited to original literature. The flow inside the cylinder does not correspond to the flow through a tube because when the hydrogen hits the back wall it bounces backwards again, to find the heat transfer coefficient in such cases a CFD model can be created or experimental data can be used. Dicken and Mrida [12] carried out the first test on temperature development inside a cylinder and compared the results with CFD calculations. It was shown that a uniform temperature distribution could be assumed. In this study the heat transfer coefficient used for charging a tank, has been determined experimentally by Monde and Woodfield [9].

2.3.2. Pressure losses

The pressure loss equations used in the model can be seen in Table 2.

The new pressure loss model of a tube is standard equations for calculating pressure loss at turbulent flow through a tube.

Table 1 – Equations for heat transfer.

Model	Reference	Equations	
Heat Transfer differential equation	[8]	$Q_i = (\rho \cdot c\Delta V)_i \cdot \frac{dT_i}{dt}$	(12)
Energy balance	[8]	$Q_i = Q_{i-1} + Q_{i+1}$	(13)
		$Q_{i-1} = \frac{T_i - T_{i-1}}{R_{i-1}}$	(14)
		$Q_{i+1} = \frac{T_i - T_{i+1}}{R_{i+1}}$	(15)
Boundary conditions	[5]	$\left.\frac{dT_i}{dx}\right\|_{x=0} = \frac{\alpha_g}{k}(T_g - T_i\|_{x=0})$	(16)
		$\left.\frac{dT_i}{dx}\right\|_{x=L} = \frac{\alpha_a}{k}(T_i\|_{x=L} - T_a)$	(17)
Charging heat transfer coefficient	[9,10]	$150 - 500\frac{W}{m^2\,K}$	(18)
Discharging heat transfer coefficient	[11]	$\alpha = \frac{Nu \cdot k}{d}$	(19)
Nusselt's number	[11]	$Nu = 0.104Ra^{0.352}$	(20)
Rayleigh's number	[11]	$Ra = \frac{g\beta d^3 c_p \rho^2 (T_w - T_g)}{\mu k}$	(21)

Table 2 – Equations for pressure losses.

Model	Reference	Equations
Valves	[13]	$P_{out} = P_{in} - \rho \cdot \left(\frac{k_v}{\dot{V} * 3600}\right)^{-2} * \rho_{water}^{-1}$ (22)
Filter and Mass flow meter	[14]	$\Delta P = 0.5 k_p \rho \left(\frac{\dot{m}}{A\rho}\right)^2$ (23)
Tubing	[15]	$\Delta P = f \frac{L}{d} \frac{\rho v^2}{2}$ (24)
Friction factor	[15]	$f = \left(-1.8 \log\left(\left(\frac{6.9}{Re}\right) + \left(\frac{3.7r}{d}\right)^{1.11}\right)\right)^{-2}$ (25)
Reynolds number	[15]	$Re = \frac{\rho v d}{\mu}$ (26)

2.3.3. *Cooling demand*

The cooling demand in the model is calculated using the energy balance in the heat exchanger.

$$Q = \Delta h \dot{m} \tag{27}$$

where Q is the cooling demand, Δh the enthalpy difference and $\dot{m}$ the mass flow. The energy consumption which the refrigeration facility requires to deliver the cooling demand is found from:

$$W = \frac{Q}{COP} \tag{28}$$

where *COP* is the coefficient of performance for the refrigeration facility; power to cooling ratio.

2.4. *Software used for model*

The model has been implemented into the software Dymola, which is an extension of the free simulation software Modelica. The programming language is unified object-oriented for physical modeling and the approach is non casual and it uses true ordinary differential equations and algebraic equations. The software is capable of solving large dynamic complex systems using the build in solvers.

2.5. *Changes made in the model*

To analyze the energy consumption a thermodynamic model has been made in Dymola. A similar model has been used to show the thermodynamic properties of hydrogen refueling and how the pressure losses in the system affect the refueling [5]. The new model enables the possibility to mix streams. It improved and accounts for more generalized compressor equations of a piston compressor as well as improved pressure loss equations enabling a more precise pressure loss calculation that can be related to industrial pressure loss values for the component. Further the model is able to have reverse and zero mass flow in any part of the system while other parts are running simultaneously. These changes enable the possibility to do a vehicle refueling while the compressor is running and when the refueling has finished the refueling part can be "shut down" while the compressor refuels the tanks in the cascade system through the same tubing as the refueling was using.

2.6. *Hydrogen refueling system description*

The model used for simulation of hydrogen refueling complies with the protocol by Society of Automotive Engineers, TIR J2601. The refueling system that is modeled is shown in Fig. 1. The system is separated into two main sections, the refueling station and the hydrogen vehicle. The hydrogen refueling station is divided into two, the refueling system used for refueling the vehicle and the compressor system used to refuel the tanks at the station. The main refueling system consists of a number of high pressure tanks setup in a cascade system for refueling the vehicle and the components used to assure the refueling comply with J2601. The compressor system consists of a medium pressure bank of tanks, a compressor and a heat exchanger that removes the heat after the compression. A short walk through of a refueling follows here. The vehicle pulls up to the station and is connected at the nozzle. The refueling station measures the pressure of the hydrogen in the vehicle before it sends in a pulse were the mass is known, the pressure in the vehicle is measured again, by knowing the pressure rise and the mass which was in the pulse, the size of the tank can be decided. The pressure in the tank and the ambient temperature is then used to set the average pressure ramp rate that is to be used for the refueling. The volume of the tank indicates how much the reduction valve should be opened when the refueling starts. The system now opens for tank 1 and let the hydrogen flow to the vehicle tank. At the same time the compressor starts up and deliver hydrogen to the stream going from tank 1 to the vehicle, if the mass flow from the compressor is larger than needed for the refueling, then the excess hydrogen is stored in the tank.

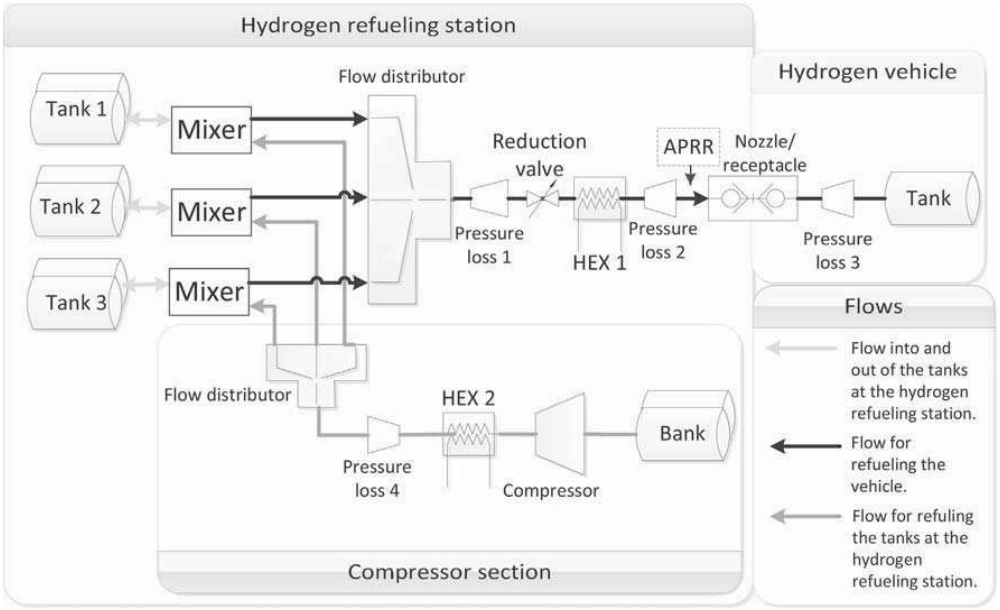

Fig. 1 – Sketch of a hydrogen refueling station with three tanks in a cascade setup and a compressor section to refuel the station.

When the pressure across the reduction valve reaches a certain limit, the station changes to tank 2 which is at higher pressure than tank 1 and the refueling continues. The compressor fills tank 1 back to starting mass/pressure before it start filling tank 2. When the pressure in tank 2 becomes to low to keep up the average pressure ramp rate the station changes to tank 3 which is at a higher pressure than tank 2. When the outlet of the station reaches the final pressure, the refueling of the vehicle is aborted. The compressor keeps running until all the tanks at the station are back to starting mass/pressure. The process of refueling the vehicle and bringing the tanks at the station back to starting pressure, is referred to as; a complete refueling cycle. As one may have noticed the pressure losses in the systems are collected at four different strategically selected places. There is a pressure loss before the reduction valve (pressure loss 1) which takes into account tubing and valves together. This pressure loss influences the pressure into the reduction valve and thereby when to change the tank in the cascade system. Decreasing the pressure loss before the reduction valve increases the time before shifting from the first tank. The second pressure loss (pressure loss 2) is between the reduction valve and the average pressure ramp rate (APRR). This takes into account the pressure loss in the heat exchanger and some valves. This is also the pressure loss the reduction valve needs to adjust for in order to have the average pressure ramp rate at the nozzle. The third pressure loss (pressure loss 3) is the pressure loss in the vehicle. Pressure loss 3 influences the mass flow of the refueling; low pressure loss gives an earlier and higher peak in mass flow. When increasing the pressure loss in the vehicle the peak mass flow rate is decreased and will peak later in the refueling. This has a large influence on the station as an early mass flow peak results in more mass is drawn from the tanks at lower pressures and with a late mass flow peak more mass is drawn from the tanks with higher pressure. The last pressure loss (pressure loss 4) accounts for the pressure losses between the compressor and the mixer. The compressor has to make up such loss while delivering hydrogen. The mixers are ideal mixers where the flow from the compressor is mixed with the mass flow for the refueling of the vehicle. The flow distributor controls the flow, only one flow can pass through at a time. The heat exchanger at the outlet of the refueling system cools the hydrogen to the desired temperature set by the fueling protocol J2601. The heat exchanger after the compressor cools the hydrogen to the same temperature as ambient. For the model the station can have up to 8 tanks in the cascade system. The extra tanks are connected like tank 1, 2, and 3 in Fig. 1.

3. Analysis and discussion

The following section presents and discusses the results obtained from the energy optimization of the cascade system at the hydrogen refueling station. Table 3 contains the volumes used for the tanks and Table 4 contains the pressures used. For the parameter variation of the tank sizes and pressures, the given volumes and pressures are the ones at which it was not possible to go further down in volume or pressure.

3.1. *Simulation comparisons*

The three different scenarios that are compared in this section are; first, the effect of adding more tanks to the cascade

Table 3 – Volumes of the tanks.

Number of tanks at station	Scenario	Tank 1 (m^3)	Tank 2 (m^3)	Tank 3 (m^3)	Tank 4 (m^3)	Tank 5 (m^3)	Tank 6 (m^3)	Tank 7 (m^3)	Tank 8 (m^3)
1	1,3	1							
	2	1							
2	1,3	1	1						
	2	1	0.75						
3	1,3	1	1	1					
	2	1	0.75	0.50					
4	1,3	1	1	1	1				
	2	1	1	0.75	0.5				
5	1,3	1	1	1	1	1			
	2	1	1	0.75	0.25	0.25			
6	1,3	1	1	1	1	1	1		
	2	1	0.50	0.25	0.25	0.25	0.25		
7	1,3	1	1	1	1	1	1	1	
	2	0.25	0.25	0.25	0.25	0.25	0.25	0.25	
8	1,3	1	1	1	1	1	1	1	1
	2	0.25	0.25	0.25	0.25	0.25	0.25	0.25	0.25

system at the station is analyzed. This is done for both the maximum allowed pressure loss in the vehicle and for a low pressure loss in the vehicle. Second, the volume of the tanks is changed decreasing the volume as the pressure increases. Third, a variation of the pressures in the tanks is done by lowering the pressures to a minimum in order for the refueling to take place. The first parameter variation shows the effect of adding another tank to the cascade system, the second parameter variation shows the effect of decreasing the volume of the tanks and the third parameter variation shows the gain by having the minimum required pressures in the tanks. The trade-off between power consumption, tank size and tank pressures are interesting both from an energy point of view, but also from an economical point of view as the investment cost of the tanks increases with increasing volume and pressure. Though, it is up to the manufacture to judge where the best trade of is between energy consumption and investment costs of tanks. This paper shows the trends and can therefore not be used as a final dimension of refueling stations to be used for manufacturing. The pressures and sizes reached in this paper are specific for the pressure losses used at this particular station and all other stations should be evaluated individually to find the best tank size/pressure setup. Though the energy savings should be of the same magnitude, for all stations with a similar layout. When adding more tanks to the refueling station the volume of each tank is 1 m^3 and the pressures are as follows, when only 1 tank is present it is 950 bars for two tanks it is 400 and 900 bars and for more than two tanks the pressure is distributed in between 400 and 900 bars with equal pressure rise between each tank, this is shown i Table 4. The parameter variation of the tank sizes allows 4 different sizes to be used 0.25 m^3, 0.50 m^3, 0.75 m^3 and 1 m^3. The variation is done by decreasing the tank volumes to a minimum starting with the highest pressure tank, then

Table 4 – The pressures used for the comparisons.

Number of tanks at station	Scenario	Tank 1 (bar)	Tank 2 (bar)	Tank 3 (bar)	Tank 4 (bar)	Tank 5 (bar)	Tank 6 (bar)	Tank 7 (bar)	Tank 8 (bar)
1	1,2	950							
	3	925							
2	1,2	400	950						
	3	550	925						
3	1,2	400	675	950					
	3	350	650	875					
4	1,2	400	583	767	950				
	3	350	551	712	840				
5	1,2	400	538	675	813	950			
	3	350	503	630	737	825			
6	1,2	400	510	620	730	840	950		
	3	350	475	582	674	753	820		
7	1,2	400	492	583	675	767	858	950	
	3	350	455	548	629	699	761	815	
8	1,2	400	479	557	635	714	793	871	950
	3	350	441	522	594	658	715	765	810

moving down gradually decreasing the volumes until the refueling of the vehicle just succeeds, the final volumes can be seen in Table 3. The third parameter variation with constant volume of the tanks of 1 m^3 allows the pressures to be set between 350 and 950 bars. The main constrain is that the pressure when the refueling of the vehicle is finished is between 10 and 20 bars across the reduction valve. Further all the tanks in the cascade system have to be used. The pressures for this variation were tested both using the same pressure difference between each tank and then with the same pressure ratio between each tank in the cascade system instead. By having the same pressure ratio, a decrease in pressure difference between each tank step in the cascade system can be provided. It was found that using the same pressure ratio between tanks next to each other, gave the lowest energy consumption. Therefore all results shown here are with the equal pressure ratio.

3.1.1. *Other system assumptions*

The hydrogen fueling station considered is for refueling of hydrogen vehicles without communication. The pressure loss in the vehicle is the highest allowed which peaks at 200 bars during the refueling. This pressure loss gives the most demanding refueling of the vehicle for the station in terms of pressures and sizes of the tanks. Using a lower pressure loss will fill a larger mass to the vehicle, but the mass flow will peak earlier and be lower towards the end of the refueling. This result in more mass is drawn in the beginning of the refueling, from the tanks at lower stages in the cascade system. Thereby does the high pressure tank get a lower demand and decrease less in pressure, hence less mass is drawn from them. It means that if the station is able to fulfill this refueling of a vehicle with high pressure loss it can also satisfy all refueling; this will be explained further in Section 3.2. The two heat exchangers in the system are connected to a refrigeration facility, which for the heat exchanger after the compressor (HEX2) has a $COP = 2$ and after the reduction valve (HEX1) has a $COP = 1.5$. The compressor has a peak mass flow capacity of 0.015 kg/s, which is obtained when the pressure ratio are close to one. The peak mass flow corresponds to the largest hydrogen compressors which is present available.

3.2. *General thermodynamics of the system*

To explain the properties of the system further, a complete cycle for a three tanks cascade refueling station is used as example. Fig. 2 shows the mass flows for a refueling with a high pressure loss (HPL) and for a low pressure loss (LPL) refueling. It is clear that the mass flow peak later when a large pressure loss is present in the vehicle. Further the total mass refueled is less with a high pressure loss than with a low pressure loss, this is because the refueling finishes when the pressure at the outlet of the station reaches a certain value. Therefore the pressure is higher in the tanks when the pressure loss in the vehicle is lower. The mass flow through the compressor decreases as it shifts tank to refuel. For the station to recover after refueling a low pressure loss vehicle it takes longer time as more mass has been fueled to the vehicle. It may seems contradictory to consider the high pressure loss refueling as more mass is refueled with low pressure loss, but

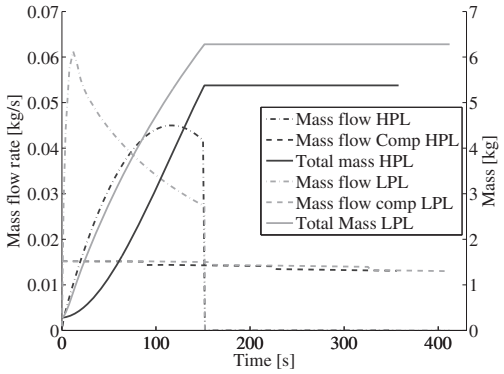

Fig. 2 – The mass flows and total mass for a refueling of a vehicle with both low pressure loss (LPL) and high pressure loss (HPL).

when considering the pressures in the tanks at the station, it becomes clear why the higher pressure loss refueling is of larger importance. Fig. 3 shows the pressures in the system at the reduction valve, out of the compressor and at the nozzle (the average pressure ramp rate). The pressures into the reduction valve have two changes in pressure (the steep lines), which is due to change of tank in the cascade system. Considering the pressure into the reduction valve, the low pressure tank in the cascade system finishes at lower pressure for refueling a low pressure loss vehicle compared to a high pressure loss vehicle. A lower finishing pressure means that more mass has been drawn from the low pressure tank in the cascade system. It therefore changes earlier to the second tank in the cascade system. The medium pressure tank delivers approximately the same amount of mass as they end at the same pressure, Fig. 3. The high pressure in the cascade system ends at a higher pressure for the low pressure loss vehicle refueling than for the high pressure loss vehicle refueling. This shows that less mass has been drawn from the higher pressure for a low pressure loss vehicle refueling than for a higher pressure loss vehicle refueling. When deciding the

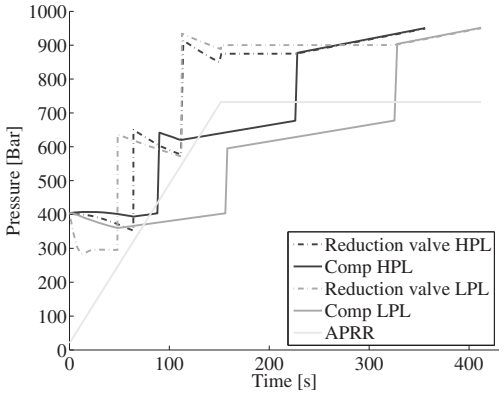

Fig. 3 – The pressures for a refueling of a vehicle with both low pressure loss (LPL) and high pressure loss (HPL).

INTERNATIONAL JOURNAL OF HYDROGEN ENERGY 39 (2014) 582–592

pressures in the tanks at the refueling station, it is most energy efficient if the pressure into the reduction valve is close to the outlet of the reduction valve when the fueling finishes, hence the compressor has not used work to compress hydrogen to a higher pressure than necessary. Fig. 4 shows the pressure losses in the system shown in Fig. 1. The pressure loss; pressure loss 3 HPL is uses the second y-axes in Fig. 4. The suddenly changes in pressure loss 2 is due to change of tank at the station for the refueling. After 152 s the only place there is a pressure loss, is between the compressor and the tank it is refueling, as the refueling of the vehicle has finished. The refueling in Fig. 3 is therefore not the most energy effective, because there are more than 100 bars differences between the reduction valve, the average pressure ramp rate and the pressure loss between the reduction valve and the nozzle is only 17 bars.

3.3. *Results*

The first simulation has a constant volume of the tanks of 1 m^3 and a variation of number of tanks is done from 1 to 8 tanks. This is the reference case for further comparisons with variable tanks size and with variable pressure. The energy consumption of a complete cycle is shown in Fig. 5(a) for a refueling done to a vehicle with a low pressure loss and a high pressure loss. The energy consumption is decreasing approaching an exponential function as one more tanks is added to the refueling station. It is clear that using a cascade system compared to one tank is favorable from an energy consumption point of view. The hydrogen which is fueled to the vehicle has an energy content of approximately 240 kWh and the largest amount of energy used for a full cycle with a high pressure loss vehicle is 5.97 kWh, which is 2.5% of the energy fueled. Fig. 5(a) also shows that the energy consumption for a complete refueling cycle with a low pressure loss vehicle changes from being more energy consuming at 3 tanks to being less at 4 tanks. This fact proofs the point that even though more mass is fueled, it is taken from the lower pressure tanks. The distribution of the energy consumption between the components is shown in Fig. 5(b). The compressor account for more than 50% and the refrigeration facility for

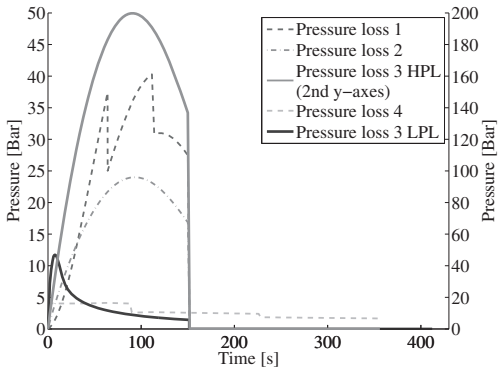

Fig. 4 – The pressure losses for a refueling of a vehicle with high pressure loss (HPL) and the pressure loss for a vehicle with low pressure loss (LPL).

the heat exchanger after the compressor for approximately 30%, the lowest energy consumption is for the cooling of the hydrogen at the exit of the station accounting for approximately 20%. Fig. 6 shows the energy saving when adding more tanks to the cascade system, the savings are showed for each component and the total saving. The saving from going from one to two tanks is 18% and the saving for the compressor which accounts for more than 50% of the total energy used is 20%. The energy savings by adding another tank to the cascade system are approaching exponential. Fig. 6 shows that the energy saving is significant until three tanks are present in the cascade system. From four to five tanks the saving is app. 5% and after going from four to five tanks the energy saving by adding an extra tank is less than 3% for each additional tank. It should be noted that for the cascade system using 6, 7 and 8 tanks, the high pressure tank of 950 bars were not in use for the vehicle refueling, as the other tanks could satisfy the demand. This will be examined further when studying the effect of reducing the tank sizes and changing the pressures so that the pressure difference in the cascade system does not necessarily has even pressure difference between them. Decreasing the sizes of the tanks will have an effect on the energy consumption of the refueling. First, by lowering the volume the final pressure in the tanks will be lowered after having refueled the vehicle; this gives a lower pressure ratio for the compressor at the beginning of refueling the cascade system. Second, by decreasing the volume of the tanks and thereby decreasing the pressure faster during refueling of a vehicle, the cascade system will change tank in earlier stage. This results in that more mass is taken from the higher pressure tanks, which increases the energy consumption when the compressor has to refuel the station. The minimum size of tanks which can be obtained with the given pressures can be seen in Table 3. For four and five tanks, the second tank has to be 1 m^3 which might seem strange comparing to 3 tanks where the medium tank is 0.75 m^3, but that is because the pressure is lower in the medium range tank compared to 3 tanks and the high pressure tanks are smaller, see Tables 3 and 4. Fig. 7 shows the energy saving compared to the corresponding system with 1 m^3 tanks. For cascade systems up to 5 tanks the energy saving is between 1% and 2.7%, when having more than 5 tanks in the cascade system, the energy consumption increases. This is a results of not all of the tanks were used in the reference case with a constant volume and linear pressure distribution. The compressor never had to refuel up to 950 bars but by decreasing the volumes all the tanks are taken into use, which in return results in an energy increase between 1% and 1.6%. The third parameter variation is the pressures in the tanks. This is done for tanks with constant volume of 1 m^3. Fig. 8 shows the energy saving compared to the reference scenario. The energy savings are for all the cascade systems between 4% and 5%, for a single tank the saving is lower 2.5%. It is obvious that the largest saving is gained from the compressor section; this is because the pressures have been lowered. It results in lower compression ratio and a decreased temperature out of the compressor which means that less energy is required for compression as well as a lower cooling demand. The pressures in the tanks was both lowered using the same pressure difference between each tank but with different boundary

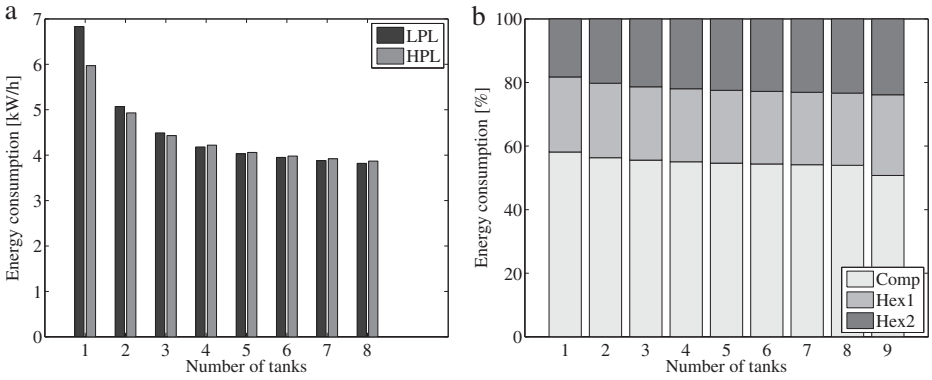

Fig. 5 – The thermodynamics of hydrogen refueling (a) Energy consumption as a function of tanks in the cascade system, both shown for a low pressure loss (LPL) and a high pressure loss (HPL) in the vehicle (b) Energy distribution between the compressor and the cooling facilities.

pressures and by having the same pressure ratio between each step with different boundary pressures. It was found that using 350 bars as lower pressure when there are 3 tanks or more in the cascade system and having the same pressure ratio between each step in the cascade system, gave the lowest energy consumption.

3.4. *General considerations*

The results show that the design of the hydrogen refueling station influences the energy consumption and thereby the operation costs but it also influences the investment costs, as the high pressure tanks are expensive if the volume of the high pressure tanks are decreased the investment cost decreases. The trade-off between tank volumes, pressures and costs must be considered for the specific station taking into account for the daily demand. With small tanks at the station, the mass stored is low and the possibility of doing another refueling before the station has completed the cycle is nonexistent. The larger tanks allows for more flexible use and the possibility to set the pressure in the tanks to cover more than one refueling before recovery is necessary or the pressure can be lower for decreasing energy consumption. The number of tanks at the station should be selected carefully, as the energy consumption is approaching an exponential function, too few tanks will result in high energy consumption by the station and too many tanks do not have a significant energy saving compared to the investment costs of adding more tanks. It is therefore important to consider each station individually with respect to number of tanks, the volumes of the tanks and the pressure in the tanks. Having 3 or 4 tanks at the station in a cascade setup optimizing the pressures is probably the best solution. The energy saving by increasing the volume of the high pressure tanks to 1 m^3 is app. 2.5%, but it also allows for more flexible use. Going from 3 to 4 tanks has an energy saving of 5% and it should be considered if a fourth tank is worth it.

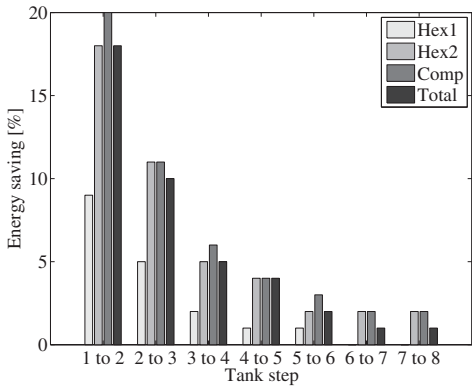

Fig. 6 – Energy saving by adding an extra tank to the refueling station.

4. Conclusion

A thermodynamic model based on the first principles has been made in the modeling software Dymola. The model takes into account heat transfer from the tanks, pressure loses in the system, cooling demands, compressor work and it complies with the protocol for refueling hydrogen vehicle for personal transportation. The analysis was done in 3 steps. First the effect of numbers of tanks in the cascade system was studied with respect to the energy consumption of the individual component and the overall consumption. When going from one tank at the refueling station to eight tanks the energy consumption decreased approaching an exponential function with the largest energy saving between having one and two tanks at the station of 18% per complete refueling cycle. The energy consumption starts leveling out when more than 4 tanks are present in the cascade system. The second analysis with varying tank volumes showed that decreasing the volume of the tanks, with the largest decrease in the high pressure tanks gave a small reduction in energy consumption when 5 tanks or less was used for the vehicle refueling. By lowering the volumes in the lower pressure tanks more mass

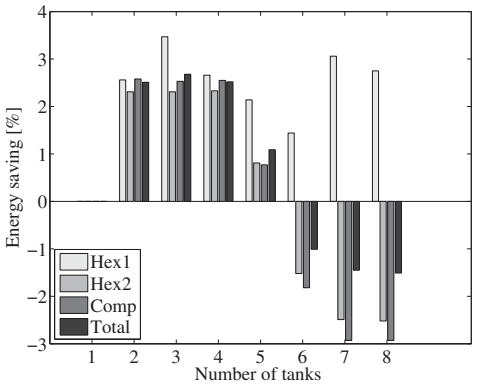

Fig. 7 – The energy difference for decreasing the tank volume.

was drawn from the higher pressure tanks, which in principle means higher pressure ratio for the compressor. However, because the volumes were decreased, the pressure ratio was also decreased and the overall energy consumption lowered with 2.5%. The third analysis showed that by having a constant volume of 1 m^3 in all the tanks and then changing the pressures in the tanks, starting from 350 bars and then increasing with equal pressure ratio between tanks next to each other and then ending a pressure difference across the reduction valve on 10 to 20 bars lowered the energy consumption with approximately 5% compared to have fixed pressures between 400 and 950 bars. The analysis shows that an optimal number of tanks in a cascade refueling system is 3–4 tanks and that it is important to consider the pressure loss in the station in order to determine the pressures that are used in the tanks. Further the hydrogen refueling station should be designed according to refuel a vehicle with a high pressure loss even though the mass refueled is considerable lower than when refueling a vehicle with a low pressure loss. This is because the mass flow curve is dependent on the vehicles pressure loss. A lower pressure loss means that the mass flow peaks earlier and the extra mass that is fueled is taken from the lower pressure tanks at the station. This in turn results in that every refueling station that can handle a vehicle with a high pressure loss, will also be able to handle a vehicle with a lower pressure loss. The results from this analysis can be conducted to refueling stations, but the values set as pressures and volumes are only valid with the pressure losses of this specific case. Therefore all hydrogen refueling stations should be examined individually in order to obtain the optimal pressure and volumes of the tanks in the cascade system.

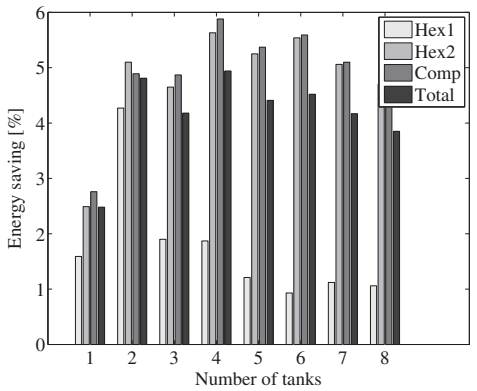

Fig. 8 – The energy difference when optimizing the pressure in the tanks.

Acknowledgments

The authors would like to thank the Danish Energy Agency for financial support and our industrial partner, H2Logic, for their collaboration and technical support.

Nomenclature

A	area of tank, m^2
c	specific heat capacity, J/(kg K)
d	diameter, m
f	friction factor, –
g	gravity, m/s^2
h	enthalpy, J/kg
k	conductivity, W/(m K)
k_v	pressure loss constant, m^3/h
k_p	pressure loss constant, –
L	length, m
$\dot{m}$	mass flow rate, kg/s
M	mass, kg
n	number of strokes, strokes/s
Nu	Nusselt number, –
P	pressure, Pa
Q	heat loss, J/s
R	resistance, (J/K)
r	roughness, mm
Ra	Rayleigh number, –
T	temperature, K
t	time, s
U	internal energy, J
V	volume, m^3
$\dot{V}$	volume flow, m^3/s
v	velocity, m/s
W	work, J/s
x	thickness, m

Greek

α	heat transfer coefficient, $W/(m^2 K)$
β	thermal expansion coefficient, T^{-1}
η	efficiency, –
γ	heat capacity ratio, –
μ	dynamic viscosity, kg/(sm)
ρ	density, kg/m^3

Subscript

a	ambient
cyl	cylinder
g	gas

i	node number
in	into component
is	isentropic
k	conductivity
L	total thickness
out	out of component
P	pressure
v	volumetric
w	wall
water	water properties at 15 °C

Abbreviations

APRR	average pressure ramp rate
HPL	high pressure loss
LPL	low pressure loss
SAE	Society of Automotive Engineers
TIR	technical information report

REFERENCES

[1] Society of Automotive Engineers. Fueling protocols for light duty gaseous hydrogen surface vehicle; 2010. Technical Information Report J2601.

[2] Society of Automotive Engineers. Compressed hydrogen vehicle fueling connection devices; 2008. Technical Information Report J2600.

[3] Farzaneh-Gord M, Deymi-Dashtebayaz M, Rahbari H, Niazmand H. Effects of storage types and conditions on compressed hydrogen fuelling stations performance. Int J Hydrogen Energy 2012;37:3500–9.

[4] Hosseini M, Dincer I, Naterer GF, Rosen MA. Thermodynamic analysis of filling compressed gaseous hydrogen storage tanks. Int J Hydrogen Energy 2012;37:5063–71.

[5] Rothuizen E, Merida W, Rokni M, Wistoft-Ibsen M. Optimization of hydrogen vehicle refueling via dynamic simulation. Int J Hydrogen Energy 2013;38:4221–31.

[6] Kaern MR. Analysis of flow maldistribution in fin-and-tube evaporators [Ph.D. thesis]. The Technical University of Denmark; 2011. DCAMM special report no. S132.

[7] Smith R. Chemical process. 1 ed. New York: John Wiley & Sons; 2005. p. 273–5.

[8] Kaviany M. Principles of heat transfer. 1 ed. New York: John Wiley & Sons; 2002. p. 294–6.

[9] Monde M, Woodfield P, Takano T, Kosaka M. Estimation of temperature change in practical hydrogen pressure tanks being filled at high pressure of 35 and 70 MPa. Int J Hydrogen Energy 2012;37:5723–34.

[10] Woodfield P, Monde M, Mitsutake Y. Measurement of averaged heat transfer coefficient in high-pressure vessel during charging with hydrogen nitrogen and argon gas. J Therm Sci Tech-JPN 2007;2:180–91.

[11] Daney DE. Turbulent natural convection of liquid deuterium hydrogen and nitrogen within enclosed vessels. Int J Heat Mass Transf 1976;19:431–41.

[12] Dicken CBJ, Mérida W. Measured effects of filling time and initial mass on the temperature distribution within a hydrogen cylinder during refueling. J Power Sources 2006;165:324–36.

[13] Burkert. Data sheet. http://www.burkert.dk/productsd ata/datasheets/DS 2836-Standard-EU-EN.pdf; 2013. 1, The 10th of June 2013.

[14] Krex H. Maskin staabi. 9 ed. Copenhagen: Nyt Teknisk Forlag; 2004. p. 143–51.

[15] Cengel Y, Cimbala J. Fluid mechanics: fundamentals and applications. 1 ed. New York: McGraw-Hill; 2006. p. 321–54.

Appendix F

Paper III

Erasmus Rothuizen, Martin Abel, Masoud Rokni and Brian Elmegaard

Using a potassium acetate solution for cooling high pressure hydrogen in a prototype heat exchanger

23rd International Congress of Refrigeration. IIR/IFF. Prague, Czech Republic. (2011)

ID: 536

USING A POTASSIUM ACETATE SOLUTION FOR COOLING HIGH PRESSURE HYDROGEN IN A PROTOTYPE HEAT EXCHANGER

E. D. ROTHUIZEN (*), M. ABEL, M. ROKNI, B. ELMEGAARD
(*) Department of Thermal energy Systems at Institute for Mechanical Engineering, Technical University of Denmark , Nils Koppels Allé building 403, Kgs. Lyngby, 2800, Denmark
edro@mek.dtu.dk

ABSTRACT

A statement of intent assures more than 100.000 hydrogen vehicles will enter the market by 2015. A uniform approach for filling the vehicles has been developed and it states that cooling of the hydrogen is needed. For this purpose a test refrigeration facility was build. As the hydrogen is to be delivered at high pressure a heat exchanger was designed and constructed. The paper presents a detailed study of construction of the heat exchanger which has been tested and compared to theory to predict and verify its performance. The method presented by Nellis and Klein for laminar flow in annulus tubes was the most accurate of the methods compared. At low mass flows the calculated result was larger than the measured and at large mass flows the calculated results was lower than the measured. The used approach gives a reasonably accurate calculation for further investigations of cooling hydrogen.

1. INTRODUCTION

A statement of intent assures that more than 100.000 hydrogen vehicles will be deployed into the European, American, Japanese and Korean markets by 2015. The implementation of such a large amount of hydrogen vehicles into the market requires a universal procedure for filling the high pressure hydrogen vessels in the vehicles. Society of Automotive Engineers (SAE) has therefore made a technical information report containing a fuelling protocol for light duty gaseous hydrogen surface vehicles, SAE TIR J2601 (SAE, 2010). SAE TIR J2601 establishes guidelines for the fuelling protocol of gaseous hydrogen vehicles. The fuelling station should comply with these guidelines for working pressures at 35 MPa and 70 MPa for which the standard assures a safe filling within reasonable time. The use of the protocol is entirely voluntary and is not prerequisite for building hydrogen filling stations. The protocol states an average pressure ramp rate (APRR) into the vehicles high pressure vessel depending on the ambient temperature, the pressure in the vessel before the fuelling and the temperature of the hydrogen as it enters the vehicles hydrogen storage system (HSS). Figure 1 shows a sketch of the refrigeration cycles. The protocol describes the fuelling procedure for three different entrance temperatures for the hydrogen where it is cooled and one with no cooling; D = no cooling, C = 0°C, B = -20°C and A = -40°C. The fuelling stations are categorised depending on the maximum working pressure and the hydrogen temperature at the inlet of the vehicle e.g. B-35 or A-70. In order to have the necessary capacity to service all hydrogen vehicles, either an A or B station is needed with ‘A’ as the most favourable with shortest fuelling times and highest working pressure.

In order to fuel hydrogen with a temperature below the ambient temperature, energy needs to be removed from the hydrogen. This can only be done by cooling the hydrogen, due to hydrogen’s Joule-Thomson inversion temperature which never exceeds 217 K (16 MPa) and is non-existing above 17 MPa pressure. Due to this, the temperature of hydrogen will always increase during expansion at the hydrogen filling station. The cooling demand varies throughout the filling as the only factor kept constant is the APRR. The duration of one filling is between 2.5 and 6 minutes depending on the initial conditions. The cooling should operate instantly as the vehicle connects. The hydrogen is stored at a pressure of 80 MPa at the fuelling station and the vehicle is filled to around 70 MPa, this outlines the limiting operating pressure of the heat exchanger which cools the hydrogen.

The tubes for the hydrogen should be certified for 150 MPa pressure in order to carry the high pressure hydrogen.

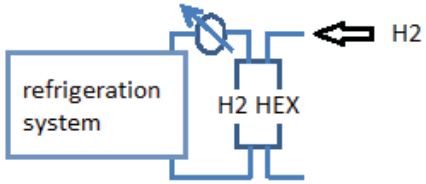

Figure 1 –Sketch of refrigeration system for a hydrogen filling station.

This paper will firstly describe the important factors which influence the cooling demand of the hydrogen. Secondly the use of brine for cooling hydrogen is described and finally is an analysis of the prototype heat exchanger for hydrogen. The heat exchanger performance is compared to theory in order to assess and verify the performance calculations of the heat exchanger.

2. METHODS

2.1. Cooling demand and properties of hydrogen

In order to determine the cooling demand, a dynamic model of a hydrogen filling system was used for calculating the cooling demand and the temperature profile across the heat exchanger. The filling simulated was an A70 (cooling to -40 C and a target pressure of 70 MPa) at an ambient temperature of 30 C. The temperature in the storage tank at the filling station (T_fb), the temperature at the inlet of the heat exchanger (T_hi), the mass flow of hydrogen (m_dot) at a constant average pressure ramp rate (APRR) and the cooling demand (Q_dot) are shown in Figure 2. The most important parameters for the cooling demand are the temperature after the expansion valve and the mass flow, as the cooling demand is a direct function of the two and the temperature out of the heat exchanger. Figure 2 shows the important dynamic parameters for a fuelling as a function of fuelling time. The cooling demand reaches a peak before the mass flow does. This is due to higher inlet temperature at the heat exchanger.

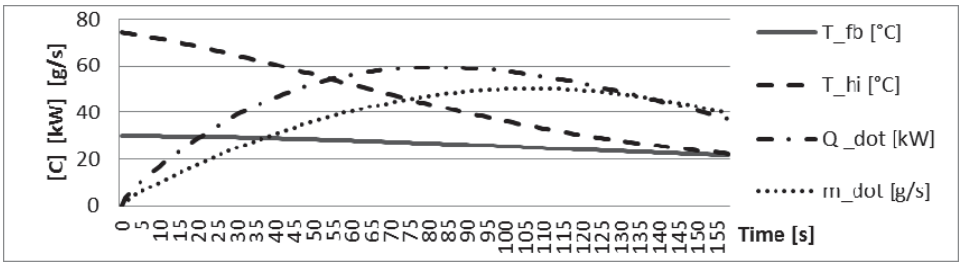

Figure 2 - Temperatures, mass flow and cooling demand during a filling.

At first the temperature at the heat exchanger inlet (T_hi) is high compared to the temperature out of the hydrogen bank (T_fb) at the filling station, as shown in Figure 1. This is due to the reverse Joule-Thomson effect of hydrogen at temperatures about 210 K and at pressures higher than 17 MPa. The joule Thomson effect occurs when a gas is throttled, as is the case for refrigerants, the difference between refrigerants and hydrogen is that refrigerants cools down where hydrogen heats up. The Joule-Thomson effect has a positive impact on the heat exchangers area as the temperature increases with up to 35 K during the throttling of the hydrogen. Leaving the cooling demand unchanged due to constant enthalpy when throttled the larger temperature difference between

hot and cold fluid decreases the size of the heat exchanger. With no Joule Thomson effect the temperature out of the hydrogen storage and after the throttling would be the same. The Joule-Thomson coefficient for hydrogen at different pressures is shown in Figure 3. The throttling of the hydrogen is at the largest 78 MPa, corresponding to a temperature increase of app. 35 K.

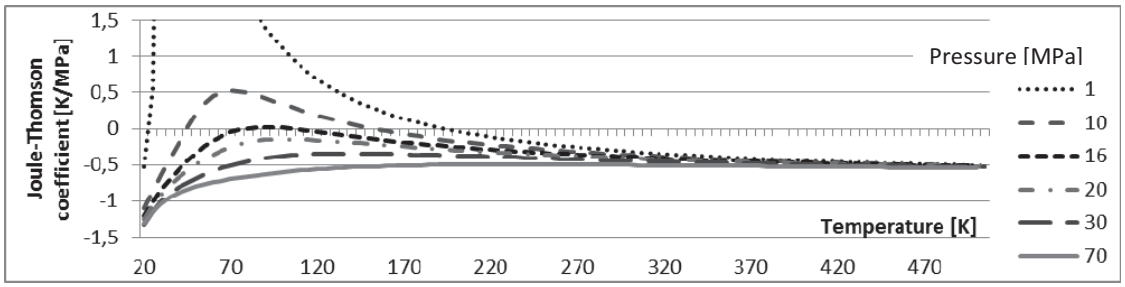

Figure 3 - The Joule-Thomson coefficient for hydrogen as a function of pressure and temperature

2.2. The refrigeration system for cooling the hydrogen.

The refrigeration facility for cooling the hydrogen consisted of a primary refrigeration system and a secondary cycle, as shown in Figure 1. The primary refrigeration system was used to cool the secondary refrigerant in the secondary cycle. The secondary refrigerant was a potassium acetate solution. The system was chosen due to the advantages of brine. Brine is a fluid consisting of water mixed with salts or chemicals to lower the temperature at which the water freezes. Brine is not pressurised and it was therefore interesting to test it for use with high pressure hydrogen, as the hydrogen has to flow in the inner tube, shown in Figure 4. A normal evaporator usual cools from the inside out on to the media which should be cooled. The brine can be used to cool from the outside in to the hydrogen. Brine is a very simple system consisting of the brine as energy carrier, two heat exchangers and a pump to circulate the brine as shown in Figure 1. The negative aspect of brine is its poor properties of heat transfer and the need for the whole refrigeration system to be running constantly in order to assure a sufficient brine temperature instantly for a filling. The energy consumption is therefore large.

Brines can both be used at laminar and turbulent flow. When it receives heat, it unlike e.g. butane and slurry ice decreases in temperature proportional to the heat received. Butane and slurry ice uses a phase change which is better at transferring heat and the temperature is constant until all refrigerant has completed the phase change. It could be of interest to compare the performance of brines with the one for slurry ice. Slurry ice has a higher local heat transfer coefficient and the advantage would be a smaller secondary system for the same cooling demand.

2.3. The heat exchanger for cooling the hydrogen.

A heat exchanger for testing purpose was designed and constructed. The heat exchanger consists of 10, 6 meters long, high pressure tubes made out of stainless steel which each are connected in parallel through a manifold. The tubes have three 180 degree bends and 4 straight sections. The tubes were placed on top of each other in parallel as shown in Figure 4, where the dimensions for the brine shell around each hydrogen tube are also given. The shell and tube heat exchanger has a total height of 0,72 meters and each channel has a width of 0,10 m. The hydrogen tube used is 3/8 inch (0,00957 m).

The design of the heat exchanger was made from estimates built on limited knowledge of heat transfer at laminar flow. Fully developed laminar flow has poor heat transfer properties as the fluid does not mix and the boundary layer does not change, therefore large temperature difference can occur across the flow. The bends are made in order to mix the flow and thereby restart the thermal development and increase the heat transfer coefficient. The designed heat exchanger was for testing purpose only and the dimensions were decided due to the simplicity of the construction rather than for the best heat transfer case. The primary purpose of the heat exchanger was to

investigate how it behaved compared to theory, in order to be able to dimension future heat exchangers for hydrogen filling stations using a potassium acetate solution to cool on high pressure hydrogen.

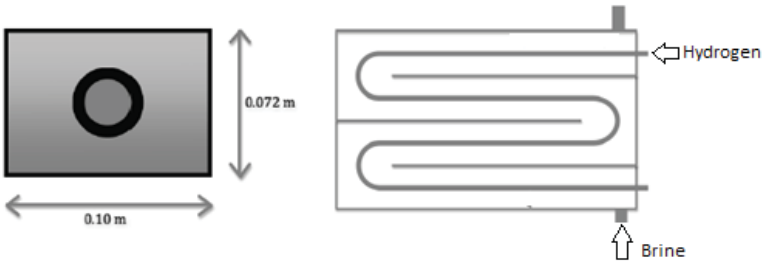

Figure 4 - The design and dimensions of the heat exchanger

2.4. Heat transfer calculations

The brine flow through the heat exchanger is laminar, with developing flow in the entrance region. Each bend is considered to restart the thermal development, hence there is an entrance length every time after each bend. In general, theory on heat transfer is very well described in the heat transfer textbooks, however the use of laminar flow in annulus tubes is often less described when the entrance region is considered. The theory on a laminar flow in a single tube is well described for the developing flow at the entrance region as well as for fully developed flow. Both the Nusselt number for annulus tubes and for a single tube has been compared in order to investigate which methods suit best for the hydrogen/brine heat exchanger dimensioning. Developing laminar flow may be categorized by heat transfer mode. The first is for constant heat flux which is most likely to occur in counter flow heat exchangers, the second is for constant wall temperature which is most likely to occur in co-flow heat exchangers. The third one is for a mixture of constant heat flux and constant wall temperature which in the most cases may be the best assumption. The values of Nusselt number for a developing flow at the entrance region has a lower limit which is the Nusselt number for constant wall temperature and the upper limit is the Nusselt number for constant heat flux (Incropera, Dewitt, Bergman, & Lavine, 2007). This paper only considers constant heat flux as the system is a counter flow heat exchanger. The solution presented by Nellis and Klein (Nellis & Klein, 2009) which is based on the results from London and Shah's (Shah and London, 1978) laminar flow through annulus ducts is for constant heat flux given by the two following equations.

$$Nu_H = Nu_{H,fd} + Nu_{D,r} * Nu_{D,H} \quad (1)$$

Where $Nu_{h,fd}$ is the contribution from the fully developed laminar flow, $Nu_{D,H}$ is the contribution due to thermally developing flow with respect to constant heat flux, $Nu_{D,r}$ is a correction factor for Prandtl numbers different from 0,7. For laminar flow in a tube Nellis and Klein suggest equation 2 for constant heat flux:

$$Nu_H = 4.36 + \frac{0.1156 + \left(\frac{0.08569}{Pr^{0.4}}\right)\frac{D}{L} Re_D Pr}{1 + 0.1158\left(\frac{D}{L} Re_D \Pr\right)^{0.6}} \quad (2)$$

Where D [m] is the hydraulic diameter, L [m] the length of the section, Re is Reynolds number and Pr is the Prandtl number. This equation is similar to other equations for developing laminar flow with constant heat flux in a tube presented by Hausen (Hausen H., 1959), Kays (Kays, 1955) and Shah (Shah, 1975).

The output of the test results was the inlet and outlet temperatures of the heat exchanger for both hydrogen and brine. The mass flows of brine and hydrogen was also measured and hydrogen fluid property data was found from the National Institute of Standardization (NIST) (NIST, 2008). The properties of the brine were found using SecCool (DESIK, 2007). The most important result was whether the capacity of the heat exchanger was sufficient, so it could transfer enough heat to cool the hydrogen down to the prescribed temperature interval given by the standard SAE TIR J2601. The outlet temperature was measured and in order to compare it with the

calculated outlet temperature the overall heat transfer coefficient was found using equation 1 and 2 for Nusselt number. The ε-NTU method was used to calculate the outlet temperature from the heat exchanger. The input for the calculations was the measured inlet temperature, pressure and mass flow and the output was the outlet temperature which was used to calculate the heat transfer capacity of the heat exchanger. The heat transferred from the hydrogen was found through enthalpy differences at the inlet and outlet of the heat exchanger. The test carried out did not follow the APRR according to the standard SAE TIR J2601 as the test was done without a receiving hydrogen pressure vessel. Instead the test was made with constant mass flow at different flow rates and the hydrogen was released to the ambient after the heat exchanger. The heat exchanger was tested using different number of hydrogen tubes. This was done by physically blocking out some of the tubes. It has been assumed that the mass flow of the hydrogen is evenly distributed in the tubes and that the cooling in each tube is the same. All analyses are made on one tube, hence the amount of connected tubes is eliminated for this comparison between measured data and calculated results.

3. RESULTS

The problem was approached as a calculation of 7 individual heat exchangers in a serial connection. The first input for the first calculation was the measured inlet temperature into the heat exchanger and the following calculations used the output temperature from the previous calculation. This is assumed to be valid as the thermal development restarts at the entrance and exit of the bends in the heat exchanger. An example of a calculation using equation 1 for the heat exchanger is shown in Figure 5. The entrance temperature (T_{hi}) is measured, the temperatures stated T_s are after a straight section and the temperatures T_b are after a bend. The last T_s are the calculated outlet temperature. For comparison, the measured outlet temperature has been plotted as T_{ho}.

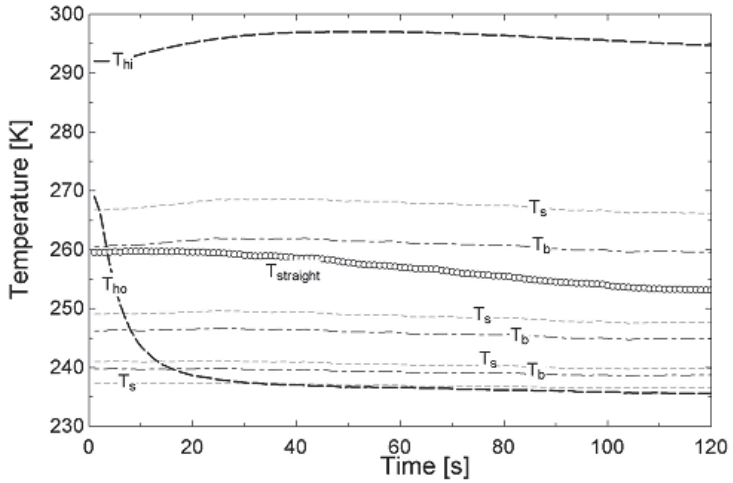

Figure 5 - Calculated hydrogen temperature after each section in the HEX and inlet and outlet temperature measured (T_{hi} and T_{ho}) for a full test.

$T_{straight}$ is the temperature out of the heat exchanger if the thermal development is not restarted at the bends, hence the heat exchanger is calculated as one long tube. In the test results shown in Figure 5 the calculated outlet temperature fits the measured, test 2 in Table 1, but this is not a general tendency. The results from a series of tests compared to the measured data from the inlet and outlet of the heat exchanger can be seen in Table 1. The results have been arranged so that the hydrogen mass flow increases from top to the bottom of the table.

Table 1 - Test measurement and results.

Test	m_dot [kg/s]	Q_r [kW]	d1 [%]	d2 [%]	UA_r [W/K]	T_hi [K]	T_ho [K]	ΔT [K]	ε - HEX [%]
1	8,94E-04	0,951	-0,016	0,120	42,17	309,7	237,8	71,9	0,958
2	1,03E-03	0,909	-0,002	0,161	48,03	296,0	236,1	59,9	0,957
3	1,26E-03	1,113	-0,081	0,143	37,05	300,9	241,2	59,7	0,859
4	1,35E-03	1,386	-0,085	0,156	38,04	314,6	245,6	69,0	0,847
5	1,53E-03	1,578	0,050	0,284	64,18	308,2	238,2	70,0	0,941
6	1,63E-03	1,675	-0,004	0,257	50,67	312,5	243,0	69,5	0,875
7	1,76E-03	1,624	0,093	0,342	78,67	300,6	237,9	62,7	0,951
8	1,85E-03	1,706	0,105	0,360	81,67	299,8	237,3	62,5	0,949
9	2,01E-03	1,663	0,015	0,312	54,72	298,7	242,7	56,0	0,837
10	2,29E-03	2,116	0,105	0,395	73,03	306,0	243,4	62,6	0,882
11	3,16E-03	2,317	0,105	0,441	68,18	297,2	247,6	49,6	0,761
12	3,46E-03	2,722	0,141	0,473	73,72	303,8	250,4	53,4	0,759
13	3,78E-03	2,596	0,142	0,485	73,37	296,5	250,1	46,4	0,722
14	4,79E-03	3,076	0,195	0,537	80,10	297,4	254,2	43,2	0,666

The table shows the hydrogen mass flow per tube (m_dot), the heat transferred (Q_r), the deviation between calculated and measured heat transfer using both equation 1(d1) and 2(d2). The UA value of the heat exchanger, the temperature at the inlet and outlet of the heat exchanger as well as the temperature difference between inlet and outlet of hydrogen and last the effectiveness (ε) of the heat exchanger.

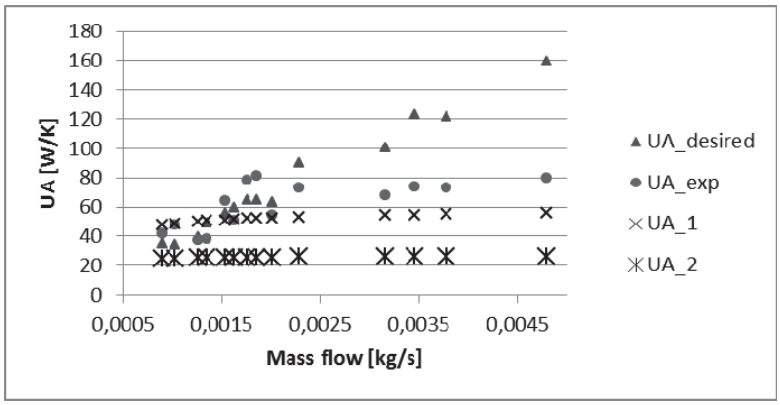

Figure 6 - The UA values for the HEX calculated and measured as a function of the hydrogen mass flow

Figure 6 shows the UA values for the heat exchanger, UA_desired is the lowest UA value which is needed in order to comply with SAE 2601, UA_exp is the UA number obtained from the experimental data, UA_1 is the theoretical UA number found for brine flow in annulus tubes using equation 1 to find Nusselt number and UA2 is the theoretical UA number if correlations for flow in a tube are supplied, equation 2. Figure 7 shows the corresponding heat transferred for the different tests. The abbreviations are the same as above, so Q_desired is

the needed heat transferred to comply with J2601, Q_exp is the heat transferred for the heat exchanger, Q_1 is for calculations for laminar flow in annulus tubes (equation 1) and Q_2 is for laminar flow through a tube (equation 2).

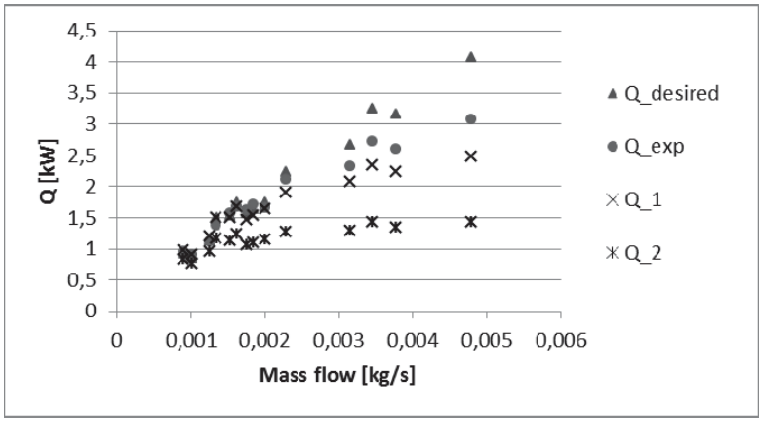

Figure 7 - The heat transferred between brine and hydrogen in the HEX as a function of the mass flow through one hydrogen tube.

4. DISCUSSION

Figure 5 shows the temperature difference after each section in the heat exchanger. The temperature decrease in each section decreases as the hydrogen temperature approaches the brine temperature. This was expected, the lower the temperature difference between hot and cold fluid, the larger the area of the heat exchanger needs to be.

The comparison between equation 1 and 2 for calculating Nusselt number shows significant differences. Using equation 2; the lowest deviation is 12 % and it increases as the mass flow increases. The deviation reaches 19,5% using equation 1 for calculating the Nusselt number. At mass flows less than 1,75 g/s the calculated heat transfer is larger than the measured and the deviation is below 8,5 %. At higher mass flows between 1,75 g/s and 3,16 the deviation is between 9,3 % and 10,5 %. As the mass flow increases above 3,16 g/s the deviation between the calculated and measured heat transfer increases.

Figure 6 shows the calculated results compared to the experimental results and the desired UA value. As expected, the UA value does increase as the mass flow increases in both tests and calculations. The calculated and measured UA values are at low mass flows higher than the lowest UA value desired. This can also be seen in Table 1 as the outlet temperature is lower than 240 K. The desired UA value increases proportionally to the mass flow. At mass flows higher than 1,75 g/s the heat exchangers cannot transfer the heat required between the hydrogen and the brine. The highest mass flow for a filling will be around 50 g/s. The prototype heat exchanger had 10 tubes with a mass flow for each tube of 5 g/s. It can be seen from the test that the UA value for a hydrogen mass flow of 4,79 g/s is approximately half of the desired UA value. This is also expressed in the effectiveness in Table 1, which shows how close the temperature of the outlet of the hydrogen is to the brine temperature. Figure 7 shows the heat transferred between the hydrogen and the brine. It is similar to Figure 6 but the relative differences between the calculated, measured and desired heat transfer are smaller than for the UA values. This is because of the decreasing temperature difference between the hydrogen and the brine as the hydrogen flows through the heat exchanger, as seen in Figure 5. The difference between the desired heat transfer and the actual heat transfer is in tests 12 and 13 about 19 % but the difference in the UA values is around 38 %. The last heat which should be removed requires a larger area as the temperature difference between the hydrogen and brine decreases. As the mass flow increases it seems like the UA_exp stabilises around 80 W/K, this should then be the maximum UA value possible under the given conditions.

The flow considered is laminar and it would be of interest to try to change it to turbulent flow, as the heat transfer properties increases for turbulent flow (Melinder, 2002).

It should be noted, that this heat exchanger has been tested during Danish summer conditions and control the temperature of the hydrogen at the inlet to the heat exchanger was not possible. It would be of interest to perform tests with controlled temperature between hydrogen inlet and brine. This would give a better understanding of the behaviour of this kind of heat exchangers.

5. CONCLUSION

The refrigeration facility for the hydrogen refuelling station is designed with refrigeration system cooling on a brine in the secondary system. The secondary system uses a potassium acetate solution which cools at laminar flow without phase change. This has a negative impact on the size of the heat exchanger due to low heat transfer properties. If it is possible to make the flow turbulent, it would enhance the heat transfer though a phase changing refrigerant would still have better performance.

The prototype heat exchanger was built for testing purposes and for investigating its heat transfer properties for cooling hydrogen with brine at laminar flow. Equation 1 for Nusselt number at laminar flow in annulus tubes was most accurate of the two calculations methods compared. At low mass flows the heat transfer calculated is larger than measured and for high mass flow it is up to 20 % lower than measured. It is acceptable as for low mass flow the heat exchanger performed better than the minimum requirement to comply with SAE J2601. For higher mass flow where the heat exchanger did not have enough capacity the predicted heat transfer was smaller than the actual heat transfer as the equation used to calculate Nusselt number was not precise enough. Thus using equation 1 would in this case be a worst case calculation and assure that the heat exchanger is large enough for cooling the hydrogen at peak mass flow. In conclusion we find that it would be preferred to find a more precise way to determine the size of the brine-hydrogen heat exchanger, but that the described approach gives a reasonably accurate calculation for further investigations of the cooling system of the hydrogen filling station.

REFERENCES

DESIK. (2007). SecCool. (1.3). Copenhagen, Denmark.

Hausen H. (1959). Neue Gleichungen für die Wärmeübertragung bei freier und erzwungener Strömung. *Allg. Warmtechnik, 9*, 75-79.

Incropera, F. P., Dewitt, D. P., Bergman, T. L., & Lavine, A. S. (2007). *Introduction to Heat Transfer* (Fifth ed.). Wiley.

Kays, W. M. (1955). Trans. *ASME*, 77.

Melinder, Å. (2002). *Update on Secondary Refrigerants for Indirect Systems.* The Royal Institut of Technology (KTH), Sweden.

Nellis, G., & Klein, S. (2009). *Heat Transfer.* Cambridge University Press.

NIST. (2008). *National Institute of Standardiztion*. Retrieved 1 2011, from NIST: http://webbook.nist.gov/

SAE. (2010). *Fueling protocols for light duty gaseous hydrogen surface vehicles.* Technical Report J2601, Society of automotive Engineers, Fuel cell Standard Committee.

Shah, R. K. (1975). *Thermal entry length solutions for the circular tube and parallel plates.* Proc. 3rd National Heat Mass Transfer Conference.

Shah, R. K., & London, A. L. (1978). *laminar Flow Forced Convection In Ducts.* Acedemic Press.

Appendix G

Paper IV

Erasmus Rothuizen and Masoud Rokni

The effect on overall energy consumption at a hydrogen refueling station by cascade fueling a hydrogen vehicle

6th International Conference of Sustainable Energy and Environmental Protection, Maribor, Slovenia. (2013)

SEEP-2013 27

THE EFFECT ON OVERALL ENERGY CONSUMPTION AT A HYDROGEN REFUELING STATION BY CASCADE FUELLING A HYDROGEN VEHICLE

E. D. Rothuizen[1] and M. Rokni[2]

1. Department of Mechanical Engineering, Section for Thermal Energy, Technical University of Denmark, Denmark. email: edro@mek.dtu.dk
2. Department of Mechanical Engineering, Section for Thermal Energy, Technical University of Denmark, Denmark. email: mr@mek.dtu.dk

ABSTRACT

Hydrogen vehicles are predicted to become an important part of the transition for the future sustainable energy supply. Several car manufactures have signed a statement of intent securing hydrogen vehicles on the market from year 2015. Society of Automotive Engineers has made protocols for the refuelling process in order to develop standardization for safety and couplings. Until now main concerns have been focused on vehicle refuelling and less attention has been paid to the hydrogen refuelling stations. This study considers the refueling of the high pressure cascade system at the hydrogen refueling station. This is important for the design of the refuelling stations when considering: energy savings, cooling after compression, recovering time between refuelling and safety at the stations. In order to do the analysis, a dynamic model has been developed in Dymola, based on first principle and taking into account pressure losses and heat transfer. The simulations show that adding extra tanks at the station decreases the energy demand for a refuelling cycle approaching an exponential correlation. The largest energy saving (i.e. 16 %) is obtained when going from one to two tanks. The yearly saving for 20.000 refuelling's will be 32.000 kWh.

Keywords: Hydrogen refuelling station, Cascade system, Thermodynamics, Optimization

1 INTRODUCTION

Hydrogen vehicles have been pronounced to be one of the best alternatives to vehicles driving on fossil fuels. This was made clear in 2010 when several of the world's largest car manufactures signed a statement of intent to produce a total of 200.000 hydrogen vehicles to enter the market by 2015. Unfortunately not all of the manufactures can meet the deadline by 2015 but are instead aiming to have their share of hydrogen vehicles out by 2017. Further, in 2010 the first protocol for refuelling of hydrogen vehicles was released by Society of Automotive Engineers: Fuelling protocols for light duty gaseous hydrogen surface vehicle (J2601) [1]. The protocol describes a safe, convenient and fast refuelling of hydrogen vehicles taking into account tank type, ambient conditions and type of refuelling station. The primary intent is to describe the hydrogen properties at the outlet of the station, aiming to depict temperature rise and pressure changes. A refuelling where the hydrogen is cooled down to –40°C and the pressure rises with a constant ramp rate of 282 bar per minute can fill a vehicle tank from 20 bar to 700 bar in 2.5 minutes. Cooling is needed in order to keep the temperature inside the vehicle tank beneath 85°C at all-time avoiding stressing the materials in the tank. The advantage of knowing the exact outlet conditions of the refuelling process is that the refuelling station is not affected by the station but only by the vehicles pressure loss. This means that a vehicle, from a refuelling point of view, will behave in the exact same way at every station following the protocol. Beside the protocol for refuelling stations, a protocol for the coupling between the refuelling station and the vehicle was released in 2008 [2]. The two

protocols assure that any hydrogen vehicles can be refuelled at any station worldwide. Until now the research within refuelling of hydrogen has primarily been focused on the vehicles system and very little research has been done on the refuelling station. It has previously been shown that the hydrogen refuelling station does not affect the refuelling [3], as long as it complies with J2601. The pressure loss in the vehicle is decisive for the mass flow rate and the final pressure in the tank, hence for the total fuelled mass. A low pressure loss results in a higher mass flow peak and in a higher final pressure and total mass in the vehicle tank. With increased pressure loss in the vehicles storage system, the final pressure and total mass decreases. The reason for this behaviour is that the refuelling finishes when a certain pressure is reach at the outlet of the station. The energy usage at the hydrogen refuelling station has not been of any concern until now as the aim was to make the stations comply with J2601. It has been shown that cascade refuelling lowers both cooling demand and compressor energy to refuel the hydrogen refuelling station [3], and that the exergy destruction decreases compared to using a single higher pressure tank [4]. This paper studies the actual energy consumption for hydrogen refuelling and an optimization of the cascade system considering the number of tanks which is used, the total cooling demand, both for the cooling during vehicle refuelling and after the compressor that refuels the hydrogen refuelling station.

2 METHODS

This section contains the basic information about the systems, the calculations and the program used.

2.1 The system

The system that is considered in this paper is a simple system, shown in Fig. 1. The tank for refuelling is situated in the left side, the compressor section at the bottom, the reduction valve and heat exchanger controlling the outlet conditions (according to the standard) in the middle while in the right side of Fig. 1, the vehicle is placed. Table 1 explains the different components. The dark grey lines represents the stream of hydrogen from the compressor, the black line depicts the stream of hydrogen for the refuelling of the vehicle and the light grey line shows where the hydrogen flow can go depending on how the station is operated. The pressure losses for each part of the system have been added together and are at the station placed

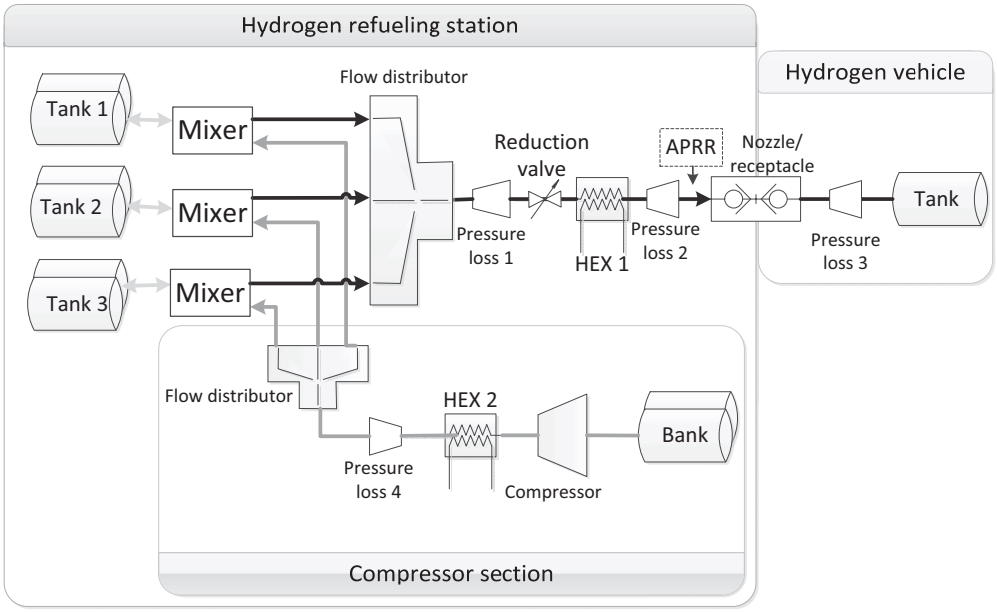

Figure 1. Reference sketch of a hydrogen refuelling station with cascade refuelling

before the reduction valve and before the outlet (nozzle) taking into account the heat exchanger, tubing and valves. The vehicle has pressure losses due to tubing, valves and safety equipment. The maximum allowed pressure loss in the vehicle is 200 bars. There is also a small pressure loss after the heat exchanger in the compressor section to account for the heat exchanger, tubing and valves. The hydrogen is stored at the refuelling station at different pressures and the refuelling proceeds starting with fuelling from the tank with the lowest pressure i.e. Tank 1. At the same time the compressor starts delivering hydrogen to the mixer. The hydrogen from the compressor mixes with the hydrogen from the tank into the stream going to the refuelling of the vehicle.

Table 4. Explanation of the components in figure 1

Component	Function
Tank	Storage tank for hydrogen
Bank	300 bar infinite hydrogen storage
Mixer	Can mix flows from different directions
Flow distributor	Distributes the flow, only one flow can Passat a time
Pressure loss	Different pressure losses
Reduction valve	Controls the flow and assure the constant pressure ramp rate
HEX	Heat exchanger
APRR	The place where the constant pressure ramp rate is defined
Nozzle/receptacle	Coupling between refuelling station and vehicle

If the mass flow out of the compressor becomes larger than what is needed for the refuelling the excess hydrogen is filled into the tank at the station. When the pressure drop across the reduction valve is 10 bars, the station switches to the next tank in the system, i.e. Tank 2. The compressor switches tank when the first tank is back at start pressure. The variation of the number of tanks in the cascade refuelling setup at the station is simply done by adding a tank and connecting it to the compressor and the refuelling system.

2.2 Adiabatic compression and cooling of hydrogen

The thermodynamic equations of the system are described inn; Optimization of hydrogen vehicle refuelling via dynamic simulation [3]. The compressor is modelled as an isentropic compressor with the isentropic efficiency given by equation 1 [5].

$$\eta_{is} = 0.1091 \log\left(\frac{P_{out}}{P_{in}}\right)^3 - 0.5247 \log\left(\frac{P_{out}}{P_{in}}\right)^2 + 0.8577 \log\left(\frac{P_{out}}{P_{in}}\right) + 0.3727 \quad (1)$$

The enthalpy out of the compressor is found by equation 2.

$$h_{out} = \frac{h_{out,is} - h_{in}}{\eta_{is}} - h_{in} \quad (2)$$

The temperature out of the compressor can be determined with state equations by implementing coolprop [6] in Dymola; $T_{out}(P_{out}, h_{out})$.
The compression is adiabatic, which is the worst case scenario for the hydrogen temperature out of the compressor. The work performed by the compressor is given by Eq. 3.

$$W = \dot{m}(h_{out} - h_{in}) \quad (3)$$

Were the mass flow out of the compressor is found by,

$$\dot{m} = V_{cyl} * \rho * \eta_v * n \quad (4)$$

Were ρ is the density at the inlet, n is number of strokes, V_{cyl} is the volume of the cylinder and η_v is the volumetric efficiency. The volumetric efficiency has a maximum of 90% and it decreases by 5% per single increment in the pressure ratio value.

The work required to satisfy the cooling demand after the compressor and at the outlet of the station is found by:

$$W = \frac{\dot{m}(h_{out} - h_{in})}{COP} \quad (5)$$

COP is the coefficient of performance for the refrigeration facilities. The temperature out of the heat exchanger is set as a fixed value and the enthalpy out of it is found using state equations $h_{out}(T_{out}, P_{out})$. The total energy consumption for one refuelling at the hydrogen refuelling station is found by Eq. 6.

$$W_{total} = W_{comp} + W_{hex1} + W_{hex2} \quad (6)$$

2.3 The model

The model is developed in Dymola software which is a dynamic simulation programme. The language is unified object-orientated for physical system modelling. The software is capable of solving large dynamic complex systems using ordinary differential equations. The model is build up by objects which can be connected in any order as they all receive and pass on the same information. Each object represents a system object like a valve, heat exchanger, tank etc.

3 RESULTS

This section first explains the conditions for the system used for the simulation. Then the results of the simulation are shown and analysed.

3.1 Input values

The considered refuelling is the most demanding for vehicles assigned as personal transportation. It is a 7 kg refueling within 2.5 minutes. The hydrogen is cooled down to 20°C in the heat exchanger after the compressor and the outlet temperature of the hydrogen leaving the station is –40°C. The vehicles tank is at 20 bars when starting and the refuelling end when the pressure out of the station reaches 720 bars. The cascade systems analysed has 950 bars as the highest pressure, while the pressure for the other tanks starts at 400 bars and equally increases until 950 bars are reached. All the tanks have a size of 1m^3. The low pressure tank at which the compressor draws the hydrogen is assumed to be large enough with 300 bars. The value of 300 bars has been chosen because steel tanks can withstand this pressure. The coefficient of performance (COP) for *Hex1* and *Hex2* (Fig. 1) is set to 1.5 and 2 respectively. These values are in the lower end of the expected values for the refrigeration facilities [7]. The pressure drop after the reduction valve (pressure loss 2) and in the vehicle (pressure loss 3), are the same in all scenarios. The pressure drop before the reduction valve (pressure loss 1) and after the compressor (pressure loss 4) will depend on the specific system. The pressure drops can be seen in Fig. 2 were pressure loss 1 and 4 are for a three tanks cascade system. The compressor has a maximum mass flow of 0.015 kg/s while the maximum mass flow to the vehicle for this refuelling is 0.046 kg/s. The mass flows can be seen in Fig. 3, valid for the compressor with a three tank cascade system.

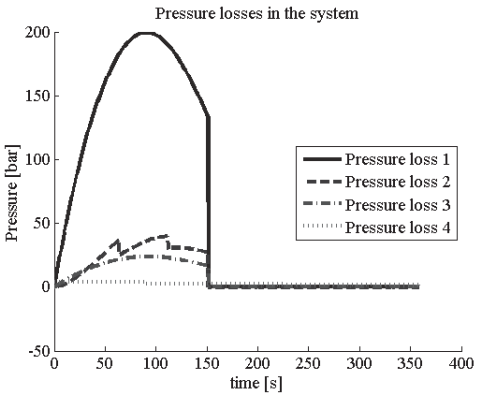

Figure 2. The pressure losses in the system

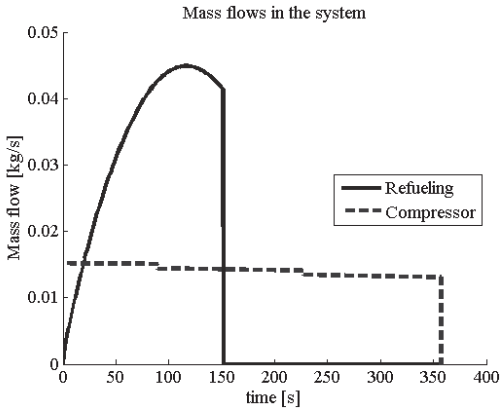

Figure 3. Mass flows for refuelling and the compressor

The drops in pressure loss 2 are due to tank switch at the station during refuelling while the drops in the compressor´s mass flow are due to the switch among the tanks at the station being fuelled.

3.2 Energy consumption

For the energy optimization a system like the one presented in Fig. 1 is used. The only change is that the number of tanks at the station varies from 1 to 6. The energy consumption is the total of cooling and compression during a full cycle at the refuelling station. The electronic equipment and the filling of the large 300 bars bank are not included, as this is the same for all the different designs. The energy consumption of the system can be seen in Fig. 4. The consumption of energy is highest when using a single tank at the station and then it decreases exponentially as more tanks are added. The highest energy consumption is 5.7 kWh for one refuelling cycle which is approximately 2.4 % of the energy of the hydrogen fuelled to a 7 kg capacity vehicle tank which contains 240 kWh when full. The largest contribution to the overall energy consumption is given by hydrogen compression and it represents more than half of the total energy consumption. The second highest energy consumption comes from the cooling needed after the compressor while the lowest energy consumption comes from the cooling needed during the refuelling of the vehicle. Increasing the number of tanks in the cascade system decreases the energy consumption of all three components.

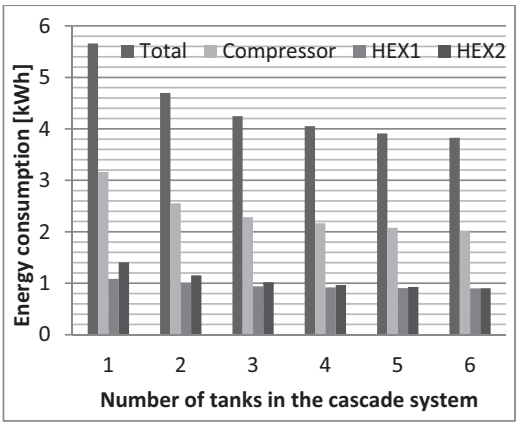

Figure 4. Energy usage at the refuelling station for a full hydrogen refuelling cycle

The energy saving of using more tanks in the cascade system can be seen in Fig. 5, where "energy savings" stands for the energy saving obtained by adding an extra tank to the system (e.g. from one to two tanks or from three to four tanks). The energy saving is larger for the compressor at all times as it uses more energy than refrigeration facilities, though the difference between two and three tanks is the refrigeration facility after the compressor, which has the largest relative energy saving of 11 % of its own use. The energy saving is lower than 5 % for each extra tank added when at least three tanks are present in the system. Though the energy saving for the compressor and the refrigeration facility after the compressor are both more than 5 %. This is first when going from four to five tanks that the energy saving for each component is under 5 %.

If a hydrogen refuelling station yearly services 55 vehicles a day, then the energy saving by having multiple tanks is at least 19.000 kWh. Figure 6 shows the yearly savings of having more than a single tank in the cascade system.

Summing up in Fig. 6, the saving of having 4 tanks instead of 1 is app. 32.000 kWh per year.

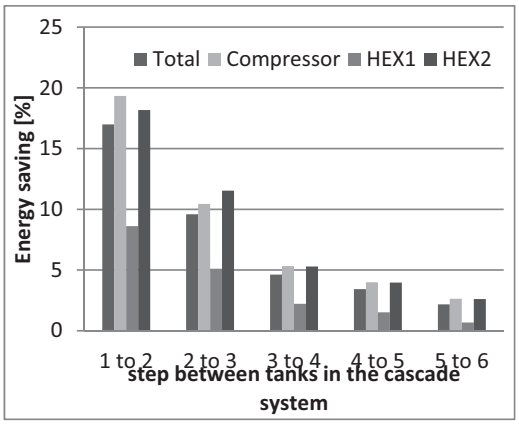

Figure 5. Saving gained when introducing an additional tank to the system.

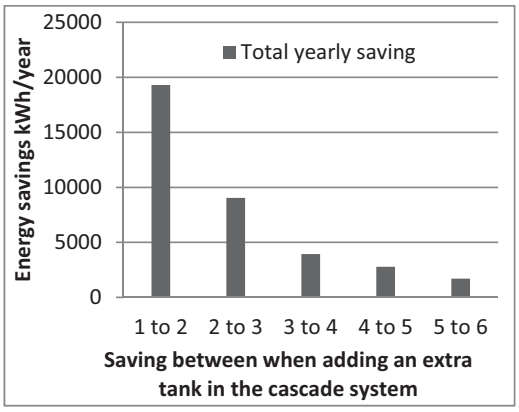

Figure 6. Yearly energy saving for approximately 20.000 refuelling's

4 CONCLUSION

Using thermodynamic simulation for predicting the process enables to optimize systems without having to build a physical test station. This study used the most demanding hydrogen refuelling process fuelling 7 kg of hydrogen at 700 bars in the vehicle. The energy consumption of 1 refuelling cycle can be reduced from 5.7 kWh using 1 tank to 3.9 kWh using 6 tanks at the station. The energy saving is approaching an exponential function and the largest savings are retrieved when the refuelling station expands from one tank to two tanks. The largest contributor to the energy consumption is the compressor which uses half of the energy during a refuelling cycle, but the compressor is also the component with the largest percentage of energy saving when adding additional tanks.

It is beneficial to build refuelling stations with at least 3 tanks in a cascade system, but also adding more than three tanks should be considered with respect to the trade-off between the increase of system´s capital investment and the total saving over its lifetime. Since today a refuelling station typically services only a limited number of vehicles, the optimum tank number to be introduced in the system would be around 3. When more hydrogen vehicles enter the market, adding more tanks could be beneficial.

ACKNOWLEDGEMENTS

The authors would like to thank the Danish Energy Agency for financial support and the industrial partner H2Logic for the collaboration.

REFERENCES

[1] Society of automotive engineers, *Fueling protocols for light duty gaseous hydrogen surface vehicle. Tecnical information report J2601*, 2010.

[2] Society of automotive engineers, *Fueling protocols for light duty gaseous hydrogen surface vehicle. Tecnical information report J2601*, 2010.

[3] E. Rothuizen, W, Merida and M. Rokni, Optimization of hydrogen vehicle refuelling via dynamic simulation, *Int. J Hydrogen Energy,* Vol. 38, pp. 4421-4231, 2013.

[4] M. Hosseini, Thermodynamic analysis of filling compressed gaseous hydrogen storage, *Int. J Hydrogen Energy,* Vol. 37, pp. 5063-5071, 2012.

[5] R. Smith, *Chemical process design and integration*, John-Wiley, 2005.

[6] Ian H. Bell, Sylvain Quoillin, Jorrit Wronski, Vincent Lemort, Coolprop: An open-source reference-quality thermophysical property library, *2nd International Seminar on ORC Power Systems*, 2013.

[7] J. K. Jensen, hydrogen cooling specialist, personal conversation, Technical University of Denmark, June 2013.

DTU Mekanik
Sektion for Termisk Energi
Danmarks Tekniske Universitet

Nils Koppels Allé, Bygn. 403
2800 Kgs. Lyngby

Tlf.: 4525 4131
Fax: 4588 4325
www.mek.dtu.dk
ISBN: 978-87-7475-371-1

DCAMM
Danish Center for Applied Mathematics and Mechanics

Nils Koppels Allé, Bld. 404
DK-2800 Kgs. Lyngby
Denmark
Phone (+45) 4525 4250
Fax (+45) 4593 1475
www.dcamm.dk
ISSN: 0903-1685